

©Copyright 2015

Mycah R. Uehling

Gold-Catalyzed Asymmetric Synthesis of Cyclic Ethers
and
Copper-Catalyzed Hydrofunctionalization of Alkynes

Mycah R. Uehling

A dissertation submitted in partial fulfillment of the requirements for the degree of:

Doctor of Philosophy

University of Washington

2015

Reading Committee:

Gojko Lalic, chair

Forrest Michael

Champak Chatterjee

Program Authorized to Offer Degree:

Department of Chemistry

University of Washington

Abstract

Gold-Catalyzed Asymmetric Synthesis of Cyclic Ethers
and
Copper-Catalyzed Hydrofunctionalization of Alkynes

Mycah R. Uehling

Chair of the Supervisory Committee:

Professor Gojko Lalic

Department of Chemistry

Gold-catalyzed cyclization of enantioenriched trisubstituted allenols to form enantioenriched α -tetrasubstituted cyclic ethers has been developed. This structural motif can be found in many natural products that have useful biological properties. The cyclization reaction is compatible with multiple functional groups and can be used to prepare enantioenriched furans, pyrans, and chromans all containing an α -tetrasubstituted stereocenter. The reaction development, scope, and a preliminary mechanistic study are discussed. In addition, a method to synthesize the required enantioenriched trisubstituted allenols based on copper-catalyzed cross coupling of enantioenriched propargylic phosphates and organoboron reagents has been developed. This allows the overall sequence to be practical and convergent.

Copper-catalyzed hydrobromination and hydroalkylation of alkynes have been developed. The reactions are compatible with many functional groups and can be used to prepare functionalized alkenes in high yield and as one regio- and diastereoisomer. The reaction development, scope, and preliminary mechanism studies are discussed for both reactions. The development of copper-catalyzed hydrobromination and hydroalkylation of alkynes demonstrates that copper-catalyzed

hydrofunctionalization of alkynes is a general approach to the synthesis of different types of functionalized alkenes.

Table Of Contents

List of Abbreviations.....	9
List of Figures.....	13
List of Schemes	14
List of Tables.....	15
Part 1: Asymmetric Synthesis of Cyclic Ethers Containing an α -Tetrasubstituted Stereocenter.....	18
Chapter 1: Copper-Catalyzed Asymmetric Synthesis of Trisubstituted Allenenes	19
1.1 Introduction.....	19
1.2 Reaction Optimization	22
1.3 Scope.....	24
1.4 Mechanism Studies	26
1.5 Conclusion	32
1.6 Experimental.....	33
1.6.1 General Information.....	33
1.6.2 Materials	33
1.6.3 Synthesis of Propargylic Alcohols.....	34
1.6.4 Chiral Resolution of Propargylic Alcohols.....	34
1.6.5 Characterization Data for Propargylic Alcohols	34

1.6.6 Synthesis of Propargylic Phosphates	36
1.6.7 Characterization Of Propargylic Phosphates	36
1.6.8 Substitution of Propargylic Phosphates	38
1.6.9 Characterization of Allene Products	39
1.6.10 Determination of Absolute Stereochemistry	46
1.6.11 Synthesis of Boronate	47
1.6.12 Reaction Between Alkylborane And Various Alkali Metal Alkoxides	47
1.6.13 Reactivity Studies Using Borane or Borate Nucleophiles	47
1.6.14 Synthesis of ICyCuMe	48
1.6.15 Stoichiometric Reaction Between ICyCuMe and Phosphate	48
1.6.16 Catalytic Reaction Using ICyCuMe as the Catalyst	48
Chapter 1 References	49
Chapter 2: Catalytic Asymmetric Synthesis of Cyclic Ethers Containing an α-Tetrasubstituted Stereocenter	53
2.1 Introduction.....	53
2.2 Reaction Optimization	56
2.3 Furan and Pyran Synthesis Scope	59
2.4 Chroman Synthesis Optimization	60
2.5 Chroman Synthesis Scope.....	62
2.6 Mechanism of Ether Formation	63
2.6.1 Mechanism of Furan and Pyran Formation.....	63
2.6.2 Mechanism of Chroman Formation	66
2.7 Conclusions.....	69
2.8 Experimental	69
2.8.1 General.....	69
2.8.2 Cyclization of Enantioenriched Hydroxy Allenes	70
2.8.3 Cyclization of Enantioenriched Phenoxy Allenes.....	77
2.8.4 Attempted Synthesis of Oxetanes and Oxepanes	81
2.8.5 Investigation of Reaction Mechanism.....	82
Chapter 2 References	88
Part 2: Copper-Catalyzed Hydrofunctionalization of Alkynes.....	91

Chapter 3: Catalytic Anti-Markovnikov Hydrobromination of Alkynes 93

3.1 Introduction.....	93
3.2 Reaction Development.....	94
3.2.1 Background Reaction 1: Formation of Bromoalkyne	99
3.2.2 Background Reaction 2: Alkyne Semireduction.....	101
3.3 Optimized Reaction	102
3.4 Hydrobromination Scope	103
3.4 Hydrobromination Mechanism	107
3.5 Hydrobromination Conclusions	109
3.6 Experimental.....	109
3.6.1 Reaction Development:.....	110
3.6.2 Hydrobromination of Terminal Alkynes:.....	111
3.6.3 Large Scale Hydrobromination Procedure.....	112
3.6.4 Characterization Data for Alkenyl Bromides.....	112
3.6.5 Characterization Data for Starting Materials	120
3.6.6 Mechanism Experiments.....	126
Chapter 3 References	129

Chapter 4: Copper-Catalyzed Hydroalkylation of Terminal Alkynes.. 132

4.1 Introduction.....	132
4.2 Hydroalkylation of Alkynes Reaction Development	134
4.3 Hydroalkylation of Alkynes Scope	137
4.4 Hydroalkylation Mechanism.....	138
4.5 Conclusion	141
4.6 Experimental.....	141
4.6.1 Reaction Development.....	143
4.6.2 General Procedure for Hydroalkylation of Alkynes	145
4.6.3 Characterization Data for Alkene Products.....	145
4.6.4 Alkyne Starting Materials	152
4.6.5 Primary Alcohol Starting Materials	154
4.6.7 General Procedure for the Triflation of Primary Alcohols	157
4.6.8 General Procedure for the Synthesis of Benzylic Triflates	159

4.6.9 Mechanism and Kinetics Experiments.....	160
4.6.10. Synthesis of Organometallic Starting Materials and Intermediates	165
Chapter 4 References	168

List of Abbreviations

Ac:	Acetyl
Ad:	Adamantyl
Ar:	Aryl
BBN:	Borabicyclononane
Bn:	Benzyl
Boc:	<i>tert</i> -Butyloxycarbonyl
Bz:	Benzyl
C:	Celsius
Cy:	Cyclohexyl
dr:	Diastereomeric ratio
E ⁺ :	Electrophile
ee:	Enantiomeric excess
er:	Enantiomeric Ratio
eq:	Equation
equiv:	Equivalent
ESI-MS:	Electrospray ionization mass spectrometry
Et:	Ethyl

FTIR:	Fourier transform infrared spectroscopy
h:	Hour
HPLC:	High performance liquid chromatography
HRMS:	High resolution mass spectrometry
Hz:	Hertz
ICy:	1,3-dicyclohexyl imidazolium
IMes:	1,3-Bis-(2,4,6-trimethylphenyl)imidazolium
<i>i</i> Pr:	isopropyl
IPr:	1,3-Bis-(2,6-diisopropylphenyl)imidazolium
Me:	Methyl
Mes:	Mesityl
MHz:	Megahertz
MOC:	Methoxycarbonyl
mol:	Mole
MOM:	methoxymethyl ether
mp:	Melting point
NHC:	N-heterocyclic carbene
NMR:	Nuclear magnetic resonance

Abbreviations for NMR splitting patterns

s:	singlet
d:	doublet
t:	triplet
q:	quartet
p:	pentet
m:	multiplet
br:	broad
Nu:	Nucleophile
OTf:	Trifluoromethanesulfonate
OTFA	Trifluoroacetate
OTs:	<i>p</i> -Toluenesulfonate
PG:	Protecting Group
Ph:	Phenyl
Phth:	Phthalyl
pin:	pinacol
PMHS:	polymethylhydrosiloxane
ppm:	parts per million

rt:	room temperature
<i>t</i> Bu:	<i>tert</i> -butyl
TBS:	<i>Tert</i> -butyldimethylsilyl
TFA:	Trifluoroacetic acid
THF:	Tetrahydrofuran
TIPS:	Triisopropylsilyl
TLC:	Thin layer chromatography
TMDSO:	Tetramethyldisiloxane
TMS:	Trimethylsilyl
tol:	Tolyl
Ts:	<i>p</i> -Toluenesulfonyl
SIPr:	1,3-Bis-(2,6-diisopropylphenyl)imidazolium

List of Figures

Figure 1. Allene Bonding, Stereochemistry, and Absolute Stereochemical Assignment	20
Figure 2. Cyclic Ether Natural Products Containing an α -Tetrasubstituted Stereocenter	54
Figure 3. Hydroalkylation Reaction Time Courses Comparing Stir Rate and Catalyst	140
Figure 4. Product Yield Over Time Using 1.1 equiv or 2.0 equiv CsF	161
Figure 5. Product Yield Over Time Using SIPrCuOTf or SIPrCuF	162
Figure 6. Product Yield over Time with Varying Concentrations of Alkyne	163
Figure 7. Product Yield over Time with Varying Concentrations of TMDSO.....	164
Figure 8. Product Yield over Time With Varying Concentration of Alkyl Triflate.	165

List of Schemes

Scheme 1. Synthetic Approach to Cyclic Ether Synthesis.....	18
Scheme 2. Enantioselective Rh-Catalyzed 1,6-Addition of Aryltitanates to Enynes	20
Scheme 3. Selected Examples of General Asymmetric Allene Synthesis	21
Scheme 4. Reactivity of Copper (I) Salts with a) Grignard Reagents and b) Organoboron/NaO <i>t</i> Bu	22
Scheme 5. Propargylic Phosphate Isomerization	24
Scheme 6. Absolute Stereochemical Assignment	27
Scheme 7. Proposed Mechanism of Propargylic Substitution	28
Scheme 8. Mechanistic Proposals for Boron-to-Copper Transmetalation	29
Scheme 9. ¹¹ B NMR Experiments.....	30
Scheme 10. Reactivity of Potassium Borate in the Catalytic Reaction.....	31
Scheme 11. Reactivity of ICyCuMe.....	32
Scheme 12. Use of ICyCuMe as a Catalyst	32
Scheme 13. Selected Example of Asymmetric <i>endo</i> -Selective Cyclic Ether Synthesis	55
Scheme 14. Gold-Catalyzed <i>exo</i> -Selective Cyclization of Alleneol.	56
Scheme 15. Synthesis of Enantioenriched Trisubstituted Allenols.....	56
Scheme 16. First Attempt at Enantioenriched Cyclic Ether Synthesis	57
Scheme 17. Experiment Showing Allene Racemization Before Cyclization	57
Scheme 18. Mechanism of Cyclic Ether Formation.....	63
Scheme 19. Protonation of Alkenyl Gold with Mono-methylterephthalic Acid.	66
Scheme 20. Catalytic Competency of Vinyl Gold Intermediate	67
Scheme 21. Kinetic Isotope Effect Experiment.	67
Scheme 22. Copper-Catalyzed Hydrofunctionalization of Alkynes	92
Scheme 23. Stoichiometric Hydrometallation Followed by Bromination	94
Scheme 24. Alkyne Semireduction and Hydrobromination.....	95
Scheme 25. Alkyne Semireduction Mechanism.....	96
Scheme 26. Proposed Catalytic Cycle of Hydrobromination of Alkynes	96
Scheme 27. Initial Attempts at Catalytic Hydrobromination of Alkynes	98
Scheme 28. Proposed Background Reactions.....	99
Scheme 29. Transmetalation of IPrCuO(2- <i>t</i> Bu)Ph and Ph ₂ SiH ₂	101
Scheme 30. Scale Up of Hydrobromination Reaction.....	105
Scheme 31. Proposed Catalytic Cycle for Hydrobromination	108
Scheme 32. Conversion of IPrCuCl to IPrCuOAr.....	108
Scheme 33. Bromination of Alkenyl Copper in the Presence of TEMPO.....	108
Scheme 34. Known Alkyne Hydroalkylation Strategies.....	133
Scheme 35. Stoichiometric Alkylation of Alkenyl Copper	134
Scheme 36. First Attempt at Hydroalkylation of Alkynes.....	135
Scheme 37. Copper-Catalyzed Reduction of Alkyl Triflates	135
Scheme 38. Optimization of Hydroalkylation of Alkynes.	136
Scheme 39. Formation of SIPrCuH.....	139
Scheme 40. Proposed Catalytic Cycle of Hydroalkylation of Alkynes	139
Scheme 41. Formation of SIPrCH from SIPrCuF	160

List of Tables

Table 1. Optimization of Asymmetric Allene Synthesis	23
Table 2. Alkylation of Propargylic Phosphates	24
Table 3. Arylation of Propargylic Phosphates	26
Table 4. Optimization of Gold-Catalyzed Allene Hydroalkoxylation	58
Table 5. Asymmetric Synthesis of Tetrahydrofurans and Tetrahydropyrans	59
Table 6. Optimization of Chroman Synthesis	61
Table 7. Scope of Asymmetric Chroman Synthesis	62
Table 8. Stoichiometric Bromination of Alkenyl Copper	97
Table 9. Investigation of Bromoalkyne Formation	100
Table 10. Development of Hydrobromination of Alkynes.....	102
Table 11. Hydrobromination of Alkyl Alkynes	103
Table 12. Hydrobromination of Aryl Acetylenes	105
Table 13. Reaction Parameters for Hydroalkylation of Alkynes.....	136
Table 14. Hydroalkylation of Alkynes Scope	137
Table 15. Hydroalkylation Catalyst Screen.....	143
Table 16. Solvent Screen	143
Table 17. Silane Screen	144
Table 18. Electrophile Screen in Catalytic Reaction	145

Acknowledgements

Behind each graduate student is a network of people who have worked incredibly hard to ensure the success of the student. In my case those people have supported me immensely by showing love and encouragement along the way, sacrificed more than is reasonable, and mentored with great patience.

My Family - Mom and Dad, Thank you for your endless love, support, and sacrifice as I grew up. Thank you for believing in me no matter what I was doing. You are both role model parents and I am indebted to you for life. I can't remember a time when you doubted a goal that I had. Jessie, I have known you longer than anyone and I thank you for your energy, love, support, and, humor, especially as we were both in graduate school and could relate to each other's experiences. Love you forever sister. Helena Yan He, you are a boundless source of joy in my life and I would not be the person that I am today without you. Thank you for understanding when I stayed late at work, or went in early on the weekends. Thank you for encouraging me to always work as hard as I can and for your love.

Prof. Gojko Lalic - Thank you for your patience, trust, energy, and mentorship. You taught me what it means to be a scientist and created an environment where I was able to grow beyond anything I thought was possible. Joining your lab is one of the best decisions I have ever made.

Lalic Lab Coworkers, past and present - A special thanks to Sam Marionni, Nick Cox, Karl Haelsig, Richard Rucker, and Alison Suess who I worked with on various projects. Aaron, Nick, Richard, Alison, Hester, Melrose, Karl, Zoha, Mary, Julia, and Bing Yan thank you for your friendship. My undergrads, Alex, Karl, and Zoha, thanks for your dedication and willingness to work so hard. Best of luck in the future to all of my Lalic Lab coworkers past and present. I hope to stay in contact with all of you.

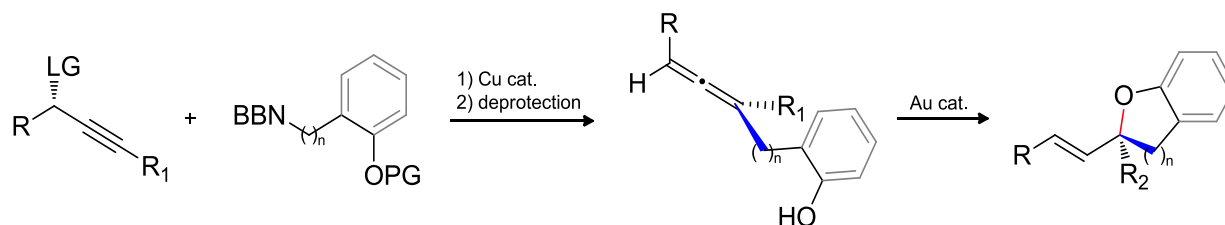
PLU Professors - A special thanks to Dr. Yakelis and Dr. Fryhle. My time at PLU under your guidance inspired me to study organic chemistry and for that I am forever in your debt. Especially important is the time I spent as an undergraduate researcher in Dr. Yakelis's lab. Thanks Dr. Yakelis for the encouragement and support to attend graduate school.

Dedication

To my family for always believing in me and supporting me in everything I do.

Part 1: Asymmetric Synthesis of Cyclic Ethers Containing an α -Tetrasubstituted Stereocenter

The focus of this section is asymmetric synthesis of cyclic ethers containing an α -tetrasubstituted stereocenter. This structural motif is found in many natural products and bioactive compounds. Our synthetic strategy is outlined in Scheme 1. Starting with an enantioenriched propargylic electrophile, copper-catalyzed S_N2' substitution yields an enantioenriched trisubstituted allene (1st transformation, Scheme 1). After deprotection, an enantioenriched cyclic ether containing an α -tetrasubstituted stereocenter is formed through gold catalyzed cyclization. (2nd transformation, Scheme 1). The first transformation will be discussed in Chapter 1 and the second transformation will be discussed in Chapter 2 (Scheme 1).



Scheme 1. Synthetic Approach to Cyclic Ether Synthesis

Chapter 1: Copper-Catalyzed Asymmetric Synthesis of Trisubstituted Allenes

Portions of this chapter as well as figures, schemes, and tables were adapted or reproduced from the following manuscript co-authored by Mycah R. Uehling, Asymmetric Synthesis of Trisubstituted Allenes: Copper-Catalyzed Alkylation and Arylation of Propargylic Phosphates, *Organic Letters*, **2012**, 14, 362. Copyright **2012** American Chemical Society

1.1 Introduction

Allenenes play a prominent role in organic chemistry.¹ Hundreds of natural products that contain the allene structural motif have been identified and allenes have been utilized as enzyme inhibitors, anti-viral agents, cytotoxic agents,² and even as ligands for asymmetric catalysis.³ Allenenes have also been used as substrates in a variety of transformations throughout organic chemistry.⁴

The allene central carbon is sp hybridized and involved in two orthogonal π -bonds to the neighboring carbons (See Figure 1). These π bonds are offset by 90° around the allenic axis. The barrier of rotation about an allene C-C π bond has been noted at 43 Kcal/mol.⁵ Therefore, enantioenriched allenes that can be synthesized usually do not racemize under ambient conditions. This allows for the isolation, storage, and use of enantioenriched allenes as intermediates in asymmetric synthesis.⁶

The method of assigning absolute stereochemistry of allenes is much like the one used to assign the absolute configuration of stereocenters. The substituents on the allene are first ranked according to the Cahn-Ingold-Prelog system. The substituent on the same side as the highest ranked substituent is automatically ranked second. When viewing the allene from the highest ranked substituent end, if moving from the highest ranked substituent to the lowest in the clockwise direction, the allene is assigned R, if counter clockwise, S. The allene drawn in Figure 1 is the R enantiomer.

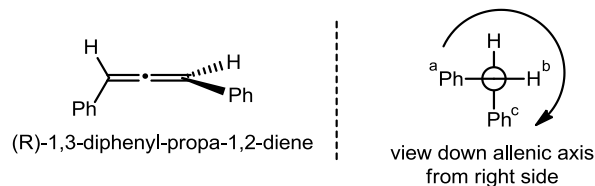
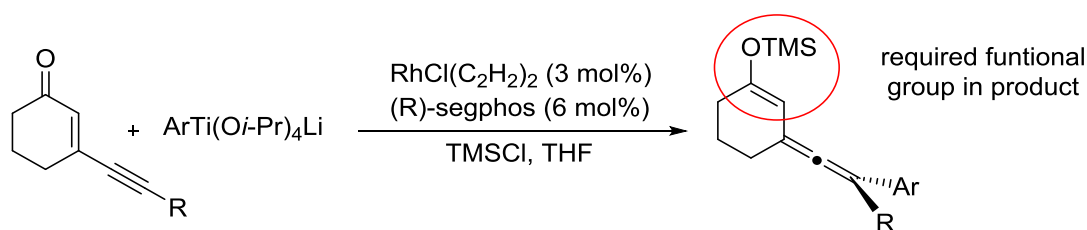


Figure 1. Allene Bonding, Stereochemistry, and Absolute Stereochemical Assignment

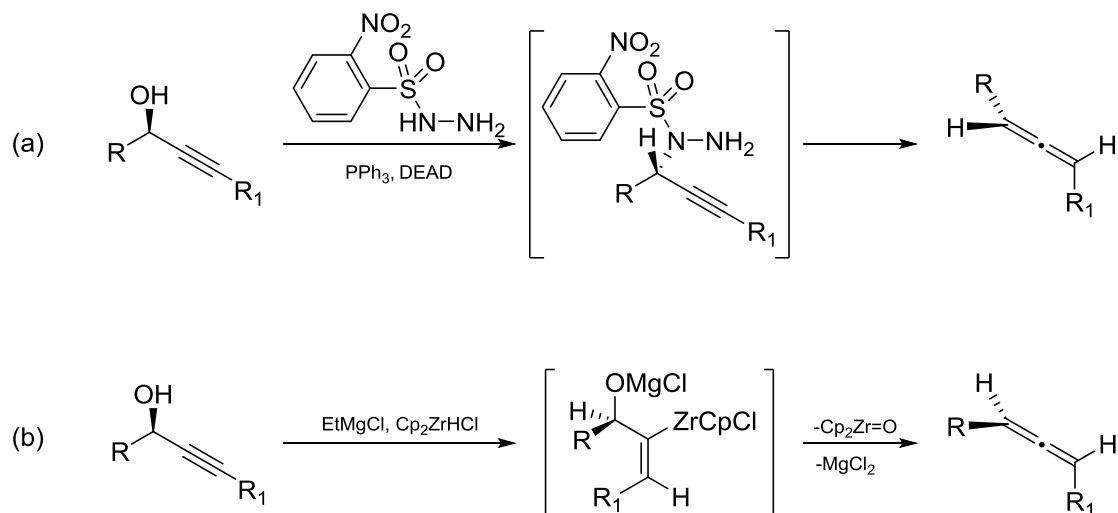
While many strategies for the synthesis of allenes have been developed,⁷ asymmetric synthesis of allenes is still a considerable challenge.⁸ In most cases, asymmetric synthesis of allenes requires that a specific functional group be present in the product.⁹ For example, Hayashi has developed a reaction that can be used to prepare tetrasubstituted¹⁰ enantioenriched allenes based on rhodium catalyzed conjugate addition of aryl titanates to enynones (see Scheme 2).¹¹ The products can be isolated in a highly enantioenriched form. However, only compounds with this general structure where an allene is conjugated to a silyl enol ether are possible.



Scheme 2. Enantioselective Rh-Catalyzed 1,6-Addition of Aryltitanates to Enynones

Two specific examples of asymmetric allene syntheses are worth noting as they are the most general. The first is a reaction that was developed in the Myers lab (see Scheme 3a).¹² Enantioenriched secondary propargylic alcohols can be converted into enantioenriched disubstituted allenes in the presence of a sulfonyl hydrazine reagent, triphenylphosphine, and DEAD. This reaction proceeds via an initial Mitsunobu inversion followed by a rearrangement to form the allene product. The second reaction worth noting is one reported by the Ready lab (see Scheme 3b).¹³ In this work, Ready and coworkers showed that enantioenriched secondary propargylic alcohols can be converted into disubstituted

enantioenriched allenes in the presence of an alkyl Grignard base and Schwartz's reagent. Both of these reactions proceed with high chirality transfer and are compatible with many functional groups. However, they are both limited to the synthesis of disubstituted allenes.

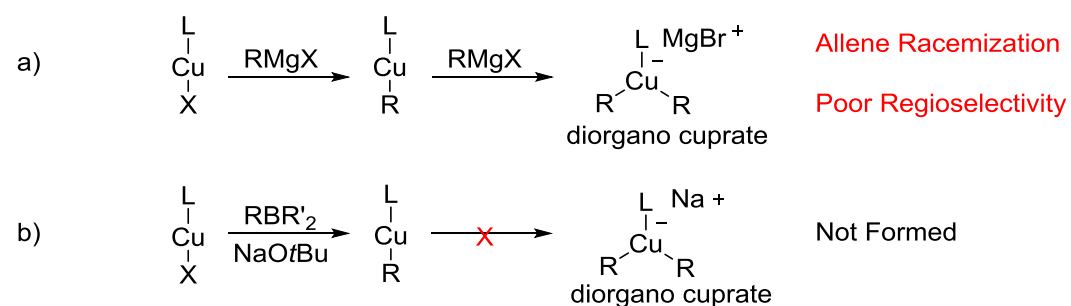


Scheme 3. Selected Examples of General Asymmetric Allene Synthesis

The current limitations of asymmetric allene synthesis are twofold: 1) available methods rely upon pendant functional group reactivity and are therefore not general; 2) most general methods cannot be used to prepare trisubstituted allenes, only disubstituted allenes. To address these limitations, we set out to develop a general synthesis of allenes that can be used to prepare enantioenriched trisubstituted allenes.

We focused on copper-catalyzed substitution of propargylic electrophiles¹⁴ because in this transformation a C-C bond is formed and the reaction has broad scope.¹⁵ In addition, the starting materials are readily or commercially available. Most asymmetric reactions of this type are based on chirality transfer¹⁶ from an enantioenriched propargylic electrophile to an enantioenriched allene. Asymmetric allene synthesis using the propargylic substitution reaction has been limited to the use of terminal propargylic substrates,¹⁷ substrates that have a pendant alkoxy group,¹⁸ or to electrophiles with cyclic leaving groups such as lactones¹⁹ or carbonates.²⁰

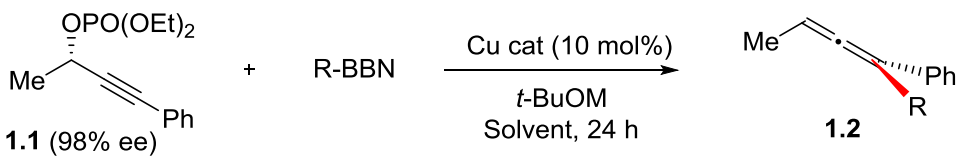
The most common carbon nucleophiles used in copper-catalyzed propargylic substitution reactions are Grignard and organolithium reagents. These highly reactive nucleophiles react with copper to form organocuprates before propargylic substitution (Scheme 4a). In the context of asymmetric allene synthesis, organocuprates are known to cause problems such as allene racemization²¹ and low regioselectivity.²² In addition, small changes in the type of electrophile, nucleophile, and leaving group have been observed to affect regio- and stereoselectivity. One way to avoid the problems associated with organocuprates is to use a milder, less reactive organometallic reagent that might be less likely to form cuprates. In 2010, our group developed boron-to-copper transmetalation as a mild way to form catalytic amounts of organocopper (Scheme 4b).²³ We speculated that the formation of organocuprates might be slower when using organoboron nucleophiles because they are much less basic than Grignard reagents and that the use of organoboron reagents might help solve the problems associated with asymmetric copper-catalyzed propargylic substitution, allene racemization and poor regioselectivity. We set out to develop a copper catalyzed S_N2' substitution of enantioenriched propargylic electrophiles utilizing boron-to-copper transmetalation.



Scheme 4. Reactivity of Copper (I) Salts with a) Grignard Reagents and b) Organoboron/NaOtBu

1.2 Reaction Optimization

Our first experiment during reaction development was to take phosphate **1.1** and subject it to reaction conditions that were developed for allylic chloride arylation²⁴ (Table 1, entry 1). The allene product **1.2** was formed in modest yield and poor chirality transfer.

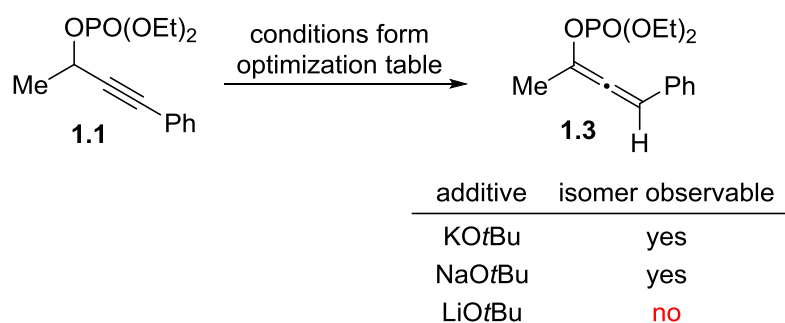
Table 1. Optimization of Asymmetric Allene Synthesis


entry ^{a,b}	catalyst	t (°C)	solvent	M	yield	ee
1	IMesCuOt-Bu	60	1,4-dioxane	Na	45%	30%
2	IPrCuCl	60	1,4-dioxane	Na	35%	26%
3	IMeCuCl	60	1,4-dioxane	Na	33%	29%
4	It-BuCuCl	60	1,4-dioxane	Na	16%	37%
5	ICyCuCl	60	1,4-dioxane	Na	79%	30%
6	ICyCuCl	60	pentane	Na	47%	81%
7	ICyCuCl	35	1,4-dioxane	Li	86%	94%
8	ICyCuCl	35	pentane	Li	95%	96%
9 ^c	ICyCuCl	35	pentane	Li	34%	96%
10 ^d	ICyCuCl	35	pentane	Li	75%	96%
11 ^e	ICyCuCl	35	pentane	Li	93%	41%

R = (CH₂)₄Ph, a) alkyl borane prepared in 1,4-dioxane (1.0 M, 60 °C, 12 h) from 4-phenyl-1-butene (1.5 equiv) and 9-BBN (1.5 equiv), b) phosphate (1.0 equiv), *t*-BuOM (1.0 equiv), c) 2.5 mol% ICyCuCl, d) 1.3 equiv alkyl borane, e) 1.5 equivalents LiOtBu

However, we were optimistic when we discovered that only the allene regioisomer was observable by GC/MS in the crude reaction mixture. This observation validated our strategy of using organoboron nucleophiles to avoid the formation of organocuprates allowing for a highly regioselective propargylic substitution. We found that the NHC ligand on copper has a substantial influence on yield (Table 1, Entries 1-5). This is most likely a steric effect as the NHC ligands listed in Table 1 are similar electron donors.²⁵ We observed that changing the solvent to pentane allowed for a considerable increase in chirality transfer (Table 1, Entry 6). However the yield was diminished. In some cases, where the yield was lower (Table 1, Entries 1-6), we observed that the allenic phosphate **1.3**²⁶ was being formed under the reaction conditions, and this byproduct accounted for the missing mass balance of phosphate starting material (Scheme 5). Remarkably, we found that this background reaction can be effectively turned off by

using LiOtBu as the additive for transmetalation instead of NaOtBu (Table 1, Entry 8, Scheme 5). We observed that the reaction yield is sensitive to catalyst loading (Table 1, entry 9) and equivalents of alkylborane used (Table 1, entry 10). Lastly, if excess LiOtBu was used, the enantioselectivity was diminished (Table 1, entry 11).²⁷

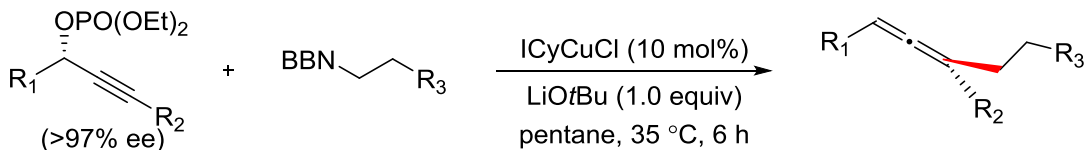


Scheme 5. Propargylic Phosphate Isomerization

1.3 Scope

Our next objective was to explore the scope of the reaction (Table 2). Using the developed reaction as shown in Table 1 entry 8, we were able to prepare allenes containing various functional groups such as silyl ethers, alkyl and aryl ethers, alkyl chlorides, thioacetals,²⁸ aryl bromides, and esters. In addition, 1,1-disubstituted alkenes can be used as coupling partners (Table 2, entry 5). All of the products were isolated as one regioisomer with high chirality transfer. Even propargylic phosphates that are sterically biased against S_N2' substitution work well in the developed reaction (Table 2, entries 6-10). Lastly, propargylic phosphates where the alkyne terminus is silylated also work as substrates (Table 2, entries 9-10).²⁹

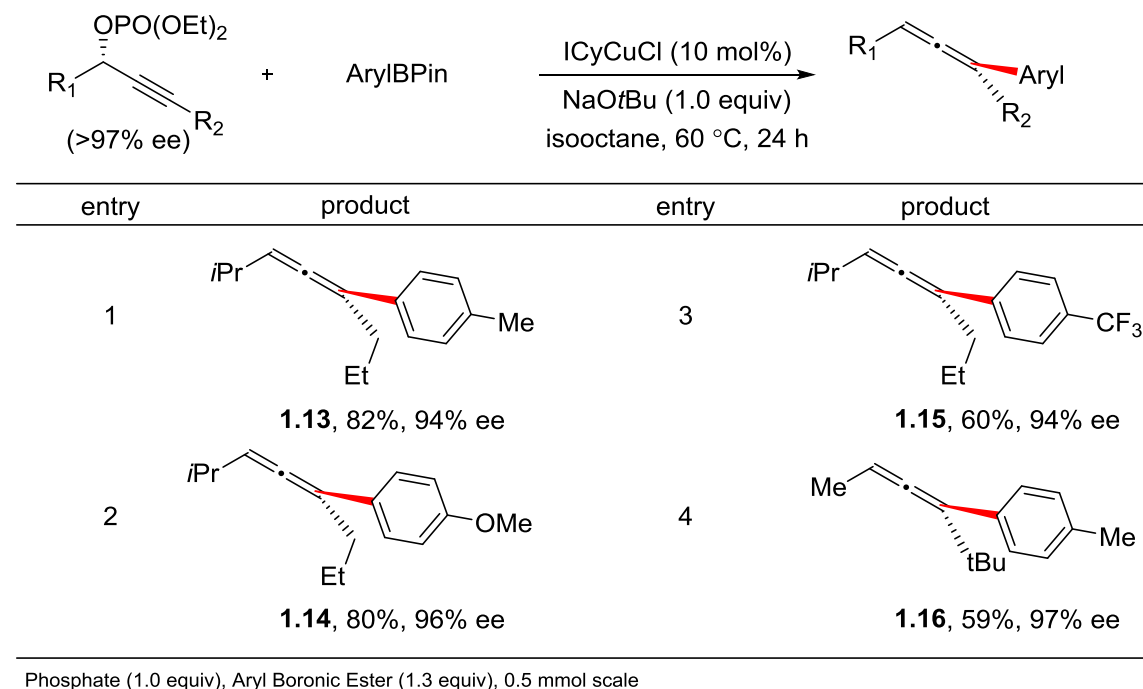
Table 2. Alkylation of Propargylic Phosphates



entry	product	entry	product
1	<p>1.2, 93%, 96% ee</p>	6	<p>1.8, 51%, 96% ee</p>
2	<p>1.4, 80%, 96% ee</p>	7	<p>1.9, 78%, 97% ee</p>
3	<p>1.5, 85%, 94% ee</p>	8	<p>1.10, 83%, 96% ee</p>
4	<p>1.6, 76%, 98% ee</p>	9	<p>1.11, 77%, 97% ee</p>
5	<p>1.7, 75%, 96% ee</p>	10	<p>1.12, 78%, 98% ee</p>

alkyl borane prepared in 1,4-dioxane (1.0 M, 60 °C, 12 h) from terminal alkene (1.5 equiv) and 9-BBN (1.5 equiv)

In addition to propargylic alkylation, we also developed a propargylic arylation using related reaction conditions (Table 3). We found that both electron rich and electron poor arylboronic esters can be used as nucleophiles and the allene products are formed in high yield, excellent regioselectivity, and as one regioisomer. Even with a sterically biased substrate, the allene product is obtained as one regioisomer (Table 3, entry 4).

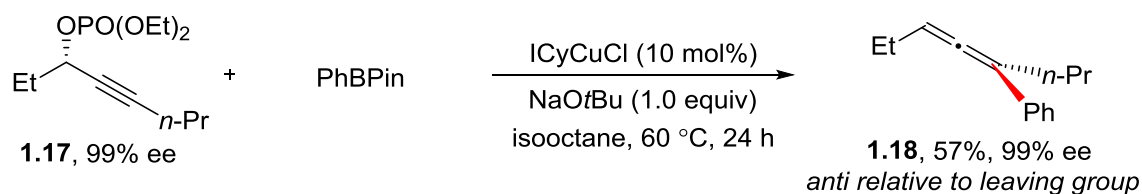
Table 3. Arylation of Propargylic Phosphates

This is the first example of a Cu-catalyzed arylation of propargylic substrates that is S_N2' -selective.^{30,31} In addition, this is the first example of propargylic arylation that proceeds with greater than 95% chirality transfer, except for a report from 2004 where one example is presented.³² Overall, the development of this copper-catalyzed propargylic substitution using organoboron nucleophiles has greatly expanded the scope of enantioenriched trisubstituted allene synthesis.

1.4 Mechanism Studies

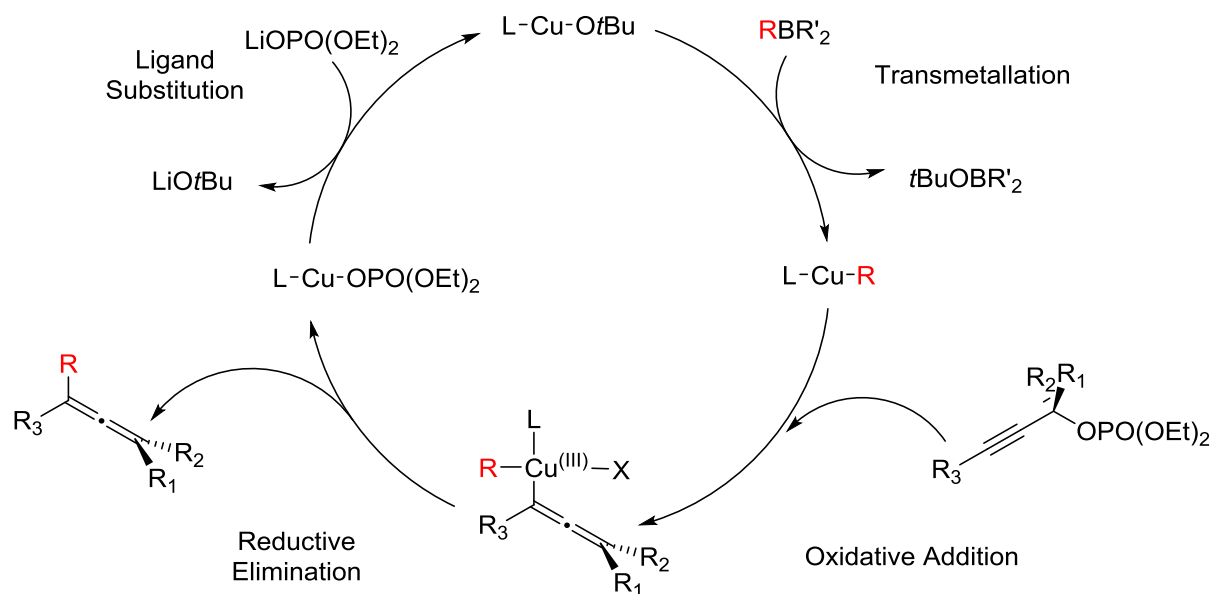
In propargylic and allylic substitutions, usually the anti-pathway is dominant,³³ unless there is an energetically favorable interaction between the leaving group and incoming nucleophile. We performed an experiment to probe the stereoselectivity in this propargylic substitution to see if the reaction proceeds with *syn* or *anti* stereoselectivity relative to the leaving group (Scheme 6). When the phosphate **1.17** was allowed to react with the pinacol phenyl boronic ester under standard conditions, the allene **1.18** was formed in 57% yield and 99% ee. This allene is a known compound³⁴ and the optical rotation of the compound synthesized with our method matched the literature value in both sign and magnitude, when

measured in the same solvent at the same concentration. Therefore, the reaction proceeds with *anti* stereoselectivity.



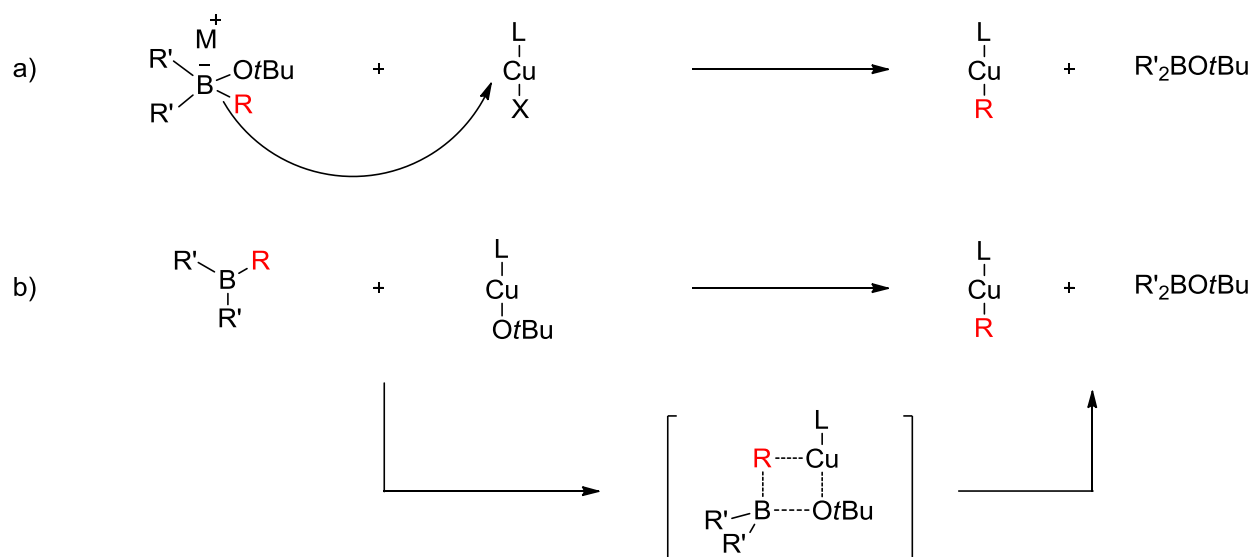
Scheme 6. Absolute Stereochemical Assignment

Based on previous reactions developed around boron-to-copper transmetalation reported by our lab³⁵ and others,³⁶ we propose that the mechanism of propargylic substitution proceeds as outlined in Scheme 7. In the first step, a copper(I) alkoxide undergoes transmetalation with an organoboron reagent to form the organometallic nucleophile. The organocopper intermediate is able to react with a propargylic phosphate to form an allenyl copper(III) complex through oxidative addition. Copper(III) formation has been shown in the context of similar allylic substitution reactions,³⁷ but to the best of our knowledge, has never been observed in the context of propargylic substitution. Reductive elimination gives the product and a ligated copper(I) phosphate. Finally, ligand substitution of the copper(I) phosphate with LiOtBu forms the catalyst.³⁸



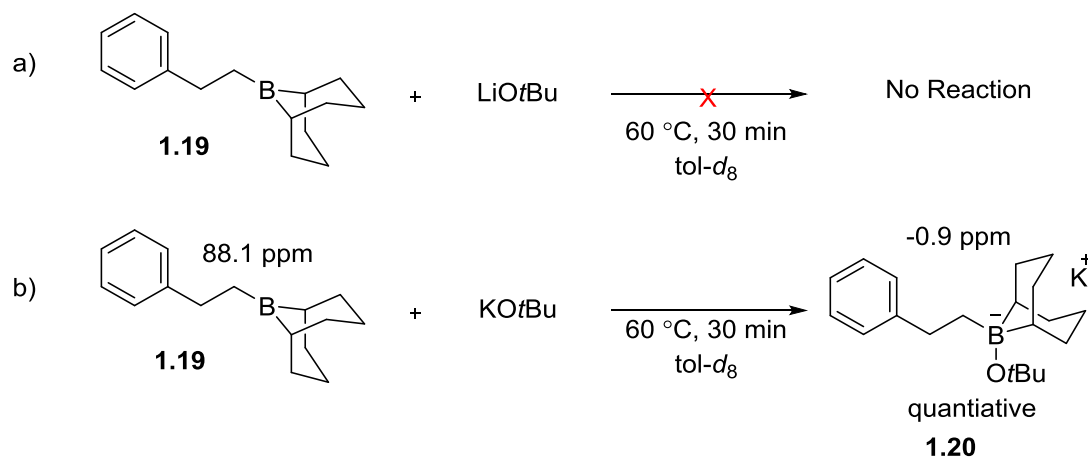
Scheme 7. Proposed Mechanism of Propargylic Substitution

While boron-to-copper transmetallation is now common in the literature, it is still not agreed upon through which mechanism the transmetallation reaction takes place.³⁹ Even among papers published from the same group, multiple mechanisms for boron-to-copper transmetallation have been proposed.⁴⁰ In analogy to boron-to-palladium transmetallation,⁴¹ two basic mechanisms have been put forward (Scheme 8). The first mechanism is one where the organoboron reagent reacts with the additive to form a borate. The borate then acts as a nucleophile to form the organocopper (Scheme 8a). Alternatively, it has been proposed that a copper alkoxide and trivalent organoboron react through a sigma bond metathesis to form organocopper (see Scheme 8b).



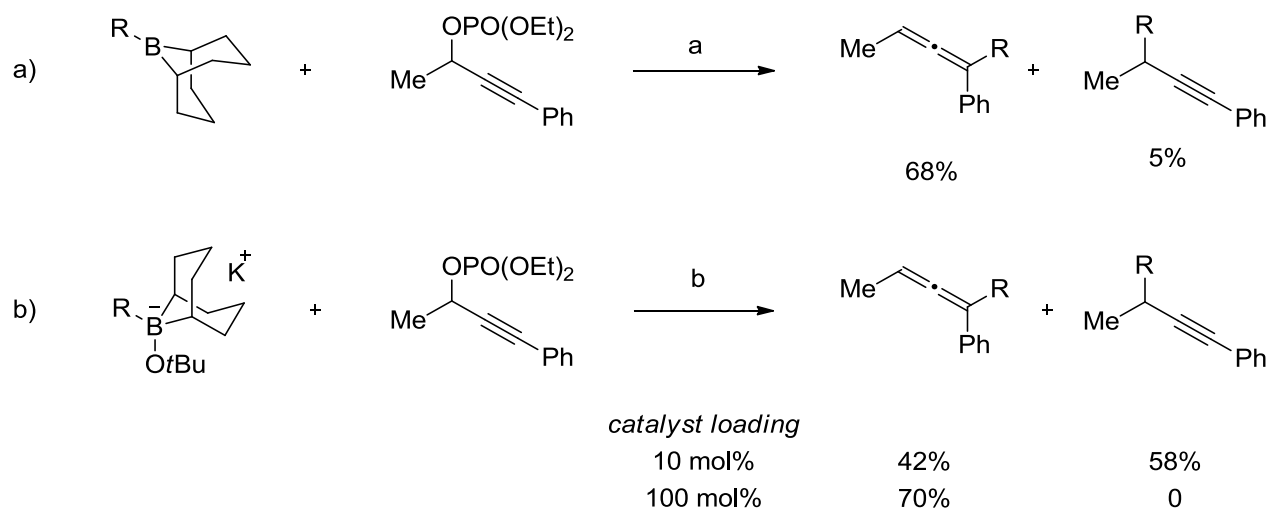
Scheme 8. Mechanistic Proposals for Boron-to-Copper Transmetallation

In an effort to understand the elementary step of boron-to-copper transmetallation, both in the context of this reaction, and others where boron-to-copper transmetallation is invoked, we performed the following mechanistic experiments. In the first experiment, we sought to understand which boron species is most abundant in solution in the presence of different alkoxide additives. We allowed trialkylborane **1.19** to react with one equivalent of either LiO*t*Bu or KO*t*Bu in toluene-*d*₈ for thirty minutes at 60 °C, then monitored the reactions by ¹¹B NMR.⁴² In the case of LiO*t*Bu, no borate was observable (Scheme 9). It is not clear if that is because the reaction is too slow or if the reaction is unfavorable. However, in the case of KO*t*Bu, only the potassium borate **1.20** was observable and no free trialkylborane was present. These results suggest that the most abundant species in the catalytic reaction, where LiO*t*Bu is used to promote transmetallation, is probably a free organoboron species, and not a lithium borate. Therefore, we propose that transmetallation proceeds through a free organoboron species and a copper alkoxide similar to the reaction drawn in Scheme 8b. However, it is possible that when using LiO*t*Bu, a fast equilibrium is established where a small amount of borate is present that is undetectable using NMR and this borate is responsible for transmetallation in the catalytic reaction.



Scheme 9. ^{11}B NMR Experiments

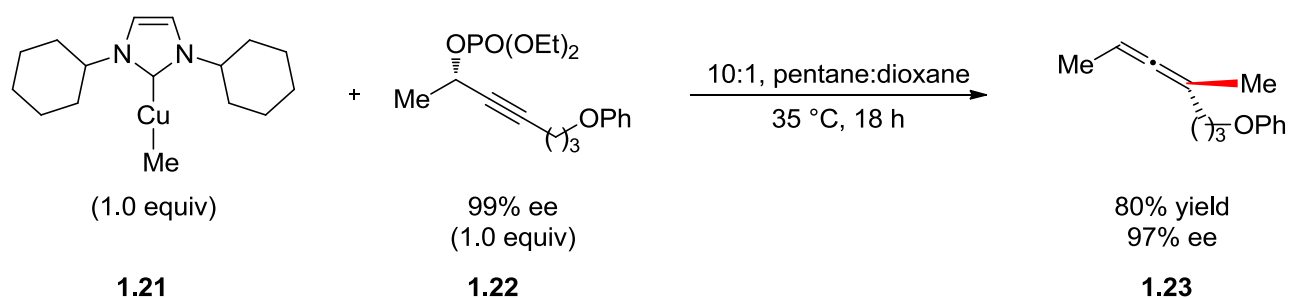
To investigate the possibility of this scenario, we performed the following experiments. In the first experiment, the cross coupling reaction was conducted in the usual manner, except that LiOtBu was replaced with KOtBu . In this reaction, the dominant product was the allene (Scheme 10a). When a similar reaction was performed using a preformed potassium borate, the product ratio of regioisomers was near 1:1 (Scheme 10b),⁴³ much different than the product ratio observed in the optimized reaction. In addition, only the allene **1.2** is formed when a stoichiometric amount of copper is used, implying that organoboron compounds might form cuprates under certain reaction conditions. Based on these observations, we propose that transmetalation in the propargylic substitution reaction proceeds through a free organoboron intermediate and not a borate because the regioselectivity observed in the catalytic reaction is closest to that observed when using a free organoboron reagent as shown in Scheme 10a. Overall, these results suggest that transmetalation can occur through multiple pathways and the outcome of the reaction may depend upon which organoboron species is used.



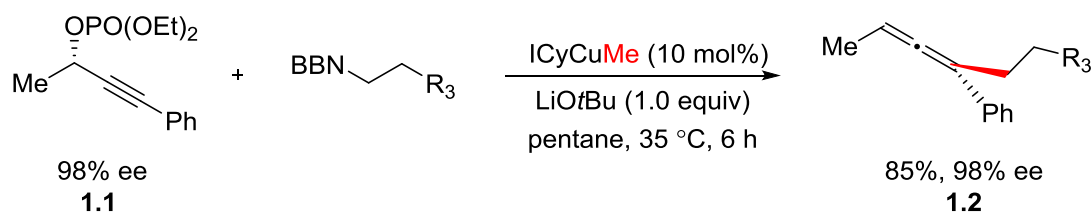
R = (CH₂)₄Ph, a) 1.5 equiv trialkylborane, 1.0 equiv phosphate, 1.0 equiv KOtBu, 10 mol% ICyCuCl, pentane, 35 °C, 24 h b) 1.0 equiv borate, 1.0 equiv phosphate, ICyCuCl, pentane, 35 °C, 24 h.

Scheme 10. Reactivity of Potassium Borate in the Catalytic Reaction

To provide support for the organocopper intermediate⁴⁴ in the proposed catalytic cycle, ICyCuMe (**1.21**) was synthesized and tested in a stoichiometric reaction with enantioenriched phosphate. The allene **1.23** was formed in 80% yield and 97% ee after 18 h (Scheme 11). This stoichiometric reaction provides support for the proposed step in the catalytic cycle where the organocopper intermediate reacts with a propargylic phosphate. In addition, when this complex was used as a catalyst under the optimized reaction conditions, the reaction outcome matched that of the catalytic reaction (Scheme 12). One observation worth noting is that the rate of the stoichiometric reaction between ICyCuMe (**1.21**) and phosphate **1.22** is much lower than the catalytic one. The catalytic reactions were done after six hours. The stoichiometric reaction proceeded to 80% yield after 18 hours and was not done after 6 hours. Based on this observation it is possible that the active nucleophile in the propargylic substitution is a more complicated species such as an alkoxyorganocuprate or maybe the Li from LiOtBu acts as a Lewis acid to activate the phosphate.



Scheme 11. Reactivity of ICyCuMe



alkyl borane prepared in 1,4-dioxane (1.0 M, 60 °C, 12 h) from terminal alkene (1.5 equiv) and 9-BBN (1.5 equiv)

Scheme 12. Use of ICyCuMe as a Catalyst

1.5 Conclusion

We have developed a practical method for the asymmetric synthesis of trisubstituted allenes based on copper-catalyzed substitution of propargylic electrophiles. The developed reaction proceeds with good to excellent yield, excellent regioselectivity, and high chirality transfer. The reaction is compatible with many functional groups and both propargylic alkylation and arylation are now possible. The key to the success of the reaction is to use boron-to-copper transmetallation as a mild way to form an organocopper intermediate and avoid the formation of diorganocuprates, which have previously been shown to cause low regioselectivity and low chirality transfer in propargylic substitution reactions. In addition, the use of organoboron along with a reagent for transmetallation is a mild alternative to adding a more traditional organometallic reagent such as a Grignard or organolithium. The mildness of this approach allows for reactions developed using boron-to-copper transmetallation to have a broad scope.

1.6 Experimental

1.6.1 General Information

All reactions were performed under a nitrogen atmosphere, using flame-dried glassware unless otherwise indicated. Column chromatography was performed on a Biotage Iso-1SV flash purification system using silica gel (Agela Technologies Inc., 60Å, 40-60 µm, 230-400 mesh). Infrared (IR) spectra were recorded on a Perkin Elmer Spectrum RX I spectrometer. IR peak absorbencies are represented as follows: s = strong, m = medium, w = weak, br = broad. ¹H and ¹³C NMR spectra were recorded on a Bruker AV-300 or AV-500 spectrometer. ¹H NMR chemical shifts (δ) are reported in parts per million (ppm) downfield of TMS and are referenced relative to residual CHCl₃ (7.26 ppm), C₆H₆ (7.16 ppm), or CH₂Cl₂ (5.32 ppm). ¹³C chemical shifts are reported in parts per million downfield of TMS and are referenced to the carbon resonance of the solvent CDCl₃ (δ 77.2 ppm), C₆D₆ (128.4), CD₂Cl₂ (54.0). Data are represented as follows: chemical shift, multiplicity (s = singlet, d = doublet, t = triplet, q = quartet, m = multiplet), integration, and coupling constants in Hertz (Hz). Mass spectra were collected on a JEOL HX-110 Mass spectrometer, a Bruker Esquire 1100 Liquid Chromatograph – Ion Trap Mass Spectrometer, or a Hewlett Packard 5971A gas chromatograph – Mass Spectrometer. Chiral GC analysis was performed on a Shimadzu GC-2010 with a flame ionization detector and a Supelco Beta DEXTM 120 column (30 m x 0.25 mm x 0.25 µm). Chiral HPLC analysis was performed on a Shimadzu LC-6AD with a SPD-20A UV/Vis-detector and a Daicel Chiralcel OD-H column (.46 cm x 25 cm).

1.6.2 Materials

THF, CH₂Cl₂, Et₂O and toluene were degassed and dried on columns of neutral alumina. 1,4-dioxane was distilled from purple Na/benzophenone ketyl, and stored over 4Å molecular sieves. Deuterated solvents were purchased from Cambridge Isotope Laboratories, Inc. 1,4-Dioxane-*d*8 was distilled from purple Na/benzophenone ketyl. All other deuterated solvents were degassed, and dried over 4Å molecular sieves.

Commercial reagents were purchased from Sigma-Aldrich Co., VWR international, LLC., or STREM Chemicals, Inc., and were used as received.

1.6.3 Synthesis of Propargylic Alcohols

4-phenylbut-3-yn-2-ol (**1.24**), 5-dimethylhex-3-yn-2-ol (**1.25**), 6-methylhept-4-yn-3-ol (**1.26**), 2-methyloct-4-yn-3-ol (**1.27**), 1-(trimethylsilyl)pent-1-yn-3-ol (**1.28**), and octa-4-yne-3-ol (**1.29**) were all synthesized according to literature procedure.⁴⁵

1.6.4 Chiral Resolution of Propargylic Alcohols

General procedure for chiral resolution⁴⁶:

An air-free reaction flask was flame dried under vacuum, allowed to cool under nitrogen, and charged with a stir bar and Novozyme (100mg/10 mmols alcohol). The flask was filled with 28 mL vinylacetate. To the flask was added 1-phenyl-2-butyn-3-ol (4.14 g, 28.3 mmols). The flask was then heated at 60 °C with gentle stirring. The reaction progress was monitored by chiral HPLC or chiral GC. After the alcohol was enantioenriched to a satisfactory level, the whole reaction mixture was filtered through a plug of celite. The celite plug was washed with copious CH₂Cl₂. The solution was concentrated and the crude products were purified by silica gel column chromatography (0 → 30% EtOAc/Hex).

1.6.5 Characterization Data for Propargylic Alcohols

(S)-4-phenylbut-3-yn-2-ol (1.30), (98% ee): Compound isolated as a yellow oil (2.6 g, 39% yield). Spectral data match the previously reported values.⁴⁷ ¹H NMR (300 MHz, C₆D₆) δ 7.42 (m, 2H), 6.97 (m, 3H), 4.74 – 4.27 (m, 1H), 1.51 (d, *J* = 5.0 Hz, 1H), 1.33 (d, *J* = 6.6 Hz, 3H). The optical purity was determined by chiral HPLC analysis. Chiralcel OD-H HPLC column, 4% IPA/Hex, 1 ml/min, 254 nm detection, *t*_{minor} = 8.4 minutes, *t*_{major} = 19.8 minutes.

(S)-5,5-dimethylhex-3-yn-2-ol (1.31), (98% ee): Compound isolated as a clear oil (0.9 g, 28% yield). Spectral data matches the previously reported values.⁴⁸ ¹H NMR (300 MHz, C₆D₆) δ 4.33 (q, *J* = 6.5 Hz, 1H), 1.28 (m, 4H), 1.17 (s, 9H). The optical purity was determined by chiral GC analysis. Supelco Beta

DEX 120 GC column, 75 °C (21 min), ramp to 90 °C at 4 °C/min, 90 °C (10 min.), $t_{\text{minor}} = 20.9$ minutes, $t_{\text{major}} = 21.2$ minutes.

(S)-6-methylhept-4-yn-3-ol (1.32), (97% ee): Compound isolated as a clear oil (1.0 g, 31% yield). ^1H NMR (300 MHz, C_6D_6) δ 4.17 (dd, $J = 10.8, 4.9$ Hz, 1H), 2.50 – 2.31 (m, 1H), 1.72 – 1.50 (m, 2H), 1.27 (m, 1H), 1.04 (d, $J = 6.9$ Hz, 6H), 0.94 (t, $J = 7.4$ Hz, 3H). The optical purity was determined by chiral GC analysis. Supelco Beta DEX 120 GC column, 75 °C (30 min), ramp to 90 °C at 4 °C/min, 90 °C (10 min), $t_{\text{minor}} = 31.3$ minutes, $t_{\text{major}} = 32.4$ minutes.

(R)-2-methyloct-4-yn-3-ol (1.33), (97% ee): Compound isolated as a clear oil (1.0 g, 40% yield). $[\alpha]_{\text{D}}^{23} = 2.6^\circ$ ($c = 1.0$, CH_2Cl_2) ^1H NMR (300 MHz, C_6D_6) δ 4.06 (d, $J = 3.4$ Hz, 1H), 1.98 (td, $J = 7.0, 2.0$ Hz, 2H), 1.79 (m, 1H), 1.45 – 1.25 (m, 3H), 1.00 (dd, $J = 17.8, 6.7$ Hz, 6H), 0.86 (t, $J = 7.3$ Hz, 3H). ^{13}C NMR (75 MHz, CDCl_3) δ 86.21, 80.08, 68.29, 34.81, 22.29, 20.81, 18.27, 17.55, 13.61. GC/MS calculated for $[\text{M}]^+$ 140, found 140. FTIR (neat, cm^{-1}): 3362 (br), 2690 (s), 1464 (m), 1381 (m), 1024 (s). The optical purity was determined by chiral GC analysis. Supelco Beta DEX 120 GC column, 80 °C (60 min), ramp to 85 °C at 0.2 °C/min, ramp to 190 °C at 4 °C/min, $t_{\text{minor}} = 60.8$ minutes, $t_{\text{major}} = 62.5$ minutes.

(S)-1-(trimethylsilyl)pent-1-yn-3-ol (1.34), (>99% ee): Compound isolated as a clear oil (1.6 g, 33% yield). Spectral data matches the previously reported values.⁴⁹ ^1H NMR (300 MHz, CDCl_3) δ 4.21 (t, $J = 6.4$ Hz, 1H), 1.99 – 1.39 (m, 3H), 0.91 (t, $J = 7.4$ Hz, 3H), 0.07 (s, 9H). The optical purity was determined by chiral GC analysis. Supelco Beta DEX 120 GC column, 50 °C (60 minutes), ramp to 80 °C at 0.15 °C/min, ramp to 160 °C at 4 °C/min. $t_{\text{major}} = 178.5$ minutes, $t_{\text{minor}} = 180.0$ minutes.

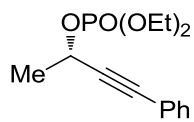
(S)-octa-4-yne-3-ol (1.35), (>99% ee) : Compound isolated as a clear oil (1.0 g, 30%) Spectral data matches previously reported values. $[\alpha]_{\text{D}}^{23} = -8.75^\circ$ ($c = 1.3$, CH_2Cl_2) ^1H NMR (300 MHz, C_6D_6) δ 4.18 (ddd, $J = 6.3, 4.4, 2.0$ Hz, 1H), 1.98 (td, $J = 7.0, 2.0$ Hz, 2H), 1.70 – 1.45 (m, 2H), 1.41 – 1.22 (m, 3H), 0.95 (t, $J = 7.4$ Hz, 3H), 0.86 (t, $J = 7.3$ Hz, 3H). The optical purity was determined by chiral GC analysis.

Supelco Beta DEX 120 GC column, 75 °C (15 minutes), ramp to 88 °C at 0.2 °C/min, ramp to 140 °C at 4 °C/min. $t_{\text{minor}}=54.7$ minutes, $t_{\text{major}}=56.4$ minutes.

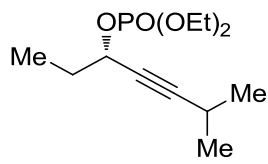
1.6.6 Synthesis of Propargylic Phosphates

An air free reaction flask was charged with a stir bar, flame dried under vacuum, and allowed to cool under nitrogen. Alcohol (1.0 equiv), 4-dimethylaminopyridine (0.1 equiv), dry CH_2Cl_2 , and diethylchlorophosphate (1.25 equiv) were added to the reaction flask. The mixture was cooled to 0 °C and triethylamine (1.2 equiv) was added. The reaction mixture was allowed to warm to room temperature with constant stirring. After consumption of the alcohol starting material the mixture was diluted with diethyl ether and washed with concentrated ammonium chloride three times. The organic phase was then washed with brine, dried with MgSO_4 , and concentrated. The crude material was purified by silica gel chromatography.

1.6.7 Characterization Of Propargylic Phosphates

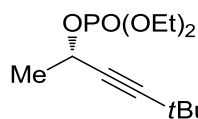


(S)-diethyl (4-phenylbut-3-yn-2-yl) phosphate (1.1) (99% ee): Compound was isolated as a clear yellow oil after purification by silica gel chromatography (20 → 50% EtOAc in hexanes). $[\alpha]_{\text{D}}^{23} = -64^\circ$ ($c = 1.0$, CH_2Cl_2). $^1\text{H NMR}$ (300 MHz, CD_2Cl_2) δ 7.56 – 7.36 (m, 2H), 7.38 – 7.23 (m, 3H), 5.54 – 5.05 (m, 1H), 4.29 – 3.90 (m, 4H), 1.64 (d, $J = 6.6$ Hz, 3H), 1.48 – 1.21 (m, 6H). $^{13}\text{C NMR}$ (75 MHz, CD_2Cl_2) δ 132.04, 129.18, 128.78, 122.49, 87.84 (d, $J = 5.5$ Hz), 85.70, 65.03 (d, $J = 5.4$ Hz), 64.22 (dd, $J = 8.7, 5.9$ Hz), 23.75, 23.67, 16.38, 16.29. HRMS calculated for $[\text{M}+\text{H}]^+$ 283.10998, found 283.10929. FTIR (neat, cm^{-1}): 3055 (w), 2986 (s), 2238 (w), 1490 (s), 1273 (s), 1029 (s), 757 (m).

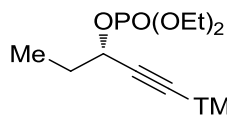


(S)-diethyl (6-methylhept-4-yn-3-yl) phosphate (1.36) (97% ee): Compound was isolated as a clear oil after purification by silica gel chromatography (20 → 50% EtOAc in hexanes).

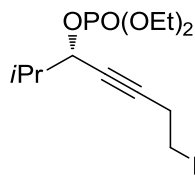
$[\alpha]_D^{22} = -30^\circ$ ($c = 0.56$, CH_2Cl_2). $^1\text{H NMR}$ (300 MHz, C_6D_6) δ 5.22 (m, 1H), 4.11 – 3.90 (m, 4H) minor impurity, 2.36 (dtd, $J = 13.8, 6.8, 1.7$ Hz, 1H), 1.86 – 1.74 (m, 2H), 1.07 (dt, $J = 14.3, 7.1$ Hz, 6H) minor impurity, 0.97 (dd, $J = 12.5, 7.1$ Hz, 9H). $^{13}\text{C NMR}$ (126 MHz, CD_2Cl_2) δ 128.70, 93.06, 77.07 (d, $J = 4.6$ Hz), 69.93 (d, $J = 5.6$ Hz), 64.00 (dd, $J = 11.4, 5.9$ Hz), 30.61, 30.57, 22.94, 20.88, 16.34, 16.29, 9.33. HRMS calculated for $[\text{M}+\text{H}]^+$ 263.14127, found 263.14130. FTIR (neat, cm^{-1}): 3051 (w), 2975 (w), 2250 (w), 1464 (w), 1272 (s), 1035 (2), 995 (s), 735 (m).



(S)-5,5-dimethylhex-3-yn-2-yl diethyl phosphate (1.37) (98% ee): Compound was isolated as a clear oil after purification by silica gel chromatography (20 → 50% EtOAc in hexanes). $[\alpha]_D^{23} = -46^\circ$ ($c = 0.76$, CH_2Cl_2). $^1\text{H NMR}$ (300 MHz, C_6D_6) δ 5.39 – 5.28 (m, 1H), 4.09 – 3.88 (m, 4H), 1.45 (d, $J = 6.5$ Hz, 3H), 1.12 (s, 9H), 1.11 – 0.98 (m, 6H). $^{13}\text{C NMR}$ (126 MHz, CD_2Cl_2) δ 128.71, 94.84, 77.67 (d, $J = 4.7$ Hz), 65.07 (d, $J = 3.5$ Hz), 63.99 (dd, $J = 11.6, 5.6$ Hz), 30.89, 27.64, 24.13, 24.09, 16.35, 16.30. HRMS calculated for $[\text{M}+\text{H}]^+$ 263.14127, found 263.14160. FTIR (neat, cm^{-1}): 3052 (w), 2972 (s), 2243 (w), 1474 (m), 1267 (m), 991 (s), 735 (s).



(S)-diethyl (1-(trimethylsilyl)pent-1-yn-3-yl) phosphate (1.38) (>99% ee): Compound was isolated as a clear oil after purification by silica gel chromatography (20 → 50% EtOAc in hexanes). $[\alpha]_D^{23} = -47^\circ$ ($c = 0.72$, CH_2Cl_2). $^1\text{H NMR}$ (300 MHz, C_6D_6) δ 5.19 (m, 1H), 4.12 – 3.89 (m, 4H), 1.77 (p, $J = 7.1$ Hz, 2H), 1.07 (dt, $J = 18.8, 7.1$ Hz, 6H), 0.94 (t, $J = 7.4$ Hz, 3H), 0.12 (s, 9H). $^{13}\text{C NMR}$ (126 MHz, CD_2Cl_2) δ 128.70, 102.92 (d, $J = 3.9$ Hz), 91.67, 69.72 (d, $J = 5.5$ Hz), 64.13 (dd, $J = 9.9, 5.7$ Hz), 30.25, 30.21, 16.34, 16.29, 9.28, -0.25. HRMS calculated for $[\text{M}+\text{H}]^+$ 293.13382, found 293.13308. FTIR (neat, cm^{-1}): 2977 (s), 2177 (m), 1393 (m), 1277 (s), 1251 (s), 1034 (s), 845 (s), 760 (m).



(S)-diethyl (2-methyloct-4-yn-3-yl) phosphate (1.39) (97% ee): Compound was isolated as a clear oil after purification by silica gel chromatography (20 → 50% EtOAc in hexanes). $[\alpha]_D^{23} = -36^\circ$ ($c = 1.8$, CH_2Cl_2). $^1\text{H NMR}$ (500 MHz, CDCl_3) δ 4.89 – 4.65 (m, 1H), 4.24 – 3.89 (m, 4H), 2.17 (td, $J = 7.0, 1.9$ Hz, 2H), 2.04 – 1.91 (m, 1H), 1.55 – 1.43 (m, 2H), 1.30 (tdd, $J = 7.1, 3.0, 1.0$ Hz, 6H), 0.98 (d, $J = 6.7$ Hz, 3H), 0.94 (t, $J = 6.7$ Hz, 6H). $^{13}\text{C NMR}$ (126 MHz, CDCl_3) δ 128.27 (s), 87.77 (s), 76.26 (d, $J = 3.7$ Hz), 73.55 (d, $J = 6.1$ Hz), 63.61 (dd, $J = 11.7, 5.9$ Hz), 34.04 (d, $J = 6.3$ Hz), 21.92 (s), 20.65 (s), 17.96 (s), 17.13 (s), 16.06 (dd, $J = 7.1, 3.3$ Hz), 13.38 (s). HRMS calculated for $[\text{M}+\text{H}]^+$ 277.15692, found 277.15608. FTIR (neat, cm^{-1}): 3024 (w), 2970 (w), 2250 (w), 1460 (w), 1270 (s), 1040 (2), 100 (s), 721 (m).

1.6.8 Substitution of Propargylic Phosphates

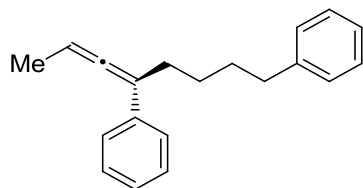
General Alkylation Procedure:

In a glove box a scintillation vial was charged with a stir bar. To the vial was added 9-borabicyclo[3.3.1]nonane (1.6 equiv, 0.77 mmol). An alkene (1.5 equiv, 0.72 mmol) was weighed out in a shell vial and added to the scintillation vial by rinsing with 0.7 mL dioxane. The mixture was heated at 60 °C. After 12 hours, cyclohexene (0.2 equiv, 0.096 mmol) was added and the mixture was heated at 60 °C for 2 hours. To the reaction mixture LiOtBu (0.50 equiv, 0.25 mmol) and ICyCuCl (0.10 equiv, 0.050 mmol) were added. The mixture was diluted to a volume of 7.0 mL with pentane. The enantioenriched phosphate (1.0 equiv, 0.50 mmol) was then added to the reaction mixture. The mixture was heated at 35 °C with stirring for three hours. After three hours another portion of LiOtBu (0.5 equiv, 0.25 mmol) was added and the mixture was heated at 35 °C with stirring. After complete consumption of the phosphate, the mixture was filtered through a plug of silica gel using EtOAc as eluent. The solution was concentrated to yield a thick oil which was loaded onto a silica gel column and purified by flash chromatography.

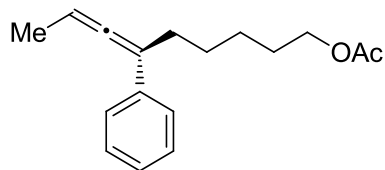
General Arylation Procedure:

In a glove box under a N₂ atmosphere, a scintillation vial was charged with a stir bar. To the vial was added boronic ester (1.25 equiv, 0.625 mmol), sodium tert-pentoxide (1.00 equiv, 0.500 mmol), ICyCuCl (0.10 equiv, 0.025 mmol), the propargylic phosphate (1.00 equiv, 0.500 mmol), and isooctane (2.5 mL). The mixture was stirred at 60 °C for 24 h. The vial was removed from the glove box, diluted with Et₂O, filtered through a plug of silica, concentrated in vacuo, and the crude reaction mixture was purified by silica gel chromatography.

1.6.9 Characterization of Allene Products

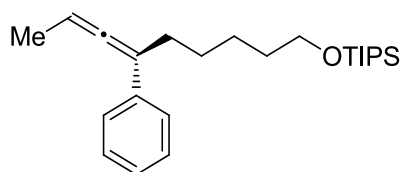


(S)-octa-5,6-diene-1,5-diyldibenzene (1.2): Compound was isolated as a clear oil (123 mg, 93% yield, 96% ee) after purification by silica gel column chromatography (0% → 10% EtOAc/Hex). $[\alpha]_D^{22} = 90.6^\circ$ ($c = 1.4$, CH₂Cl₂). ¹H NMR (300 MHz, CD₂Cl₂) δ 7.40 (d, $J = 7.6$ Hz, 2H), 7.30 (dd, $J = 15.5, 7.6$ Hz, 4H), 7.20 (d, $J = 7.2$ Hz, 4H), 5.55 – 5.37 (m, 1H), 2.66 (t, $J = 7.5$ Hz, 2H), 2.46 (t, $J = 5.5$ Hz, 2H), 1.85 – 1.68 (m, 5H), 1.62 (dd, $J = 14.4, 7.1$ Hz, 2H). ¹³C NMR (75 MHz, CD₂Cl₂) δ 204.96, 143.28, 137.98, 128.77, 128.61, 128.58, 126.70, 126.35, 125.93, 105.28, 89.29, 36.19, 31.63, 30.08, 28.01, 14.56. HRMS calculated for [M]⁺ 262.17217, found 262.17176. FTIR (neat, cm⁻¹): 3082 (w), 2926 (w), 2043 (m), 1944 (m), 1596 (m), 1407 (s), 1435 (m), 745 (s), 694(s). The optical purity was determined by chiral HPLC analysis. Chiralcel OD-H HPLC column, 100 %Hex, 0.9 ml/min, 254 nm detection, $t_{\text{minor}} = 18.1$ minutes, $t_{\text{major}} = 23.0$ minutes.



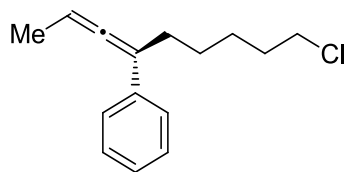
(S)-6-phenylnona-6,7-dien-1-yl acetate (1.4): Compound was isolated as a clear oil (96 mg, 80% yield, 96% ee) after purification by silica gel column chromatography (0% →

10% EtOAc/Hex). $[\alpha]_D^{22} = 101^\circ$ ($c = 0.88$, CH_2Cl_2). $^1\text{H NMR}$ (300 MHz, C_6D_6) δ 7.45 (d, $J = 7.4$ Hz, 2H), 7.21 (t, $J = 7.7$ Hz, 2H), 7.07 (t, $J = 7.3$ Hz, 1H), 5.40 – 5.26 (m, 1H), 3.96 (t, $J = 6.6$ Hz, 2H), 2.30 (m, 2H), 1.69 (s, 3H), 1.59 (d, $J = 7.0$ Hz, 3H), 1.53 – 1.36 (m, 4H), 1.32 – 1.18 (m, $J = 14.0, 8.5, 5.2$ Hz, 2H). $^{13}\text{C NMR}$ (75 MHz, CDCl_3) δ 204.73, 171.36, 137.52, 128.40, 126.50, 126.04, 104.83, 89.06, 64.73, 29.80, 28.62, 27.59, 25.77, 21.13, 14.49. HRMS calculated for $[\text{M}]^+$ 259.17018, found 259.16911. FTIR (neat, cm^{-1}): 3082 (w), 2936 (s), 1945 (m), 1738 (s), 1439 (m), 1365 (m), 1238 (s), 1045 (m). The optical purity was determined by chiral HPLC analysis. Chiralcel OD-H HPLC column, 0.5% IPA/Hex, 0.8 ml/min, 254 nm detection, $t_{\text{minor}} = 11.6$ minutes, $t_{\text{major}} = 14.4$ minutes.



(S)-triisopropyl((6-phenylnona-6,7-dien-1-yl)oxy)silane (1.5):

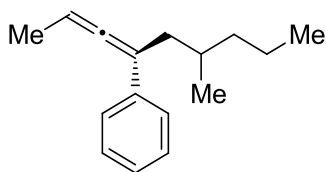
Compound was isolated as a clear oil (146 mg, 85% yield, 94% ee) after purification by silica gel column chromatography (0% → 10% EtOAc/Hex). $[\alpha]_D^{22} = 57^\circ$ ($c = 2.0$, CH_2Cl_2). $^1\text{H NMR}$ (300 MHz, CDCl_3) δ 7.42 (d, $J = 7.7$ Hz, 2H), 7.32 (t, $J = 7.6$ Hz, 2H), 7.20 (t, $J = 7.2$ Hz, 1H), 5.60 – 5.37 (m, 1H), 3.72 (t, $J = 6.4$ Hz, 2H), 2.43 (dd, $J = 10.5, 4.6$ Hz, 2H), 1.79 (d, $J = 7.0$ Hz, 3H), 1.71 – 1.37 (m, 7H) (minor impurity), 1.10 (s, 25H) (minor impurity). $^{13}\text{C NMR}$ (75 MHz, CDCl_3) δ 204.72, 137.60, 128.28, 126.33, 126.00, 105.00, 88.82, 63.49, 33.00, 29.95, 27.84, 25.69, 18.09, 14.42, 12.06. HRMS calculated for $[\text{M}]^+$ 373.29254, found 373.29253. FTIR (neat, cm^{-1}): 3082 (w), 2941 (s), 1946 (m), 1596 (m), 1461 (s), 1382 (m), 1109 (s), 882(s). The optical purity was determined by chiral HPLC analysis. Chiralcel OD-H HPLC column, 100% Hex, 0.8 ml/min, 254 nm detection, $t_{\text{minor}} = 8.2$ minutes, $t_{\text{major}} = 9.5$ minutes.



(S)-(10-chlorodeca-2,3-dien-4-yl)benzene (1.6): Compound was isolated

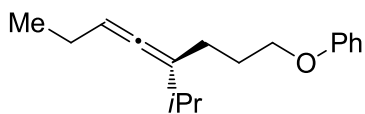
as a clear oil (81 mg, 64% yield, 98% ee) after purification by silica gel column chromatography (0% →

10% EtOAc/Hex). $[\alpha]_D^{22} = 68^\circ$ ($c = 1.6$, CH_2Cl_2). $^1\text{H NMR}$ (300 MHz, CD_2Cl_2) δ 7.40 (dd, $J = 11.0$, 3.6 Hz, 2H), 7.31 (t, $J = 7.6$ Hz, 2H), 7.19 (t, $J = 7.2$ Hz, 1H), 5.63 – 5.38 (m, 1H), 3.56 (t, $J = 6.8$ Hz, 2H), 2.64 – 2.26 (m, 2H), 1.90 – 1.68 (m, 5H), 1.66 – 1.30 (m, 6H). $^{13}\text{C NMR}$ (75 MHz, CD_2Cl_2) δ 204.98, 138.00, 128.63, 126.72, 126.35, 105.31, 89.28, 45.71, 33.12, 30.16, 29.00, 28.14, 27.22, 14.57. HRMS calculated for $[\text{M}]^+$ 248.13315, found 248.13311. FTIR (neat, cm^{-1}): 3081 (w), 2932 (s), 2857 (s), 1945 (m), 1739 (w), 1595 (m), 1492 (s), 1387 (m), 742 (s). The optical purity was determined by chiral HPLC analysis. Chiralcel OD-H HPLC column, 100% Hex, 0.9 ml/min, 254 nm detection, $t_{\text{minor}} = 15.9$ minutes, $t_{\text{major}} = 22.0$ minutes.



((3S)-6-methylnona-2,3-dien-4-yl)benzene (1.7): Compound was isolated

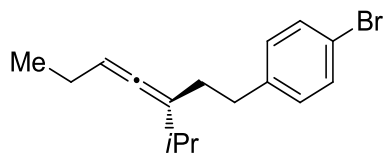
as a clear oil (76 mg, 75% yield, 96% ee) after purification by silica gel column chromatography (0% → 10% EtOAc/Hex). $[\alpha]_D^{22} = 131^\circ$ ($c = 0.56$, CH_2Cl_2). $^1\text{H NMR}$ (300 MHz, C_6D_6) δ 7.49 (d, $J = 7.7$ Hz, 2H), 7.21 (t, $J = 7.7$ Hz, 2H), 7.07 (t, $J = 7.3$ Hz, 1H), 5.55 – 5.11 (m, 1H), 2.55 – 2.38 (m, 1H), 2.29 – 2.11 (m, 1H), 1.85 – 1.70 (m, 1H), 1.61 (d, $J = 7.0$ Hz, 3H), 1.48 – 1.27 (m, 2H), 1.27 – 1.03 (m, 2H), 0.96 (d, $J = 6.6$ Hz, 3H), 0.87 (t, $J = 7.0$ Hz, 3H). $^{13}\text{C NMR}$ (75 MHz, CD_2Cl_2) δ 205.75, 138.19, 128.65, 126.58, 104.20, 88.37, 39.82, 38.51, 31.72, 20.74, 20.55, 20.04, 14.69, 14.55. HRMS calculated for $[\text{M}]^+$ 214.17213, found 214.17285. FTIR (neat, cm^{-1}): 3024 (w), 2955 (w), 2094 (w), 1948 (w), 1596 (w), 1493 (m), 1075 (w), 692 (s). The optical purity was determined by chiral HPLC analysis. Chiralcel OD-H HPLC column, 100% Hex, 0.3 ml/min, 254 nm detection, $t_{\text{minor}} = 18.8$ minutes, $t_{\text{major}} = 20.1$ minutes.



(S)-((4-isopropylocta-4,5-dien-1-yl)oxy)benzene (1.8): Compound was

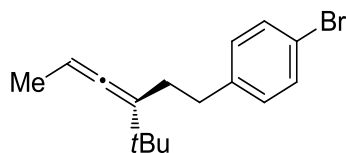
isolated as a clear oil (63 mg, 51% yield, 96% ee) after purification by silica gel column chromatography (0% → 10% EtOAc/Hex). $[\alpha]_D^{22} = -3.6^\circ$ ($c = 0.9$, CH_2Cl_2). $^1\text{H NMR}$ (300 MHz, C_6D_6) δ 7.19 (d, $J = 3.6$ Hz, 2H), 6.90 (m, 3H), 5.40 – 5.11 (m, 1H), 3.77 (t, $J = 6.1$ Hz, 2H), 2.18 – 2.02 (m, 3H), 2.01 – 1.85 (m, 4H),

1.09 (d, $J = 4.6$ Hz, 6H), 1.00 (t, $J = 7.2$ Hz, 3H). ^{13}C NMR (75 MHz, C_6D_6) δ 199.56, 159.81, 129.74, 120.77, 114.83, 111.38, 95.37, 67.46, 31.65, 31.65, 28.15, 27.61, 22.86, 22.26, 22.04, 13.80. GC/MS calculated for $[\text{M}]^+$ 244, found 244. FTIR (neat, cm^{-1}): 3061 (w), 2960 (s), 1955 (m), 1601 (s), 1469 (s), 1687 (m), 1380 (m), 1245 (s), 1042 (s), 752 (s), 690 (s). The optical purity was determined by chiral HPLC analysis. Chiralcel OD-H HPLC column, 100% Hex, 0.3 ml/min, 254 nm detection, $t_{\text{minor}} = 13.2$ minutes, $t_{\text{major}} = 12.6$ minutes.



(S)-1-bromo-4-(3-isopropylhepta-3,4-dien-1-yl)benzene (1.9):

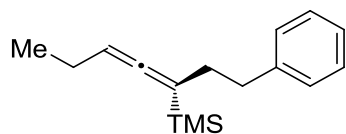
Compound was isolated as a clear oil (117 mg, 78% yield, 97% ee) after purification by silica gel column chromatography (0% to 10% EtOAc/Hex). $[\alpha]_{\text{D}}^{23} = -36^\circ$ ($c = 0.9$, CH_2Cl_2). ^1H NMR (300 MHz, C_6D_6) δ 7.25 (d, $J = 8.3$ Hz, 2H), 6.69 (d, $J = 8.3$ Hz, 2H), 5.26 (m, 1H), 2.54 (t, $J = 7.6$ Hz, 2H), 2.08 (ddd, $J = 9.7, 6.6, 3.1$ Hz, 2H), 2.03 – 1.96 (m, 1H), 1.95 – 1.85 (m, 2H), 1.04 (dd, $J = 6.7, 2.1$ Hz, 6H), 0.94 (t, $J = 7.4$ Hz, 3H). ^{13}C NMR (75 MHz, C_6D_6) δ 199.74, 141.61, 131.59, 130.52, 119.84, 111.23, 96.04, 34.04, 32.79, 31.60, 22.86, 22.24, 22.03, 13.79. HRMS calculated for $[\text{M}]^+$ 292.08229, found 292.08312. FTIR (neat, cm^{-1}): 3062 (w), 2960 (s), 1957 (m), 1890 (w), 1487 (m), 1072 (m), 1011 (m), 804 (m). The optical purity was determined by chiral GC analysis. Supelco Beta DEX 120 GC column, 120 °C (400 minutes), ramp to 200 °C at 1.5 °C/min, 200 °C (4 min). $t_{\text{minor}} = 382.5$ minutes, $t_{\text{major}} = 377.5$ minutes.



(S)-1-bromo-4-(3-(tert-butyl)hexa-3,4-dien-1-yl)benzene (1.10):

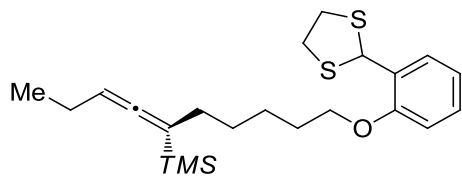
Compound was isolated as a clear oil (124 mg, 83% yield, 96% ee) after purification by silica gel column chromatography (0% to 10% EtOAc/Hex). $[\alpha]_{\text{D}}^{23} = -6.2^\circ$ ($c = 2.1$, CH_2Cl_2). ^1H NMR (300 MHz, CD_2Cl_2) δ 7.39 (d, $J = 8.3$ Hz, 2H), 7.10 (d, $J = 8.2$ Hz, 2H), 5.12 (m, 1H), 2.80 – 2.50 (m, 2H), 2.39 – 2.07 (m, 2H), 1.59 (d, $J = 6.8$ Hz, 3H), 1.03 (s, 9H). ^{13}C NMR (75 MHz, CD_2Cl_2) δ 201.04, 142.44, 131.49, 130.70,

119.46, 112.79, 88.70, 34.31, 33.86, 29.50, 29.00, 15.21. HRMS calculated for $[M]^+$ 292.08229, found 292.08229. FTIR (neat, cm^{-1}): 3085 (w), 1945 (m), 1891 (w), 1776 (w), 1591 (w), 1487 (s), 1360 (m), 1072 (s), 1011 (m), 802 (s). Method: Hold at 120 °C for 300 minutes, then ramp to 200 ° at 1.5 C/min, then hold at 200 for 4 minutes. Column: Supleco Beta-Dex 120. The optical purity was determined by chiral GC analysis. Supelco Beta DEX 120 GC column, 120 °C (300 min), ramp to 200 °C at 1.5 C/min, 200 °: $t_{\text{minor}} = 302.2$ minutes, $t_{\text{major}} = 297.6$ minutes.



(S)-trimethyl(1-phenylhepta-3,4-dien-3-yl)silane (1.11): Compound was

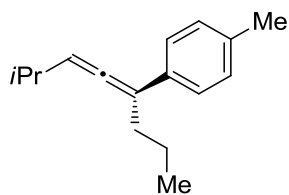
isolated as a clear oil (96 mg, 77% yield, 97% ee) after purification by silica gel column chromatography (0% to 10% EtOAc/Hex). $[\alpha]_{\text{D}}^{22} = 13$ ($c = 0.70$, CH_2Cl_2). $^1\text{H NMR}$ (300 MHz, C_6D_6) δ 7.15 – 7.03 (m, 5H), 4.93 (m, 1H), 2.92 – 2.61 (m, 2H), 2.36 – 2.10 (m, 2H), 2.03 – 1.74 (m, 2H), 0.94 (t, $J = 7.4$ Hz, 3H), 0.10 (s, 9H). $^{13}\text{C NMR}$ (75 MHz, CD_2Cl_2) δ 205.55, 143.18, 128.81, 128.55, 125.98, 97.29, 88.48, 35.92, 31.67, 21.91, 14.11, -1.45. HRMS calculated for $[M]^+$ 244.16471, found 244.16422. FTIR (neat, cm^{-1}): 3026 (w), 2959 (s), 1935 (m), 1603 (w), 1496 (m), 1452 (m), 1247 (s), 9641 (w), 837 (s), 697 (s). The optical purity was determined by chiral HPLC analysis. Chiralcel OD-H HPLC column, 100% Hex, 0.5 ml/min, 254 nm detection, $t_{\text{minor}} = 4.5$ minutes, $t_{\text{major}} = 5.2$ minutes.



(S)-(10-(2-(1,3-dithiolan-2-yl)phenoxy)deca-3,4-dien-5-yl)trimethylsilane (1.12): Compound was isolated as a clear oil (140 mg, 78% yield, 98% ee) after

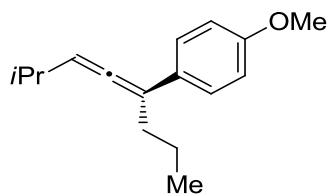
purification by silica gel column chromatography (0% to 10% EtOAc/Hex). $[\alpha]_{\text{D}}^{23} = 8.6^\circ$ ($c = 2.3$, CH_2Cl_2). $^1\text{H NMR}$ (300 MHz, C_6D_6) δ 7.95 (dd, $J = 7.6, 1.5$ Hz, 1H), 7.06 (td, $J = 8.0, 1.6$ Hz, 1H), 6.89 (t, $J = 7.2$ Hz, 1H), 6.54 (d, $J = 8.0$ Hz, 1H), 6.33 (s, 1H), 4.98 (m, 1H), 3.61 (t, $J = 6.3$ Hz, 2H), 2.88 (ddd, $J = 11.5, 8.8, 6.9$ Hz, 2H), 2.78 (ddd, $J = 9.9, 8.8, 6.9$ Hz, 2H), 2.18 – 1.82 (m, 4H), 1.59 (qd, $J = 14.1,$

7.0 Hz, 4H), 1.50 – 1.39 (m, 2H), 1.01 (t, $J = 7.4$ Hz, 3H), 0.18 (s, 9H). ^{13}C NMR (75 MHz, C_6D_6) δ 205.69, 156.61, 128.80, 128.60, 120.65, 111.48, 97.36, 88.05, 68.25, 49.70, 39.40, 29.71, 29.54, 29.37, 26.25, 22.00, 14.33, -1.17. GC/MS calculated for $[\text{M}]^+$ 358, found 358. FTIR (neat, cm^{-1}): 3068 (w), 2928 (s), 1932 (s), 1597 (s), 1486 (s), 1453 (s), 1247 (s), 1101 (s), 863 (s), 751 (s). The optical purity was determined by chiral HPLC analysis. Chiralcel OD-H HPLC column, 100% Hex, 1.5 ml/min, 254 nm detection, $t_{\text{minor}} = 34.2$ minutes, $t_{\text{major}} = 37.1$ minutes.



(R)-2-methyl-5-(4-methylphenyl)-octa-3,4-diene (1.13): Compound was

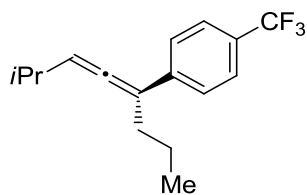
isolated as a clear oil (123 mg, 82% yield, 94% ee) after purification by silica gel column chromatography (5% benzene in hexanes). $[\alpha]_{\text{D}}^{23} = -131^\circ$ ($c = 0.73$, CH_2Cl_2). ^1H NMR (300 MHz, C_6D_6) δ 7.45 (d, $J = 8.2$ Hz, 2H), 7.06 (d, $J = 7.9$ Hz, 2H), 5.49 (dt, $J = 5.9, 3.1$ Hz, 1H), 2.50 – 2.23 (m, 3H), 2.15 (s, 3H), 1.74 – 1.47 (m, 2H), 1.04 (d, $J = 6.8$ Hz, 3H), 0.96 (t, $J = 7.4$ Hz, 3H). ^{13}C NMR (126 MHz, CDCl_3) δ 202.03, 136.03, 134.85, 129.12, 125.81, 106.59, 101.79, 77.41, 77.16, 76.91, 32.42, 28.92, 22.87, 21.46, 21.17, 14.25. HRMS calculated for $[\text{M}]^+$ 214.17213, found 214.17202. FTIR (neat, cm^{-1}): 3085 (w), 3049 (w), 3022 (m), 2958 (s), 1943 (m), 1687 (m), 1608 (m), 1511 (s), 1110 (m), 823 (s). The optical purity was determined by chiral GC analysis. Supelco Beta DEX 120 GC column, 110 $^\circ\text{C}$ (100 min), ramp to 180 $^\circ\text{C}$ at 3 $^\circ\text{C}/\text{min}$, 180 $^\circ\text{C}$ (10 min), $t_{\text{minor}} = 116.7$ minutes, $t_{\text{major}} = 116.4$ minutes.



(R)-2-methyl-5-(4-methoxyphenyl)-octa-3,4-diene (1.14): Compound was

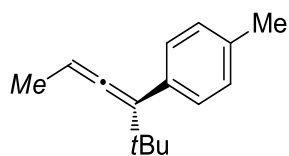
isolated as faint yellow oil (89 mg, 77% yield, 96% ee) after purification by silica gel column chromatography (5% benzene in hexanes). $[\alpha]_{\text{D}}^{23} = -121^\circ$ ($c = 0.73$, CH_2Cl_2). ^1H NMR (500 MHz, CDCl_3) δ 7.36 (d, $J = 8.8$ Hz, 2H), 6.88 (d, $J = 8.8$ Hz, 2H), 5.52 (dt, $J = 5.9, 3.0$ Hz, 1H), 3.82 (s, 3H), 2.53 – 2.22

(m, 3H), 1.71 – 1.45 (m, 2H), 1.10 (d, $J = 6.7$ Hz, 3H), 1.02 (t, $J = 7.4$ Hz, 3H). ^{13}C NMR (126 MHz, CDCl_3) δ 201.70, 158.38, 130.15, 126.94, 113.87, 106.24, 101.85, 55.42, 32.52, 28.95, 22.88, 21.44, 14.26. HRMS calculated for $[\text{M}]^+$ 230.16688, found 230.16664. FTIR (neat, cm^{-1}): 3035 (w), 2957 (s), 2931 (s), 2870 (s), 1942 (m), 1680 (m), 1607 (s), 1510 (s), 1464 (m), 1249 (s), 1177 (s), 1037 (s). The optical purity was determined by chiral HPLC analysis. Chiralcel OD-H HPLC column, 0.5% IPA/Hex, 1.2 ml/min, 275 nm detection, $t_{\text{minor}} = 4.3$ minutes, $t_{\text{major}} = 4.8$ minutes.



(R)-2-methyl-5-(4-trifluoromethylphenyl)-octa-3,4-diene (1.15) :

Compound was isolated as a clear oil (134 mg, 60% yield, 94% ee) after purification by silica gel column chromatography (5% benzene in hexanes). $[\alpha]_{\text{D}}^{23} = -87^\circ$ ($c = 1.03$, CH_2Cl_2). ^1H NMR (500 MHz, CDCl_3) δ 7.54 (d, $J = 8.4$ Hz, 2H), 7.50 (d, $J = 8.5$ Hz, 2H), 5.58 (dt, $J = 6.0, 3.1$ Hz, 1H), 2.51 – 2.32 (m, 3H), 1.63 – 1.52 (m, 2H), 1.09 (d, $J = 6.8$ Hz, 6H), 1.01 (t, $J = 7.4$ Hz, 3H). ^{13}C NMR (126 MHz, CDCl_3) δ 203.14, 141.74 (q, $J = 1.4$ Hz), 128.28 (q, $J = 32.4$ Hz), 125.99, 125.29 (q, $J = 3.8$ Hz), 124.52 (q, $J = 271.6$ Hz), 106.14, 102.55, 32.14, 28.81, 22.81 (d, $J = 1.5$ Hz), 21.35, 14.18. HRMS calculated for $[\text{M}]^+$ 268.14362, found 268.14311. FTIR (neat, cm^{-1}): 2960 (s), 2929 (s), 2872 (s), 1945 (m), 1616 (s), 1326 (s), 1165 (s), 1126 (s), 1069 (s), 1015 (s), 843 (s). The optical purity was determined by chiral GC analysis. Supelco Beta DEX 120 GC column, 160 $^\circ\text{C}$ (30 min), ramp to 180 $^\circ\text{C}$ at 3 $^\circ\text{C}/\text{min}$, $t_{\text{minor}} = 88.0$ minutes, $t_{\text{major}} = 83.6$ minutes.



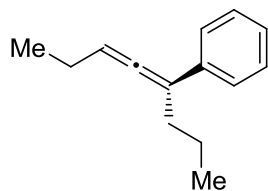
(R)-4-(4-methylphenyl)-5,5-dimethyl-hexa-2,3-diene (1.16) : Compound was

isolated as a clear oil (89 mg, 59% yield, 97% ee) after purification by silica gel column chromatography (5% benzene in hexanes). $[\alpha]_{\text{D}}^{24} = -81^\circ$ ($c = .79$, CH_2Cl_2). ^1H NMR (300 MHz, C_6D_6) δ 7.26 (d, $J = 7.9$ Hz,

2H), 7.00 (d, $J = 7.7$ Hz, 2H), 5.12 (q, $J = 6.9$ Hz, 1H), 2.13 (s, 3H), 1.58 (d, $J = 6.9$ Hz, 3H), 1.23 (s, 9H). ^{13}C NMR (126 MHz, CDCl_3) δ 202.82, 136.19, 135.73, 129.55, 128.68, 115.09, 86.08, 34.42, 30.25, 21.34, 15.19. HRMS calculated for $[\text{M}]^+$ 200.15649, found 200.156616. FTIR (neat, cm^{-1}): 3080 (w), 3046 (w), 2950 (s), 1954 (m), 1675 (w), 1608 (w), 1510 (s), 1476 (m), 1460 (m), 1359 (s), 1237 (m), 1204 (m), 1182 (m), 1152 (m), 1108 (m), 1020 (m), 956 (m), 905 (m), 823 (s). The optical purity was determined by chiral GC analysis. Supelco Beta DEX 120 GC column, 70°C ramp to 99°C at $0.15^\circ\text{C}/\text{min}$, ramp to 160°C at $4^\circ/\text{min}$, $t_{\text{minor}} = 181.4$ minutes, $t_{\text{major}} = 182.7$ minutes.

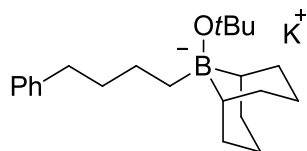
1.6.10 Determination of Absolute Stereochemistry

(*R*)-5-phenyl-octa-3,4-diene was synthesized according to general Arylation procedure and optical rotation was compared with literature value (lit. $[\alpha]_{\text{D}}^{25} = -128^\circ$ ($c = 1.27$, MeOH)).



(*R*)-5-phenyl-octa-3,4-diene (1.18): Compound was isolated as clear oil (149 mg, 57% yield, 99% ee) after purification by silica gel column chromatography (5% benzene in hexanes). $[\alpha]_{\text{D}}^{23} = -110^\circ$ ($c = 1.59$, MeOH) Characterization data matches literature values. ^1H NMR (300 MHz, C_6D_6) δ 7.48 (d, $J = 7.5$ Hz, 2H), 7.21 (d, $J = 15.2$ Hz, 2H), 7.07 (t, $J = 7.3$ Hz, 1H), 5.54 – 5.37 (m, 1H), 2.43 – 2.24 (m, 2H), 2.11 – 1.88 (m, 21H), 1.78 – 1.48 (m, 2H), 0.96 (dt, $J = 12.8, 7.4$ Hz, 3H). ^{13}C NMR (75 MHz, C_6D_6) δ 203.95, 138.02, 128.65, 126.74, 126.41, 106.77, 96.21, 32.55, 22.68, 21.70, 14.22, 13.79. The optical purity was determined by chiral GC analysis. Supelco Beta DEX 120 GC column, 110°C (100 min), ramp to 180°C at $3.0^\circ\text{C}/\text{min}$, 180°C (15 min), $t_{\text{minor}} = 75.7$ minutes, $t_{\text{major}} = 73.9$ minutes.

1.6.11 Synthesis of Boronate



: In a glove box, a scintillation vial was charged with 4-phenylbutene (1.0 equiv, 6.6 mmols), 9-borabicyclo[3.3.1]nonane (1.0 equiv, 6.6 mmol), and a stir bar. To the scintillation vial was added 6.6 mL Toluene (1 M) and the mixture was heated at 60 °C for 12 hours. To this mixture was added Potassium *t*-butoxide (1.0 equiv, 6.6 mmol). The mixture stirred vigorously at 100 °C for 30 minutes. The mixture was allowed to cool to 23 °C and the Toluene was removed by reduced pressure. The material was then suspended in dichloromethane and triterated with pentane. After removal of the solvent under reduced pressure a white solid was formed. This solid was placed on a fine frit and washed with pentane to yield potassium trialkylboronate as white solid, 86%. ^{11}B NMR (160 MHz, C_6D_6) δ -0.79, 23 °C, corresponds to known borate chemical shift. NMR taken in a quartz NMR tube.

1.6.12 Reaction Between Alkylborane And Various Alkali Metal Alkoxides

In a glove box under an atmosphere of N_2 , a dram vial was charged with 9-BBN (1.0 equiv) and styrene (1.0 equiv) in toluene- d_8 . The mixture was stirred vigorously at 60 °C for 12 hours. At this time either lithium *tert*-butoxide or sodium *tert*-butoxide was added to the mixture. The suspension was heated at 60 °C for 30 minutes. Then an aliquot was taken for NMR analysis. The mixture containing LiOtBu was homogeneous while the mixture with KOtBu was heterogeneous.

1.6.13 Reactivity Studies Using Borane or Borate Nucleophiles

When the neutral borane was used as nucleophile, the reaction was performed exactly how it is in the standard conditions except that LiOtBu is exchanged for KOtBu .

When the potassium borate is used as a nucleophile, no excess base was added and one equivalent of this nucleophile was added, otherwise it is exactly the same as the standard propargylic phosphate alkylation conditions.

1.6.14 Synthesis of ICyCuMe

In a glove box under N₂ atmosphere, a 25 mL reaction flask was charged with ICyCuCl (400 mg, 1.00 equiv), THF (4 mL), and a stir bar. The flask was then taken outside the glove box, put under N₂ atmosphere, cooled to -78 °C, and MeLi (0.75 mL of 1.6 M solution, 1.01 equiv) was added slowly with stirring. The mixture was allowed to warm to room temperature and concentrated to dryness to yield a creamy white solid. The material was put back in the glove box and dissolved in 3 mL of THF, layered with 7 mL of pentane, and placed in a -34 °C freezer. After 20 minutes the mixture was filtered on a fine frit and washed with pentane to yield 365 mg of ICyCuMe (93%). ¹H NMR (300 MHz, C6D6) δ 6.22 (s, 2H), 4.49 – 4.11 (m, 2H), 1.86 (d, J = 9.6 Hz, 2H), 1.43 (dt, J = 19.9, 10.0 Hz, 5H), 1.18 – 0.77 (m, 6H), 0.26 (s, 3H), minor impurity (THF). ¹³C NMR (75 MHz, C6D6) δ 180.36, 116.23, 60.61, 34.90, 25.56, 25.37, -11.30.

1.6.15 Stoichiometric Reaction Between ICyCuMe and Phosphate

In a glove box, a scintillation vial was charged with ICyCuMe (1.0 equiv, 0.5 mmol). To the vial was added phosphate (1.0 equiv, 0.5 mmol) and pentane/dioxane (10:1, 5 mL). The mixture was heated at 35 °C for 18 hours. After complete consumption of the phosphate, the mixture was filtered through a plug of silica gel using EtOAc as eluent. The solution was concentrated to yield a thick oil which was loaded onto a silica gel column and purified by flash chromatography.

1.6.16 Catalytic Reaction Using ICyCuMe as the Catalyst

In a glove box a scintillation vial was charged with a stir bar. To the vial was added 9-borabicyclo[3.3.1]nonane (1.6 equiv, 0.77 mmol). 4-phenylbutene (1.5 equiv, 0.72 mmol) was weighed out in a shell vial and added to the scintillation vial by rinsing with 0.7 mL dioxane. The mixture was heated at 60 °C. After 12 hours, cyclohexene (0.2 equiv, 0.096 mmol) was added and the mixture was heated at 60 °C for 2 hours. To the reaction mixture LiOtBu (1.0 equiv, 0.5 mmol) and ICyCuMe (0.10 equiv, 0.050 mmol) were added. The mixture was diluted to a volume of 7.0 mL with pentane. The enantioenriched phosphate (1), (1.0 equiv, 0.50 mmol), was then added to the reaction mixture. The

mixture was heated at 35 °C with stirring. After complete consumption of the phosphate, the mixture was filtered through a plug of silica gel using EtOAc as eluent. The solution was concentrated to yield a thick oil which was loaded onto a silica gel column and purified by flash chromatography. The product (3), was isolated in 85% yield, 98% ee.

Chapter 1 References

¹ Claesson, A. *The Chemistry of Allenes*; Landor, S. R. Ed.; Academic Press: London, **1982**.

² Hoffmann-Röder, A; Krause, N. *Angew. Chem. Int. Ed.* **2004**, 43, 1196

³ Cai, F.; Pu, X.; Qi, X.; Lynch, V.; Radha, A.; Ready, J. M. *J. Am. Chem. Soc.* **2011**, 133, 18066.

⁴ (a) Ma, S. *Acc. Chem. Res.* **2003**, 36, 701 (b) Ma, S. *Chem Rev* **2005**, 105, 2829 (c) Álvarez-Corral, M.; Muñoz-Dorado, M.; Rodríguez-García, I. *Chem. Rev.* **2008**, 108, 3174 (d) Bongers, N.; Krause, N. *Angew. Chem., Int. Ed.* **2008**, 47, 2178 (e) Widenhoefer, R. A. *Chem. Eur. J.* **2008**, 14, 5382 (f) Ma, S. *Acc. Chem. Res.* **2009**, 42, 1679 (g) Aubert, C.; Fensterbank, L.; Garcia, P.; Malacria, M.; Simonneau, A. *Chem. Rev.* **2011**, 111, 1954 (h) Corma, A.; Leyva-Pérez, A.; Sabater, M. J. *Chem. Rev.* **2011**, 111, 1657.

⁵ Hasegawa, M.; Iwata, S.; Sone, Y.; Endo, S.; Matsuzawa, H.; Mazaki, Y. *Molecules* **2014**, 19, 2829

⁶ (a) Wan, Z.; Nelson, S. G. *J. Am. Chem. Soc.* **2000**, 122, 10470 (b) Liu, Z.; Wasmuth, A. S.; Nelson, S. G. *J. Am. Chem. Soc.* **2006**, 128, 10352 (c) Volz, F.; Krause, N. *Org. Biomol. Chem.* **2007**, 5, 1519; (d) Volz, F.; Wadman, S. H.; Hoffmann-Röder, A.; Krause, N. *Tetrahedron* **2009**, 65, 1902

⁷ Selected reviews on allene synthesis: (a) Krause, N.; Hoffmann-Röder, A. *Tetrahedron* **2004**, 60, 11671; (b) Brummond, K. M.; DeForrest, J. E. *Synthesis* **2007**, 795; (c) Yu, S.; Ma, S. *Chem. Commun.* **2011**, 47, 5384.

⁸ Highlights of some asymmetric allene synthesis and application, Hoffmann-Röder, A; Krause, N. *Angew. Chem. Int. Ed.* **2002**, 41, 2933

⁹ Selected examples: (a) Han, J. W.; Tokunaga, N.; Hayashi, T. *J Am Chem Soc* **2001**, 123, 12915. (b) Ogasawara, M.; Ikeda, H.; Nagano, T.; Hayashi, T. *J. Am. Chem. Soc.* **2001**, 123, 2089. (c) Schultz-Fademrecht, C.; Wibbeling, B.; Fröhlich, R.; Hoppe, D. *Org. Lett.* **2001**, 3, 1221. (d) Sherry, B. D.; Toste, F. D. *J. Am. Chem. Soc.* **2004**, 126, 15978. (e) Trost, B. M.; Fandrick, D. R.; Dinh, D. C. *J. Am. Chem. Soc.* **2005**, 127, 14186. (f) Ogasawara, M.; Fan, L.; Ge, Y.; Takahashi, T. *Org. Lett.* **2006**, 8, 5409. (g) Kolakowski, R. V.; Manpadi, M.; Zhang, Y.; Emge, T. J.; Williams, L. J. *J. Am. Chem. Soc.* **2009**, 131, 12910. (h) Liu, H.; Leow, D.; Huang, K.-W.; Tan, C.-H. *J. Am. Chem. Soc.* **2009**, 131, 7212. (i) Cerat, P.; Gritsch, P. J.; Goudreau, S. R.; Charette, A. B. *Org. Lett.* **2010**, 12, 564. (j) Nishimura, T.; Makino, H.; Nagaosa, M.; Hayashi, T. *J. Am. Chem. Soc.* **2010**, 132, 12865. l) a recent example of asymmetric trisubstituted allene synthesis: Dabrowski, J. A.; Haeffner, F.; Hoveyda, A. H. *Angew. Chem. Int. Ed.* **2013**, 52, 7694. m) Dieter, R. K.; Chen, N.; Gore, V. K. *J. Org. Chem.* **2006**, 71, 8755 n) Kobayashi, K.; Naka, H.; Wheatley, A. E. H.; Kondo, Y. *Org. Lett.* **2008**, 15, 3375, o) a rare enantioselective trisubstituted allene synthesis: Li, C.; Wang, X.; Sun, X.; Tang, Y.; Zheng, J.; Xu, Z.; Zhou, Y.; Dai, L. *J. Am. Chem. Soc.* **2007**, 129, 1494.

¹⁰ Asymmetric higher order allene synthesis is rare. This reaction is remarkable.

¹¹ Hayashi, T.; Tokunaga, N.; Inoue, K. *Org. Lett.* **2004**, 2, 305.

¹² Myers, A. G.; Zheng, B. *J. Am. Chem. Soc.* **1996**, 118, 4492

-
- ¹³ Pu, X.; Ready, J. M. *J. Am. Chem. Soc.* **2008**, *130*, 10874.
- ¹⁴ Rona, P.; Crabbe, P. *J. Amer. Chem. Soc.* **1968**, *90*, 4733
- ¹⁵ Making a C-C bond in the allene formation step allows the developed reaction to be convergent.
- ¹⁶ Chirality transfer is defined as CT = (ee products / ee starting material)100%
- ¹⁷ Selected examples: (a) Oehlschlager, A. C.; Czyzewska, E. *Tetrahedron Lett.* **1983**, *24*, 5587; (b) Alexakis, A.; Marek, I.; Mangeney, P.; Normant, J. F. *J. Am. Chem. Soc.* **1990**, *112*, 8042; (c) Gooding, O. W.; Beard, C. C.; Jackson, D. Y.; Wren, D. L.; Cooper, G. F. *J. Org. Chem.* **1991**, *56*, 1083; (d) Myers, A. G.; Condroski, K. R. *J. Am. Chem. Soc.* **1995**, *117*, 3057; (e) Brummond, K. M.; Kerekes, A. D.; Wan, H. *J. Org. Chem.* **2002**, *67*, 5156.
- ¹⁸ Marshall, J. A.; Pinney, K. G. *J. Org. Chem.* **1993**, *58*, 7180. Marshall et al showed this pendant alkoxy groups helps to improve anti/syn ration of products.
- ¹⁹ Wan, Z.; Nelson, S. G. *J. Am. Chem. Soc.* **2000**, *122*, 10470
- ²⁰ Tang, X.; Woodward, S.; Krause, N. *Eur. J. Org. Chem.* **2009**, 2836
- ²¹ Claesson, A.; Olsson, L. I. *J. Chem. Soc., Chem. Commun.* **1979**, 524.
- ²² Ohmiya, H.; Yokobori, U.; Makida, Y.; Sawamura, M. *Org. Lett.* **2011**, *13*, 6312. This report is the first example of copper-catalyzed S_N2' alkylation of phosphates using an alkyl borane. However, the focus was on regioselectivity not chirality transfer. In our publication, all substrates were enantioenriched.
- ²³ Whittaker, A. M.; Rucker, R. P.; Lalic, G. *Org. Lett.* **2010**, *12*, 3216
- ²⁴ See Reference 23
- ²⁵ Dorta, R.; Stevens, E. D.; Scott, N. M.; Costabile, C.; Cavallo, L.; Hoff, C. D.; Nolan, S. P. *J. Am. Chem. Soc.* **2005**, *127*, 2485.
- ²⁶ Hammerschmidt, F.; Schneyder, E.; Zbiral, E. *Chem. Ber.* **1980**, *113*, 3891. This compound is a known compound and the characterization data matched that reported.
- ²⁷ This multi-variable optimization process caused reaction development to be quite confusing. One might think that adding excess LiOtBu would help make transmetalation more efficient, when instead it was effecting chirality transfer. We propose that the excess LiOtBu can react with alkyl copper, forming a cuprate, which can then participate in allene racemization through an electron transfer mechanism, see: Claesson, A.; Olsson, L. *J. Chem. Soc. Chem. Comm.* **1979**, 524
- ²⁸ The analogous acetal also worked as a substrate, but the enantiomers were inseparable using chiral-phase HPLC.
- ²⁹ The synthesis of similar substrates and their synthetic utility was the focus of a later publication. See: Yokobori, U.; Ohmiya, H.; Sawamura, M. *Organometallics*, **2012**, *31*, 7909.
- ³⁰ Since our initial report, more work has been done in this area: a) Yang, M.; Yokokawa, N.; Ohmiya, H.; Sawamura, M. *Org. Lett.* **2012**, *14*, 816, b) Nakatani, A.; Hirano, K.; Satoh, T.; Miura, M. *Org. Lett.* **2012**, 2586.
- ³¹ Alexakis published a method to convert geminal propargylic chlorides to enantioenriched trisubstituted allenes based an enantioselective Pd catalyzed S_N2' substitution followed by cross coupling of the allenyl chloride. Li, H.; Müller, D.; Gué, L.; Alexakis, A. *Org. Lett.* **2012**, *14*, 5880.

-
- ³² a) Yoshida, M.; Gotou, T.; Ihara, M. *Tetrahedron Lett.* **2004**, *45*, 5573, b) Yoshida, M.; Ueda, H.; Ihara, M. *Tetrahedron Lett.* **2005**, *46*, 6705. c) an example using special fluorinated substrates Konno, T.; Tanikawa, M.; Ishihara, T.; Yamanaka, H. *Chem. Lett.* 2000, 1360-1361.
- ³³ Falciola, C. A.; Alexakis, A. *Eur. J. Org. Chem.* **2008**, 3765-3780. Anti refers to the relative orientation of the leaving group and nucleophile.
- ³⁴ Murakami, M.; Igawa, H. *Helv. Chim. Acta.* **2002**, *85*, 4182
- ³⁵ See Reference 23
- ³⁶ First unambiguous use of boron-to-copper transmetalation in a catalytic reaction: a) Ohishi, T.; Nishiura, M.; Hou, Z. *Angew. Chem. Int. Ed.* 2008, *47*, 5792, other applications in miscellaneous reactions: b) Takaya, J.; Tadami, T.; Ukai, K.; Iwasawa, N. *Org. Lett.* 2008, *13*, 2697, c) Ohmiya, H.; Yokobori, U.; Makida, Y.; Sawamura, M. *J. Am. Chem. Soc.* **2010**, *132*, 2895, d) Ohmiya, H.; Yokokawa, N.; Sawamura, M. *Org. Lett.* **2010**, *12*, 2438, e) Ohmiya, H.; Yoshida, M.; Sawamura, M. *Org. Lett.* **2011**, *13*, 482, f) Ohmiya, H.; Tanabe, M.; Sawamura, M. *Org. Lett.* **2010**, *13*, 1086. g) Gurung, S. K.; Thapa, S.; Kafle, A.; Dickie, D. A.; Giri, R. *Org. Lett.* **2014**, *16*, 1264, h) Shido, Y.; Yoshida, M.; Tanabe, M.; Ohmiya, H.; Sawamura, M. *J. Am. Chem. Soc.* **2012**, *134*, 18573, i) Yoshida, M.; Ohmiya, H.; Sawamura, M. *J. Am. Chem. Soc.* **2012**, *134*, 11896 j) Gao, F.; Carr, J. L.; Hoveyda, A. H. *Angew. Chemie. Int. Ed.* **2012**, *51*, 6613, k) Nagao, K.; Yokobori, U.; Makida, Y.; Ohmiya, H.; Sawamura, M. *J. Am. Chem. Soc.* **2012**, *134*, 8982, l) Jung, B.; Hoveyda, A. H. *J. Am. Chem. Soc.* **2012**, *134*, 1490, m) Wada, R.; Shibuguchi, T.; Makino, S.; Oisaki, K.; Kanai, M.; Shibasaki, M. *J. Am. Chem. Soc.* **2006**, *128*, 7687
- ³⁷ This step of the catalytic cycle could also proceed through carbocupration and anti-elimination, however based on studies by Bertz and Ogle studying allylic substitution, oxidative addition is reasonable see: Bartholomew, E. R.; Bertz, S. H.; Cope, S.; Murphey, M.; Ogle, C. A. *J. Am. Chem. Soc.* **2008**, *130*, 11244. Additionally, Cu(III) has been invoked in the mechanism of the Ullman reaction, see: Huffman, L. M.; Stahl, S. *J. Am. Chem. Soc.* **2008**, *130*, 9196.
- ³⁸ This elementary step is described in the literature. See: Mankad, N. P.; Laitar, D. S.; Sadighi, J. P. *Organometallics* **2004**, 3369
- ³⁹ DFT calculations performed on transmetalation reaction: Dang, L.; Lin, Z.; Marder, T. B. *Organometallics* **2010**, *29*, 917.
- ⁴⁰ For example, see references 36i and 36k, both from the same group. In those papers, different mechanisms of transmetalation are proposed.
- ⁴¹ Here is a recent study on the mechanism of boron-to-palladium transmetalation: Carrow, B. P.; Hartwig, J. F. *J. Am. Chem. Soc.* **2011**, *133*, 2116.
- ⁴² Ideal to use quartz NMR tubes to avoid the presence of the borosilicate resonance in NMR spectrum
- ⁴³ The borate and the phosphate don't react without a copper catalyst present.
- ⁴⁴ IMesCuEt was synthesized and fully characterized by our group later, see: Rucker, R. P.; Whittaker, A. M.; Dang, H.; Lalic, G. *J. Am. Chem. Soc.* **2012**, *134*, 6571
- ⁴⁵ Tao, B.; Ruble, J. C.; Hoic, D. A.; Fu, G. C. *J. Am. Chem. Soc.* **1999**, *121*, 5091
- ⁴⁶ Kazmaier, U.; Zumpe, F. L. *Eur. J. Org. Chem.* **2001**, 4067
- ⁴⁷ Panteleev, J.; Huang, R. Y.; Lui, E. K. J.; Lautens, M. *Org. Lett.* **2011**, *19*, 5314
- ⁴⁸ Ng, S.; Jamison, T. F. *J. Am. Chem. Soc.* **2005**, *127*, 7320

⁴⁹ Denmark, S. E.; Yang, S. *J. Am. Chem. Soc.* **2004**, 126, 12432

Chapter 2: Catalytic Asymmetric Synthesis of Cyclic Ethers Containing an α -Tetrasubstituted Stereocenter

Portions of this chapter as well as figures, schemes, and tables were adapted or reproduced from the following manuscript co-authored by Mycah R. Uehling: Catalytic Asymmetric Synthesis of Cyclic Ethers Containing an α -Tetrasubstituted Stereocenter, *Angewandte Chemie International Edition*, **2013**, 52, 4878. Copyright **2013** WILEY-VCH Verlag GmbH & Co. KGaA, Weinheim

2.1 Introduction

The tetrahydrofuran and tetrahydropyran structural motifs are found in many classes of natural products such as macrodiolides,¹ acetogenins,² ionophores,³ lignans,⁴ and macarolides.⁵ In addition, arene-fused pyrans make up the chroman^{6,7} family of natural products. All of these classes of natural products are valuable and have biological properties. For example, the acetogenins are known to have cytotoxic, anti-cancer, anti-parasitic, pesticidal, anti-microbial, and immunosuppressive properties. A common structural motif found throughout the classes of natural products listed above is a sterically hindered α -substituted cyclic ether. While most cyclic ethers contain an α -trisubstituted stereocenter (one hydrogen bound to carbon of the stereocenter), there are a considerable number that contain an α -tetrasubstituted stereocenter (no hydrogen bound to carbon of stereocenter, See Figure 2, selected examples shown).

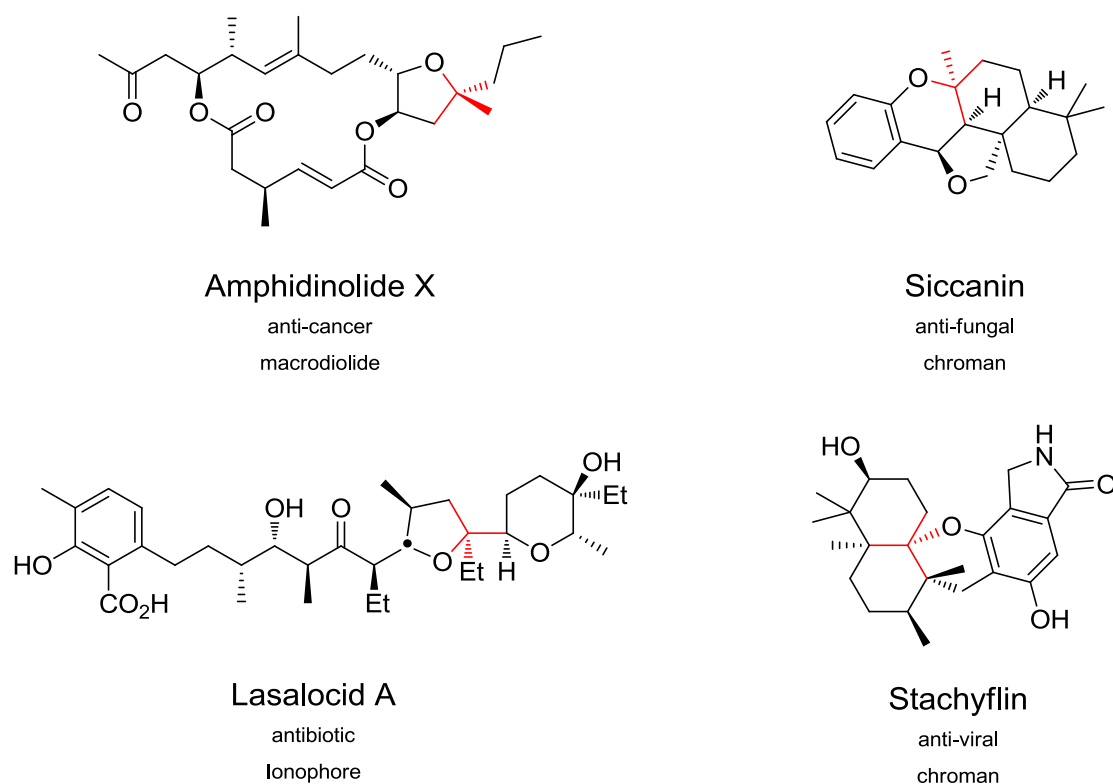
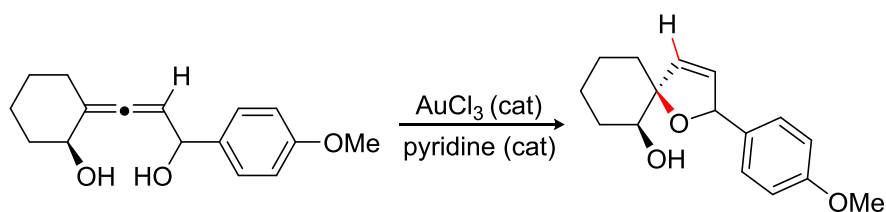


Figure 2. Cyclic Ether Natural Products Containing an α -Tetrasubstituted Stereocenter

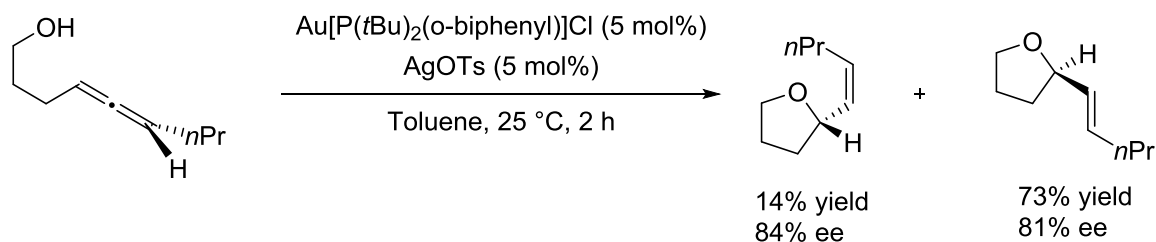
As cyclic ethers are present in natural products that are biologically active, their synthesis has been the focus of a substantial body of work.⁸ Most synthetic strategies can be grouped into one of the following categories: intramolecular S_N2 reactions where an alkyl leaving group is displaced by oxygen nucleophiles, addition of carbon nucleophiles to oxocarbenium ions, or cycloadditions. These strategies have not become applicable to asymmetric cyclic ether synthesis where the target compound contains an α -tetrasubstituted stereocenter. Recently, effort has been focused on asymmetric catalytic synthesis of cyclic ethers containing an α -tetrasubstituted stereocenter.⁹ However, these methods tend to have limited scope, generally low enantioselectivity, or require highly specialized starting materials that can be difficult to prepare. Importantly, none of the methods described above provide a general solution to the asymmetric synthesis of cyclic ethers containing an α -tetrasubstituted stereocenter.

A relatively unexplored strategy for asymmetric cyclic ether synthesis is gold-catalyzed cyclization of enantioenriched allenols. This approach to asymmetric cyclic ether synthesis is based on chirality transfer¹⁰ from an allenic axis to the cyclic ether α -stereocenter. There is some precedent in the literature for this approach to enantioenriched α -tetrasubstituted cyclic ether synthesis. The few examples are reports by Marshal¹¹ and later Krause.¹² They showed that enantioenriched trisubstituted allenols can be transformed into dihydrofurans containing an α -tetrasubstituted stereocenter through gold or silver catalyzed *endo*-selective cyclization (Scheme 13). These methods are dependent on the ability to access the required enantioenriched trisubstituted allenol¹³ starting materials and therefore have limited scope.



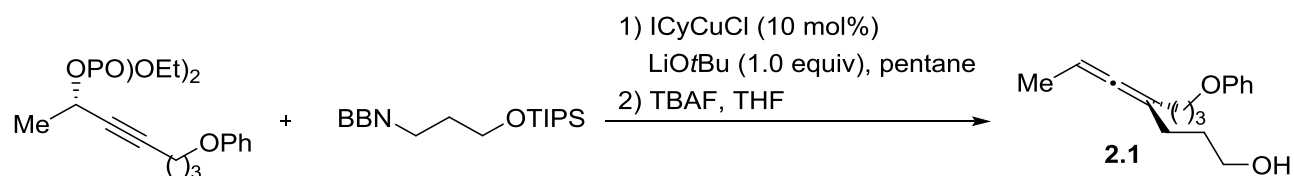
Scheme 13. Selected Example of Asymmetric *endo*-Selective Cyclic Ether Synthesis¹⁴

As an alternative to *endo*-selective cyclization, we have developed an *exo*-selective cyclization to transform enantioenriched trisubstituted allenols into enantioenriched cyclic ethers containing an α -tetrasubstituted stereocenter. This is an efficient strategy for asymmetric synthesis of cyclic ethers because there are no byproducts formed in the reaction, and more importantly, if the allene is enantioenriched, high axis-to-center chirality transfer is possible (vide infra). Our strategy is based on *exo*-selective cyclization of disubstituted allenols developed by Widenhoefer and coworkers (Scheme 14).¹⁵ In their 2006 report, they describe one example of an *exo*-selective gold-catalyzed cyclization of an enantioenriched disubstituted allenol to form a furan product. While this approach to asymmetric ether synthesis seems practical and potentially useful, this strategy has never been applied to the synthesis of cyclic ethers containing an α -tetrasubstituted stereocenter. In the case that Widenhoefer and coworkers describe, the reaction products are isolated as mixture of diastereoisomers with opposite sense of chirality (pseudoenantiomers)¹⁶ (Scheme 14).



Scheme 14. Gold-Catalyzed *exo*-Selective Cyclization of Allenol.

We speculated that the main reason that gold-catalyzed *exo*-selective cyclization hadn't been applied to the asymmetric synthesis of cyclic ethers containing an α -tetrasubstituted stereocenter is that there was no way to easily prepare the required enantioenriched trisubstituted allenes. However, using the method described in Chapter 1, access to enantioenriched trisubstituted allenes such as **2.1** was possible (Scheme 15). This synthetic advantage allowed us to systematically study *exo*-selective cyclization of enantioenriched trisubstituted allenols to form α -tetrasubstituted cyclic ethers. Based on the observations of Widenhoefer and coworkers (Scheme 14), we expected that a major challenge in reaction development will be controlling diastereoselectivity of the reaction. In addition, it was unclear if chirality transfer would be a problem because trisubstituted allenols had never been systematically studied in this context.

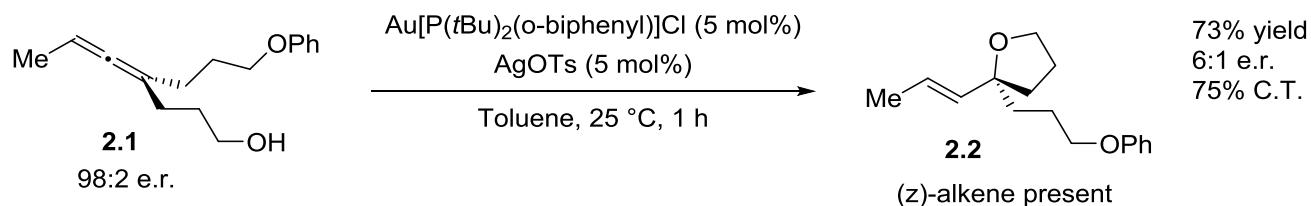


Scheme 15. Synthesis of Enantioenriched Trisubstituted Allenols

2.2 Reaction Optimization

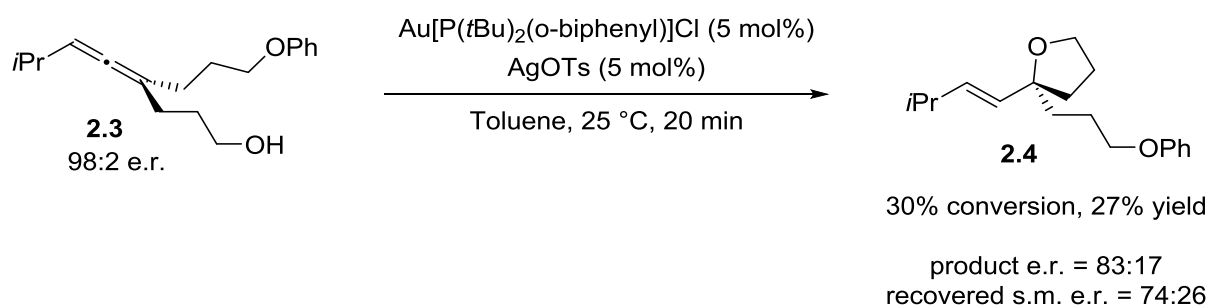
With enantioenriched trisubstituted allenols in hand we began optimization of the reaction. In our first experiment, we exposed allenol **2.1** to the same reaction conditions Widenhoefer had used in the cyclization of disubstituted allenols (Scheme 16). Consistent with Widenhoefer's results, we observed multiple diastereomers. However, we observed poor chirality transfer (75%, Widenhoefer

observed >95%). This is surprising in light of a computational study that proposed that trisubstituted allenes racemize slower in the presence of cationic gold catalysts than disubstituted allenes.¹⁷ Based on our results using trisubstituted allenes, we proposed that the allene was involved in a background racemization reaction that was causing lower chirality transfer.¹⁸



Scheme 16. First Attempt at Enantioenriched Cyclic Ether Synthesis

To understand what was leading to poor chirality transfer, we performed the following experiment. Our plan was to perform a cyclization using enantioenriched trisubstituted allenol **2.3**, but stop the reaction early, and measure the enantiomeric ratio (er) of both the starting material and the product. If the er of the allene was diminished relative to the product, then background racemization is probably causing low chirality transfer. If not, the loss of enantioenrichment probably occurs during the cyclization step.¹⁹

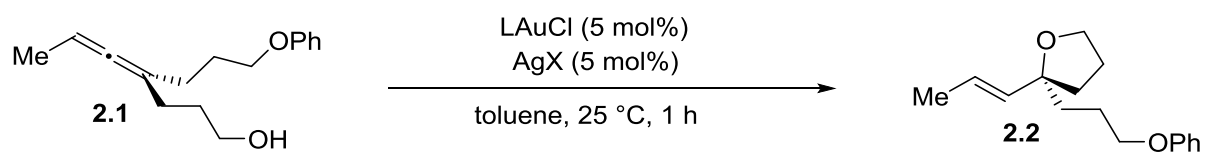


Scheme 17. Experiment Showing Allene Racemization Before Cyclization

After isolation of the product **2.4** and the starting material **2.3** at 30% conversion (Scheme 17), we analyzed the enantiopurity of both the starting material and the product. We found that the starting

material was enantioenriched at the level of 74:26 er and the product was enantioenriched at 83:17 er. These results suggest that background allene racemization is leading to poor chirality transfer. This observation gave us hope that we might be able to treat allene racemization as a background reaction and optimize allenol cyclization as the dominant reaction pathway.

Table 4. Optimization of Gold-Catalyzed Allene Hydroalkoxylation



Entry	L	X	Yield (%)	C.T. (%)
1	PtBu ₂ (o-biphenyl)	OTs	73 ^a	75
2	PPh ₃	ClO ₄	>95	0
3	PPh ₃	BF ₄	>95	2
4	PPh ₃	OTs	>95	95
5 ^b	PPh ₃	OAc	70	87
6	P(C ₆ F ₅) ₃	OAc	>95	83
7 ^c	P(C ₆ F ₅) ₃	OAc	>95	28
8 ^d	P(C ₆ F ₅) ₃	OTs	>95	16
9	PCy ₃	OTs	>95	98
10	PtBu ₃	OTs	>95	99
11 ^e	PtBu ₃	OTs	>95	99

a) mixture of diastereomers b) 60 °C, 100 h c) THF instead of toluene d) DCM instead of toluene e) 1 mol% catalyst used

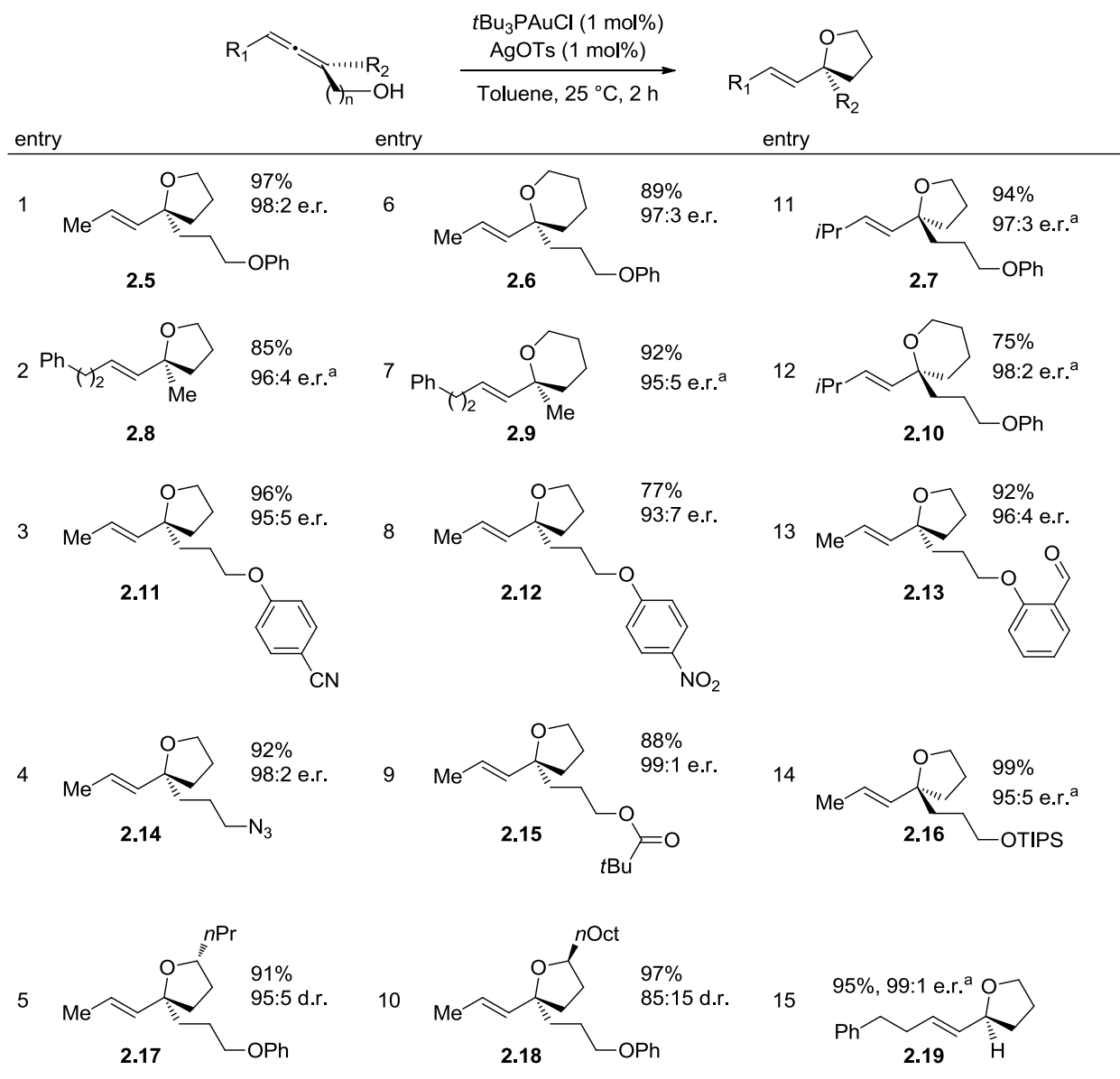
The challenges of reaction optimization were obtaining high diastereoselectivity and chirality transfer. Reaction yield was never a problem as the reaction is highly efficient using many types of gold(I) catalyst systems (Table 4). Surprisingly, we found that switching from PtBu₂(o-biphenyl) to PPh₃ solved the problem of diastereoselectivity. In all cases when simple, monodentate organophosphines were used as ligands, we found that only one diastereoisomer can be observed in the crude reaction mixture, the (*E*)-alkene. Most importantly, by varying the counterion on gold, we were able to dramatically affect the chirality transfer (Table 4, entries 2-4). If the counterion is not coordinating enough, full racemization occurs before cyclization and if the counter ion is too coordinating the reaction becomes prohibitively slow (Table 4, entry 5). The electronic nature of the ligand plays a small role in chirality transfer (Table 4,

entry 5 and 6). Lastly, choice of solvent is essential, when using more polar solvents, allene racemization can become competitive with cyclization (Table 4, entries 6-8). Overall, the most productive reaction was observed using 1 mol% of tri-*t*-butylphosphinegold tosylate as the active catalyst in toluene (Table 4, entries 9-11).

2.3 Furan and Pyran Synthesis Scope

With the optimized reaction conditions in hand, we explored the scope of the reaction. We found that our method can be used to prepare enantioenriched furans and pyrans with different sized substituents bound to the α -tetrasubstituted carbon (Table 5, entries 1-2). In addition, the size of the R₁ substituent does not seem to have an effect on the outcome of the reaction (Table 5, entries 11-12). We were able to use this method to synthesize 1.2 g of compound **2.5** (Table 5, entry 1) using 0.02 mol% of the gold catalyst,²⁰ demonstrating that this method is practical for gram scale synthesis. The reaction is compatible with many common functional groups including cyano, nitro, formyl, azido, pivaloyl, and silyloxy (Table 5, entries 3-5, 8-9, 13-14). When a secondary alcohol is used as a nucleophile, we observed a slight matched-mismatched selectivity between the secondary alcohol stereocenter and the allenic axis (Table 5, entries 5 and 10).²¹ Lastly, in contrast to Widenhoefer's results, a disubstituted allene can be successfully cyclized in high chirality transfer and high diastereoselectivity (Table 5, entry 15).²²

Table 5. Asymmetric Synthesis of Tetrahydrofurans and Tetrahydropyrans



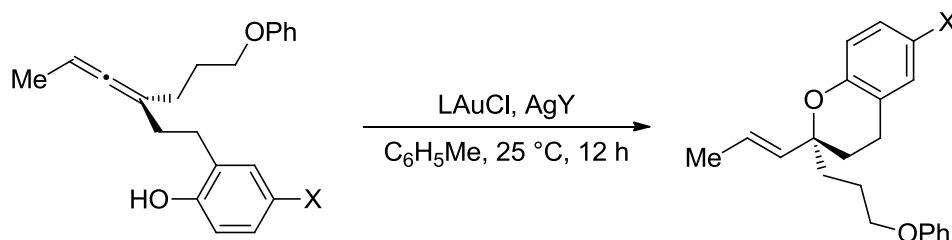
a) used allene with opposite sense of chirality

2.4 Chroman Synthesis Optimization

Building on our success with furan and pyran synthesis, we directed our focus toward the synthesis of chromans. We were drawn toward chroman synthesis because the chroman structural motif can be found in many biologically active compounds.²³ While various asymmetric approaches to the chroman structural motif exist,²⁴ we were surprised to find that chromans have never been synthesized by hydrophenoxylation of allenes. In addition, a large number of natural chromans have been characterized

that contain an α -tetrasubstituted stereocenter.²⁵ We envisioned that the *exo*-selective hydrophenyloxylation of trisubstituted allene phenols to be a practical approach to asymmetric synthesis of chromans containing an α -tetrasubstituted stereocenter.

Table 6. Optimization of Chroman Synthesis



Entry	X	% LAuCl	% AgY	Yield (%)	C.T. (%)
1	H	10% <i>t</i> -Bu ₃ P	10% OTs	92	89
2	H	10% Cy ₃ P	10% OTs	89	77
3	H	10% <i>o</i> -tol ₃ P	10% OTs	88	89
4	H	10% <i>n</i> -Bu ₃ P	10% OTs	94	52
5	H	10% <i>t</i> -Bu ₃ P	10% ClO ₄	90	5
6	H	10% <i>t</i> -Bu ₃ P	10% TFA	90	84
7 ^a	H	10% <i>t</i> -Bu ₃ P	10% OAc	80	97
8	H	10% <i>t</i> -Bu ₃ P	10% O ₂ CPh	92	98
9 ^a	OMe	10% <i>t</i> -Bu ₃ P	10% O ₂ CPh	58	- ^b
10	OMe	5% <i>t</i> -Bu ₃ P	5% O ₂ CPh	>95	89
11	OMe	2% <i>t</i> -Bu ₃ P	2% O ₂ CC ₆ H ₄ (4-CO ₂ Me)	89	94

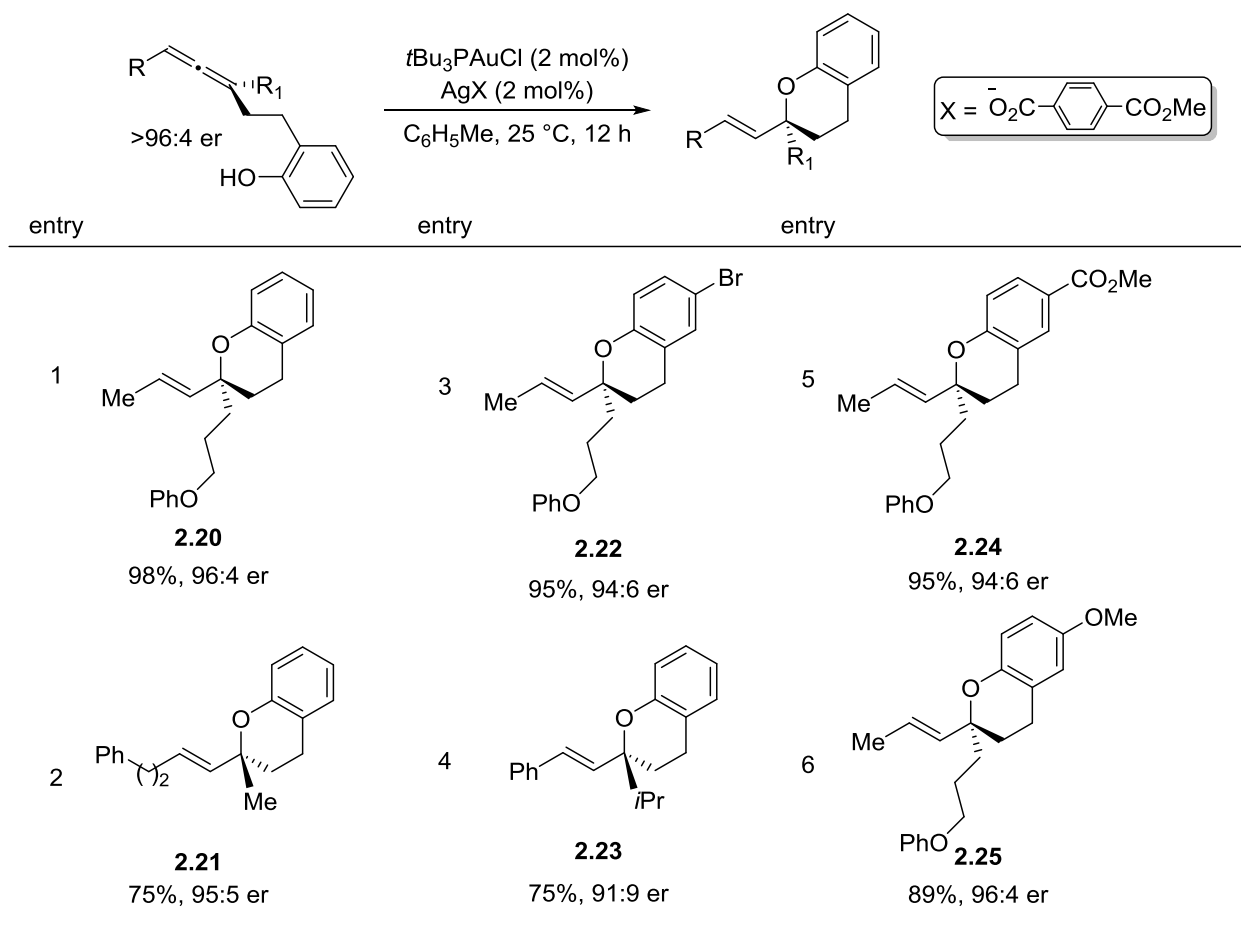
a) reaction time, 48 h b) C.T. not determined

In our initial experiment we exposed an allenyl phenol to the reaction conditions developed for furan and pyran synthesis. We found that the chroman was formed in high yield and high chirality transfer (Table 6, entry 1), but were curious to see if we could optimize the reaction further to achieve >90% chirality transfer. Based on our effort to optimize the cyclization of allenols to form furans and pyrans, we speculated that the key variables to manipulate would be the ligand and counterion on gold. Indeed, when using different triorganophosphine ligands, chirality transfer varied substantially (Table 6, entries 1-4). In terms of the counterion, we observed an effect similar to that of the furan and pyran study, where the optimal counter ion is finely tuned at the right coordination level (Table 6, entries 1, 5, and 6). Using the

acetate counter ion, the reaction proceeds with high chirality transfer, but the reaction is unreasonably slow (Table 6, entry 7). In order to balance reactivity and chirality transfer we reasoned that the benzoate counter ion might work well (Table 6, entry 8). This proved to be the case for certain allene phenols. However, we observed that if substituents on the phenol nucleophile are changed, the relative cyclization and racemization rates also changed (Table 6, entry 9).²⁶ We found that by adjusting the reaction concentration and catalyst loading, and by further tuning the counter ion to mono-methylterephthalate, we were able to achieve an optimal reaction using many types of phenols with various substitution patterns (Table 6, entry 11).

2.5 Chroman Synthesis Scope

Table 7. Scope of Asymmetric Chroman Synthesis



a) used allene with opposite sense of chirality

The scope of the developed asymmetric chroman synthesis is shown in Table 7. All compounds were isolated as one diastereomer, in high yield, and with high to excellent chirality transfer. We were able to prepare chromans containing multiple functional groups such as aryl halides, electron poor and electron rich aryl systems, and aryl-alkyl ethers (Table 7). The reaction is tolerant of multiple structural modifications in the substrate such as varying the size of the R group (Table 7) and importantly the reaction is tolerant of variable sized groups at R₁ (Table 7, entries 2,4, and 6). Entry 4 in table 7 shows that as the size of R₁ becomes too great, racemization starts to become competitive with cyclization and thus chirality transfer is lowest in this case.

2.6 Mechanism of Ether Formation

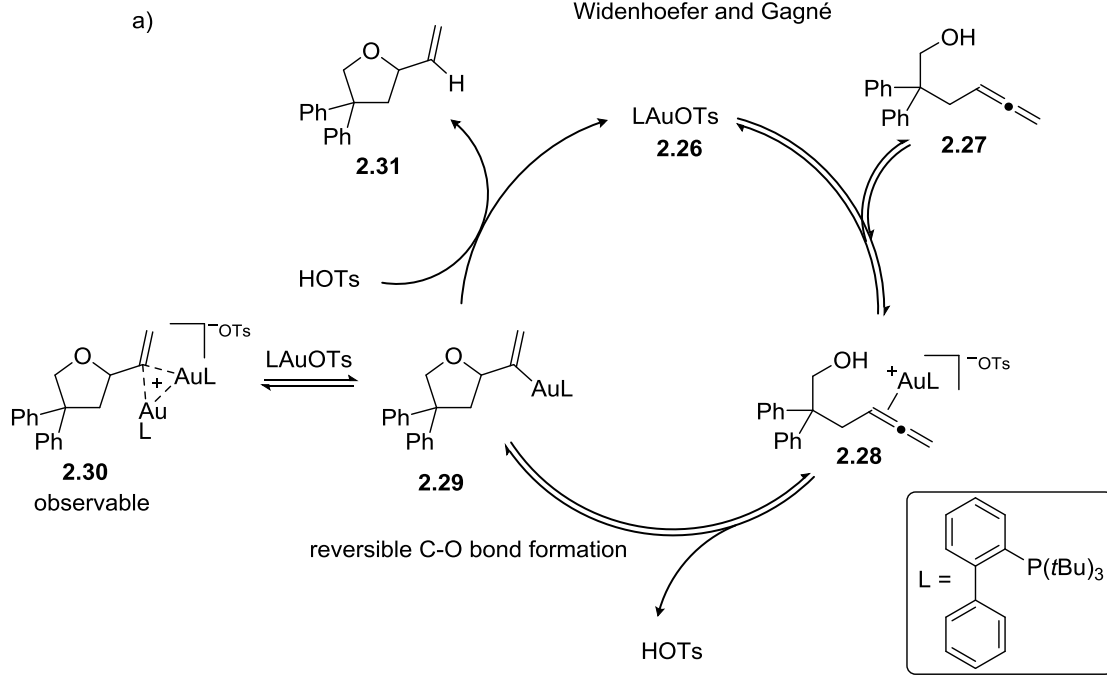
2.6.1 Mechanism of Furan and Pyran Formation

During the preparation of our manuscript Widenhoefer and Gagné published an elegant study detailing the gold-catalyzed hydroalkoxylation of allenes to form tetrahydrofurans (Scheme 18a).²⁷ A brief discussion of some of their observations are worth noting as we also did similar experiments and came to the same general conclusions.²⁸

Scheme 18. Mechanism of Cyclic Ether Formation

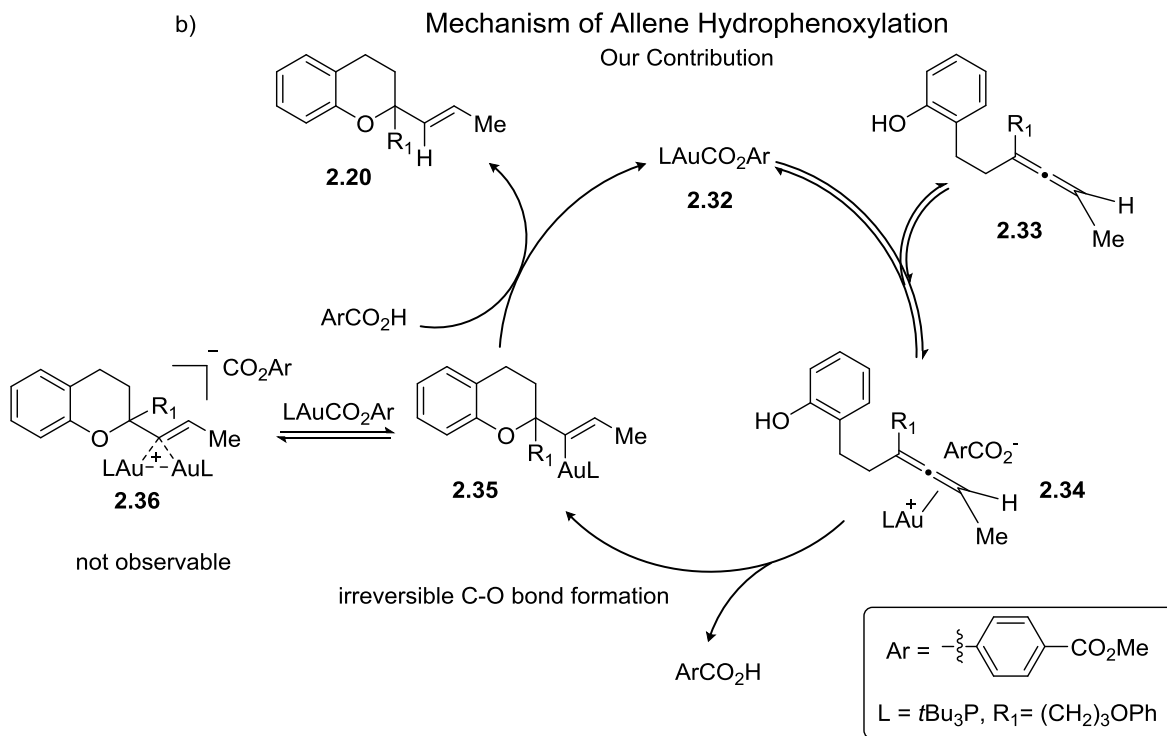
Mechanism of Allene Hydroalkoxylation

Widenhoefer and Gagné



Mechanism of Allene Hydrophenoxylation

Our Contribution



Widenhoefer and Gagné's observations were the following (See Scheme 18 a): In a stoichiometric reaction between gold complex **2.26** and alleneol **2.27** performed at -80 °C in DCM, the dominant species in solution are the bis(gold) vinyl species **2.30** and the alleneol **2.27**. After heating to -30 °C, the product **2.31** is formed quantitatively in 3 hours. In a catalytic reaction performed at -30 °C, the bis(gold) vinyl species **2.30** is observable immediately after mixing the substrate and catalyst, and is present until conversion reaches ca 95%. These observations provide evidence that a bis(gold) vinyl species **2.30** is a resting state for gold, at least at low temperature. When isolated vinylgold species **2.29** is allowed to react with TsOH at -80 °C, the product **2.31** is not formed, but rather the bis(gold) vinyl species **2.30** and free alleneol **2.27** are formed. Not until warming the solution does the product form. This observation provides evidence that the C-O bond formation is reversible. Lastly, a KIE of $k_H/k_D = 5.3$ was measured for the catalytic reaction.

Taking all this data together, Widenhoefer and Gagné propose the mechanism shown in Scheme 18a. They propose that the alleneol first coordinates to the gold tosylate catalyst to form a gold allene complex **2.28**.²⁹ Reversible C-O bond formation and elimination of HOTs yields the vinyl gold intermediate **2.29**. The vinyl gold intermediate **2.29**, can either be trapped by more gold tosylate to form the bis(gold) vinyl species **2.30** or be protonated to form the product **2.31** and form the gold tosylate complex **2.26**. A KIE of $k_H/k_D = 5.3$ was observed for the catalytic reaction (C-O bond formation is reversible), so it was concluded that the turnover-limiting step is protonation of vinylgold with TsOH.

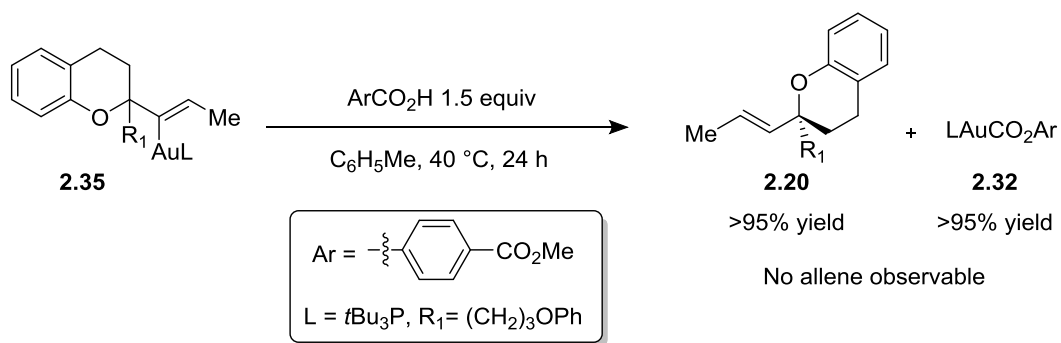
Our lab also measured the resting state of gold-catalyzed hydroalkoxylation of allenes at low temperature and concluded that it was a bis(gold) vinyl species similar to that characterized by Widenhoefer and Gagné.³⁰ We also measured a KIE of $k_H/k_D = 5.3$. We did not establish the reversibility of C-O bond formation but given the similarity in reaction conditions between those used in our asymmetric allene hydroalkoxylation and that which Widenhoefer and Gagné studied, it is reasonable to believe that our reaction follows a similar mechanism.

2.6.2 Mechanism of Chroman Formation

With the mechanism of gold-catalyzed hydroalkoxylation having recently been studied, we turned our focus to the mechanism of gold-catalyzed chroman formation. In particular we focused on trying to identify differences between the mechanism of furan and pyran formation and the mechanism of chroman formation.

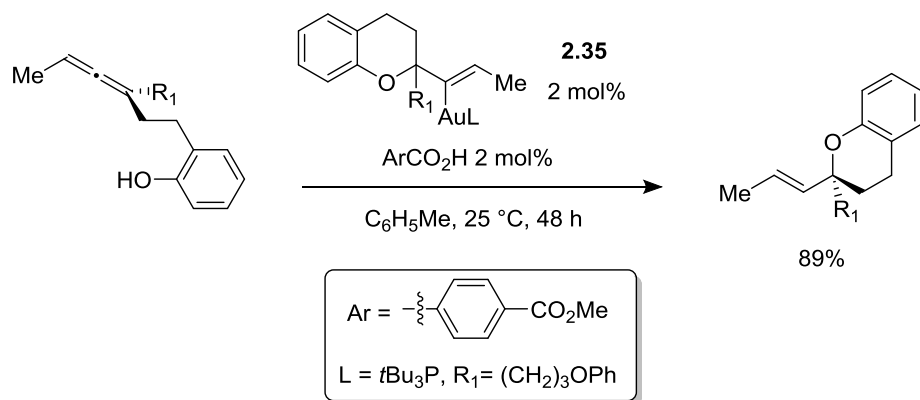
Our first goal in studying the mechanism of chroman formation was to try to identify the resting state of the catalyst and any other relevant catalytic intermediates. We observed the catalytic reaction under standard conditions by using NMR spectroscopy. We were able to identify two resting states in the catalytic reaction, a vinylgold intermediate (**2.35** in scheme 18b) and the gold complex (**2.32** in scheme 18b) using ^{31}P NMR. The reaction mixture remained homogeneous throughout the course of the reaction and no bis(gold) vinyl species (similar to complex **2.36**) was observable.³¹

We were able to independently prepare and characterize the vinyl gold species **2.35** that we observed in the catalytic reaction.³² When the vinyl gold intermediate **2.35** was allowed to react with a stoichiometric amount of mono-methylterephthalic acid, the product **2.20** and the gold complex **2.32** were formed in greater than 95% yield respectively (Scheme 19). Interestingly, no free allene was observable during the course of the reaction, leading us to believe that C-O bond formation is irreversible.



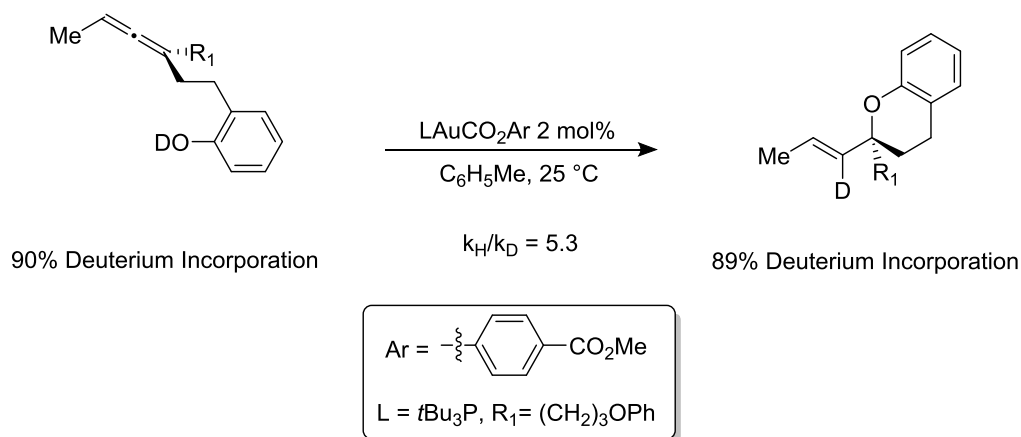
Scheme 19. Protonation of Alkenyl Gold with Mono-methylterephthalic Acid.

When vinyl gold species **2.35** was used as a catalyst in the presence of a catalytic amount of mono-methylterephthalic acid, the product was formed in 89% yield after 48 hours (Scheme 20). The result of this experiment shows that the vinyl gold intermediate **2.35** is catalytically competent.



Scheme 20. Catalytic Competency of Vinyl Gold Intermediate

Lastly, when a deuterated allenyl phenol was prepared and used as a substrate, a KIE of $k_{\text{H}}/k_{\text{D}} = 5.3$ was observed and high deuterium labeling at the vinyl position near the tetrasubstituted stereocenter was measured (Scheme 21).



Scheme 21. Kinetic Isotope Effect Experiment.

Taking into account the work of Widenhoefer and Gagné on furan and pyran formation (described above), the body of literature on gold catalyzed addition of nucleophiles to allenes,³³ and the

observations we made studying the mechanism of gold-catalyzed hydrophenoxylation of allenes, we propose the following catalytic cycle for chroman formation (Scheme 18b). An allene gold complex forms between the gold mono-methylterephthalate catalyst **2.32** and the allene **2.33**. The phenol will then attack the allene forming the vinyl gold intermediate **2.35**. Protonation of the vinyl gold intermediate **2.35** forms the product and reforms the catalyst **2.32**.

Based on the experiments we performed studying the mechanism of hydrophenoxylation of allenes, and what is understood about hydroalkoxylation of allenes, a few points are worth mentioning. 1) Under the standard reaction conditions for hydrophenoxylation, no bis(gold) vinyl intermediate is observable. This is in contrast to the mechanistic observations made regarding the mechanism of pyran and furan formation. We propose that because the gold-terephthalate catalyst is more electron rich than the gold tosylate catalyst, it is less likely that a gold cation will trap the vinyl gold intermediate to form a dimer. A similar trend has been observed in bis(gold) aryl dimers.³⁴ 2) C-O bond formation is irreversible. We believe this to be true because when the vinyl gold intermediate **2.35** is allowed to react with mono-methylterephthalic acid, no free allene is observable (Scheme 19). C-O bond formation is reversible in the case of pyran and furan formation as shown by Widenhoefer and Gagné. We believe this difference arises from the difference in acidity of the conjugate acid of the gold counterions. In the case of furan and pyran formation, TsOH is acidic enough to protonate the vinyl gold ethereal oxygen and eliminate gold cation to form the allene. In the case of chroman formation, the mono-methylterephthalic acid is not acidic enough to protonate the vinyl gold ethereal oxygen, rendering C-O bond formation irreversible. Overall, whether or not C-O bond formation is reversible, high chirality transfer is possible. 3) In the gold-catalyzed allene hydrophenoxylation mechanism, there are two irreversible steps. The reaction itself is not reversible and the C-O bond formation is not reversible. There is no free allene formed when vinyl gold is allowed to react with mono-methylterephthalic acid and both the catalyst **2.32** and vinyl gold intermediate **2.35** are observable during the catalytic reaction. This is a rare scenario in catalytic reactions, but can occur if two steps proceed at about the same rate and the first step is irreversible.

2.7 Conclusions

We have developed a catalytic method to convert enantioenriched trisubstituted allenes containing an alcohol or phenol into enantioenriched cyclic ethers containing an α -tetrasubstituted stereocenter. Our method can be used to prepare highly enantioenriched cyclic ethers such as tetrahydrofurans, tetrahydropyrans, and chromans. Our method is compatible with a variety of common functional groups and substrate substitution patterns. In all cases the enantioenriched cyclic ethers were isolated in high yield and as one diastereomer. This method is especially powerful when used in tandem with the trisubstituted asymmetric allene synthesis described in Chapter 1. Lastly, we studied the mechanism of chroman formation in detail and found that gold-catalyzed allene hydrophenoxylation and hydroalkoxylation proceed under slightly different mechanisms.

2.8 Experimental

2.8.1 General

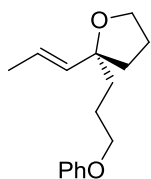
All reactions were performed under a nitrogen atmosphere, using flame-dried glassware unless otherwise indicated. Column chromatography was performed on a Biotage Iso-1SV flash purification system using silica gel (Agela Technologies Inc., 60Å, 40-60 μm , 230-400 mesh). Infrared (IR) spectra were recorded on a Perkin Elmer Spectrum RX I spectrometer. IR peak absorbencies are represented as follows: s = strong, m = medium, w = weak, br = broad. ^1H , ^{13}C , and ^{31}P NMR spectra were recorded on a Bruker AV-300 or AV-500 spectrometer. ^1H NMR chemical shifts (δ) are reported in parts per million (ppm) downfield of TMS and are referenced relative to residual CHCl_3 (7.26 ppm), C_6H_6 (7.16 ppm), or CH_2Cl_2 (5.32 ppm). ^{13}C chemical shifts are reported in parts per million downfield of TMS and are referenced to the carbon resonance of the solvent CDCl_3 (δ 77.16 ppm), C_6D_6 (128.06), or CD_2Cl_2 (54.00). ^{31}P chemical shifts are reported in parts per million downfield of H_3PO_4 and are referenced to the phosphorus resonance of either an internal capillary or external standard of H_3PO_4 (0.00). Data are represented as follows: chemical shift, multiplicity (s = singlet, d = doublet, t = triplet, q = quartet, m = multiplet, bs = broad singlet), integration, and coupling constants in Hertz (Hz). Mass spectra were collected on a JEOL

HX-110 Mass spectrometer, a Bruker Esquire 1100 Liquid Chromatograph – Ion Trap Mass Spectrometer, or a Hewlett Packard 5971A gas chromatograph – Mass Spectrometer. GC analysis was performed on a Shimadzu GC-2010 with a flame ionization detector and a SHRXI-5MS column (15 m x 0.25 mm x 0.25 μm) or for chiral GC analysis, a Supelco Beta DEXTM 120 column (30 m x 0.25 mm x 0.25 μm). Chiral HPLC analysis was performed on a Shimadzu LC-6AD with a SPD-20A UV/Vis-detector and a Daicel Chiralcel OD-H/AD-H column (.46 cm x 25 cm). Preparative-scale HPLC was performed using an Agilent ZORBAX PrepHT CN, 21.2 x 250mm, 7 μm cartridge.

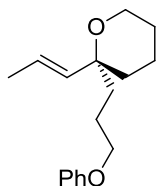
Materials: THF, CH_2Cl_2 , Et_2O and toluene were degassed and dried on columns of neutral alumina. 1,4-dioxane was distilled from purple Na/benzophenone ketyl, and stored over 4 \AA molecular sieves. Deuterated solvents were purchased from Cambridge Isotope Laboratories, Inc., degassed, and dried over 4 \AA molecular sieves. Cy_3PAuCl ,³⁵ $t\text{-Bu}_3\text{PAuOTs}$,²⁷ $\text{AgO}_2\text{CC}_6\text{H}_4(4\text{-CO}_2\text{Me})$,³⁶ and $\text{AgO}_2\text{CC}_6\text{H}_4(4\text{-NO}_2)$ were prepared according to procedures described in existing literature. All other commercial reagents were purchased from AK Scientific, Inc., Oakwood Products, Inc., Sigma-Aldrich Co., STREM Chemicals, Inc., Tokyo Chemical Industry Co., Ltd., or VWR international, LLC. and were used as received.

2.8.2 Cyclization of Enantioenriched Hydroxy Allenes

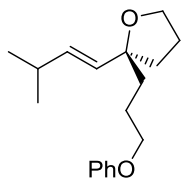
In a nitrogen-filled glovebox, a 1-dram vial was charged with a stir bar, silver(I) tosylate (0.005 mmol, 0.01 equiv), and chlorotri-*t*-butylphosphinegold(I) (0.005 mmol, 0.01 equiv). The mixture was diluted with 0.5 mL toluene, removed from the glove box, and allowed to stir at room temperature for 20 minutes. The catalyst mixture was then poured into a dram vial containing the allenol (0.5 mmol, 1 equiv). The mixture was diluted with 1 mL toluene to reach a final concentration of 0.3 M and allowed to stir at room temperature. After consumption of the starting material, the mixture was poured directly onto a silica gel column and purified with silica gel chromatography.



(*R,E*)-2-(3-phenoxypropyl)-2-(prop-1-en-1-yl)tetrahydrofuran (2.5): Compound was isolated as a clear oil (116 mg, 97% yield, 98:2 er) after purification by silica gel column chromatography (0% → 10% EtOAc/Hex). $[\alpha]_D^{22} = +2.7$ ($c = 0.0058$, CH_2Cl_2). ^1H NMR (300 MHz, CD_2Cl_2) δ 7.29 (t, $J = 7.9$ Hz, 2H), 6.93 (dd, $J = 13.2, 7.6$ Hz, 3H), 5.71 – 5.57 (m, 1H), 5.45 (dd, $J = 15.4, 1.2$ Hz, 1H), 3.96 (td, $J = 6.4, 1.6$ Hz, 3H), 3.84 (t, $J = 6.6$ Hz, 3H), 1.97 – 1.64 (m, 11H). ^{13}C NMR (75 MHz, CD_2Cl_2) δ 159.6, 135.9, 129.8, 123.6, 120.8, 114.8, 84.7, 68.7, 67.7, 37.0, 36.6, 25.8, 25.1, 17.9. GC/MS (EI) calculated for $[\text{M}]^+$ 246.3, found 246.2. FTIR (neat, cm^{-1}): 3027 (w), 2956 (w), 2867 (m), 1890 (w), 1672 (w), 1600 (w), 1497 (w), 1245 (s), 1038 (m), 752 (m). The optical purity was determined by chiral HPLC analysis: Chiralcel OD-H HPLC column, 2% IPA/Hex, 0.25 ml/min, 220 nm detection, $t_{\text{minor}} = 21.2$ minutes, $t_{\text{major}} = 23.9$ minutes.

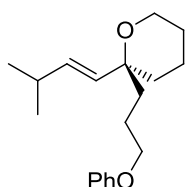


(*R,E*)-2-(3-phenoxypropyl)-2-(prop-1-en-1-yl)tetrahydro-2H-pyran (2.6): Compound was isolated as a clear oil (66 mg, 89% yield, 97:3 er) after purification by silica gel column chromatography (0% → 25% EtOAc/Hex). $[\alpha]_D^{22} = +24.9$ ($c = 0.005$, CH_2Cl_2). ^1H NMR (300 MHz, C_6D_6) δ 7.27 – 7.05 (m, 2H, C_6H_6 overlap), 6.86 (dd, $J = 13.7, 7.5$ Hz, 3H), 5.49 (dq, $J = 15.8, 6.4$ Hz, 1H), 5.29 (dd, $J = 15.9, 1.3$ Hz, 1H), 3.69 (t, $J = 6.1$ Hz, 2H), 3.65 – 3.56 (m, 2H), 1.97 – 1.71 (m, 3H), 1.75–1.50 (m, 5H), 1.48 – 1.33 (m, 4H), 1.25 (bs, 1H). ^{13}C NMR (75 MHz, CD_2Cl_2) δ 159.7, 135.2, 129.8, 126.5, 120.8, 114.9, 76.1, 68.8, 62.6, 38.6, 34.8, 26.8, 23.7, 20.3, 18.2. GC/MS (EI) calculated for $[\text{M}]^+$ 260.4, found 260.1. FTIR (neat, cm^{-1}): 3026 (w), 2937 (w), 2861 (m), 1927 (m), 1833 (m), 1769 (s), 1599 (s), 1495 (m), 1245 (m), 1080 (m), 750 (m). The optical purity was determined by chiral HPLC analysis: Chiralcel OD-H HPLC column, 5% IPA/Hex, 1.0 ml/min, 254 nm detection, $t_{\text{minor}} = 4.7$ minutes, $t_{\text{major}} = 4.3$ minutes.



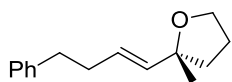
(*S,E*)-2-(3-methylbut-1-en-1-yl)-2-(3-phenoxypropyl)tetrahydrofuran (2.7): Compound was isolated as a clear oil (94 mg, 94% yield, 97:3 er) after purification by silica gel column chromatography (0% → 20% EtOAc/Hex). $[\alpha]_D^{22} = +3.4$ ($c = 0.009$, CH_2Cl_2). ^1H NMR (300 MHz, CD_2Cl_2) δ 7.27 (t, $J = 8.0$ Hz, 2H), 6.91 (dd, $J = 13.7, 7.5$ Hz, 3H), 5.58 (dd,

$J = 15.6, 6.6$ Hz, 1H), 5.35 (d, $J = 15.6$ Hz, 1H), 3.96 (dd, $J = 8.9, 3.9$ Hz, 2H), 3.82 (dd, $J = 8.4, 4.8$ Hz, 2H), 2.40 – 2.18 (m, $J = 7.7$ Hz, 1H), 1.95 – 1.62 (m, 8H), 1.00 (d, $J = 6.7$ Hz, 6H). ^{13}C NMR (75 MHz, CD_2Cl_2) δ 159.5, 136.1, 131.4, 129.7, 120.7, 114.7, 84.7, 68.6, 67.6, 37.0, 36.6, 31.1, 25.7, 25.0, 22.8. GC/MS (EI) calculated for $[\text{M}]^+$ 274.4, found 274.2. FTIR (neat, cm^{-1}): 3037 (w), 2926 (s), 2858 (s), 2074 (w), 1929 (w), 1834 (w), 1599 (s), 1495 (s), 1240 (m), 1042 (m), 754 (m). The optical purity was determined by chiral HPLC analysis: Chiralcel OD-H HPLC column, 2% IPA/Hex, 0.25 ml/min, 254 nm detection, $t_{\text{minor}} = 18.1$ minutes, $t_{\text{major}} = 20.5$ minutes.



(*S,E*)-2-(3-methylbut-1-en-1-yl)-2-(3-phenoxypropyl)tetrahydro-2H-pyran (2.10):

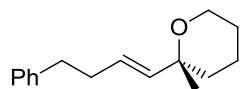
Compound was isolated as a clear oil (47 mg, 75% yield, 98:2 er) after purification by silica gel column chromatography (0% → 20% EtOAc/Hex). $[\alpha]_{\text{D}}^{22} = +19.9$ ($c = 0.009$, CH_2Cl_2). ^1H NMR (300 MHz, C_6D_6) δ 7.22 – 7.07 (m, 2H, C_6H_6 overlap), 7.00 – 6.75 (m, 3H), 5.54 (dd, $J = 16.1, 6.8$ Hz, 1H), 5.25 (d, $J = 16.1$ Hz, 1H), 3.70 (t, $J = 5.8$ Hz, 2H), 3.68-3.55 (m, 2H), 2.45 – 2.20 (m, 1H), 1.99 – 1.71 (m, 3H), 1.64 – 1.50 (m, 2H), 1.48 – 1.29 (m, 4H), 1.27 – 1.12 (m, 1H), 0.97 (d, $J = 6.7$ Hz, 6H). ^{13}C NMR (75 MHz, C_6D_6) δ 159.8, 138.6, 131.1, 129.7, 120.7, 114.9, 75.7, 68.4, 62.6, 38.8, 34.4, 31.6, 26.7, 23.7, 22.9, 20.3. ESI MS calculated for $[\text{M} + \text{Na}]^+$ 311.4, found 311.5. FTIR (neat, cm^{-1}): 3093 (w), 2953 (s), 2280 (m), 1924 (w), 1833 (w), 1601 (s), 1497 (s), 1245 (m), 1081(m), 752 (m). The optical purity was determined by chiral HPLC analysis: Chiralcel OD-H HPLC column, 2% IPA/Hex, 0.25 ml/min, 220 nm detection, $t_{\text{minor}} = 19.1$ minutes, $t_{\text{major}} = 17.9$ minutes.



(*R,E*)-2-methyl-2-(4-phenylbut-1-en-1-yl)tetrahydrofuran (2.8): Compound was

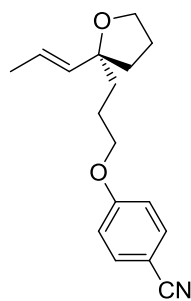
isolated as a clear oil (84 mg, 85% yield, 96:4 er) after purification by silica gel column chromatography (0% → 25% EtOAc/Hex). $[\alpha]_{\text{D}}^{22} = -10.5$ ($c = 0.008$, CH_2Cl_2). ^1H NMR (300 MHz, C_6D_6) δ 7.11 – 6.99 (m, 2H, C_6H_6 overlap), 5.70 (dt, $J = 15.4, 6.7$ Hz, 3H), 5.43 (dd, $J = 15.4, 1.1$ Hz, 1H), 3.75 (td, $J = 7.2, 2.3$ Hz, 2H), 2.56 (t, $J = 7.6$ Hz, 2H), 2.25 (dd, $J = 14.4, 7.3$ Hz, 2H), 1.68 – 1.51 (m,

3H), 1.46 – 1.35 (m, 1H), 1.29 (s, 3H). ^{13}C NMR (75 MHz, CD_2Cl_2) δ 142.6, 136.9, 128.9, 128.6, 126.9, 126.1, 82.2, 67.6, 38.0, 36.3, 34.5, 26.8, 26.1. GC/MS (EI) calculated for $[\text{M}]^+$ 216.3, found 216.1. FTIR (neat, cm^{-1}): 3075 (w), 2962 (w), 1943 (w), 1877 (w), 1797 (w), 1495 (m), 1452 (m), 1037 (s), 740(s). The optical purity was determined by chiral HPLC analysis: Chiralcel AD-H HPLC column, 100 %Hex, 1.5 ml/min, 215 nm detection, $t_{\text{minor}} = 8.4$ minutes, $t_{\text{major}} = 8.7$ minutes.



(*R,E*)-2-methyl-2-(4-phenylbut-1-en-1-yl)tetrahydro-2H-pyran (2.9):

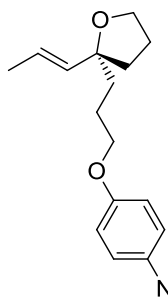
Compound was isolated as a clear oil (99 mg, 92% yield, (95:5 er) after purification by silica gel column chromatography (0% → 15% EtOAc/Hex). $[\alpha]_{\text{D}}^{22} = -33.1$ ($c = 0.099$, CH_2Cl_2). ^1H NMR (300 MHz, C_6D_6) δ 7.29 – 7.11 (m, 2H, C_6H_6 overlap), 7.06 (t, $J = 6.8$ Hz, 3H), 5.52 (dd, $J = 14.5$, 7.9 Hz, 1H), 5.38 (d, $J = 16.0$ Hz, 1H), 3.70 – 3.59 (m, 1H), 3.55 – 3.41 (m, 1H), 2.56 (t, $J = 7.5$ Hz, 2H), 2.27 (dd, $J = 14.6$, 6.9 Hz, 2H), 1.66 – 1.46 (m, 1H), 1.37 (d, $J = 6.2$ Hz, 4H), 1.29 – 1.09 (m, 4H). ^{13}C NMR (75 MHz, CD_2Cl_2) δ 142.4, 136.4, 129.4, 128.9, 128.6, 126.1, 73.9, 62.6, 36.3, 35.5, 34.9, 29.4, 26.5, 20.4. ESI MS calculated for $[\text{M} + \text{Na}]^+$ 253.3, found 253.3. FTIR (neat, cm^{-1}): 3010 (w), 2934(s), 2849 (m), 1948 (w), 1867 (w), 1797 (w), 1655 (w), 1452 (m), 1080 (s), 967 (m). The optical purity was determined by chiral HPLC analysis: Chiralcel OD-H HPLC column, 100 % Hex, 0.9 ml/min, 215 nm detection, $t_{\text{minor}} = 13.8$ minutes, $t_{\text{major}} = 12.6$ minutes.



(*R,E*)-4-(3-(2-(prop-1-en-1-yl)tetrahydrofuran-2-yl)propoxy)benzotrile (2.11):

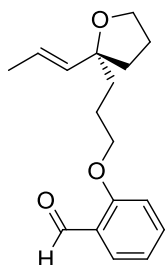
Compound was isolated as a white solid (79 mg, 96% yield, 95:5 er) after purification by silica gel column chromatography (0% → 40% EtOAc/Hex). $[\alpha]_{\text{D}}^{22} = -6.9$ ($c = 0.007$, CH_2Cl_2). ^1H NMR (300 MHz, C_6D_6) δ 7.05 (d, $J = 7.7$ Hz, 2H), 6.44 – 6.37 (m, 2H), 5.66 (dq, $J = 15.2$, 6.5 Hz, 1H), 5.29 (dd, $J = 15.3$, 1.4 Hz, 1H), 3.79 – 3.63 (m, 2H), 3.54 – 3.42 (m, 2H), 2.09 – 1.11 (m, 11H). ^{13}C NMR (75 MHz, C_6D_6) δ 162.4, 135.9, 133.9, 123.4, 119.3, 115.2, 104.4, 84.4, 68.7, 67.6, 37.0, 36.8, 25.6, 24.7, 17.7. GC/MS (EI) calculated for $[\text{M}]^+$ 271.4, found 271.4. FTIR (neat, cm^{-1}): 3082 (w), 2962 (m), 2858 (m), 2217 (m), 1869 (w), 1764 (w), 1665 (w), 1603 (s), 1504 (s), 1259 (m), 830 (w). The optical purity was determined by chiral HPLC analysis: Chiralcel

OD-H HPLC column, 5% IPA/Hex, 1.0 ml/min, 254 nm detection, $t_{\text{minor}} = 7.6$ minutes, $t_{\text{major}} = 8.7$ minutes.



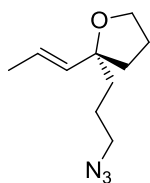
(*R,E*)-2-(3-(4-nitrophenoxy)propyl)-2-(prop-1-en-1-yl)tetrahydrofuran (2.12):

Compound was isolated as a light yellow solid (90 mg, 77% yield, 93:7 er) after purification by silica gel column chromatography (0% → 40% EtOAc/Hex). $[\alpha]_{\text{D}}^{22} = -8.9$ ($c = 0.006$, CH_2Cl_2). $^1\text{H NMR}$ (300 MHz, C_6D_6) δ 7.90 (d, $J = 9.2$ Hz, 2H), 6.35 (d, $J = 9.2$ Hz, 2H), 5.69 (dq, $J = 15.2, 6.5$ Hz, 1H), 5.30 (dd, $J = 15.3, 1.6$ Hz, 1H), 3.80 – 3.63 (m, 2H), 3.52 – 3.34 (m, 2H), 1.96 – 1.30 (m, 11H). $^{13}\text{C NMR}$ (75 MHz, C_6D_6) δ 164.1, 141.8, 135.9, 125.9, 123.5, 114.4, 84.4, 69.1, 67.6, 37.0, 36.8, 25.6, 24.6, 17.7. ESI MS calculated for $[\text{M} + \text{Na}]^+$ 314.3, found 314.3. FTIR (neat, cm^{-1}): 3113 (w), 2926 (m), 2867 (m), 2443 (2), 1901 (w), 1759 (w), 1589 (s), 1504 (s), 1259 (m), 1108 (m), 735 (m). The optical purity was determined by chiral HPLC analysis: Chiralcel OD-H HPLC column, 5% IPA/Hex, 1.0 ml/min, 254 nm detection, $t_{\text{minor}} = 7.9$ minutes, $t_{\text{major}} = 9.1$ minutes.

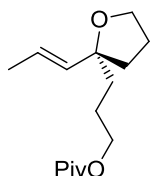


(*R,E*)-2-(3-(2-(prop-1-en-1-yl)tetrahydrofuran-2-yl)propoxy)benzaldehyde (2.13):

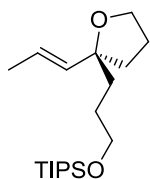
Compound was isolated as a clear oil (78 mg, 92% yield, 96:4 er) after purification by silica gel column chromatography (0% → 40% EtOAc/Hex). $[\alpha]_{\text{D}}^{22} = -9.1$ ($c = 0.007$, CH_2Cl_2). $^1\text{H NMR}$ (300 MHz, C_6D_6) δ 10.76 (s, 1H), 8.00 (dd, $J = 7.7, 1.6$ Hz, 1H), 7.11 – 7.02 (m, 1H), 6.67 (t, $J = 7.5$ Hz, 1H), 6.47 (d, $J = 8.4$ Hz, 1H), 5.76 – 5.60 (m, 1H), 5.31 (dd, $J = 15.3, 1.4$ Hz, 1H), 3.80 – 3.64 (m, 2H), 3.57 (td, $J = 6.5, 3.0$ Hz, 2H), 1.92 – 1.33 (m, 11H). $^{13}\text{C NMR}$ (75 MHz, CD_2Cl_2) δ 190.0, 162.1, 136.2, 135.7, 128.2, 125.4, 123.7, 120.7, 113.1, 84.7, 69.4, 67.7, 36.9, 36.7, 25.7, 24.9, 17.8. GC/MS (EI) calculated for $[\text{M}]^+$ 274.4, found 274.4. FTIR (neat, cm^{-1}): 3082 (w), 2943 (s), 2867 (m), 1688 (s), 1485 (s), 1287 (m), 1042 (w), 977 (m), 764(m). The optical purity was determined by chiral HPLC analysis: Chiralcel OD-H HPLC column, 5% IPA/Hex, 0.5 ml/min, 254 nm detection, $t_{\text{minor}} = 7.6$ minutes, $t_{\text{major}} = 8.7$ minutes.



(*S,E*)-2-(3-azidopropyl)-2-(prop-1-en-1-yl)tetrahydrofuran (2.14): Compound was isolated as a clear oil (47 mg, 92% yield, 98:2 er) after purification by silica gel column chromatography (0% → 30% EtOAc/Hex). $[\alpha]_D^{22} = -11.4$ ($c = 0.0045$, CH_2Cl_2). ^1H NMR (300 MHz, C_6D_6) δ 5.63 (dq, $J = 19.5, 6.5$ Hz, 1H), 5.22 (dd, $J = 15.3, 1.4$ Hz, 1H), 3.74 – 3.60 (m, 2H), 2.79 (t, $J = 6.0$ Hz, 2H), 1.67 – 1.24 (m, 11H). ^{13}C NMR (75 MHz, C_6D_6) δ 135.8, 123.3, 84.3, 67.5, 51.9, 37.5, 36.9, 25.5, 24.5, 17.7. ESI MS calculated for $[\text{M} + \text{Na}]^+$ 218.3, found 218.3. FTIR (neat, cm^{-1}): 2926 (m), 2094 (m), 1268 (m), 1259 (m), 764 (m), 731 (s). The optical purity was determined by chiral HPLC analysis of the *p*-nitrobenzene amide³⁷: Chiralcel OD-H HPLC column, 5% IPA/Hex, 0.25 ml/min, 254 nm detection, $t_{\text{minor}} = 171$ minutes, $t_{\text{major}} = 162$ minutes.

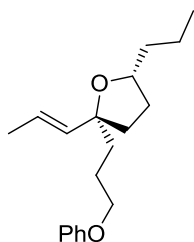


(*R,E*)-3-(2-(prop-1-en-1-yl)tetrahydrofuran-2-yl)propyl pivalate (2.15): Compound was isolated as a clear oil (92 mg, 88% yield, >99:1 er) after purification by silica gel column chromatography (0% → 10% EtOAc/Hex). $[\alpha]_D^{22} = -5.3$ ($c = 0.0085$, CH_2Cl_2). ^1H NMR (300 MHz, C_6D_6) δ 5.64 (dq, $J = 15.3, 6.5$ Hz, 1H), 5.28 (dd, $J = 15.3, 1.5$ Hz, 1H), 4.06 (t, $J = 6.7$ Hz, 2H), 3.78 – 3.59 (m, 2H), 1.82 – 1.34 (m, 11H), 1.16 (s, 9H). ^{13}C NMR (75 MHz, C_6D_6) δ 177.7, 136.0, 123.3, 84.3, 67.5, 64.9, 38.8, 36.9, 36.8, 27.4, 25.6, 24.5, 17.7. GC/MS (EI) calculated for $[\text{M}]^+$ 254.4, found 254.4. FTIR (neat, cm^{-1}): 2962 (s), 2867 (m), 1726 (s), 1481 (w), 1283 (m), 1160 (s), 1042 (m). The optical purity was determined by chiral HPLC analysis of the *p*-nitrobenzoate ester³⁸: Chiralcel OD-H HPLC column, 5% IPA/Hex, 1.0 ml/min, 254 nm detection, $t_{\text{minor}} = 9.4$ minutes, $t_{\text{major}} = 7.5$ minutes.



(*S,E*)-triisopropyl(3-(2-(prop-1-en-1-yl)tetrahydrofuran-2-yl)propoxy)silane (2.16): Compound was isolated as a clear oil (119 mg, 99% yield, 95:5 er) after purification by silica gel column chromatography (0% → 20% EtOAc/Hex). $[\alpha]_D^{22} = -13.0$ ($c = 0.0053$, CH_2Cl_2). ^1H NMR (300 MHz, C_6D_6) δ 5.89 – 5.56 (m, 1H), 5.40 (dd, $J = 15.3, 1.5$ Hz, 1H), 3.94 – 3.54 (m, 4H), 1.75 (dd, $J = 10.1, 3.3$ Hz, 4H), 1.67 – 1.41 (m, 7H), 1.25 – 0.88 (m, 21H). ^{13}C NMR (75 MHz, C_6D_6) δ 136.5, 123.0, 84.7, 67.4, 64.3, 37.3, 36.8, 28.8, 25.7, 18.3, 17.8, 12.4. ESI MS calculated for $[\text{M} +$

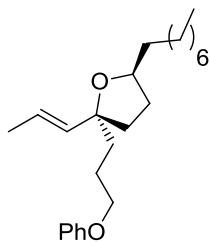
Na]⁺ 349.6, found 349.6. FTIR (neat, cm⁻¹): 2934 (s), 2058 (s), 1457 (m), 1099 (s), 877 (m), 674 (m). The optical purity was determined by chiral HPLC analysis of the *p*-nitrobenzoate ester³⁹: Chiralcel OD-H HPLC column, 100 % Hex, 0.9 ml/min, 254 nm detection, *t*_{minor} = 10.1 minutes, *t*_{major} = 8.1 minutes.



(2*S*,5*R*)-2-(3-phenoxypropyl)-2-((*E*)-prop-1-en-1-yl)-5-propyltetrahydrofuran

(2.17): Compound was isolated as a clear oil (124 mg, 91% yield, 95:5 dr) after purification by silica gel column chromatography (0% → 10% EtOAc/Hex). $[\alpha]_D^{22} =$

11.4 (*c* = 0.0092, CH₂Cl₂). dr = 1:1. ¹H NMR (500 MHz, C₆D₆) δ 7.23 – 7.10 (m, 2H, C₆H₆ overlap), 6.90 (dd, *J* = 7.8, 6.0 Hz, 4H), 6.85 (t, *J* = 7.3 Hz, 2H), 5.79 (dq, *J* = 15.3, 6.5 Hz, 1H), 5.70 (dq, *J* = 16.6, 6.5 Hz, 1H), 5.43 (dd, *J* = 15.2, 1.6 Hz, 1H), 5.37 (dd, *J* = 15.3, 1.6 Hz, 1H), 3.96 – 3.87 (m, 1H), 3.87 – 3.80 (m, 1H), 3.79 – 3.66 (m, 4H), 2.07 – 1.27 (m, 32H), 0.92 (t, *J* = 7.2 Hz, 6H). dr = 1:1 ¹³C NMR (75 MHz, CD₂Cl₂) δ 159.6, 137.3, 136.5, 129.8, 123.2, 123.0, 120.7, 114.8, 84.6, 84.5, 79.7, 78.7, 68.7, 68.7, 39.1, 38.9, 37.9, 37.5, 37.2, 36.1, 31.8, 31.5, 25.0, 25.0, 20.1, 19.9, 17.9, 14.5. dr = 20:1 ¹H NMR (500 MHz, C₆D₆) δ 7.25 – 7.7.10 (m, 5H C₆H₆ overlap), 6.89 (d, *J* = 7.8 Hz, 2H), 6.84 (t, *J* = 7.3 Hz, 1H), 5.70 (dq, *J* = 15.2, 6.5 Hz, 1H), 5.36 (dd, *J* = 15.3, 1.6 Hz, 1H), 3.94 – 3.86 (m, 1H), 3.79 – 3.65 (m, 2H), 1.98 – 1.80 (m, 2H), 1.81 – 1.70 (m, 1H), 1.70 – 1.51 (m, 8H), 1.50 – 1.45 (m, 1H), 1.42 – 1.26 (m, 3H), 0.91 (dd, *J* = 9.2, 5.2 Hz, 3H). dr = 20:1 ¹³C NMR (75 MHz, CD₂Cl₂) δ 159.7, 136.5, 129.8, 123.0, 120.7, 114.8, 84.6, 78.7, 68.7, 39.1, 37.9, 36.1, 31.5, 25.0, 19.9, 17.8, 14.5. GC/MS (EI) calculated for [M]⁺ 288.4, found 288.1. FTIR (neat, cm⁻¹): 3028 (w), 2934 (w), 2858 (m), 1919 (w), 1834 (w), 1759 (w), 1599 (s), 1495 (s), 1240 (s), 1037 (m), 754 (m).

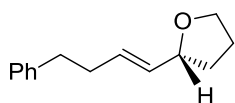


(2*S*,5*S*)-2-(3-phenoxypropyl)-2-((*E*)-prop-1-en-1-yl)-5-octyltetrahydrofuran

(2.18): Compound was isolated as a clear oil (135 mg, 97% yield, 85:15 dr) after purification by silica gel column chromatography (0% → 10% EtOAc/Hex). $[\alpha]_D^{22} =$

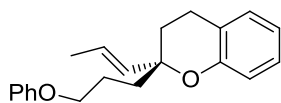
15.0 (*c* = 0.014, CH₂Cl₂). ¹H NMR (500 MHz, C₆D₆) δ 7.25 – 7.00 (m, 2H, C₆H₆ overlap), 6.91 (d, *J* = 7.8 Hz, 2H), 6.85 (t, *J* = 7.3 Hz, 1H), 5.83 (dq, *J* = 13.1, 6.5 Hz, 1H), 5.45 (dd, *J* = 15.2, 1.6 Hz, 1H), 3.88 (dt, *J* = 12.0, 5.2 Hz, 1H), 3.80 – 3.68 (m, 1H), 2.01 – 1.55 (m, 16H), 1.55 – 1.15

(m, 15H, minor impurity), 0.91 (t, $J = 6.9$ Hz, 3H). ^{13}C NMR (126 MHz, C_6D_6) δ 159.9, 137.6, 136.7, 129.7, 128.4, 128.0, 123.0, 120.7, 114.9, 84.4, 79.7, 78.8, 68.3, 38.2, 37.8, 37.5, 37.0, 36.8, 36.4, 32.4, 31.8, 30.3, 30.1, 29.8, 27.1, 26.9, 25.1, 25.0, 23.1, 17.8, 14.4. ESI MS calculated for $[\text{M} + \text{Na}]^+$ 381.5, found 381.5. FTIR (neat, cm^{-1}): 3028 (w), 2934 (s), 2858 (s), 2280(w), 1834 (w), 1765 (w), 1601 (m), 1497 (m), 1245 (s), 1034 (m), 754 (m). The diastereomeric ratio was determined by GC analysis: SHRXI-5MS column, $t_{\text{minor}} = 27.68$ minutes, $t_{\text{major}} = 28.36$ minutes.



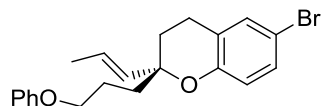
(*R,E*)-2-(4-phenylbut-1-en-1-yl)tetrahydrofuran (2.9): Compound was isolated as a clear oil (19 mg, 95% yield, 99:1 er) after purification by silica gel column chromatography (0% \rightarrow 20% EtOAc/Hex). $[\alpha]_{\text{D}}^{22} = -26.3$ ($c = 0.002$, CH_2Cl_2). ^1H NMR (300 MHz, C_6D_6) δ 7.47 – 6.71 (m, 5H), 5.67 (dtd, $J = 15.3, 6.5, 0.8$ Hz, 1H), 5.50 (ddt, $J = 15.3, 6.4, 1.2$ Hz, 1H), 4.18 (q, $J = 6.8$ Hz, 1H), 3.77 (td, $J = 7.7, 6.1$ Hz, 1H), 3.60 (td, $J = 7.8, 6.1$ Hz, 1H), 2.61 – 2.42 (m, 2H), 2.32 – 2.10 (m, 2H), 1.75 – 1.23 (m, 4H). ^{13}C NMR (75 MHz, C_6D_6) δ 142.1, 132.5, 130.5, 128.8, 128.6, 126.1, 79.7, 67.8, 36.0, 34.5, 32.6, 26.0. ESI MS calculated for $[\text{M} + \text{Na}]^+$ 225.3, found 225.3. FTIR (neat, cm^{-1}): 3082 (w), 2928 (s), 2236 (w), 1945 (w), 1804 (w), 1496 (m), 1453 (s), 1052 (s). The optical purity was determined by chiral HPLC analysis: Chiralcel OD-H HPLC column, 100 % Hex, 1.5 ml/min, 215 nm detection, $t_{\text{minor}} = 23.3$ minutes, $t_{\text{major}} = 18.7$ minutes.

2.8.3 Cyclization of Enantioenriched Phenoxy Allenes



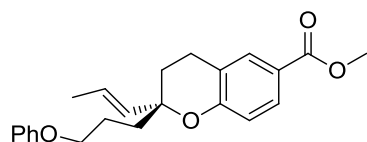
(*R,E*)-2-(3-phenoxypropyl)-2-(prop-1-en-1-yl)chroman (2.20): In a nitrogen-filled glovebox and in the dark, $t\text{-Bu}_3\text{PAuCl}$ (4.3 mg, 0.01 mmol, 0.02 equiv) was suspended in 500 μL of dry toluene and added to a vial containing $\text{AgO}_2\text{CC}_6\text{H}_4(4\text{-CO}_2\text{Me})$ (2.9 mg, 0.01 mmol, 0.02 equiv). The resulting mixture was stirred at 25 $^\circ\text{C}$ for 15 minutes, at which point it turned cloudy and slightly purple. At this point, the mixture was transferred to a vial containing (*S*)-2-(3-(3-phenoxypropyl)hexa-3,4-dien-1-yl)phenol (154 mg, 0.50 mmol, 1.00 equiv). This mixture was stirred

at 25 °C for 24 h, at which point TLC indicated the disappearance of the allene. Other chromans were made analogously. The entire reaction volume was then loaded onto a 10 g silica gel column and chromatographed using a solvent gradient of 0-10% EtOAc in hexanes over 6 column volumes. After washing with PhH (3 mL) to remove residual EtOAc, **(32)** was isolated as a clear, colorless liquid (151 mg, 98% yield, 96:4 er). $[\alpha]_D^{24} = -70^\circ$ (c = 0.007, CH₂Cl₂). ¹H NMR (300 MHz, CD₂Cl₂) δ 7.32 – 7.20 (m, 2H), 7.12 – 6.96 (m, 2H), 6.96 – 6.73 (m, 3H), 6.83 – 6.73 (m, 2H), 5.57 (dq, 2H), 5.40 (dd, *J* = 15.5, 1.4 Hz, 2H), 4.07 – 3.88 (m, 2H), 2.80 – 2.57 (m, 2H), 2.07 – 1.72 (m, 2H), 1.65 (dd, *J* = 6.3, 1.3 Hz, 3H). ¹³C NMR (75 MHz, CD₂Cl₂) δ 159.6, 154.6, 133.2, 129.8, 129.7, 127.6, 126.2, 122.4, 120.8, 120.0, 117.0, 114.8, 78.7, 68.5, 37.4, 31.1, 23.9, 22.7, 18.0. GC/MS calculated for [M]⁺ 308.4, found 308.2. FTIR (neat, cm⁻¹): 3037 (m), 2937 (s), 2359 (w), 1929 (w), 1777 (w), 1673 (w), 1600 (s), 1485 (s), 1456 (s), 1389 (m), 1302 (s), 1241 (s), 1172 (s), 1124 (s), 1040 (s), 969 (s), 882 (m), 753 (s), 695 (s). The optical purity was determined by chiral HPLC analysis: Chiralcel OD-H HPLC column, 5% IPA/Hex, 0.25 ml/min, 220 nm detection, *t*_{minor} = 19.9 minutes, *t*_{major} = 20.7 minutes.



(*S,E*)-6-bromo-2-(3-phenoxypropyl)-2-(prop-1-en-1-yl)chroman (2.22):

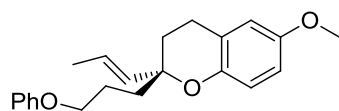
Compound was isolated as a white solid (92 mg, 95% yield over 2 steps, 94:6 er) after chromatography on silica (0 to 10% EtOAc in hexanes) and washing with PhH (3 mL) to remove residual EtOAc. $[\alpha]_D^{24} = -57^\circ$ (c = 0.007, CH₂Cl₂). ¹H NMR (300 MHz, CD₂Cl₂) δ 7.35 – 7.23 (m, 2H), 7.23 – 7.09 (m, 2H), 6.99 – 6.82 (m, 3H), 6.74 (d, *J* = 8.4 Hz, 1H), 5.57 (dq, *J* = 15.4, 6.4 Hz, 1H), 5.38 (dd, *J* = 15.5, 1.5 Hz, 1H), 4.10 – 3.82 (m, 2H), 2.85 – 2.52 (m, 2H), 2.13 – 1.72 (m, 6H), 1.67 (dd, *J* = 6.4, 1.4 Hz, 3H). ¹³C NMR (75 MHz, CD₂Cl₂) δ 159.5, 153.8, 132.6, 132.2, 130.3, 129.8, 126.5, 124.8, 120.8, 118.9, 114.8, 111.7, 79.1, 68.4, 37.3, 30.6, 23.8, 22.6, 17.9. GC/MS calculated for [M]⁺ 387.3, found 387.1. FTIR (dry film, cm⁻¹): 3030 (m), 2915 (s), 2358 (w), 1600 (s), 1495 (s), 1243 (s), 814 (m), 751 (m). The optical purity was determined by chiral HPLC analysis: Chiralcel OD-H HPLC column, 5% IPA/Hex, 0.25 ml/min, 220 nm detection, *t*_{minor} = 20.8 minutes, *t*_{major} = 21.8 minutes.



(*R,E*)-methyl 2-(3-phenoxypropyl)-2-(prop-1-en-1-yl)chroman-6-carboxylate (2.24): Compound was isolated as a clear, colorless liquid

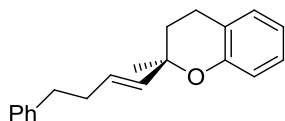
(52 mg, 95% yield, 94:6 er) after chromatography on silica (0 to 10% EtOAc in hexanes) and washing with PhH (3 mL) to remove residual EtOAc. $[\alpha]_D^{24} = -39^\circ$ ($c = 0.004$, CH_2Cl_2). $^1\text{H NMR}$ (300 MHz, CD_2Cl_2) δ 7.80 – 7.72 (m, 2H), 7.32 – 7.22 (m, 2H), 6.98 – 6.80 (m, 4H), 5.55 (dq, $J = 15.4, 6.3$ Hz, 1H), 5.40 (dd, $J = 15.5, 1.3$ Hz, 1H), 4.07 – 3.90 (m, 2H), 3.84 (s, 3H), 2.84 – 2.61 (m, 2H), 2.09 – 1.76 (m, 6H), 1.65 (dd, $J = 6.2, 1.1$ Hz, 3H). $^{13}\text{C NMR}$ (75 MHz, CD_2Cl_2) δ 167.2, 159.5, 158.8, 132.5, 131.8, 129.8, 129.3, 126.6, 122.3, 122.0, 120.8, 117.0, 114.8, 79.9, 68.4, 52.0, 37.4, 30.8, 23.8, 22.6, 17.9. GC/MS calculated for $[\text{M}]^+$ 366.5, found 366.2. FTIR (neat, cm^{-1}): 3030 (m), 2951 (s), 2359 (w), 1701 (s), 1599 (s), 1497 (s), 1437 (s), 1244 (s), 1129 (s), 1038 (s), 973 (s), 883 (m), 835 (s), 738 (s). The optical purity was determined by chiral HPLC analysis: Chiralcel AD-H HPLC column, 5%

IPA/Hex, 0.25 ml/min, 220 nm detection, $t_{\text{minor}} = 37.6$ minutes, $t_{\text{major}} = 40.4$ minutes.



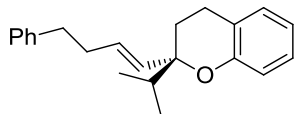
(*R,E*)-6-methoxy-2-(3-phenoxypropyl)-2-(prop-1-en-1-yl)chroman

(2.25): Compound was isolated as a clear, colorless liquid (150 mg, 89% yield, 96:4 er) after chromatography on silica (0 to 10% EtOAc in hexanes) and washing with PhH (3 mL) to remove residual EtOAc. $[\alpha]_D^{24} = -58^\circ$ ($c = 0.005$, CH_2Cl_2). $^1\text{H NMR}$ (300 MHz, CD_2Cl_2) δ 7.34 – 7.19 (m, 2H), 6.98 – 6.79 (m, 3H), 6.73 (d, $J = 8.8$ Hz, 1H), 6.65 (dd, $J = 8.8, 3.0$ Hz, 1H), 6.57 (d, $J = 2.9$ Hz, 1H), 5.57 (dq, $J = 15.5, 6.4$ Hz, 1H), 5.38 (dd, $J = 15.5, 1.5$ Hz, 1H), 4.07 – 3.88 (m, 2H), 3.72 (s, 3H), 2.79 – 2.55 (m, 2H), 2.06 – 1.68 (m, 6H), 1.65 (dd, $J = 6.4, 1.4$ Hz, 3H). $^{13}\text{C NMR}$ (75 MHz, CD_2Cl_2) δ 159.6, 153.4, 148.5, 133.2, 129.8, 126.2, 122.8, 120.8, 117.5, 114.8, 114.1, 113.6, 78.3, 68.5, 55.9, 37.3, 31.0, 23.9, 23.1, 17.9. GC/MS calculated for $[\text{M}]^+$ 338.4, found 338.2. FTIR (neat, cm^{-1}): 3029 (m), 2937 (s), 2359 (w), 1838 (w), 1673 (w), 1599 (s), 1494 (s), 1431 (s), 1389 (m), 1300 (s), 1222 (s), 1042 (s), 969 (s), 813 (s), 755 (s), 695 (s). The optical purity was determined by chiral HPLC analysis: Chiralcel AD-H HPLC column, 5% IPA/Hex, 0.25 ml/min, 220 nm detection, $t_{\text{minor}} = 21.9$ minutes, $t_{\text{major}} = 25.3$ minutes.



(*R,E*)-2-methyl-2-(4-phenylbut-1-en-1-yl)chroman (2.21): Compound was isolated as a clear, colorless liquid (119 mg, 86% yield, 95:5 er) after chromatography on silica (0 to 10% EtOAc in hexanes) and washing with PhH (3 mL) to remove residual EtOAc. $[\alpha]_D^{24} = +43^\circ$ ($c = 0.01$, CH_2Cl_2). $^1\text{H NMR}$ (300 MHz, CD_2Cl_2) δ 7.28 – 7.19 (m, 2H), 7.19 – 6.99 (m, 5H), 6.89 – 6.73 (m, 2H), 5.70 – 5.54 (m, 1H), 5.45 (d, $J = 15.6$ Hz, 1H), 2.66 – 2.57 (m, 4H), 2.37 – 2.22 (m, 2H), 1.92 – 1.69 (m, 2H), 1.37 (s, 3H). $^{13}\text{C NMR}$ (75 MHz, CD_2Cl_2) δ 154.5, 142.2, 134.3, 129.8, 129.2, 128.9, 128.6, 127.5, 126.0, 122.1, 119.9, 117.0, 76.6, 36.1, 34.6, 32.4, 27.8, 22.9. GC/MS calculated for $[\text{M}]^+$ 278.4, found 278.1. FTIR (neat, cm^{-1}): 3061 (s), 2926 (s), 2359 (w), 1610 (m), 1584 (s), 1238 (s), 988 (s), 747 (s). The optical purity was determined by chiral HPLC analysis: Chiralcel OD-

H HPLC column, 5% IPA/Hex, 0.25 ml/min, 220 nm detection, $t_{\text{minor}} = 16.2$ minutes, $t_{\text{major}} = 17.0$ minutes.

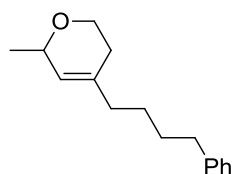
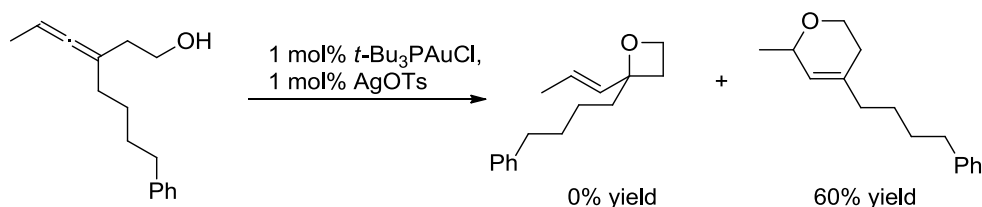


(*R,E*)-2-isopropyl-2-(4-phenylbut-1-en-1-yl)chroman (2.23): Compound was isolated as a clear, colorless liquid (151.9 mg, 84% yield, 91:9 er) after chromatography on silica (0 to 10% EtOAc in hexanes) and washing with PhH (3 mL) to remove residual EtOAc. $[\alpha]_D^{19} = -51^\circ$ ($c = 0.006$, CH_2Cl_2). $^1\text{H NMR}$ (300 MHz, C_6D_6) δ 7.14 – 7.00 (m, 5H), 6.96 (d, $J = 7.3$ Hz, 1H), 6.90 – 6.78 (m, 3H), 5.59 (dt, $J = 15.5$, 6.9 Hz, 1H), 5.09 (dt, $J = 15.5$, 1.3 Hz, 1H), 2.50 – 2.26 (m, 4H), 2.21 – 2.01 (m, 2H), 1.79 (hept, $J = 6.8$ Hz, 1H), 1.61 – 1.40 (m, 2H), 0.99 (d, $J = 6.8$ Hz, 3H), 0.88 (d, $J = 6.9$ Hz, 3H). $^{13}\text{C NMR}$ (75 MHz, CD_2Cl_2) δ 154.8, 142.2, 131.3, 130.6, 129.6, 128.9, 128.6, 127.4, 126.0, 122.6, 119.7, 116.9, 81.3, 37.3, 36.2, 34.8, 27.9, 22.7, 17.5, 16.8. GC/MS calculated for $[\text{M}]^+$ 306.4, found 306.2. FTIR (neat, cm^{-1}): 3062 (m), 3027 (m), 2930 (m), 1942 (w), 1811 (w), 1667 (w), 1607 (m), 1583 (m), 1488 (m), 1455 (m), 1305 (m), 1247 (m), 1113 (m), 975 (m), 750 (m), 699 (m). The optical purity was determined by chiral HPLC analysis: Chiralcel OD-H HPLC column, 0.5% IPA/Hex, 0.25 ml/min, 220 nm detection, $t_{\text{minor}} = 14.0$ minutes, $t_{\text{major}} = 15.0$ minutes.

2.8.4 Attempted Synthesis of Oxetanes and Oxepanes

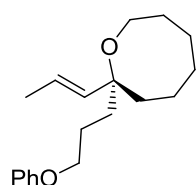
Our attempt at synthesizing oxetanes via the gold-catalyzed 4-*exo* cyclization of tri-substituted hydroxy-allenes resulted only in 6-*endo* cyclization to form the corresponding 5,6-dihydro-2*H*-pyran as shown below.

Attempted Synthesis of Oxetane:



5,6-Dihydro-2-methyl-4-(4-phenylbutyl)-2*H*-pyran : Compound was isolated as a clear oil (60 mg, 60% yield) after purification by silica gel column chromatography (0% → 20% EtOAc/Hex). ¹H NMR (300 MHz, C₆D₆) δ 7.61 – 6.89 (m, 5H), 5.20 (s, 1H), 4.15 – 4.09 (m, 1H), 3.89 (ddd, *J* = 11.1, 5.7, 2.3 Hz, 1H), 3.58 – 3.36 (m, 1H), 2.48 (t, *J* = 7.6 Hz, 2H), 2.09 – 1.93 (m, 1H), 1.83 (t, *J* = 7.5 Hz, 2H), 1.58 – 1.40 (m, 3H), 1.32 (dd, *J* = 15.4, 8.2 Hz, 2H), 1.23 (d, *J* = 6.6 Hz, 3H).

Although we were able to successfully prepare oxepanes via the gold-catalyzed 7-*exo* cyclization of trisubstituted hydroxy-allenes, we were unable to do so with high chirality transfer. Below is an example of an oxepane prepared using the general approach described above:



(*R*)-2-(3-phenoxy-propyl)-2-(prop-1-en-1-yl) oxepane : only with heating at 60 °C for 18 h. Compound was isolated as a clear oil (66 mg, 66% yield, 75:25 er) after purification by silica gel column chromatography (0% → 20% EtOAc/Hex). ¹H NMR

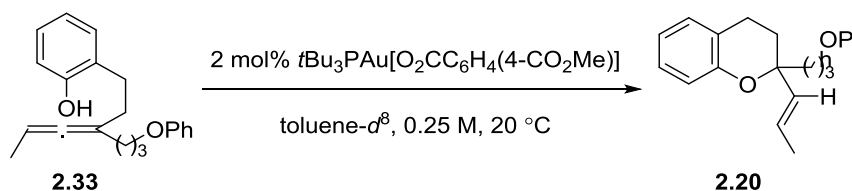
(300 MHz, C₆D₆) δ 7.14 (d, *J* = 9.1 Hz, 20H), 7.00 – 6.69 (m, 3H), 5.71 (dq, *J* = 15.1, 6.3 Hz, 1H), 5.24 (d, *J* = 15.7 Hz, 1H), 3.73 (q, *J* = 6.1 Hz, 2H), 3.45 (dd, *J* = 9.4, 3.8 Hz, 2H), 2.04 – 1.89 (m, 1H), 1.85 – 1.71 (m, 2H), 1.64 (d, *J* = 6.5 Hz, 3H), 1.59 – 1.30 (m, 9H). ¹³C NMR (75 MHz, CD₂Cl₂) δ 159.7, 136.5,

129.7, 124.1, 120.7, 114.8, 79.6, 68.8, 63.5, 39.2, 36.7, 32.3, 30.2, 24.5, 22.8, 18.0. GC/MS (EI) calculated for $[M]^+$ 274.2, found 274.1.

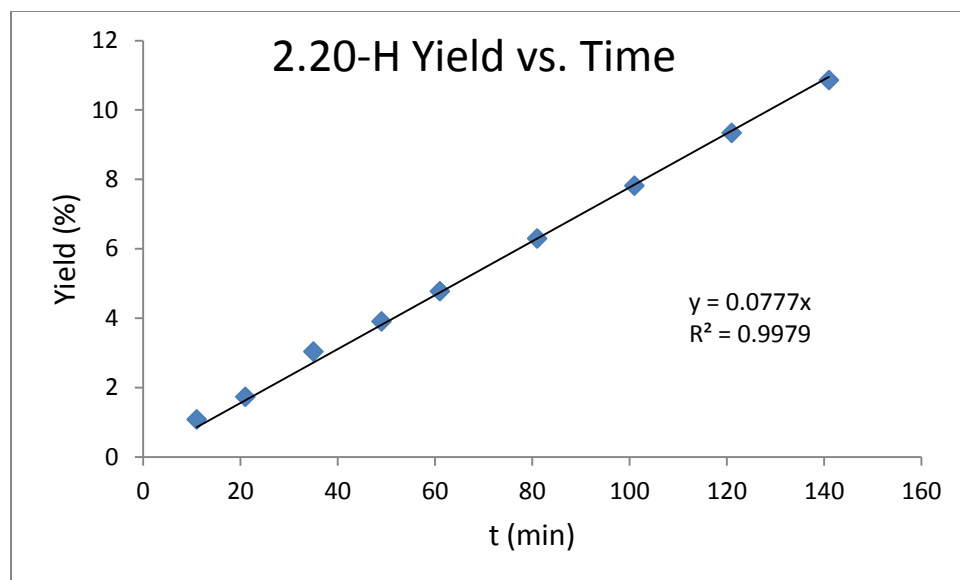
2.8.5 Investigation of Reaction Mechanism

Kinetic Isotope Effect

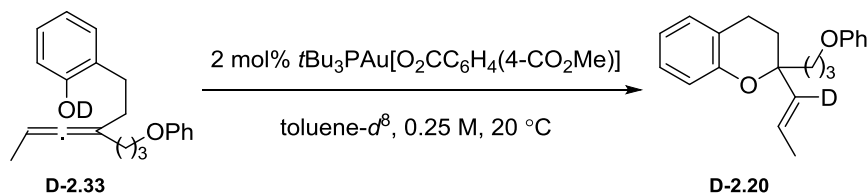
Initial Rate Experiment with Protonated Phenoxy-Allene:



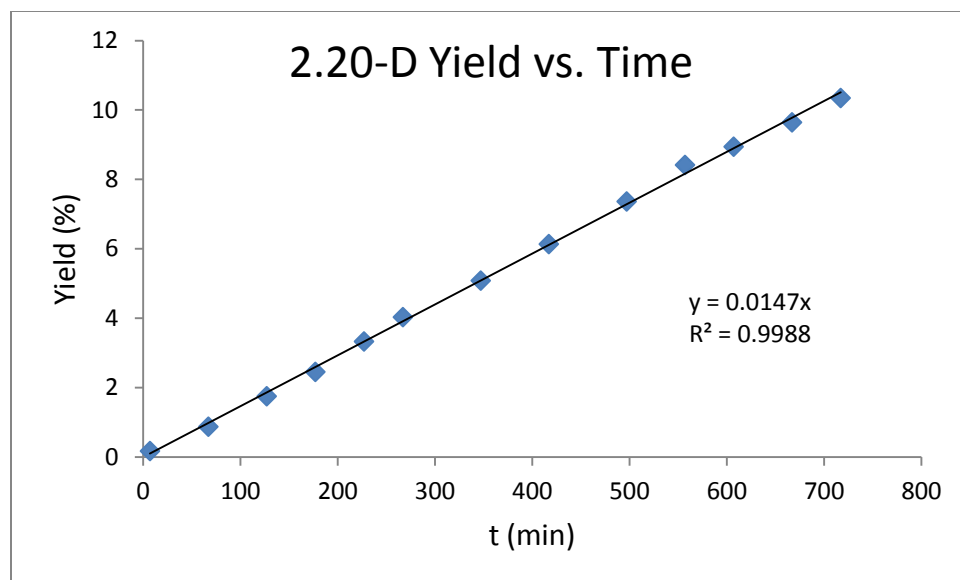
In a nitrogen-filled glovebox, racemic allene-phenol **2.33** (30.8 mg, 0.100 mmol, 1.00 equiv), trimethoxybenzene (8.4 mg, 0.05 mmol, 0.50 equiv), and $\text{toluene-}d^8$ (350 μL) were added to an NMR tube which had been sealed to a vacuum valve with jointed side-arm. The valve was sealed and the apparatus was moved to a Schlenk line outside of the glovebox and placed under nitrogen, and the contents of the NMR tube were frozen in liquid nitrogen. To this was added $t\text{Bu}_3\text{PAu}[\text{O}_2\text{CC}_6\text{H}_4(4\text{-CO}_2\text{Me})]$ (1.2 mg, 0.002 mmol, 0.02 equiv) as a solution in $\text{toluene-}d^8$ (50 μL). Once the solution of catalyst was also frozen, the tube was placed under vacuum and flame-sealed. The contents of the tube remained frozen until just before the NMR experiment was begun. The reaction progress was monitored by ^1H NMR and the initial rate was measured (0-10% yield) by comparison of peak areas corresponding to the aromatic protons of trimethoxybenzene and the downfield vinylic proton of **2.20**. The temperature of the probe was measured at 293 K throughout the initial rate experiment.



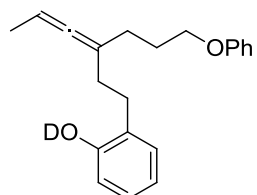
Initial Rate Experiment with Deuterated Phenoxy-Allene



This experiment was performed exactly as described for the experiment described above, except that all glassware had been washed with D_2O and dried in an oven prior to use. A comparison of initial rates for the proteo- and deuterio- cases afforded a measurement of kinetic isotope effect of 5.3. Based on comparison of peak areas between the vinylic protons of the chroman product, deuterium incorporation of (**D-2.20**) was determined to be 89% at 96% yield.

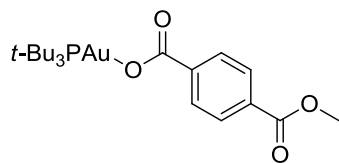


Synthesis of Deuterium-Labeled Phenoxy-Allene



2-(3-(3-phenoxypropyl)hexa-3,4-dien-1-yl)phenol-OD (2.20-D): All steps were performed with glassware that had been rinsed with D₂O and dried for at least 8 hours in an electric oven. In a nitrogen-filled glovebox, 2-(3-(3-phenoxypropyl)hexa-3,4-dien-1-yl)phenol (247 mg, 0.800 mmol, 1.00 equiv) was combined with degassed D₂O (490 μL) in a scintillation vial which was sealed with a PTFE-line cap and stirred vigorously for 2 h at 110 °C. At this point, the mixture was cooled and extracted once with Et₂O (2 mL). The aqueous layer was removed and discarded, and the Et₂O layer was concentrated under vacuum. This process was repeated 4 times. At this point, the resulting residue was suspended in C₆D₆ and concentrated under vacuum for 18 h to afford a clear, colorless oil (220 mg, 89% yield, 97% deuterium enrichment). ¹H NMR (500 MHz, C₆D₆) δ 7.21 – 7.12 (m, 2H), 7.07 (dd, *J* = 7.5, 1.5 Hz, 1H), 7.00 – 6.94 (m, 1H), 6.94 – 6.85 (m, 3H), 6.85 – 6.80 (m, 1H), 6.27 (d, *J* = 7.9 Hz, 1H), 5.19 – 4.99 (m, 1H), 3.73 (t, *J* = 6.4 Hz, 2H), 2.94 – 2.78 (m, 2H), 2.29 (td, *J* = 7.9, 2.9 Hz, 2H), 2.15 – 1.99 (m, 2H), 1.98 – 1.82 (m, 2H), 1.52 (d, *J* = 6.8 Hz, 3H).

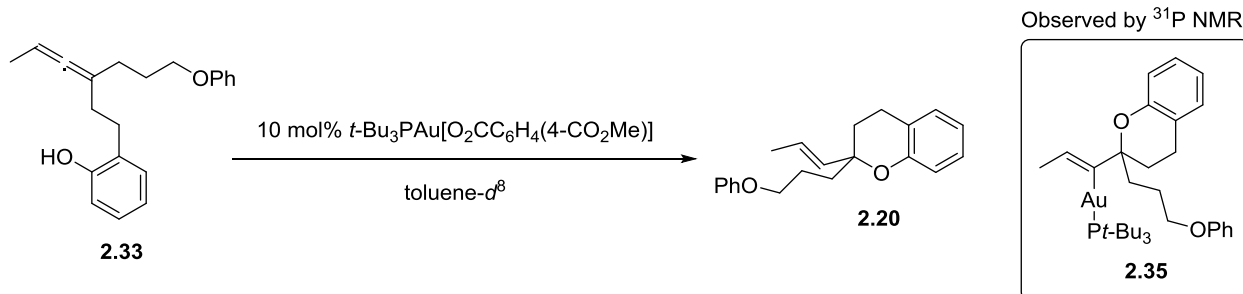
Synthesis of *t*-Bu₃PAu[O₂CC₆H₄(4-CO₂Me)]



***t*-Bu₃PAu[O₂CC₆H₄(4-CO₂Me)] (2.32):** In a nitrogen-filled glovebox, a 1-dram vial was charged with *t*-Bu₃PAuCl (278 mg, 0.62 mmol, 1.0 equiv), AgO₂CC₆H₄(4-CO₂Me) (178 mg, 0.62 mmols, 1.0 equiv), and a stir bar.

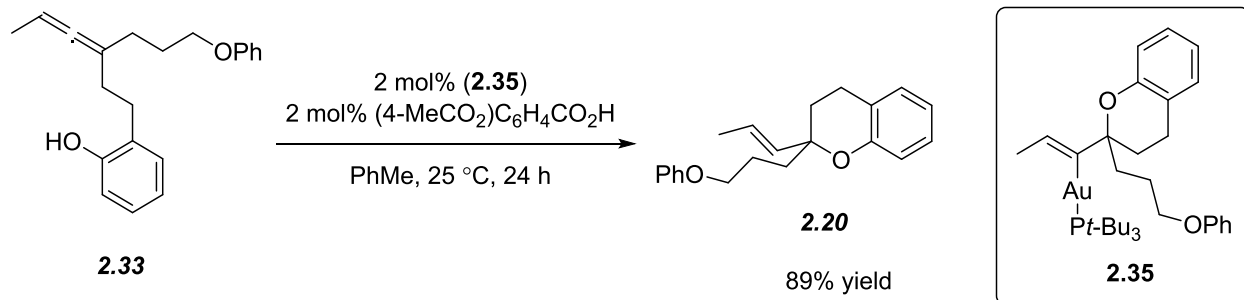
The mixture was diluted with 10 mL dichloromethane and stirred in the dark for 18 hours. At this time, the mixture was filtered through celite and concentrated to form a white solid. The material was dissolved in 1 mL dichloromethane and layered with 7 mL pentane. After 18 hours in a -35 °C freezer a white solid had precipitated. The material was filtered and washed with pentane to yield *t*-Bu₃PAu[O₂CC₆H₄(4-CO₂Me)] (250 mg, 70% yield) as a white solid. ¹H NMR (300 MHz, CDCl₃) δ 8.05 (d, J = 8.3 Hz, 2H), 7.94 (d, J = 8.3 Hz, 2H), 3.81 (s, 3H), 1.46 (d, J = 13.9 Hz, 27H). ³¹P NMR (121 MHz, C₆D₆) δ 84.2.

Catalyst Resting State



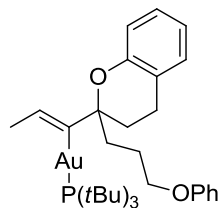
In a nitrogen-filled glovebox, an NMR tube was charged with phenoxy-allene (20 mg, 65 μmol, 1.0 equiv) and diluted with 430 μL of toluene-*d*⁸. To this mixture was added *t*-Bu₃PAu[O₂CC₆H₄(4-CO₂Me)] (3.8 mg, 6.5 μmol, 0.1 equiv). Reaction conversion was monitored by ¹H NMR, while the catalyst resting state was observed by ³¹P NMR at 20% conversion and 50% conversion. At 20% conversion, the ratio of vinyl gold complex to the catalyst was 1:3.2. After 50% conversion, this ratio was 1:5.5. The resonance at 84.7 ppm corresponds to *t*-Bu₃PAu[O₂CC₆H₄(4-CO₂Me)] and the resonance at 92.7 ppm corresponds to the vinyl gold complex shown above. Even at low temperature (-90 °C), only these two species were observable.

Catalytic Competency of Vinyl-Gold



In a nitrogen-filled glovebox, vinyl-gold complex (10.6 mg, 0.020 mmol, 0.20 equiv) and mono-methyl terephthalate (2.7 mg, 0.020 mmol, 0.20 equiv) were combined and suspended in dry toluene (750 μL). Then, a 75 μL aliquot (1/10th) of this solution was combined with phenoxy allene (23.1 mg, 0.075 mmol, 1.00 equiv) for an overall catalyst loading of 2 mol%, and the mixture was stirred at 25 $^\circ\text{C}$ for 24 h as shown above. At this point, the reaction mixture was chromatographed on silica with a solvent gradient of 0-10% EtOAc in hexanes to afford a clear, colorless liquid (20.7 mg, 89% yield).

Synthesis of Vinyl Gold

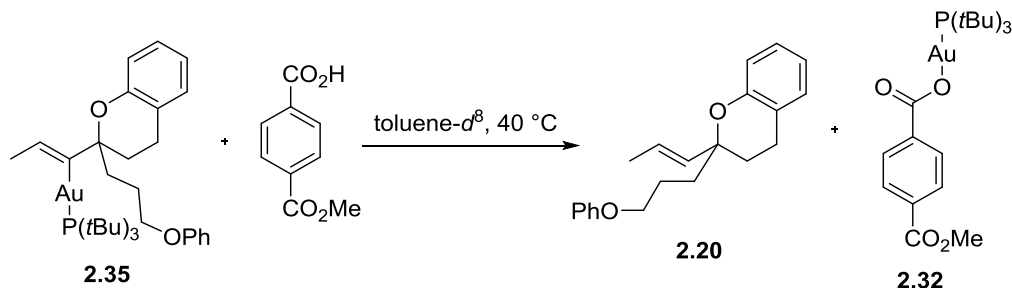


[(2-(3-phenoxypropyl)chroman-2-yl)-prop-1-en-1-yl]AuPt-Bu₃ (2.35): In a nitrogen-filled glovebox, a 1-dram vial was charged with *t*Bu₃PAuOTs (41.5 mg, 0.13 mmol, 1.0 equiv), a magnetic stir bar, and diluted with 1 mL of benzene. At this time, a mixture of triethylamine (67.8 mg, 0.70 mmol, 5.0 equiv) and phenoxy-allene

(40 mg, 0.13 mmol, 1.0 equiv) in benzene (0.6 mL) was added. The reaction mixture was allowed to stir for 5 minutes until consumption of the starting material was observed based on TLC. At this time, the mixture was diluted with hexane until a precipitate formed. The mixture was filtered through celite and the volatiles removed to give the vinyl gold complex **2.35** as a white residue (80 mg, 85% yield). ¹H NMR (300 MHz, CD₂Cl₂) δ 7.37 – 7.25 (m, 2H), 7.12 – 6.88 (m, 4H), 6.87 – 6.69 (m, 2H), 6.40 – 6.20 (m, 1H), 4.06 (t, *J* = 6.6 Hz, 2H), 3.04 – 2.87 (m, 1H), 2.67 – 2.51 (m, 1H), 2.40-2.25 (m, 1H), 2.19 – 1.67 (m, 6H), 1.56 (d, *J* = 12.7 Hz, 27H). ¹³C NMR (126 MHz, CD₂Cl₂) δ 176.4 (d, *J* = 96.9 Hz), 159.8, 155.7, 129.7, 129.5, 127.0, 125.7, 123.4, 120.5, 118.8, 116.7, 114.8, 86.7 (d, *J* = 7.2 Hz), 69.2, 40.2, 39.2 (d, *J* =

13.4 Hz), 34.1, 32.58 (d, $J = 4.3$ Hz), 24.0, 23.0, 20.7. ^{31}P NMR (202 MHz, CD_2Cl_2) δ 93.0. ^{31}P NMR (202 MHz, toluene- d^8) δ 92.8. ESI MS calculated for $[\text{M} + \text{H}]^+$ 707.7, found 707.6.

Protonation of Vinyl Gold



An NMR tube was charged with mono-methyl terephthalate (3.7 mg, 20.7 μmol , 1.5 equiv), vinyl gold complex (12 mg, 13.8 μmol , 1.0 equiv, [470 μL of a stock solution in toluene- d^8 . 0.025 $\text{mg}/\mu\text{L}$]), and trimethoxy benzene as an internal standard (1.16 mg, 6.9 μmol , 0.5 equiv, [26.6 μL of a stock solution in toluene- d^8 0.044 $\text{mg}/\mu\text{L}$]). The final volume of the reaction was 497 μL (0.03 M). The reaction was monitored by ^1H and ^{31}P NMR. The mixture was heated at 40°C for 24 hours to give >95% yield of the chroman product and >95% yield of the gold complex $\text{tBu}_3\text{PAu}[\text{O}_2\text{CC}_6\text{H}_4(4\text{-CO}_2\text{Me})]$. At 50% conversion we did not observe the formation of even a trace amount of the allene.

In an effort to investigate the reversibility of the formation of vinyl gold, the same experiment was repeated using slightly modified conditions. A scintillation vial was charged with mono-methyl terephthalate (1.7 mg, 9.2 μmol , 1.0 equiv), vinyl gold complex (8 mg, 9.2 μmol , 1.0 equiv, [220 μL of a stock solution in toluene- d^8 , 0.036 $\text{mg}/\mu\text{L}$]), and trimethoxybenzene as an internal standard (1.3 mg, 7.7 μmol , 0.84 equiv). The final volume of the reaction was 3.41 mL (0.027 M). The reaction mixture was stirred at room temperature and the progress of the reaction was occasionally monitored by ^1H NMR. At 10% conversion, ^1H NMR revealed that allene was not present. Similarly, at 40% conversion, allene could not be detected in the reaction mixture. After 18 h, the chroman product and the gold complex $\text{tBu}_3\text{PAu}[\text{O}_2\text{CC}_6\text{H}_4(4\text{-CO}_2\text{Me})]$ were formed in >95% yield, as determined by ^1H NMR using trimethoxybenzene as the internal standard.

Chapter 2 References

- ¹ Kang, E. J.; Lee, E. *Chem. Rev.* **2005**, 105, 4348.
- ² Bermejo, A.; Figadre, B.; Zafra-Polo, M. C.; Barrachina, I.; Estronell, E.; Cortes, D. *Nat. Prod. Rep.* **2005**, 22, 269.
- ³ Faul, M. M.; Huff, B. E. *Chem. Rev.* **2000**, 100, 2407.
- ⁴ Saleem, M.; Kim, H. J.; Ali, Y. S.; *Nat. Prod. Rep.* **2005**, 22, 696.
- ⁵ Yeung, K. S.; Patterson, I. *Chem. Rev.* **2005**, 105, 4237.
- ⁶ Ellis, G. P.; Lockhart, I. M. in *The Chemistry of Heterocyclic Compounds, Chromenes, Chromanones, and Chromones*, VCH, New York **2007**
- ⁷ Shen, H. C. *Tetrahedron* **2009**, 65, 3931.
- ⁸ a) Wolf, J. P.; Hay, M. B. *Tetrahedron*, **2007**, 63, 261. b) Elliot, M. C. *J. Chem. Soc. Perkin Trans. 1*, **2000**, 1291. c) Elliot, M. C.; Williams, E.; *J. Chem. Soc. Perkin Trans. 1*, **2001**, 2303. d) Boivin, T. L. B.; *Tetrahedron*, **1987**, 43, 3309. e) Jalce, G.; Frank, X.; Figarde, B. *Tetrahedron: Asymmetry*, **2009**, 20, 2537. f) McDonald, R. I.; Liu, G.; Stahl, S. S. *Chem. Rev.* **2011**, 111, 2981.
- ⁹ a) Ward, A. F.; Wolfe, J. P. *Org. Lett.* **2010**, 12, 1268. b) Asano, K.; Matsubara, S. *J. Am. Chem. Soc.* **2011**, 133, 16711. c) Trost, B. M.; Bringley, D. A.; Silverman, S. M. *J. Am. Chem. Soc.* **2011**, 133, 7664. d) Parsons, A. T.; Johnson, J. S. *J. Am. Chem. Soc.* **2009**, 131, 3122. e) Schuch, D.; Fries, P.; D önges, M.; Pérez, B. M.; Hatrung, J. *J. Am. Chem. Soc.* **2009**, 131, 12918. f) Miller, Y.; Miao, L.; Hosseini, A. S.; Chemler, S. R. *J. Am. Chem. Soc.* **2012**, 134, 12149. g) Zhang, G.; Cui, L.; Wang, Y.; Zhang, L. *J. Am. Chem. Soc.* **2010**, 132, 1474. h) Trend, R. M.; Ramtohl, Y. K.; Stoltz, B. M. *J. Am. Chem. Soc.* **2005**, 127, 17778.
- ¹⁰ a) Chirality transfer is defined as $CT = (ee_{\text{products}} / ee_{\text{starting material}}) * 100\%$. b) Recently, Denmark introduced enantiospecificity (with the same definition) as an alternative to CT. See: Denmark, S. E.; Burk, M. T. Hoover, J. A. *J. Am. Chem. Soc.* **2010**, 132, 1232.
- ¹¹ Marshall, J. A.; Pinney, K. G. *J. Org. Chem.* **1993**, 58, 7180.
- ¹² a) Volz, F.; Krause, N. *Org. Biomol. Chem.* **2007**, 5, 1519. b) Volz, F.; Wadman, S. H.; Hoffmann-Röder, A.; Krause, N. *Tetrahedron*, **2009**, 65, 1902.
- ¹³ The substrates used in these studies were prepared using procedures that are not broadly applicable.
- ¹⁴ Deutsch, C.; Gockel, B.; Hoffmann-Röder, A.; Krause, N. *Synlett* 2007, **2007**, 1790
- ¹⁵ Zhang, Z.; Liu, Z.; Kinder, R. E.; Han, X.; Qian, H.; Widenhofer, R. A. *J. Am. Chem. Soc.* **2006**, 128, 9066.
- ¹⁶ This complicates purification and further synthetic manipulations.
- ¹⁷ a) Grandon, V.; Lemi ère, G.; Hours, A.; Fensterbank, L. Malacria, M. *Angew. Chem. Int. Ed.* **2008**, 47, 7534. In addition and contrasting Malacria's calculations, it has been proposed that trisubstituted allenes might racemize faster than disubstituted allenes. Widenhofer eludes to this idea in this reference: b) Zhang, Z.; Bender, C. F.; Widenhofer, R. A. *J. Am. Chem. Soc.* **2007**, 129, 14148.
- ¹⁸ This is not unreasonable because cationic gold complexes are known to catalyze enantioenriched trisubstituted allene racemization, see: Sherry, B. D.; Toste, D. F.; *J. Am. Chem. Soc.* **2004**, 126, 15978

-
- ¹⁹ A possible scenario was one where *exo*-selective trisubstituted alleneol cyclization is inherently non-selective
- ²⁰ This catalyst loading is rare in gold catalyzed reactions and demonstrates how well behaved our catalyst system is. In this case, the catalyst turned over 5,000 times.
- ²¹ This is not a perfect test of matched-mismatched selectivity because the starting materials are not true diastereomers (they have different chemical formulas), but they have the opposite configuration at the secondary alcohol stereocenter. True diastereomers proved cumbersome to synthesize.
- ²² We found that there are limitations in the size of the ring that can be synthesized with this method. If the ring is too small the cyclization is selective for the endo product. If the ring is too big, racemization becomes competitive with cyclization and chirality transfer goes down, see experimental.
- ²³ a) Nicolaou, K. C.; Pfefferkon, J. A.; Roeker, A. J.; Cao, G. Q.; Barluenga, S.; Mitchel, H. J. *J. Am. Chem. Soc.* **2000**, *122*, 9939. b) Nicolaou, K. C.; Pfefferkorn, J. A.; Mitchell, H. J.; Roeker, A. J.; Baruenga, S.; Cao, G. Q.; Affleck, R. L.; Lillig, J. E. *J. Am. Chem. Soc.* **2000**, *122*, 9954.
- ²⁴ Shen, H. C. *Tetrahedron* **2009**, *65*, 3931
- ²⁵ See Reference 24
- ²⁶ This is something that we do not understand
- ²⁷ Brown, T. J.; Weber, D.; Gagné M. R.; Widenhoefer, R. A. *J. Am. Chem. Soc.* **2012**, *134*, 9134
- ²⁸ The rate of gold-catalyzed hydroalkoxylation of allenes using the tosylate counter ion is too high to make practical reaction kinetics measurements at relevant reaction conditions. Therefore, most experiments were performed at low temperature. We also experienced this issue. We found that the reaction could be monitored under perturbed conditions at room temperature. For example, when using a much lower catalyst loading or when running the reaction very dilute, the reactions become slow enough to monitor using standard techniques (NMR, GC).
- ²⁹ Allene gold complexes have been synthesized and characterized, see: a) Brown, T. J.; Sugie, A.; Leed, M. G. D.; Widenhoefer, R. A. *Chem. Eur. J.* **2012**, *18*, 6959. B) Brown, T. J.; Sugie, A.; Dickens, M. G.; Widenhoefer, R. A. *Organometallics* **2010**, *29*, 4207
- ³⁰ In our system we used the *t*Bu₃P ligand and performed the reaction in toluene
- ³¹ The phosphine ligands in the bis(gold) vinyl species in Scheme 16 are diastereotopic so they appear as a doublet in the ³¹P NMR spectrum. The signal for the Vinyl gold monomer shown in Scheme 16b is a singlet.
- ³² See experimental section for details
- ³³ a) Hashmi, A. S. K. *Angew. Chem. Int. Ed.* **2010**, *49*, 5232 b) Paton, R. S.; Maseras, F. *Org. Lett.* **2009**, *11*, 2237 c) Wang, A. J.; Benitez, D.; Tkatchouk, E. Goddard III, W. A.; Toste, F. D. *J. Am. Chem. Soc.* **2010**, *132*, 13064 d) Weber, D.; Tarselli, M. A.; Gagné M. R. *Angew. Chem. Int. Ed.* **2009**, *48*, 5733 e) Brooner, R. E. M.; Widenhoefer, R. A. *Chem. Eur. J.* **2011**, *17*, 6170 f) Brown, T. J.; Sugie, A.; Dickens, M. G. Widenhoefer, R. A. *Organometallics* **2010**, *29*, 4207.
- ³⁴ Weber, D.; Jones, T. D.; Adduci, L. L.; Gagné *Angew. Chem. Int. Ed.* **2012**, *51*, 2452
- ³⁵ Nieto-Oberhuber, C.; Muñoz, M. P.; López, S.; Jiménez-Núñez, E.; Nevado, C.; Herrero-Gómez, E.; Raducan, M.; Echavarren, A. M. *Chem. Eur. J.* **2006**, *12*, 1677.

³⁶ a) Stromnova, T. A.; Paschenko, D. V.; Boganova, L. I.; Daineko, M. V.; Katser, S. B.; Churakov, A. V.; Kuz'mina, L. G.; Howard, J. A. K. *Inorg. Chim. Acta* **2003**, 350, 283 b) Barnes, R. A.; Prochaska, R. J. *J. Am. Chem. Soc.* **1950**, 72 (7), 3188

³⁷ The azide was protected as a *p*-nitrobenzene amide following a procedure found in existing literature: Roush, R. W.; Julie, A. S.; Brown, J. R. *J. Org. Chem.* **1987**, 52, 5127

³⁸ Compound was reduced using lithium aluminum hydride and protected as the *p*-nitrobenzoate ester

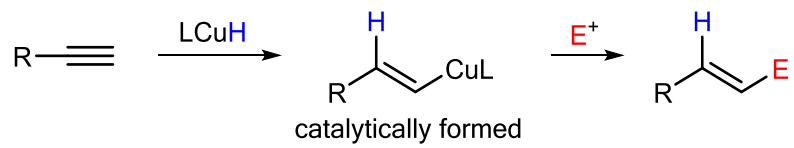
³⁹ The silyl ether was protecting group was removed with TBAF and the free alcohol was protected as the *p*-nitrobenzoate ester

Part 2: Copper-Catalyzed Hydrofunctionalization of Alkynes

Part 2 is focused on the development of copper-catalyzed hydrofunctionalization of alkynes. Functionalized alkenes are ubiquitous throughout organic chemistry and a general catalytic approach to the synthesis of different types of functionalized alkenes, from common and readily available precursors, will have a broad impact on organic synthesis. With this in mind, we focused on the development of a general approach to catalytic hydrofunctionalization of alkynes based on hydrocupration of alkynes followed by electrophilic functionalization (Scheme 22). The stereospecificity and high regioselectivity of the key step in this sequence, hydrocupration of terminal alkynes, ensures exclusive formation of the (*E*)-alkene products of anti-Markovnikov addition. This approach can be used to accomplish different hydrofunctionalization reactions by varying the electrophile.

In addition to the inherent value of developing new catalytic reactions, developing catalytic reactions based on the reactivity shown in Scheme 22 will help to improve our fundamental understanding of catalysts, reactive intermediates, and reagents. This is because a major challenge of developing a reaction of this type is chemoselectivity. For example, the copper hydride intermediate shown in scheme 22 must reduce the alkyne selectively over the electrophile, then the electrophile must react with the alkenyl copper intermediate. In addition, developing reactions based on Scheme 22 should allow the reaction to have an inherently high level of functional group compatibility because the copper hydride reagent must reduce the alkyne selectively over the electrophile. Therefore, functional groups that are less reactive than the electrophile should, in theory, be compatible.

Using the general approach outlined in Scheme 22, we were able to develop the first catalytic method for hydrobromination of alkynes (Chapter 3) and the first catalytic method for hydroalkylation of alkynes (Chapter 4).



Scheme 22. Copper-Catalyzed Hydrofunctionalization of Alkynes

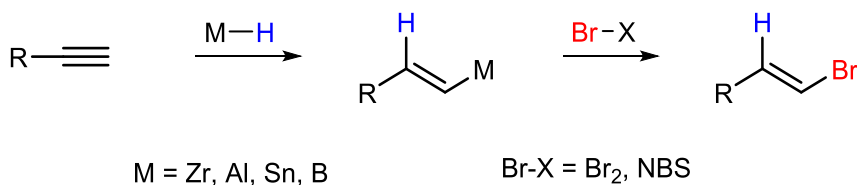
Chapter 3: Catalytic Anti-Markovnikov Hydrobromination of Alkynes

Portions of this chapter as well as figures, schemes, and tables were adapted or reproduced from the following manuscript co-authored by Mycah R. Uehling: Catalytic Anti-Markovnikov Hydrobromination of Alkynes, *Journal of The American Chemical Society*, **2014**, 136, 8799. Copyright **2014** American Chemical Society.

3.1 Introduction

Vinyl bromides are ubiquitous intermediates in organic synthesis. They are used as substrates in transition metal catalyzed cross coupling reactions¹ and as precursors to organometallic reagents such as organolithium, organozinc, and Grignard reagents.² Remarkably, while transition metal-catalyzed cross coupling has been highly developed, the most common methods used to prepare vinyl bromides, a key substrate class for cross coupling, have remained mostly unchanged for 40 years.

The most common method for the preparation of vinyl bromides is the anti-Markovnikov hydrobromination of alkynes.³ This transformation involves stoichiometric hydrometallation of an alkyne followed by electrophilic bromination (Scheme 23). Common metal hydride reagents used for hydrometallation of alkynes are based on aluminum,⁴ zirconium,⁵ tin,⁶ and boron.⁷ Common electrophilic brominating reagents are Br₂ and NBS. The hydrometallation step tends to be highly *syn*- and regioselective leading to the anti-Markovnikov⁸ *E*-alkenyl metal species.⁹ After electrophilic bromination, the alkenyl bromides can be isolated in high yield as one regio- and diastereoisomer.



Scheme 23. Stoichiometric Hydrometallation Followed by Bromination

The main limitation of this approach is the use of stoichiometric metal hydride reagents. For example, the high level of reactivity of aluminum and zirconium hydrides leads to poor functional group compatibility¹⁰ and these reagents can be sensitive to light and moisture.¹¹ Tin hydride reagents tend to be highly functional group compatible,¹² and can therefore be used with high chemoselectivity, but the reagents and byproducts are toxic. Lastly, the use of borohydride reagents tends to give lower yields in the hydrometallation electrophilic bromination reaction sequence.¹³

In addition to the limitations associated with stoichiometric metal hydrides, bromination using strong oxidants such as Br₂ and NBS can limit the functional group compatibility of the approach outlined in Scheme 23. For example, it is well established that Br₂ can oxidize electron rich aromatic rings and alkenes. In addition, Br₂ can be challenging to obtain and keep moisture-free as a neat material.

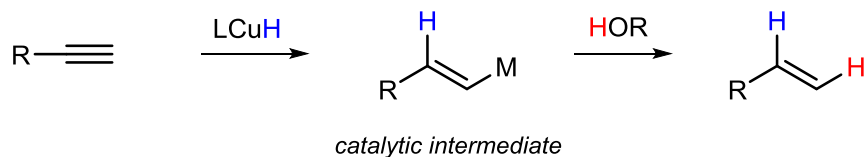
While much progress has been made in alkenyl bromide synthesis, the limitations in the state of the art for alkenyl bromide synthesis are twofold: 1) the use of a stoichiometric metal hydride reagents and 2) the use of harsh oxidizing agents such as Br₂. Our vision was to develop a catalytic method to accomplish hydrobromination of alkynes that might address both limitations.

3.2 Reaction Development

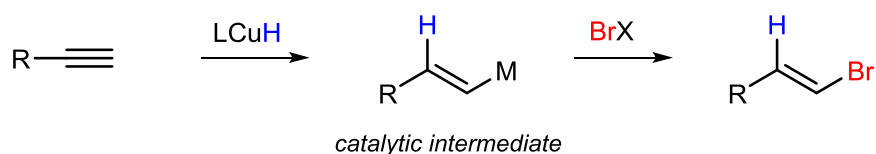
A major challenge in developing catalytic hydrobromination of alkynes is the efficient formation of an appropriate metal hydride reagent under catalytic conditions. Building on the work of Sadighi and coworkers,¹⁴ our lab recently developed an alkyne semireduction¹⁵ reaction where a copper hydride catalyst reduces an alkyne to form an alkenyl copper intermediate. The alkenyl copper intermediate is then protonated to form an alkene (Scheme 24a). This study provides proof of principle for copper-catalyzed alkyne hydrofunctionalization reactions based on the use of a catalytic amount of copper-hydride. Specifically, it shows that it is possible to reduce an alkyne in the presence of an electrophile, in this case the proton of an alcohol.¹⁶ We planned to use a similar strategy to develop copper-catalyzed

hydrobromination of alkynes except that instead of alkenyl copper protonation, we would implement alkenyl copper bromination (Scheme 24b).

a) Semireduction

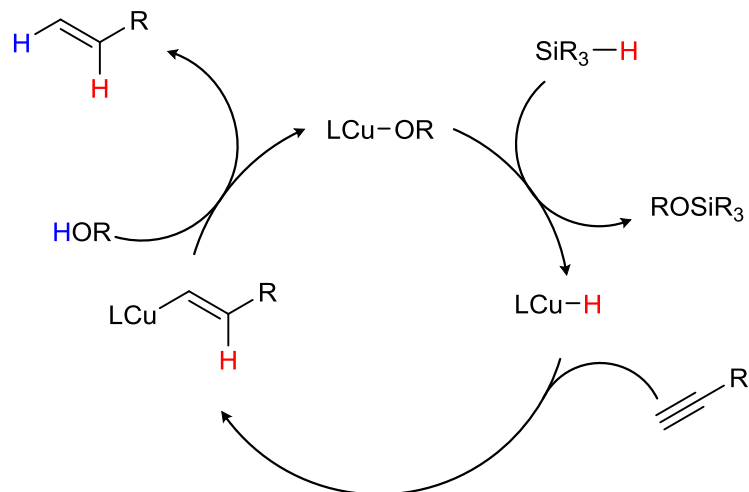


b) Hydrobromination



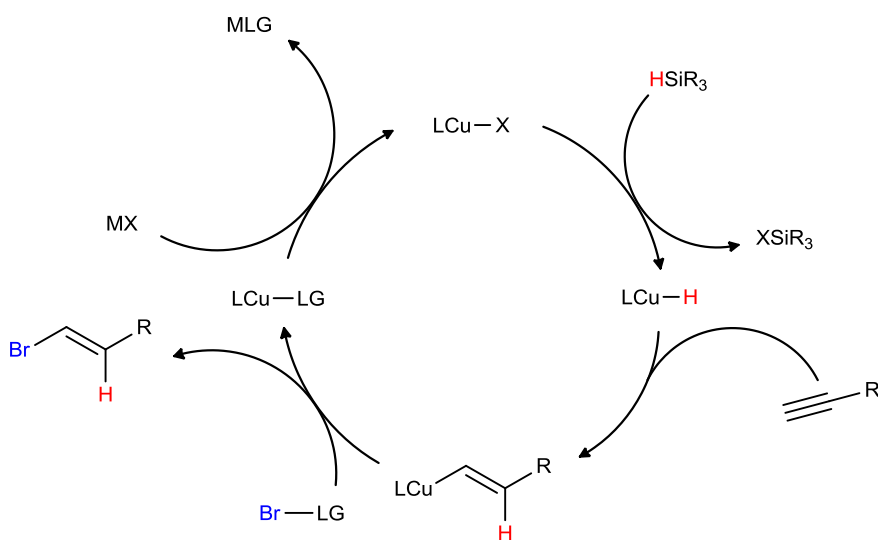
Scheme 24. Alkyne Semireduction and Hydrobromination

In the proposed mechanism of alkyne semireduction, a copper-hydride species reacts with an alkyne to form an alkenyl copper intermediate (Scheme 25). The alkenyl copper intermediate is then protonated by an alcohol to give the alkene product and a copper alkoxide (Scheme 25) This intermediate is set up perfectly to transmetallate with a silane to form copper hydride. Not all copper(I) salts are able to transmetallate with silanes. The most common copper(I) salts that have been invoked in transmetallation are copper alkoxides and fluorides. However, recently copper(I) benzoate has been proposed to transmetallate with silane to form a copper hydride intermediate.¹⁷



Scheme 25. Alkyne Semireduction Mechanism

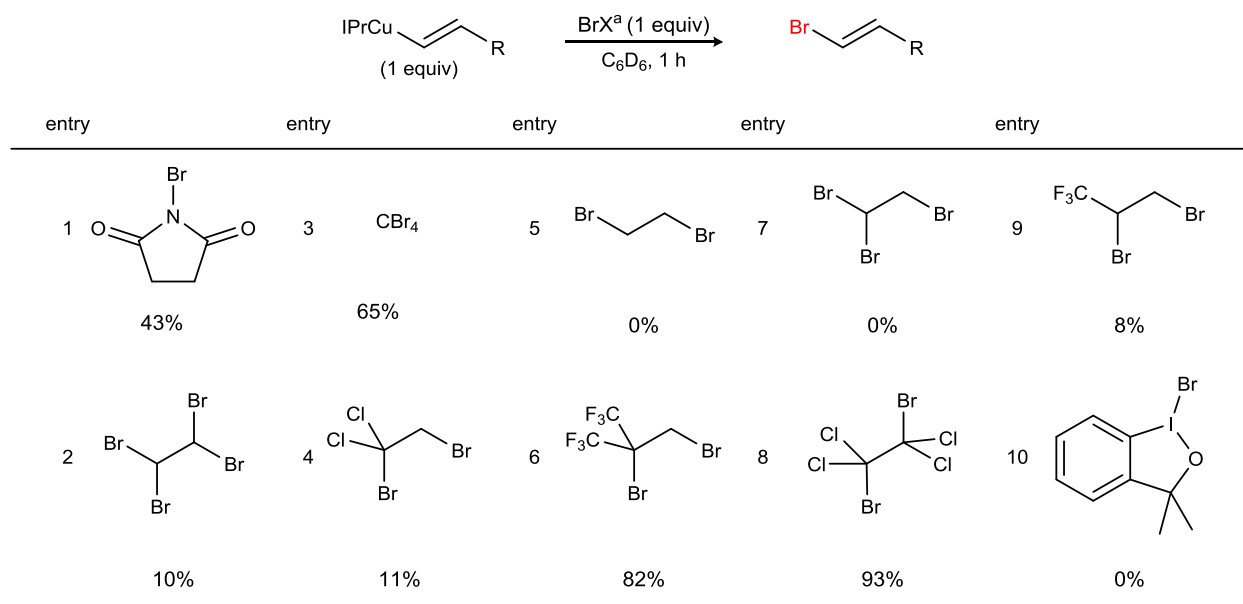
In the case of catalytic hydrobromination (Scheme 26), we anticipated that the catalytic cycle may be more complicated than that of semireduction. The main challenges we foresaw are 1) identification of an appropriate brominating reagent and 2) implementation of a catalyst turnover reagent to allow efficient formation of copper hydride.



Scheme 26. Proposed Catalytic Cycle of Hydrobromination of Alkynes

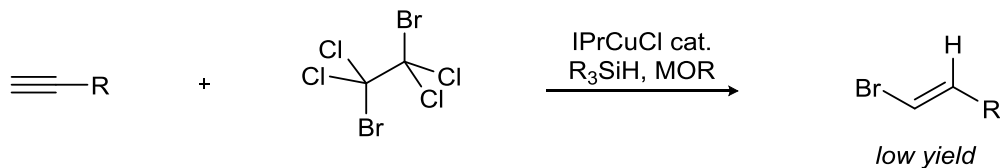
In the proposed mechanism for hydrobromination of alkynes (Scheme 26), the first two steps, copper hydride formation and hydrocupration were well understood at the time of reaction development.¹⁸ We surmised that if the reaction is possible as outlined in Scheme 26, it depends on an efficient bromination of alkenyl copper.¹⁹ In order to find the appropriate reagent, we performed stoichiometric reactions between alkenyl copper and various brominating reagents. After testing classic brominating reagents such as NBS and carbon tetrabromide, the alkenyl bromide product was formed in modest yield (Table 8, entries 1 and 3). However, when using these reagents in catalytic reactions, no product was formed. We next turned our attention to less common brominating reagents such as those shown in entries 5-10. By far the most productive reaction was observed when using 1,2-dibromotetrachloroethane as a bromine source (Table 8, entry 8). This reagent is a crystalline solid that can be weighed out in the air.²⁰ To the best of our knowledge, 1,2-dibromotetrachloroethane has never been used to brominate an alkenyl metal species. We propose that the reactivity of this oxidant is tuned to match that of the IPrCuAlkenyl complex (Table 8). Comparing the efficiency of the reaction when using 1,2-dibromoethane (entry 5) or more electrophilic versions (entries 5-9), the reaction yield gets higher as more electron withdrawing groups are incorporated. At this time the exact mechanism of bromination is not well understood.

Table 8. Stoichiometric Bromination of Alkenyl Copper

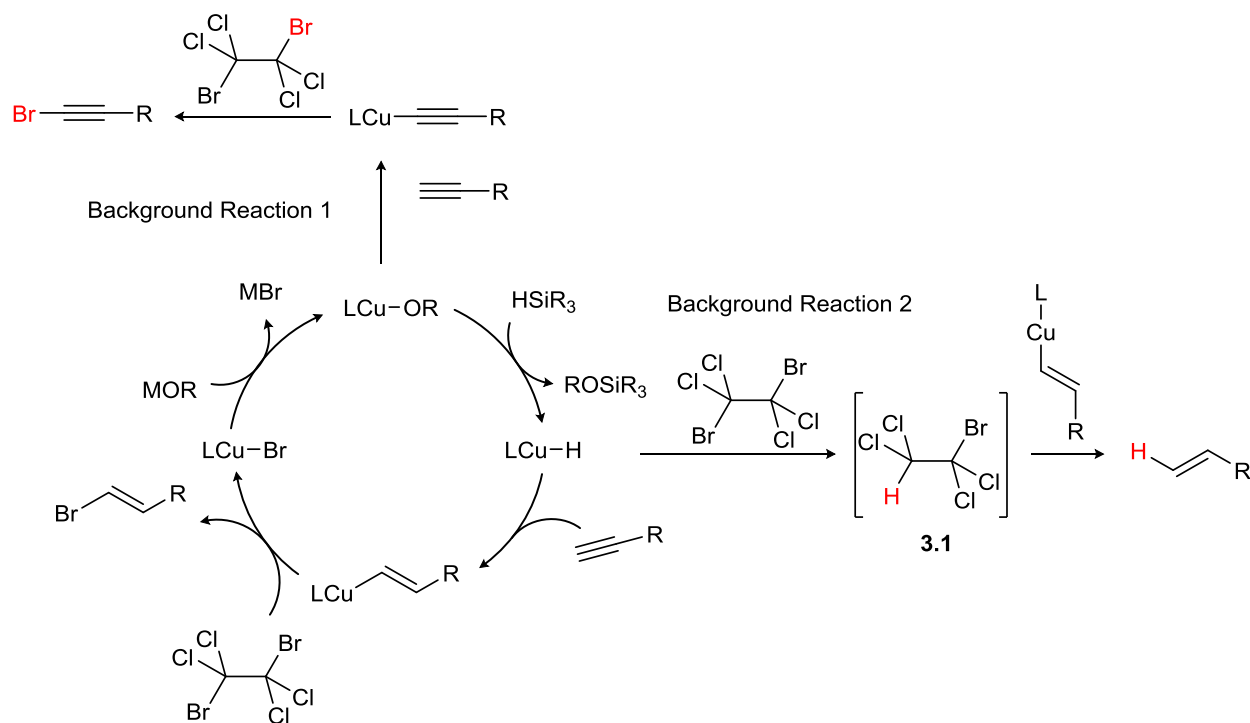


a) R = $(\text{CH}_2)_3\text{Ph}$

After establishing that 1,2-dibromotetrachloroethane is able to efficiently brominate alkenyl copper, we next focused our attention on trying to develop a catalytic alkyne hydrobromination reaction using this reagent. As a starting point, we used reaction conditions similar to those used in the semireduction reaction, except that we substituted the alcohol additive for 1,2-dibromotetrachloroethane and added additional alkali metal alkoxides for catalyst turnover (Scheme 27). We tested various NHCCuX complexes, silanes, alkoxides additives, temperatures, and concentrations. In all cases, we observed little to none of the alkenyl bromide product. However, through these experiments, we identified some key background reactions that were contributing to our diminished yields (Scheme 28).



Scheme 27. Initial Attempts at Catalytic Hydrobromination of Alkynes



Scheme 28. Proposed Background Reactions

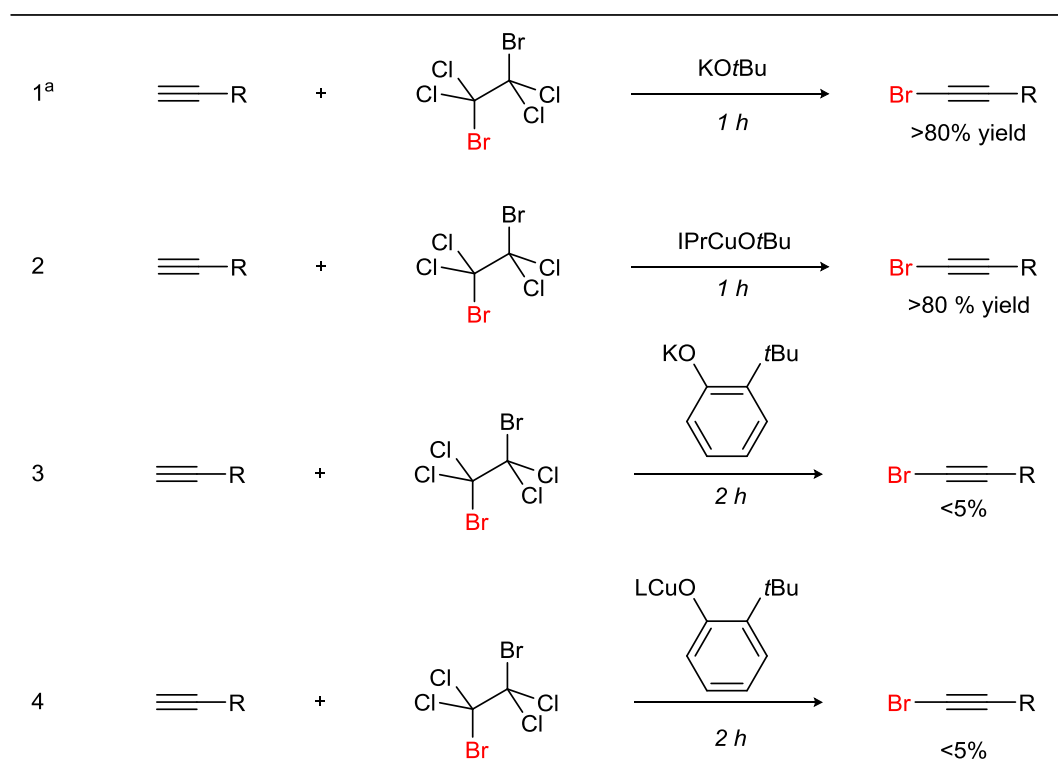
Two key background reactions that we identified are 1) the formation of bromoalkyne and 2) the formation of an alkene through semireduction (Scheme 28). In background reaction 1, we propose that the bromoalkyne is formed through a pathway that involves a copper acetylide intermediate that is oxidized by 1,2-dibromotetrachloroethane to form the bromoalkyne. In background reaction 2, we propose that copper hydride is able to reduce 1,2-dibromotetrachloroethane to form²¹ an acid that is able to protonate alkenyl copper. The background reactions outlined in scheme 28 will be discussed individually below.

3.2.1 Background Reaction 1: Formation of Bromoalkyne

The formation of bromoalkyne presumably depends on a base being present to remove the proton from the terminus of the alkyne. Our thinking was that it may be possible to slow down bromoalkyne formation relative to the productive reaction pathway by using additives that are less basic.

We first studied the bromoalkyne formation reaction to determine if we could affect the reaction rate by using bases with varying reactivity levels. We found that the bromoalkyne can be formed in high yield in the presence of KO*t*Bu or IPrCuO*t*Bu (Table 9, entries 1 and 2). When performing the same reaction in the presence of potassium 2-*t*Bu-phenoxide salts, the reaction was much slower (Table 9, entries 3 and 4). After 2 hours only trace amounts of bromoalkyne are formed. Based on these observations, we proposed that if we use a potassium phenoxide in the hydrobromination reaction, we might be able to avoid bromoalkyne formation.

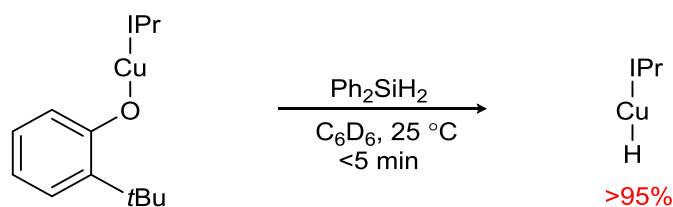
Table 9. Investigation of Bromoalkyne Formation



a) R = (CH₂)₃Ph, reactions performed in toluene

While we had identified a way to slow down bromoalkyne formation, it was not clear if a copper phenoxide was able to efficiently transmetallate with silane to form copper hydride. At the time of this research, this elementary reaction step was unknown in the literature. Gratifyingly, after mixing IPrCuO(2-*t*Bu)Ph with diphenyl silane, IPrCuH is formed in >95% yield (Scheme 29). From this point on,

we focused our attention on using alkali metal phenoxides as additives to promote the formation of copper hydride in the catalytic alkyne hydrobromination reaction and avoid background reaction 1.



Scheme 29. Transmetalation of IPrCuO(2-*t*Bu)Ph and Ph₂SiH₂

3.2.2 Background Reaction 2: Alkyne Semireduction

Based on our group's research on catalytic alkyne semireduction,¹⁵ we were aware that alkenyl copper can easily be converted into an alkene through protonation. We proposed that if the copper hydride intermediate is oxidized, it will form an acid. While the exact structure of this acid was never determined, we suspected that the reduction of the brominating reagent results in formation of **3.1**, a mild carbon based acid (Scheme 28). This is reasonable because our lab recently developed a reaction where copper hydride reduces alkyl halides to form alkanes.²² We proposed that intermediate **3.1** is able to protonate alkenyl copper forming the semireduction product.

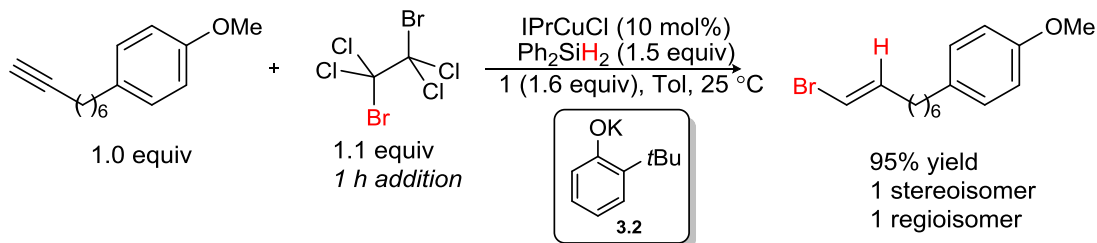
One way to avoid the oxidation of copper-hydride which presumably leads to semireduction (background reaction 2, Scheme 28), is to never allow copper-hydride to be in the same reaction vessel at the same time as the oxidant. In order to achieve this scenario, we added the brominating reagent slowly. In doing so, the brominating reagent never has an opportunity to react with copper hydride and therefore alkyne semireduction is minimized. Overall, we found that optimization of the addition rate of the brominating reagent was the key to minimizing alkene formation (background reaction 2, Scheme 28).

3.3 Optimized Reaction

Despite the initial challenges associated with reaction development, 1) determination of the appropriate reagent for bromination and 2) implementation of a compatible catalyst turnover reagent, we were able to develop the reaction shown in Table 10. The success of the reaction depends upon the use of potassium (2-*t*-Bu)OPh as an additive for transmetallation and the slow addition 1,2-dibromotetrachloroethane.

In addition to the observations discussed above in the background reaction sections, we also made the following observations while developing the reaction. We found that the IPrCuCl catalyst is necessary and uniquely effective in promoting the reaction. Even closely related NHC (*N*-heterocyclic carbene) copper complexes were completely ineffective as catalysts (Table 10, entry 1-3). Other silanes commonly used in copper-catalyzed reactions provided significantly lower yields of the desired product (Table 10, entry 4-5). In general, when using aromatic solvents the yield is high, but when using more polar solvents such as DCM or THF, the yield is lower (Table 10 entries 6-8). Lastly, we found that the phenoxide **3.2** proved to be an especially effective additive at promoting the reaction. When using other closely related phenoxides such as potassium phenoxide (Table 10, entry 9), the yield is lower.

Table 10. Development of Hydrobromination of Alkynes

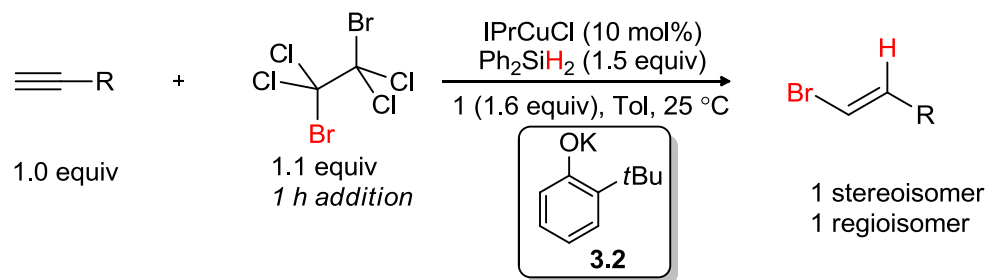


Entry	Change From Optimal Conditions	Yield
1	no catalyst	0%
2	ICyCuCl instead of IPrCuCl	0%
3	IMesCuCl instead of IPrCuCl	0%
4	PMHS instead of Ph ₂ SiH ₂	24%
5	(EtO) ₃ SiH instead of Ph ₂ SiH ₂	17%
6	Chlorobenzene instead of toluene	86%
7	DCM instead of toluene	66%
8	THF instead of toluene	4%
9	KOPh instead of 1	79%

3.4 Hydrobromination Scope

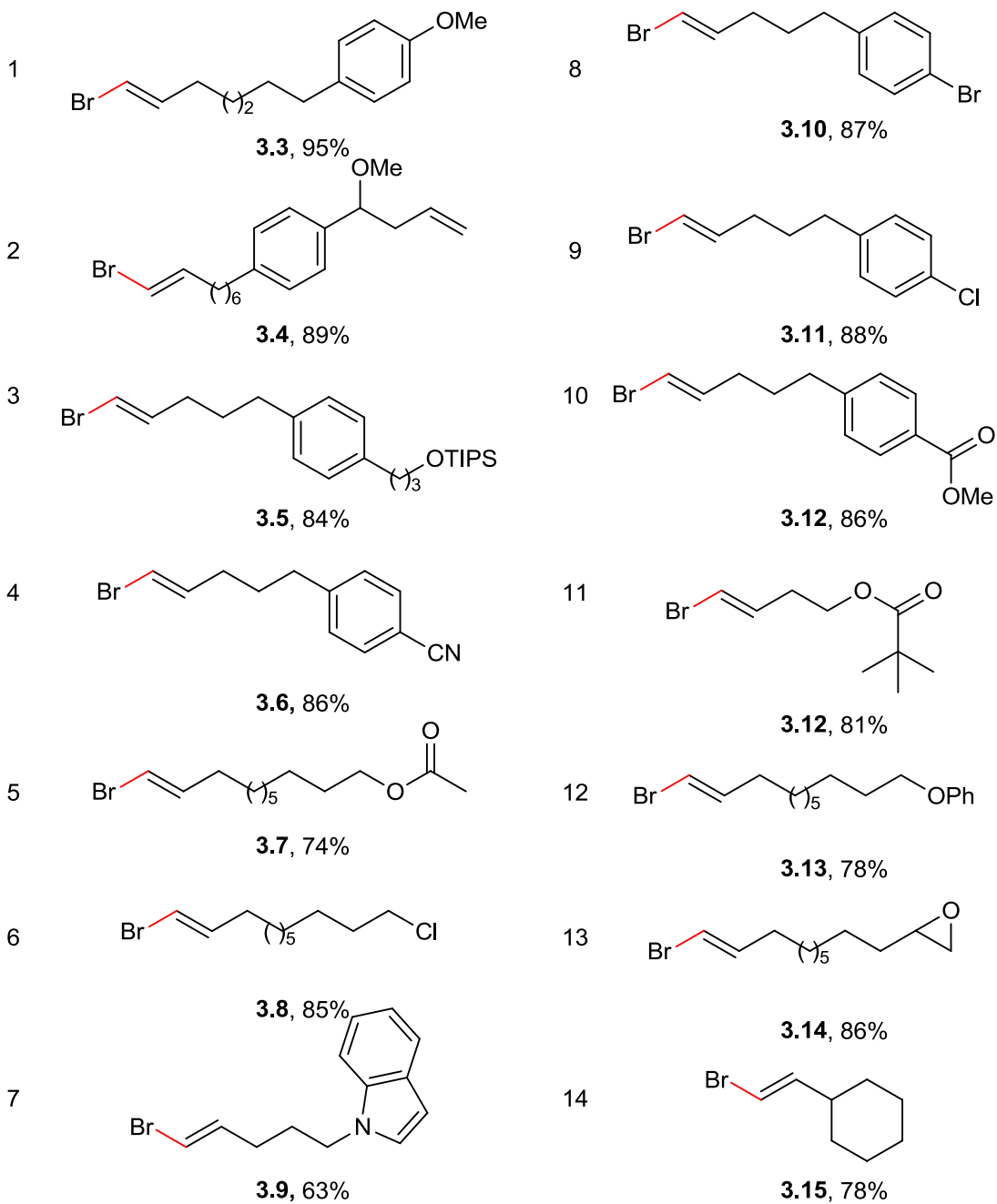
The optimized reaction conditions proved to be effective for the hydrobromination of a variety of alkyl substituted alkynes. The reaction is compatible with functional groups such as esters, nitriles, epoxides, alkyl halides, silyl ethers, aryl-alkyl ethers, and aryl halides (Table 11, entry 1-14). The compatibility of the indole substrate **3.9** demonstrates the mild nature of the optimized reaction conditions (Table 11, entry 7). Finally, alkynes that are α -branched are also compatible (Table 11, entry 14). In all cases, we observed only the formation of a single regio- and diastereoisomer of the alkenyl bromide.

Table 11. Hydrobromination of Alkyl Alkynes

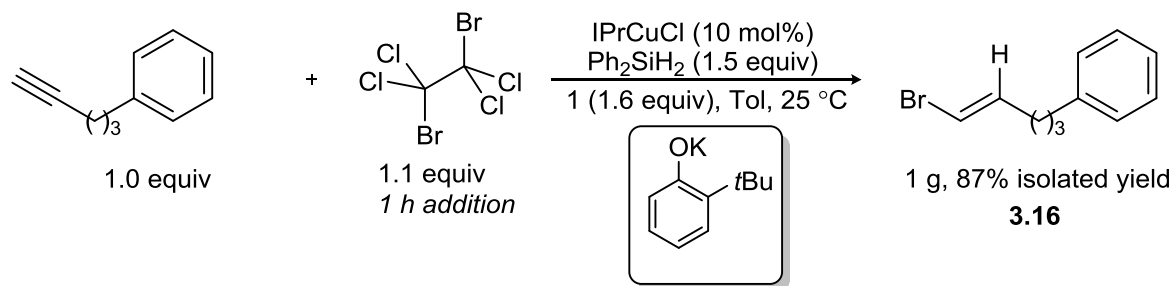


entry

entry



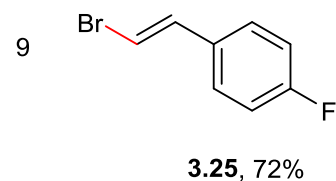
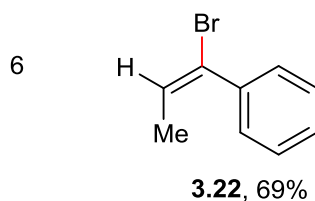
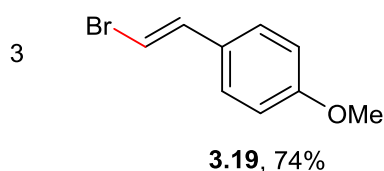
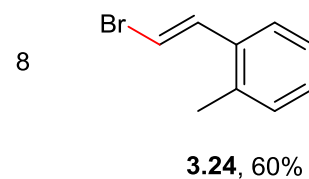
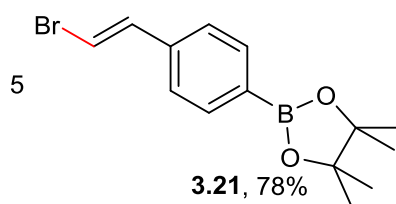
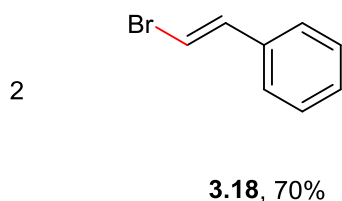
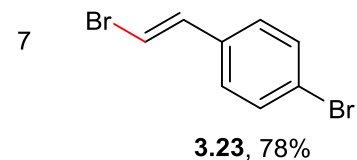
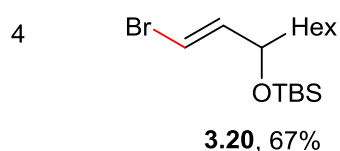
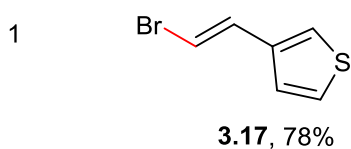
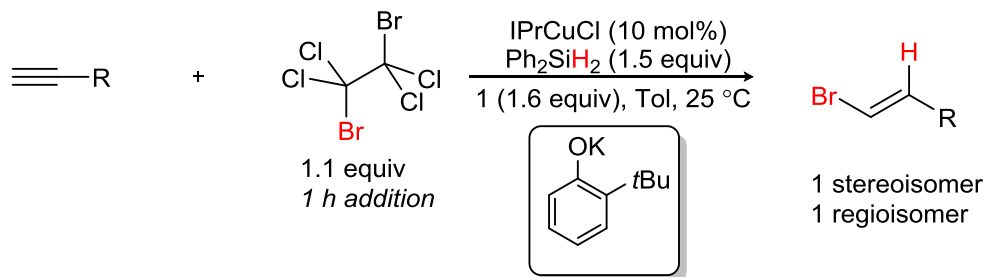
To demonstrate the utility of the hydrobromination procedure, we performed the hydrobromination reaction on a preparative scale (1 g of product). Under the standard reaction conditions described in Table 11, we were able to prepare 1 g of alkenyl bromide **3.16** in excellent yield as one regio- and stereoisomer (Scheme 30).



Scheme 30. Scale Up of Hydrobromination Reaction

We explored the reactivity of aryl-substituted alkynes, and found that styrenyl bromides with both electron-donating and electron-withdrawing substituents could be successfully prepared (Table 12). Additionally, we were surprised to find that aryl boronic esters are compatible with the hydrobromination reaction, as these compounds are known to participate in several copper-catalyzed transformations under closely-related conditions (entry 5). As demonstrated by the synthesis of **3.24**, ortho substitution is compatible with the optimized reaction. The synthesis of **3.17** shows that some heteroaryl acetylenes can also be used as substrates. Finally, the synthesis of **3.22** demonstrates that regioselective hydrobromination of a disubstituted aryl acetylene can also be accomplished. The hydrocupration of internal aryl acetylenes is known to proceed to give alkenyl copper at the carbon bound to the aromatic group.²³ In all reactions presented in Table 12, the formation of only one regio- and diastereoisomer of the product is observed.

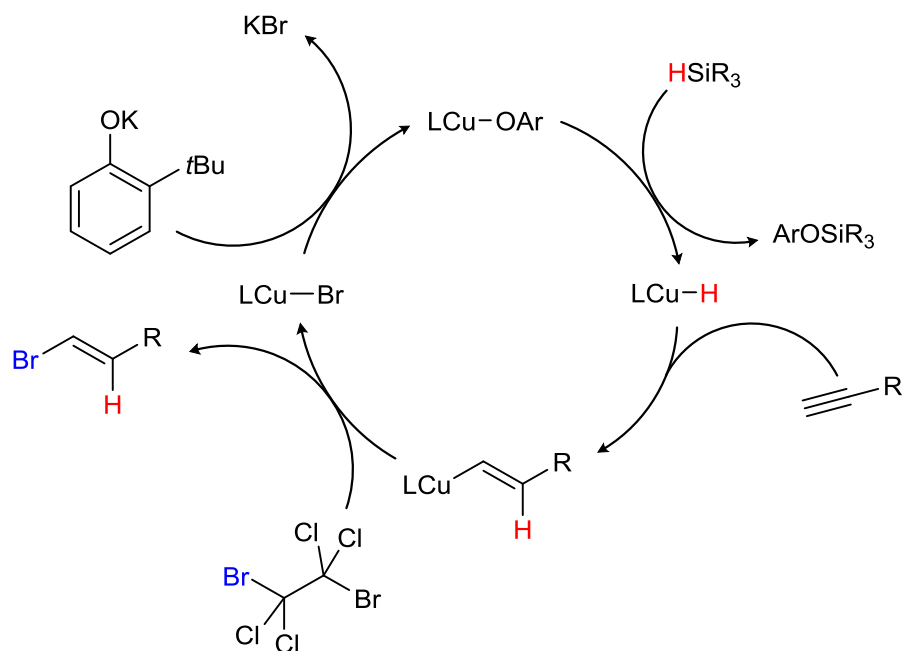
Table 12. Hydrobromination of Aryl Acetylenes



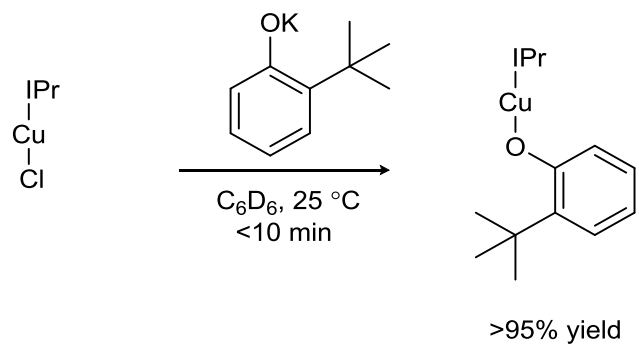
In the process of exploring the scope of the reaction, we identified some limitations. The major limitation is that electron poor aryl acetylenes do not work as substrates for the hydrobromination reaction. For example, when using *p*-cyanophenylacetylene as a substrate under the optimized reaction conditions, no alkenyl protons can be observed in the crude reaction mixture by ^1H NMR. We interpret this to mean that hydrocupration never took place. Our current hypothesis is that the electron poor aryl acetylenes get trapped as a copper acetylide or react to form a bromoalkyne and don't partake in the productive catalytic reaction. In addition, the most air sensitive component of the reaction starting materials is the potassium phenoxide **3.2**. This salt will turn black in seconds in air and must be prepared and handled in a glove box.

3.4 Hydrobromination Mechanism

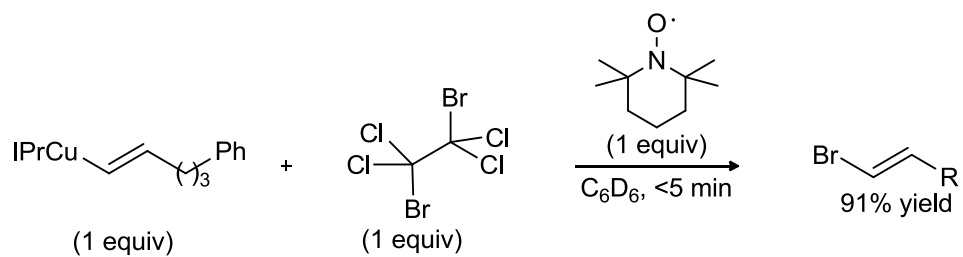
The proposed mechanism of hydrobromination of alkynes is shown in Scheme 31. Copper hydride is formed through transmetallation between copper phenoxide and silane. Then copper hydride reduces the alkyne to form alkenyl copper. After electrophilic bromination, the alkenyl bromide and IPrCuBr are formed. Lastly, the phenoxide is able to substitute IPrCuBr to form the copper phenoxide. The hydrocupration step of the catalytic cycle has strong precedent in the literature.²⁴ Therefore, we focused on providing experimental evidence for the other steps of the proposed catalytic cycle. We were able to convert IPrCuCl into IPrCuOAr in quantitative yield (Scheme 32). The result of this experiment provides support for the analogous proposed step in the catalytic cycle. The formation of copper hydride from the reaction of a copper phenoxide and silane was unknown before we conducted this research. The experiment shown in Scheme 29 provides support for the feasibility of this elementary step in the proposed catalytic cycle. Lastly, the results shown in Table 8 provide experimental evidence for the proposed bromination step of the catalytic cycle. The exact nature of the mechanism of alkenyl copper bromination is still not well understood. However, we performed the experiment described in Scheme 33 that supports the idea that this reaction does not proceed by a single electron transfer mechanism as TEMPO was not consumed during the reaction and the alkenyl bromide was formed in similar yield in the reaction without TEMPO.



Scheme 31. Proposed Catalytic Cycle for Hydrobromination



Scheme 32. Conversion of IPrCuCl to IPrCuOAr



Scheme 33. Bromination of Alkenyl Copper in the Presence of TEMPO

3.5 Hydrobromination Conclusions

We have developed the first catalytic hydrobromination of alkynes. The reaction is compatible with both alkyl and aryl-substituted alkynes, and with a wide range of functional groups, including esters, nitriles, epoxides, aryl boronic esters, alkyl halides, and aryl halides. The key step in the reaction is a catalytic hydrocupration which is highly anti-Markovnikov and *syn* selective. As a result, terminal *E*-alkenyl bromides are obtained with excellent regio- and diastereoselectivity. A preliminary study of the reaction mechanism provides support for the proposed mechanism involving hydrocupration of an alkyne followed by the electrophilic bromination of the alkenyl copper intermediate. This study also provides insight into the key properties of the brominating and turnover reagents used in the hydrobromination reaction. Finally, the discovery of phenoxides as mild turnover reagents is likely to enable the development of new reactions with copper hydrides as key catalytic intermediates.

Overall, this study provides support for the idea that catalytic reactions where hydrocupration followed by electrophilic functionalization takes place, can be used as a general approach to alkene synthesis. Through this research we have gained a better understanding for the relative reactivity of key catalytic intermediates (For example, NHCCuOAlkoxide vs. NHCuOPh) and provided a mechanistic platform for other alkyne hydrofunctionalization reactions to be developed.

3.6 Experimental

General

All reactions were performed under an atmosphere of nitrogen with flame-dried glassware, using standard Schlenk techniques, or in a glove box (Nexus II from Vacuum Atmospheres). Column chromatography was performed using a Biotage Iso-1SV flash purification system with silica gel from Agela Technologies Inc. (60Å, 40-60 µm, 230-400 mesh). Infrared (IR) spectra were recorded on a Perkin Elmer Spectrum RX I spectrometer. IR peak absorbencies are represented as follows: s = strong, m = medium, w = weak, br = broad. ¹H- and ¹³C-NMR spectra were recorded on a Bruker AV-300 or AV-500 spectrometer. ¹H

NMR chemical shifts (δ) are reported in parts per million (ppm) downfield of TMS and are referenced relative to residual protonated solvent peak (CDCl_3 (7.26 ppm), C_6D_6 (7.16 ppm), or CD_2Cl_2 (5.32 ppm)). ^{13}C chemical shifts are reported in parts per million downfield of TMS and are referenced to the carbon resonance of the solvent (CDCl_3 : δ 77.2 ppm, C_6D_6 : δ 128.1 ppm, CD_2Cl_2 : δ 54.0 ppm). Data are represented as follows: chemical shift, multiplicity (s = singlet, d = doublet, t = triplet, q = quartet, m = multiplet), integration, and coupling constants in Hertz (Hz). Mass spectra were collected on a JEOL HX-110 mass spectrometer. GC analysis was performed on a Shimadzu GC-2010 instrument with a flame ionization detector and a SHRXI-5MS column (15 m, 0.25 mm inner diameter, 0.25 μm film thickness). The following temperature program was used: 2 min @ 60 $^\circ\text{C}$, 13 $^\circ\text{C}/\text{min}$ to 160 $^\circ\text{C}$, 30 $^\circ\text{C}/\text{min}$ to 250 $^\circ\text{C}$, 5.5 min @ 250 $^\circ\text{C}$.

Materials:

Toluene and benzene were degassed and dried by passing through columns of neutral alumina. All other solvents were used as received. Deuterated solvents were purchased from Cambridge Isotope Laboratories, Inc. Commercial reagents were purchased from Sigma-Aldrich Co., VWR International, LLC., TCI Chemicals USA, or STREM Chemicals, Inc. Diphenylsilane was purchased from Oakwood Chemical. 1,2-dibromo-1,1,2,2-tetrachloroethane was purchased from Alfa Aesar and is a white easily handled crystalline solid. Potassium (2-*t*-butyl)phenoxide (**3.2**). Starting materials bearing an aryl substituent were prepared by either Suzuki²⁵ or Negishi²⁶ cross-coupling reactions. Aliphatic substrates were prepared by common functional group transformations from 10-undecyn-1-ol or 9-decen-1-ol. The indole and pivalate substrates were prepared from 4-pentyn-1-ol. Aryl acetylene starting materials were purchased from Sigma-Aldrich and used as is or distilled prior to use.

3.6.1 Reaction Development:

In a glove box, a flame-dried 25 mL Schlenk flask was charged with a stir bar, catalyst (0.1 equiv), additive for transmetalation (1.6 equiv), and toluene. Stock solutions of alkyne (1.0 equiv), silane (1.6

equiv), and brominating reagent (1.3 equiv) were prepared in the glove box. The final concentration of the reaction relative to the alkyne starting material was 0.05 M. The reaction was kept at 25 °C using an oil bath and stirred vigorously. The silane solution was added to the Schlenk flask under an atmosphere of nitrogen, followed by the alkyne solution. After 2 minutes, 1,2-dibromo-1,1,2,2-tetrachloroethane (1.1 equiv) was added with a syringe pump over one hour. After the slow addition an additional quench of 1,2-dibromo-1,1,2,2-tetrachloroethane (0.2 equiv) was added. The yield was measured by GC analysis using n-octylether as an internal standard.

3.6.2 Hydrobromination of Terminal Alkynes:

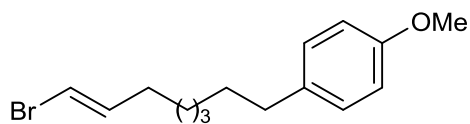
In a glove box, a flame-dried 25 mL Schlenk flask was charged with a stir bar, IPrCuCl (0.1 equiv, 0.05 mmol), potassium 2-(*t*-Bu)phenoxide (1.6 equiv, 0.72 mmol), and toluene. Stock solutions of alkyne (1.0 equiv, 0.5 mmol, 0.4 M), diphenylsilane (1.6 equiv, 0.68 mmol, 0.8 M), and 1,2-dibromo-1,1,2,2-tetrachloroethane (1.3 equiv, 0.57 mmol, 0.5 M) were prepared in the glove box. The final concentration of the reaction relative to the alkyne starting material after addition of all stock solutions was 0.05 M. The reaction was kept at 25 °C using an oil bath and stirred vigorously. Under an atmosphere of nitrogen, the diphenylsilane solution was added to the flask followed by the alkyne solution. After 2 minutes, 1,2-dibromo-1,1,2,2-tetrachloroethane (1.1 equiv) was added with a syringe pump over one hour or thirty minutes depending on the substrate. After the slow addition an additional quench of 1,2-dibromo-1,1,2,2-tetrachloroethane (0.2 equiv) was added. A sample was taken for GC analysis (n-octylether was used as an internal standard) to determine the yield of the alkenyl bromide. The crude reaction mixture was filtered through a plug of activated alumina with ether and concentrated under reduced pressure. The material was then loaded onto an alumina column and purified using standard chromatographic techniques (EtOAc/Hex).

Note: It is important to use proper air-free techniques to achieve the highest yields. We found that the use of alumina for purification was especially effective for removing silane byproducts and byproducts related to the additive **3.2**.

3.6.3 Large Scale Hydrobromination Procedure

In a glove box, a flame-dried 200 mL Schlenk flask was charged with a stir bar, IPrCuCl (0.1 equiv, 0.56 mmol), potassium 2-(*t*-Bu)-phenolate (1.6 equiv, 8.9 mmol), 5-phenyl-1-pentyne (1.0 equiv, 5.6 mmol) and toluene. Diphenylsilane (1.5 equiv, 8.3 mmol) and a stock solution of 1,2-dibromo-1,1,2,2-tetrachloroethane (1.3 equiv, 6.9 mmol) were loaded into gas-tight syringes (Hamilton). The final concentration of the reaction relative to the alkyne starting material was 0.05 M. The reaction was kept at 25 °C using an oil bath and stirred vigorously. Under an atmosphere of nitrogen, diphenylsilane was added to the reaction mixture. After 2 minutes, 1,2-dibromo-1,1,2,2-tetrachloroethane (1.1 equiv) was added over 1 hour with a syringe pump. After the slow addition an additional quench of 1,2-dibromo-1,1,2,2-tetrachloroethane (0.2 equiv) was added. The crude reaction mixture was filtered through a plug of activated alumina with ether and concentrated under reduced pressure. The material was then loaded onto an alumina column and purified using 0 to 15% EtOAc/Hex affording 1.0 grams (5 mmols) of compound **3.16**, 87% yield.

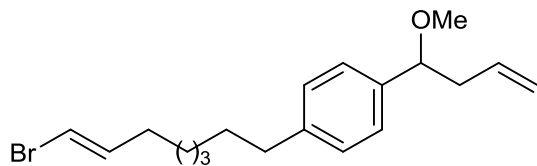
3.6.4 Characterization Data for Alkenyl Bromides



1-[(7E)-8-bromooct-7-en-1-yl]-4-methoxybenzene (3.3), 95% yield, 1h addition

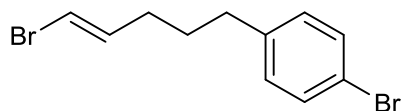
¹H NMR (300 MHz, C₆D₆) δ 7.03 (d, *J* = 8.6 Hz, 2H), 6.84 (d, *J* = 8.6 Hz, 2H), 5.96 (dt, *J* = 13.6, 7.3 Hz, 1H), 5.69 (dt, *J* = 13.5, 1.4 Hz, 1H), 3.36 (s, 3H), 2.47 (t, *J* = 7.6 Hz, 2H), 1.59 (dt, *J* = 14.0, 7.1 Hz, 2H), 1.53 – 1.41 (m, 2H), 1.21 – 0.97 (m, 6H). ¹³C NMR (75 MHz, C₆D₆) δ 158.5, 138.3, 134.8, 129.6, 114.2, 104.6, 54.8, 35.4, 33.0, 32.0, 29.1, 29.0, 28.7. GC/MS calculated for

[M]⁺ 296.1, found 296.1. FTIR (neat, cm⁻¹): 2929 (s), 2854 (m), 2359 (w), 1612 (w), 1583 (w), 1512 (s), 1254 (s), 1037 (m).



1-[(7E)-8-bromooct-7-en-1-yl]-4-(1-methoxybut-3-en-1-yl)benzene (3.4), 89% yield, 60 min addition

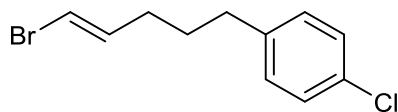
¹H NMR (300 MHz, CD₂Cl₂) δ 7.32 – 6.91 (m, 4H), 6.25 – 6.11 (m, 1H), 6.06 – 5.98 (m, 1H), 5.76 (ddt, *J* = 17.1, 10.1, 6.9 Hz, 1H), 5.00 (ddd, *J* = 11.8, 10.1, 1.4 Hz, 2H), 4.25 – 3.96 (m, 1H), 3.16 (s, 3H), 2.84 – 2.43 (m, 3H), 2.42 – 2.31 (m, 1H), 2.03 (dd, *J* = 13.7, 6.7 Hz, 2H), 1.68 – 1.49 (m, 2H, water overlap), 1.43 – 1.30 (m, 6H). ¹³C NMR (126 MHz, CD₂Cl₂) δ 142.6, 139.5, 138.9, 135.7, 128.7, 127.1, 116.7, 104.3, 83.7, 56.6, 42.8, 35.9, 33.2, 31.8, 29.4, 29.2, 28.9. ESI MS calculated for [M + Na]⁺ 373.1, found 373.3. FTIR (neat, cm⁻¹): 3071 (w), 2929 (s), 2855 (m), 2360 (m), 1612 (w), 1512 (w), 1442 (w), 1098 (s), 937 (m).



1-bromo-4-[(4E)-5-bromopent-4-en-1-yl]benzene (3.10), 87% yield, 1 h addition

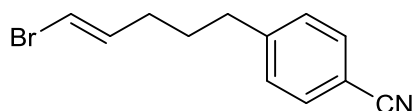
¹H NMR (300 MHz, C₆D₆) δ 7.24 (d, *J* = 8.3 Hz, 2H), 6.53 (d, *J* = 8.3 Hz, 2H), 5.94 – 5.82 (m, 1H), 5.64 (dt, *J* = 13.5, 1.3 Hz, 1H), 2.07 – 2.00 (m, 2H), 1.60 – 1.40 (m, 2H), 1.29 – 0.98 (m, 2H). ¹³C NMR (75 MHz, C₆D₆) δ 140.8, 137.5, 131.7, 130.4, 120.0, 105.1, 34.4, 32.2, 29.9.

GC/MS calculated for $[M]^+$ 301.9, found 301.9. FTIR (neat, cm^{-1}): 3055 (w), 2935 (s), 2278 (w), 1890 (w), 1765 (w), 1487 (s), 1403 (s), 1071 (s), 1010 (s), 935 (s).



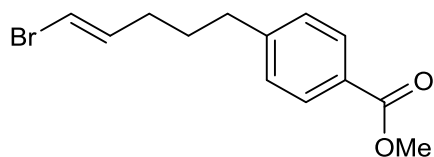
1-[(4E)-5-bromopent-4-en-1-yl]-4-chlorobenzene (3.11), 88% yield, 1 h addition

^1H NMR (300 MHz, CD_2Cl_2) δ 7.25 (d, $J = 8.4$ Hz, 2H), 7.12 (d, $J = 8.3$ Hz, 2H), 6.20 (dt, $J = 14.0, 7.1$ Hz, 1H), 6.05 (d, $J = 13.5$ Hz, 1H), 2.71 – 2.42 (m, 2H), 2.07 (q, $J = 7.2$ Hz, 2H), 1.75 – 1.63 (m, 2H). ^{13}C NMR (126 MHz, CD_2Cl_2) δ 141.0, 138.2, 131.8, 130.2, 128.7, 104.9, 34.7, 32.6, 30.5. GC/MS calculated for $[M]^+$ 258.0, found 257.9. FTIR (neat, cm^{-1}): 3030 (w), 2961 (s), 2341 (m), 1870 (w), 1752 (w), 1227 (w), 1091 (w), 935 (w).



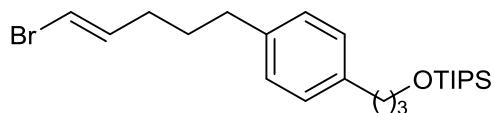
4-[(4E)-5-bromopent-4-en-1-yl]benzonitrile (3.6), 86% yield, 30 min addition

^1H NMR (300 MHz, CD_2Cl_2) δ 7.58 (d, $J = 8.2$ Hz, 2H), 7.29 (d, $J = 8.2$ Hz, 2H), 6.20 (dt, $J = 14.0, 7.1$ Hz, 1H), 6.06 (d, $J = 13.5$ Hz, 1H), 2.75 – 2.58 (m, 2H), 2.08 (q, $J = 7.1$ Hz, 2H), 1.84 – 1.61 (m, 2H). ^{13}C NMR (126 MHz, CD_2Cl_2) δ 148.1, 137.9, 132.6, 129.6, 119.4, 110.2, 105.2, 35.5, 32.6, 30.1. GC/MS calculated for $[M]^+$ 249.0, found 249.0. FTIR (neat, cm^{-1}): 3066 (w), 2935 (m), 2341 (w), 2227 (s), 1920 (w), 1805 (w), 1607 (s), 1230 (w), 938 (s), 816 (m).



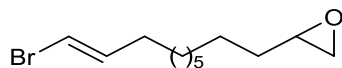
methyl 4-[(4E)-5-bromopent-4-en-1-yl]benzoate (3.12), 86% yield, 30 minute addition

^1H NMR (300 MHz, CD_2Cl_2) δ 7.93 (d, $J = 8.2$ Hz, 2H), 7.26 (d, $J = 8.1$ Hz, 2H), 6.21 (dt, $J = 14.0, 7.1$ Hz, 1H), 6.06 (d, $J = 13.5$ Hz, 1H), 3.87 (s, 3H), 2.75 – 2.55 (m, 2H), 2.08 (q, $J = 7.1$ Hz, 2H), 1.85 – 1.64 (m, 2H). ^{13}C NMR (75 MHz, CD_2Cl_2) δ 167.2, 147.9, 138.1, 129.9, 128.9, 128.4, 105.0, 52.2, 35.4, 32.7, 30.3. ESI MS calculated for $[\text{M} + \text{H}]^+$ 283.2, found 283.4. FTIR (neat, cm^{-1}): 3065 (w), 2945 (m), 2361 (w), 1928(w), 1819 (w), 1721 (s), 1607 (m), 1430 (m), 1275 (s), 1190 (m), 937 (w).



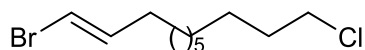
(3-{4-[(4E)-5-bromopent-4-en-1-yl]phenyl}propoxy)tris(propan-2-yl)silane (3.5), 84% yield, 30 min addition

^1H NMR (300 MHz, CD_2Cl_2) δ 7.29 – 6.92 (m, 4H), 6.21 (dt, $J = 14.1, 7.1$ Hz, 1H), 6.05 (d, $J = 13.5$ Hz, 1H), 3.71 (t, $J = 6.3$ Hz, 2H), 2.71 – 2.63 (m, 2H), 2.62 – 2.54 (m, 2H), 2.08 (dd, $J = 14.6, 7.1$ Hz, 2H), 1.89 – 1.77 (m, 2H), 1.76 – 1.63 (m, 2H), 1.20 – 0.90 (m, 21H). ^{13}C NMR (75 MHz, CD_2Cl_2) δ 140.3, 139.6, 138.5, 128.8, 128.7, 104.7, 63.0, 35.3, 35.0, 32.8, 32.1, 30.8, 18.2, 12.5. ESI MS calculated for $[\text{M} + \text{H}]^+$ 438.2, found 439.2. FTIR (neat, cm^{-1}): 3050 (m), 2941 (s), 2865 (s), 2360 (w), 1890 (w), 1781 (w), 1621 (m), 1514 (s), 1462 (s), 1104 (s), 882 (s).



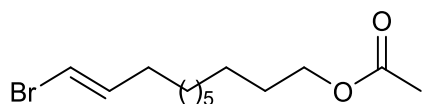
2-[(9E)-10-bromodec-9-en-1-yl]oxirane (3.14), 86% yield, 30 min addition

^1H NMR (300 MHz, C_6D_6) δ 5.99 (dt, $J = 14.5, 7.2$ Hz, 1H), 5.72 (d, $J = 13.5$ Hz, 1H), 2.64 – 2.59 (m, 1H), 2.38 (dd, $J = 5.3, 3.9$ Hz, 1H), 2.12 (dd, $J = 5.3, 2.5$ Hz, 1H), 1.63 (dd, $J = 12.1, 5.9$ Hz, 2H), 1.43 – 0.88 (m, 14H, minor impurity). ^{13}C NMR (126 MHz, C_6D_6) δ 138.3, 104.6, 51.8, 46.4, 33.0, 32.9, 29.8, 29.7, 29.6, 29.2, 28.7, 26.4. ESI MS calculated for $[\text{M} + \text{Na}]^+$ 283.1, found 283.2. FTIR (neat, cm^{-1}): 2927(m), 2855 (w), 2360 (s), 938 (w), 833 (w).



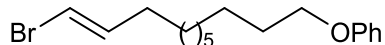
(1E)-1-bromo-11-chloroundec-1-ene (3.8), 85% yield, 60 minute addition

^1H NMR (300 MHz, C_6D_6) δ 5.99 (dt, $J = 14.5, 7.3$ Hz, 1H), 5.73 (dt, $J = 13.5, 1.3$ Hz, 1H), 3.13 (t, $J = 6.7$ Hz, 2H), 1.63 (dd, $J = 12.5, 5.9$ Hz, 2H), 1.51 – 1.38 (m, 2H), 1.26 – 0.95 (m, 12H). ^{13}C NMR (126 MHz, C_6D_6) δ 138.3, 104.6, 45.0, 33.0, 32.8, 29.6, 29.5, 29.1, 29.1, 28.7, 27.1. GC/MS calculated for $[\text{M}]^+$ 266.0, found 266.0. FTIR (neat, cm^{-1}): 3061 (w), 2928 (s), 2855 (m), 2361(m), 1283 (w), 9375 (m).



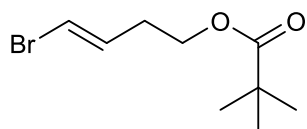
(10E)-11-bromoundec-10-en-1-yl acetate (3.7), 74% yield, 30 min addition

^1H NMR (300 MHz, C_6D_6) δ 5.99 (dt, $J = 14.4, 7.2$ Hz, 1H), 5.72 (d, $J = 13.5$ Hz, 1H), 4.01 (t, $J = 6.7$ Hz, 2H), 1.89 – 1.55 (m, 5H), 1.58 – 1.34 (m, 2H), 1.25 – 0.95 (m, 12H, minor impurity). ^{13}C NMR (126 MHz, C_6D_6) δ 170.2, 138.3, 104.6, 64.4, 33.0, 29.7, 29.6, 29.6, 29.2, 29.1, 28.7, 26.3, 20.6. ESI MS calculated for $[\text{M} + \text{Na}]^+$ 313.1, found 313.4. FTIR (neat, cm^{-1}): 2928 (s), 2855 (m), 2361(m), 1741 (s), 1620 (w), 1467 (w), 1365 (w), 1239 (s), 938 (m).



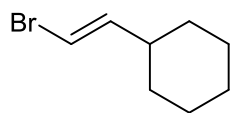
[[10E)-11-bromoundec-10-en-1-yl]oxy]benzene (3.13), 78% yield, 60 min addition

^1H NMR (300 MHz, CD_2Cl_2) δ 7.32 – 7.18 (m, 2H), 6.99 – 6.79 (m, 3H), 6.26 – 6.12 (m, 1H), 6.03 (dt, $J = 13.4, 1.2$ Hz, 1H), 3.94 (t, $J = 6.6$ Hz, 2H), 2.04 (dd, $J = 13.5, 6.8$ Hz, 2H), 1.85 – 1.68 (m, 2H), 1.51 – 1.19 (m, 12H). ^{13}C NMR (126 MHz, CD_2Cl_2) δ 159.6, 139.0, 129.8, 120.7, 114.8, 104.2, 68.3, 33.3, 29.9, 29.8, 29.7, 29.7, 29.3, 29.0, 26.4. GC/MS calculated for $[\text{M}]^+$ 324.1, found 324.1. FTIR (neat, cm^{-1}): 2928 (s), 2852 (m), 2360(m), 1852 (w), 1725 (w), 1601 (m), 1499 (m), 1247 (s), 1041 (s), 941 (m).



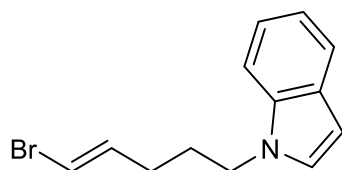
(4E)-5-bromopent-4-en-1-yl 2,2-dimethylpropanoate (3.12), 81% yield, 30 min addition

^1H NMR (300 MHz, C_6D_6) δ 5.82 (dt, $J = 14.3, 7.2$ Hz, 1H), 5.64 (d, $J = 13.6$ Hz, 1H), 3.78 (t, $J = 6.4$ Hz, 2H), 1.54 (dd, $J = 14.5, 7.0$ Hz, 2H), 1.28 – 0.97 (m, 11H). ^{13}C NMR (126 MHz, C_6D_6) δ 177.5, 137.0, 105.3, 63.3, 38.8, 29.5, 27.7, 27.3. ESI MS calculated for $[\text{M} + \text{Na}]^+$ 271.0, found 271.1. FTIR (neat, cm^{-1}): 2971(m), 2350 (s), 1720 (s), 1480 (w), 1284 (m), 1155 (s), 940 (w).



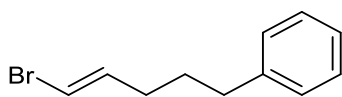
[(E)-2-bromoethenyl]cyclohexane (3.15), 78% Yield, 30 min addition

This is a known compound and has been characterized previously.²⁷



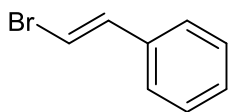
1-[(4E)-5-bromopent-4-en-1-yl]-1H-indole (3.9), 63% yield, 60 min addition

^1H NMR (300 MHz, C_6D_6) δ 7.74 (dd, $J = 6.7, 1.6$ Hz, 1H), 7.29 – 7.17 (m, 2H), 7.07 (d, $J = 7.7$ Hz, 1H), 6.56 (dd, $J = 21.8, 3.1$ Hz, 2H), 5.69 (dt, $J = 13.8, 6.9$ Hz, 1H), 5.47 (dt, $J = 13.5, 1.2$ Hz, 1H), 3.33 (t, $J = 6.6$ Hz, 2H), 1.37 – 1.12 (m, 4H). ^{13}C NMR (75 MHz, CD_2Cl_2) δ 137.2, 136.4, 129.1, 128.1, 121.7, 121.2, 119.6, 109.7, 105.6, 101.4, 45.8, 30.5, 29.4. ESI MS calculated for $[\text{M} + \text{Na}]^+$ 286.0, found 286.1. FTIR (neat, cm^{-1}): 3059 (w), 2931(m), 1612 (m), 1462 (m), 1315 (s), 937 (s).



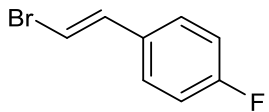
[(4E)-5-bromopent-4-en-1-yl]benzene (3.16), 87% Yield, 60 min addition

^1H NMR (300 MHz, C_6D_6) δ 7.14 – 7.02 (m, 3H, benzene overlap), 6.98 – 6.86 (m, 2H), 5.91 (dt, $J = 13.7, 7.2$ Hz, 1H), 5.63 (dt, $J = 13.5, 1.4$ Hz, 1H), 2.41 – 2.04 (m, 2H), 1.55 (dt, $J = 7.8, 4.1$ Hz, 2H), 1.39 – 1.21 (m, 2H). ^{13}C NMR (75 MHz, CD_2Cl_2) δ 142.4, 138.4, 128.8, 128.7, 126.2, 104.8, 35.4, 32.8, 30.7. GC/MS calculated for $[\text{M}]^+$ 224.0, found 224.0. FTIR (neat, cm^{-1}): 3049 (m), 3062 (s), 2857 (s), 2336 (w), 1945 (w), 1872 (w), 1805 (w), 1620 (s), 1495 (s), 1229 (m), 937 (s), 745 (s).



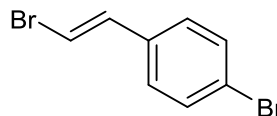
[(E)-2-bromoethenyl]benzene (3.18) 70% Yield, 30 min addition

This is a known compound and has been characterized previously.²⁸

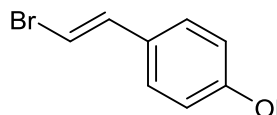


1-[(E)-2-bromoethenyl]-4-fluorobenzene (3.25), 72% Yield, 20 min

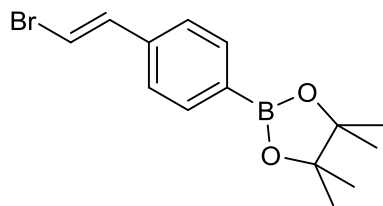
addition. This is a known compound and has been characterized previously.²⁸



1-bromo-4-[(E)-2-bromoethenyl]benzene (3.23) 78% Yield, 30 min addition. This is a known compound and has been characterized previously.²⁸

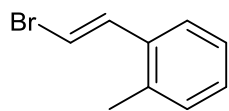


1-[(E)-2-bromoethenyl]-4-methoxybenzene (3.19) 74% Yield, 30 min addition. This is a known compound and has been characterized previously.²⁸

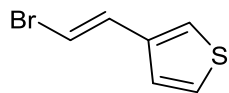


2-[4-[(E)-2-bromoethenyl]phenyl]-4,4,5,5-tetramethyl-1,3,2-dioxaborolane (3.21), 78% Yield, 15 min addition

¹H NMR (300 MHz, C₆D₆) δ 8.02 (d, *J* = 7.6 Hz, 2H), 6.87 (d, *J* = 7.8 Hz, 2H), 6.79 (d, *J* = 14.0 Hz, 1H), 6.31 (d, *J* = 14.0 Hz, 1H), 1.12 (s, 12H). ¹³C NMR (126 MHz, C₆D₆) δ 138.8, 137.4, 135.7, 128.4, 125.9, 108.2, 83.9, 25.0. GC/MS calculated for [M]⁺ 308.1, found 308.1. FTIR (neat, cm⁻¹): 2973 (w), 2360 (m), 2341 (m), 1606 (m), 1400 (m), 1360 (s), 1143 (m), 1089 (m), 859 (w), 683 (w).

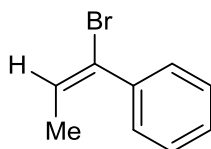


1-[(E)-2-bromoethenyl]-2-methylbenzene (3.24) 60% Yield, 30 min addition
This is a known compound and has been characterized previously.²⁹



3-[(E)-2-bromoethenyl]thiophene (3.17), 78% yield, 60 min addition

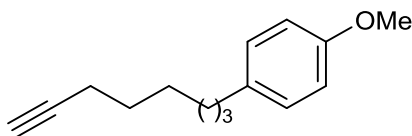
^1H NMR (300 MHz, CD_2Cl_2) δ 7.32 (dd, $J = 5.0, 3.0$ Hz, 1H), 7.22 (d, $J = 2.8$ Hz, 1H), 7.19 – 7.05 (m, 2H), 6.70 (d, $J = 13.9$ Hz, 1H). ^{13}C NMR (126 MHz, CD_2Cl_2) δ 138.2, 131.8, 127.0, 124.7, 123.3, 106.5. GC/MS calculated for $[\text{M}]^+$ 187.9, found 187.9. FTIR (neat, cm^{-1}): 2341 (m), 1772 (w), 1734 (w), 1653 (w), 1558 (w), 1202 (w), 934 (m), 745 (m).



[(E)-1-bromoprop-1-en-1-yl]benzene (3.22), 69% Yield, 60 min addition, 45 °C

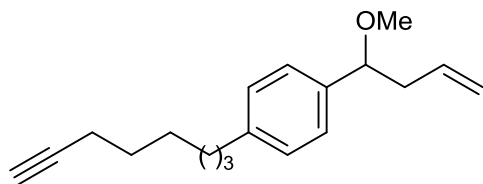
This is a known compound and has been characterized previously. The other regioisomer was not observable by GC analysis.³⁰

3.6.5 Characterization Data for Starting Materials



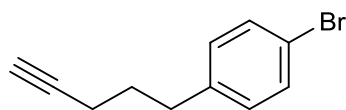
1-methoxy-4-(oct-7-yn-1-yl)benzene (3.26)

^1H NMR (300 MHz, C_6D_6) δ 7.00 (d, $J = 8.6$ Hz, 2H), 6.89 – 6.67 (m, 2H), 3.36 (s, 3H), 2.44 (t, $J = 7.6$ Hz, 2H), 1.95 (td, $J = 6.8, 2.6$ Hz, 2H), 1.79 (t, $J = 2.6$ Hz, 1H), 1.46 (dt, $J = 15.2, 7.5$ Hz, 2H), 1.39 – 1.07 (m, 6H). ^{13}C NMR (75 MHz, C_6D_6) δ 158.5, 134.8, 129.6, 114.2, 84.5, 68.9, 54.8, 35.4, 32.0, 29.0, 28.9, 28.8, 18.7. GC/MS calculated for $[\text{M}]^+$ 216.2, found 216.1. FTIR (neat, cm^{-1}): 3294 (m), 2932 (s), 2116 (w), 1869 (w), 1611 (m), 1512 (s), 1245 (s), 1037 (s), 827 (m).



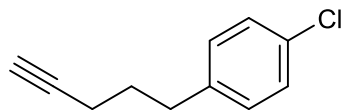
1-(1-methoxybut-3-en-1-yl)-4-(oct-7-yn-1-yl)benzene (3.27)

^1H NMR (300 MHz, C_6D_6) δ 7.22 (d, $J = 8.0$ Hz, 2H), 7.07 (d, $J = 8.0$ Hz, 2H), 5.91 (ddt, $J = 17.2, 10.2, 7.0$ Hz, 1H), 5.16 – 4.87 (m, 2H), 4.05 (dd, $J = 7.2, 6.0$ Hz, 1H), 3.09 (s, 3H), 2.68 (dt, $J = 14.2, 7.0$ Hz, 1H), 2.52 – 2.36 (m, 3H), 1.94 (td, $J = 6.8, 2.6$ Hz, 2H), 1.79 (t, $J = 2.6$ Hz, 1H), 1.45 (dt, $J = 15.2, 7.6$ Hz, 2H), 1.36 – 1.05 (m, 6H). ^{13}C NMR (75 MHz, C_6D_6) δ 142.2, 139.8, 135.5, 128.7, 127.1, 116.8, 84.4, 83.9, 68.9, 56.4, 43.2, 35.9, 31.7, 29.0, 28.8, 28.7, 18.6. ESI MS calculated for $[\text{M} + \text{Na}]^+$ 293.2, found 293.3. FTIR (neat, cm^{-1}): 3305 (w), 2933 (s), 2857 (m), 2360 (m), 1906 (w), 1641 (w), 1512 (w), 1462 (w), 1351 (w), 1098 (s), 915 (m), 1034 (m), 823 (w).



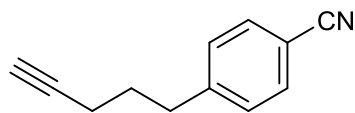
1-bromo-4-(pent-4-yn-1-yl)benzene (3.28)

^1H NMR (300 MHz, C_6D_6) δ 7.21 (d, $J = 8.3$ Hz, 2H, benzene overlap), 6.57 (d, $J = 8.3$ Hz, 2H), 2.37 – 2.14 (m, 2H), 1.89 – 1.65 (m, 3H), 1.48 – 1.36 (m, 2H). ^{13}C NMR (75 MHz, CD_2Cl_2) δ 141.1, 131.7, 130.8, 119.9, 84.3, 69.0, 34.3, 30.3, 18.0. GC/MS calculated for $[\text{M}]^+$ 222.0, found 222.0. FTIR (neat, cm^{-1}): 3300 (m), 2945 (w), 2117 (w), 1844(w), 1653 (w), 1488 (s), 1072 (s), 1011 (s), 829 (m).



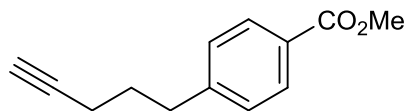
1-chloro-4-(pent-4-yn-1-yl)benzene (3.29)

^1H NMR (300 MHz, C_6D_6) δ 7.06 (d, $J = 8.4$ Hz, 2H), 6.64 (d, $J = 8.3$ Hz, 2H), 2.45 – 2.17 (m, 2H), 1.75 – 1.90 (m, 3H), 1.50 – 1.36 (m, 2H). ^{13}C NMR (75 MHz, C_6D_6) δ 140.1, 132.0, 130.1, 128.7, 83.8, 69.4, 33.9, 30.0, 17.8. GC/MS calculated for $[\text{M}]^+$ 178.1, found 178.0. FTIR (neat, cm^{-1}): 3302 (m), 2945 (m), 2862 (w), 2360 (m), 1896 (w), 1653 (w), 1492 (s), 1093 (s), 1015 (s), 832 (s), 795 (m).



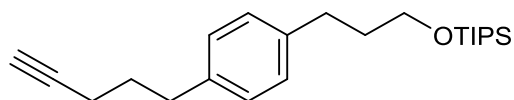
4-(pent-4-yn-1-yl)benzonitrile (3.30)

^1H NMR (300 MHz, CDCl_3) δ 7.58 (d, $J = 8.0$ Hz, 2H), 7.30 (d, $J = 8.0$ Hz, 2H), 2.81 (t, $J = 7.6$ Hz, 2H), 2.21 (td, $J = 6.8, 2.5$ Hz, 2H), 2.01 (t, $J = 2.4$ Hz, 1H), 1.93 – 1.74 (m, 2H). ^{13}C NMR (75 MHz, CD_2Cl_2) δ 147.7, 132.6, 129.7, 119.4, 110.2, 83.9, 69.3, 35.0, 29.9, 18.1. GC/MS calculated for $[\text{M}]^+$ 169.1, found 169.1. FTIR (neat, cm^{-1}): 3303 (s), 2944 (s), 2229 (s), 1928 (m), 1800 (w), 1683 (w), 1601 (m), 1506 (m), 1266 (s), 842 (s), 738 (s).



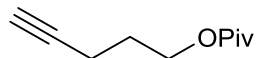
methyl 4-(pent-4-yn-1-yl)benzoate (3.31)

^1H NMR (300 MHz, CDCl_3) δ 7.96 (d, $J = 8.3$ Hz, 2H), 7.27 (d, $J = 8.1$ Hz, 2H, chloroform overlap), 3.90 (s, 3H), 2.85 – 2.73 (m, 2H), 2.20 (td, $J = 6.9, 2.6$ Hz, 2H), 2.00 (t, $J = 2.6$ Hz, 1H), 1.92 – 1.79 (m, 2H). ^{13}C NMR (75 MHz, CDCl_3) δ 167.2, 147.1, 129.9, 128.7, 128.1, 83.9, 69.1, 52.1, 34.7, 29.8, 17.9. ESI MS calculated for $[\text{M} + \text{H}]^+$ 203.1, found 203.0. FTIR (neat, cm^{-1}): 3297 (s), 2950 (s), 2117 (w), 1935 (w), 1718 (s), 1610 (m), 1435 (m), 1280 (s), 1110 (s), 859 (s).



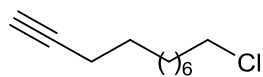
[3-[4-(pent-4-yn-1-yl)phenyl]propoxy]tris(propan-2-yl)silane (3.32)

^1H NMR (300 MHz, C_6D_6) δ 7.09 (d, $J = 8.0$ Hz, 2H), 7.00 (d, $J = 8.0$ Hz, 2H), 3.61 (t, $J = 6.2$ Hz, 2H), 2.76 – 2.63 (m, 2H), 2.59 – 2.47 (m, 2H), 1.94 (td, $J = 7.0, 2.6$ Hz, 2H), 1.88 – 1.77 (m, 3H), 1.69 – 1.55 (m, 2H), 1.18 – 1.00 (m, 21H). ^{13}C NMR (75 MHz, C_6D_6) δ 140.1, 139.1, 128.9, 128.8, 84.2, 69.2, 62.8, 35.2, 34.5, 32.1, 30.6, 30.1, 18.3, 18.0, 12.4. ESI MS calculated for $[\text{M} + \text{Na}]^+$ 381.3, found 381.4. FTIR (neat, cm^{-1}): 3313 (m), 2943 (s), 2865 (s), 2360 (w), 1894 (w), 1787 (w), 1658 (w), 1514 (m), 1462 (s), 1248 (m), 882 (m).



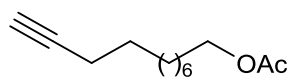
pent-4-yn-1-yl 2,2-dimethylpropanoate (3.33)

^1H NMR (300 MHz, C_6D_6) δ 3.98 (t, $J = 6.3$ Hz, 2H), 1.93 (td, $J = 7.1, 2.6$ Hz, 2H), 1.71 (t, $J = 2.6$ Hz, 1H), 1.49 (p, $J = 6.7$ Hz, 2H), 1.11 (s, 9H). ^{13}C NMR (75 MHz, C_6D_6) δ 177.5, 83.0, 69.4, 62.8, 38.7, 27.9, 27.3, 15.3. ESI MS calculated for $[\text{M} + \text{Na}]^+$ 191.1, found 191.2. FTIR (neat, cm^{-1}): 3297 (w), 2973 (s), 1728 (s), 1481 (m), 1284 (m), 1156 (s), 1038 (w).



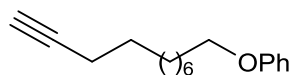
11-chloroundec-1-yne (3.34)

^1H NMR (300 MHz, C_6D_6) δ 3.12 (t, $J = 6.7$ Hz, 2H), 1.98 (td, $J = 6.9, 2.6$ Hz, 2H), 1.80 (t, $J = 2.6$ Hz, 1H), 1.51 – 1.29 (m, 4H), 1.29 – 0.92 (m, 10H). ^{13}C NMR (126 MHz, C_6D_6) δ 84.4, 68.9, 45.0, 32.9, 29.6, 29.3, 29.1, 28.9, 28.8, 27.1, 18.7. GC/MS calculated for $[\text{M}]^+$ 186.1, found 186.0. FTIR (neat, cm^{-1}): 3299 (s), 2928 (s), 2118 (m), 1465 (s), 1309 (m), 723 (m), 629 (s).



undec-10-yn-1-yl acetate (3.35)

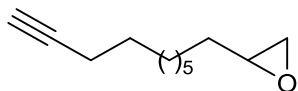
^1H NMR (300 MHz, C_6D_6) δ 4.09 (t, $J = 6.7$ Hz, 2H), 2.08 (td, $J = 6.9, 2.5$ Hz, 2H), 1.91 (t, $J = 2.6$ Hz, 1H), 1.80 (s, 3H), 1.49 (qd, $J = 14.0, 7.0$ Hz, 4H), 1.39 – 1.12 (m, 10H). ^{13}C NMR (126 MHz, CD_2Cl_2) δ 170.2, 84.5, 68.9, 64.4, 29.7, 29.5, 29.3, 29.0, 29.0, 28.8, 26.2, 20.6, 18.7. ESI MS calculated for $[\text{M} + \text{Na}]^+$ 233.2, found 233.1. FTIR (neat, cm^{-1}): 3297 (m), 2931 (s), 2857 (s), 1740 (s), 1240 (s), 1036 (m), 632 (m).



(undec-10-yn-1-yloxy)benzene (3.36)

^1H NMR (300 MHz, CD_2Cl_2) δ 7.42 – 7.07 (m, 2H), 7.01 – 6.76 (m, 3H), 3.95 (t, $J = 6.6$ Hz, 2H), 2.19 (td, $J = 7.0, 2.6$ Hz, 2H), 1.97 (t, $J = 2.6$ Hz, 1H), 1.86 – 1.70 (m, 2H), 1.60 – 1.23 (m, 12H). ^{13}C NMR (126 MHz, CD_2Cl_2) δ 159.6, 129.8, 120.7, 114.8, 85.1, 68.3, 68.2, 29.8, 29.8, 29.7, 29.4, 29.1, 29.0, 26.4, 18.7. GC/MS calculated for $[\text{M}]^+$ 244.2, found 244.2. FTIR (neat, cm^{-1}):

3307 (s), 2931 (s), 2856 (s), 2117 (w), 1926 (w), 1835 (w), 1769 (w), 1695 (w), 1600 (s), 1497 (s), 1245 (s), 1034 (m), 751 (s).

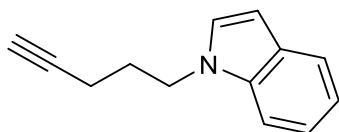


2-(dec-9-yn-1-yl)oxirane (3.37)

^1H NMR (300 MHz, C_6D_6) δ 2.64 – 2.56 (m, 1H), 2.37 (dd, $J = 5.3, 3.9$ Hz, 1H), 2.11 (dd, $J = 5.3, 2.6$ Hz, 1H), 1.98 (td, $J = 6.9, 2.6$ Hz, 2H), 1.81 (t, $J = 2.6$ Hz, 1H), 1.43 – 1.04 (m, 14H).

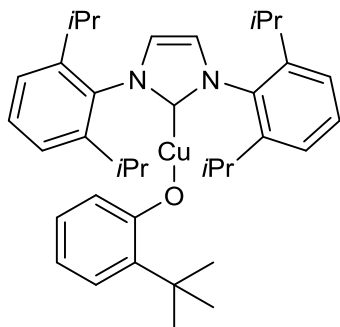
^{13}C NMR (126 MHz, C_6D_6) δ 84.5, 68.9, 51.8, 46.4, 32.9, 29.7, 29.7, 29.3, 29.0, 28.8, 26.3, 18.7.

ESI MS calculated for $[\text{M} + \text{Na}]^+$ 203.1, found 203.2. FTIR (neat, cm^{-1}): 3299 (m), 2918 (s), 2851(s), 2112 (w), 1457 (m), 1255 (w), 835 (m), 658 (w).



1-(pent-4-yn-1-yl)-1H-indole (3.38)

^1H NMR (300 MHz, CD_2Cl_2) δ 7.61 (d, $J = 7.9$ Hz, 1H), 7.40 (dd, $J = 8.2, 0.7$ Hz, 1H), 7.25 – 7.14 (m, 2H), 7.08 (ddd, $J = 7.9, 7.1, 1.0$ Hz, 1H), 6.49 (dd, $J = 3.1, 0.8$ Hz, 1H), 4.28 (t, $J = 6.7$ Hz, 2H), 2.23 – 1.95 (m, 5H). ^{13}C NMR (75 MHz, CD_2Cl_2) δ 136.3, 129.1, 128.4, 121.7, 121.2, 119.6, 109.7, 101.3, 83.4, 69.6, 45.1, 29.2, 16.1. ESI MS calculated for $[\text{M} + \text{Na}]^+$ 206.1, found 206.1. FTIR (neat, cm^{-1}): 3291(s), 3054 (s), 2117(m), 1609 (s), 1510 (s), 1455 (s), 1313 (s), 1165 (s), 1005 (m), 740 (m), 643 (m).

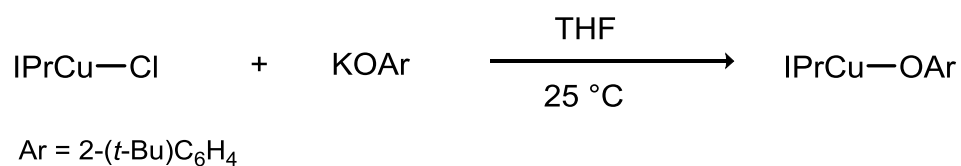


1,3-bis[2,6-bis(propan-2-yl)phenyl]-2-(2-tert-butylphenoxy)copperylidene)-2,3-dihydro-1H-imidazole (3.39)

^1H NMR (300 MHz, CD_2Cl_2) δ 7.55 (t, $J = 7.8$ Hz, 2H), 7.35 (d, $J = 7.7$ Hz, 4H), 7.20 (s, 2H), 6.84 (d, $J = 7.2$ Hz, 1H), 6.43 (t, $J = 7.9$ Hz, 1H), 6.18 (t, $J = 7.3$ Hz, 1H), 5.55 (d, $J = 7.9$ Hz, 1H), 2.70 – 2.50 (m, 4H), 1.25 (dd, $J = 12.5, 6.9$ Hz, 24H), 1.14 (s, 9H). ^{13}C NMR (126 MHz, CD_2Cl_2) δ 181.5, 146.3, 137.7, 135.2, 130.8, 126.6, 125.6, 124.6, 123.7, 122.4, 113.1, 34.9, 29.4, 29.2, 24.7, 24.1.

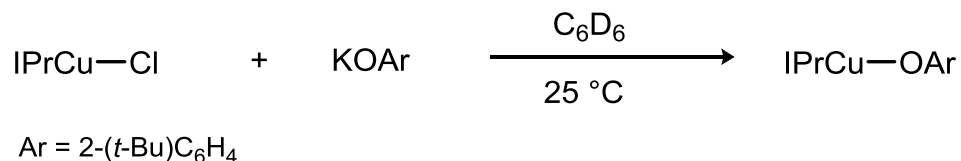
3.6.6 Mechanism Experiments

Reaction Between IPrCuCl and Potassium 2-(*t*-Bu)phenoxide:



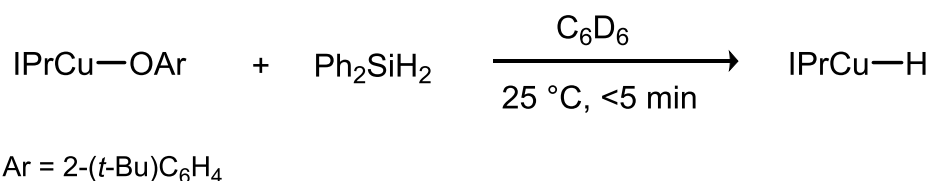
In a glove box, a scintillation vial was charged with a stir bar, IPrCuCl (1.0 equiv, 150 mg, 0.31 mmols) and potassium 2-(*t*-Bu)-phenoxide **1** (1.03 equiv, 60 mg, 0.32 mmols). The mixture was dissolved in THF (2.3 mL) and allowed to stir at 25 °C for 12 h. The suspension was then filtered through a plug of celite and concentrated. The material was suspended in dichloromethane,

layered with pentane, and placed in a -35 °C freezer. After crystallization, the crystals were filtered to yield 155 mg of IPrCuO2-(*t*-Bu)phenoxide, 84% yield.



In a glove box, a dram vial was charged with IPrCuCl (1.0 equiv, 32 mg, 0.07 mmol), KOAr (1.0 equiv, 12.2 mg, 0.07 mmol) (**1**), trimethoxybenzene (4.6 mg, 0.4 equiv), and C₆D₆ (0.05 M). Upon mixing the solution became homogeneous. A 200 uL aliquot was taken after 5 minutes and dissolved in 600 uL of C₆D₆. The IPrCuOAr complex was formed in 98% yield based on ¹H NMR relative to trimethoxybenzene internal standard.

Reaction Between IPrCuO2-(*t*-Bu)phenoxide and Diphenylsilane:



In a glove box, an NMR tube was charged with IPrCuO2-(*t*-Bu)phenoxide (1.0 equiv, 10 mg, 0.02 mmol) and C₆D₆ (0.2 mL). The NMR tube was fitted into a Cajon assembly, removed from the glove box, and placed on the manifold using standard Schlenk techniques. Separately, a solution of diphenylsilane (1.0 equiv, 3 mg, 0.02 mmol) in C₆D₆ (0.2 mL) was prepared and taken up by gas-tight syringe. The contents of the NMR tube were frozen using liquid nitrogen and the solution of diphenylsilane was added to the NMR tube. The NMR tube was sealed under

vacuum and kept frozen using liquid nitrogen. The frozen NMR tube was quickly warmed using a water bath, dried with a tissue, and placed in the NMR probe (probe operating temperature = 298 K). The reaction to form IPrCuH was too fast to monitor by NMR at room temperature. IPrCuO₂-(*t*-Bu)phenoxide was fully converted to IPrCuH within 3 minutes of mixing.

Formation of Bromoalkyne

In a glove box, a vial was charged with a stir bar and either potassium *t*-butoxide, IPrCuO-*t*-Bu, or IPrCuO₂-(*t*-Bu)C₆H₄ (1.0 equiv). Solvent (toluene or C₆D₆, 0.1 M) was added and the mixture was stirred. To the vial was added a solution of 5-phenyl-1-pentyne (1 equiv) and 1,2-dibromo-1,1,2,2-tetrachloroethane (1.0 equiv) in solvent (toluene or C₆D₆, 0.1 M) to give a final concentration of 0.05 M with respect to the alkyne. The reaction was monitored by GC (n-octyl ether used as an internal standard) or by ¹H NMR (1,3,5-trimethoxybenzene used as an internal standard). After 1 or 2 hours, the concentration of 1-bromo-5-phenylpentyne³¹ was measured.

Bromination of Alkenyl Copper Complex

In a glove box, a vial was charged with alkenyl copper complex (1.0 equiv, 0.1 mmol) and solvent (toluene or C₆D₆, 0.1 M). Brominating reagent (1 equiv, 0.1 mmol) in solvent (0.2 M) was added to the vial over one minute with stirring (final concentration of 0.1 M). The vial was capped and stirred at 25 °C. The reaction was monitored by GC (n-octylether used as an internal standard) or ¹H-NMR (hexamethylbenzene used as an internal standard).

In the case of 1,2-dibromo-1,1,2,2-tetrachloroethane, the yield was 94% after 10 minutes of stirring at 25 °C. The reaction mixture was diluted with pentane and filtered on a fine frit yielding 45 mg of IPrCuBr³² as a white powder, 85 % yield. Tetrachloroethylene was observed by GC/MS, but could not be quantified due to volatility.

In the case of using TEMPO as a reactivity probe.

In a glove box, a vial was charged with alkenyl copper complex (1.0 equiv, 0.1 mmol) and toluene (0.2 M). Brominating reagent (1 equiv, 0.1 mmol) and TEMPO (1 equiv, 0.1 mmol) were dissolved in toluene (0.2 M) and added to the vial over one minute with stirring (final concentration of 0.1 M). The vial was capped and stirred at 25 °C. The reaction was monitored by GC (n-octylether used as an internal standard).

Chapter 3 References

¹ a) Nicolaou, K. C.; Bulger, P. G.; Sarlah, D. *Angew. Chem., Int. Ed.* **2005**, *44*, 4442 b) *Metal-catalyzed cross-coupling reactions*; De Meijer, A. D., Francois, Ed.; Wiley-VCH Verlag GmbH & Co. KGaA, 2004; Vol. 1&2.

² *Organometallics in Synthesis, Third Manual*; Schlosser, M., Ed.; John Wiley & Sons, Inc., 2013.

³ Other methods include the Hunsdiecker reaction and the Takai reaction: see a) Hunsdiecker, H.; Hunsdiecker, C. *Ber. Dtsch. Chem. Ges. B* **1942**, 75B, 291, b) Naskar, D.; Roy, S. *Tetrahedron* **2000**, *56*, 1369. For the Takai reaction see: c) Corey, E. J.; Shulman, J. I.; Yamamoto, H. *Tetrahedron Lett.* **1970**, *11*, 447. d) Takai, K.; Nitta, K.; Utimoto, K. *J. Am. Chem. Soc.* **1986**, *108*, 7408. The Hunsdiecker reaction has limited scope and the Takai reaction tends to form multiple diastereomers of the alkenyl bromide.

⁴ Zweifel, G.; Miller, J. A. *Org. React.* **1984**, *32*, 1

⁵ Hart, D. W.; Blackburn, T. F.; Schwartz, J. *J. Am. Chem. Soc.* **1975**, *97*, 679

⁶ a) Zhang, H. X.; Guibe, F.; Balavoine, G. *J. Org. Chem.* **1990**, *55*, 1857 b) Chen, S.-M. L.; Schaub, R. E.; Grudzinskas, C. V. *J. Org. Chem.* **1978**, *43*, 3450 c) Leusink, A. J.; Budding, H. A.; Drenth, W. *J. Organomet. Chem.* **1968**, *11*, 541

⁷ Brown, H.; Hamaoka, T.; Ravindran, N.; Subrahmanyam, C.; Somayaji, V.; Bhat, N. G. *J. Org. Chem.* **1989**, *54*, 6075

⁸ Markovnikov selectivity can be achieved by using transition metal catalysis: a) Gao, F.; Hoveyda, A. H. *J. Am. Chem. Soc.* **2010**, *132*, 10961 b) Hibino, J.; Matsubara, S.; Morizawa, Y.; Oshima, K.; Nozaki, H. *Tetrahedron Lett.* **1984**, *25*, 2151

⁹ For examples of anti-selective hydrometalation see: (a) Asao, N.; Liu, J.-X.; Sudoh, T.; Yamamoto, Y. *J. Org. Chem.* **1996**, *61*, 4568. (b) Ohmura, T.; Yamamoto, Y.; Miyaura, N. *J. Am. Chem. Soc.* **2000**, *122*, 4990. (c) Trost, B. M.; Ball, Z. T. *J. Am. Chem. Soc.* **2005**, *127*, 17644. (d) Sundararaju, B.; Füstner, A. *Angew. Chem., Int. Ed.* **2013**, *52*, 14050. (e) Rummelt, S. M.; Füstner, A. *Angew. Chem., Int. Ed.* **2014**, *53*, 3626

¹⁰ Wipf, P.; Jahn, H. *Tetrahedron* **1996**, *52*, 12853

¹¹ Wipf, P. *Top. Organomet. Chem.* **2005**, *8*, 1

-
- ¹² a) Ahmed, F.; Forsyth, C. J. *Tetrahedron Lett.* **1998**, 39, 183. (b) Smith, A. B.; Verhoest, P. R.; Minbiole, K. P.; Schelhaas, M. J. *Am. Chem. Soc.* **2001**, 123, 4834. (c) Wang, B.; Hansen, T. M.; Wang, T.; Wu, D.; Weyer, L.; Ying, L.; Engler, M. M.; Sanville, M.; Leitheiser, C.; Christmann, M.; Lu, Y.; Chen, J.; Zunker, N.; Cink, R. D.; Ahmed, F.; Lee, C.-S.; Forsyth, C. J. *J. Am. Chem. Soc.* **2011**, 133, 1484
- ¹³ Masuda, Y.; Hoshi, M.; Arase, A. *J. Chem. Soc., Perkin Trans. 1* **1992**, 2725.
- ¹⁴ Mankad, N. P.; Laitar, D. S.; Sadighi, J. P. *Organometallics* **2004**, 23, 3369
- ¹⁵ Whittaker, A. M.; Lalic, G. *Org. Lett.* **2013**, 15, 1112
- ¹⁶ Additional key observations made in this study were that catalytic hydrocupration is highly regio- and stereoselective. The copper-hydride hydrogen atom always ends up on the internal carbon of a terminal alkyne and the semireduction is always occurs with syn stereochemistry. Therefore, we proposed that hydrobromination will be highly selective for the anti-Markovnikov syn addition product.
- ¹⁷ Zhu, S.; Niljianskul, N.; Buchwald, S. L. *J. Am. Chem. Soc.* **2013**, 135, 15746
- ¹⁸ See Ref. 14
- ¹⁹ Luckily NHCCuAlkenyl complexes are relatively easy to prepare and are stable in a glove box for months
- ²⁰ This reagent is most commonly used for bromination of aromatic rings through electrophilic aromatic substitution or allylic C-H bromination through a radical mechanism
- ²¹ The reaction between an alkyl halide and copper hydride has been recently developed by our group. See: Dang, H.; Cox, N.; Lalic, G. *Angew. Chem. Int. Ed.* **2014**, 53, 752.
- ²² See Reference 21
- ²³ See Reference 17
- ²⁴ See Reference 14
- ²⁵ Miyaura, N.; Ishiyama, T.; Sasaki, H.; Ishikawa, M.; Satoh, M.; Suzuki, A. *J. Am. Chem. Soc.* **1989**, 111, 314. Billingsley, K. L.; Anderson, K. W.; Buchwald, S. L. *Angew. Chem. Int. Ed.* **2006**, 45, 3484. Alkyl-Aryl Suzuki cross coupling reaction: hydroboration of terminal alkene with 9-BBN followed by Suzuki cross coupling. We found the Xphos ligand to be especially useful. Tricyclohexylphosphine, DPPF, and tri(o-Tol)phosphine were also used. Pd(OAc)₂ was used in all cases as the Pd source. NaOH, K₃PO₄, and Cs₂CO₃ were used as additives. Reactions were performed in either THF or Toluene at reflux temperature overnight.
- ²⁶ Procedure adapted from: Sase, S.; Jaric, M.; Metzger, A.; Malakhov, V.; Knochel, P. *J. Org. Chem.* **2008**, 73, 7380. The cross coupling was accomplished using Pd(OAc)₂ as the Pd source and SPhos as the ligand. The alkyl zinc reagents were synthesized as described in the Knochel publication. Reactions were run at room temperature over night or longer.
- ²⁷ Imazaki, Y.; Shirakawa, E.; Ueno, R.; Hayashi, T. *J. Am. Chem. Soc.* **2012**, 134, 14760
- ²⁸ Bull, J. A.; Mousseau, J. J.; Charette, A. B. *Org. Lett.* **2008**, 10, 5485
- ²⁹ Cheung, C. W.; Buchwald, S. L. *J. Org. Chem.* **2012**, 77, 7526
- ³⁰ Schiffner, J. A.; Wöste, T. H.; Oestreich, M. *Eur. J. Org. Chem.* **2010**, 174

³¹ 1-bromo-5-phenylpent-1-yne is a known compound. Yamagishi, M.; Nishigai, K.; Hata, T.; Urabe, H. *Org. Lett.* **2011**, 13, 4873

³² IPrCuBr is a known compound. Goj, L. A.; Blue, D. E.; Delp, S. A.; Gunnoe, B. T.; Chundari, T. R.; Pierpont, A. W.; Petersen, J. L.; Boyle, P. D. *Inorg. Chem.* **2006**, 45, 9032

Chapter 4: Copper-Catalyzed Hydroalkylation of Terminal Alkynes

Portions of this chapter as well as figures, schemes, and tables were adapted or reproduced from the following manuscript co-authored by Mycah R. Uehling: Copper-Catalyzed Hydroalkylation of Terminal Alkynes, *Journal of The American Chemical Society*, **2015**, 137, 1424. Copyright **2015** American Chemical Society.

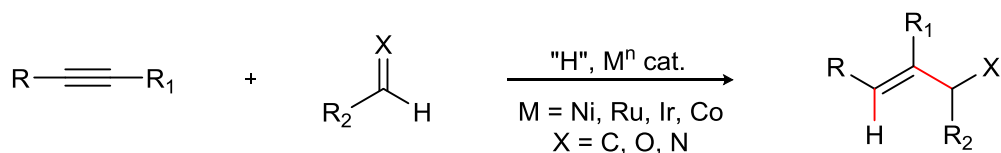
4.1 Introduction

(*E*)-Alkenes are common targets and intermediates in organic chemistry. Therefore, numerous methods for their synthesis have been developed. Classic methods such as dissolving metal reduction of alkynes,¹ Schlosser modification of the Wittig reaction,² Horner-Wadsworth Emmons reaction,³ or the Julia-Kocienski reaction,⁴ are still commonly used. In terms of catalytic methods, commonly used reactions are the Heck reaction,⁵ or methods based on cross-coupling of functionalized (*E*)-alkenes, such as alkenyl halides or alkenyl metal reagents.⁶ While the Heck reaction is usually *E* selective, it can give multiple products because of unselective β -hydride elimination and reinsertion. Methods based on cross coupling of functionalized (*E*)-alkene reagents can be cumbersome because they require the synthesis of the (*E*)-alkene reagent, which can in itself can be a challenge.⁷ Lastly, catalytic (*E*)-selective semireduction of alkynes has been developed.⁸

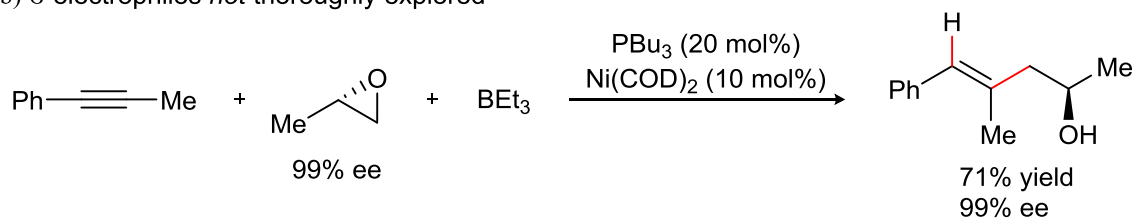
A particularly efficient, yet unexplored approach to the synthesis of alkenes, is the intermolecular hydroalkylation of alkynes. This transformation leads to an increase in both structural (new C–C bond is formed) and stereochemical (double bond geometry) complexity and offers potential for complete control of both regio- and diastereoselectivity. Furthermore, terminal alkynes and alkyl electrophiles are readily available starting materials. Despite the potential of hydroalkylation as a method for the synthesis of (*E*)-alkenes, there are still no catalytic methods for simple hydroalkylation of terminal alkynes.⁹

While there has been a considerable amount of effort focused on reductive coupling of alkynes with π electrophiles (Scheme 34a),¹⁰ reactions with alkyl electrophiles (σ) are exceedingly rare. To the best of our knowledge the only example of such a transformation was developed by Jamison and coworkers where the reductive coupling of an epoxide and an alkyne yields homoallylic alcohols (Scheme 34b).¹¹ In addition, most reductive coupling of alkynes are performed on internal alkynes. This has been proposed to be because terminal alkynes tend to form benzenes through a reductive trimerization mechanism.¹²

a) π electrophiles thoroughly explored



b) σ electrophiles *not* thoroughly explored



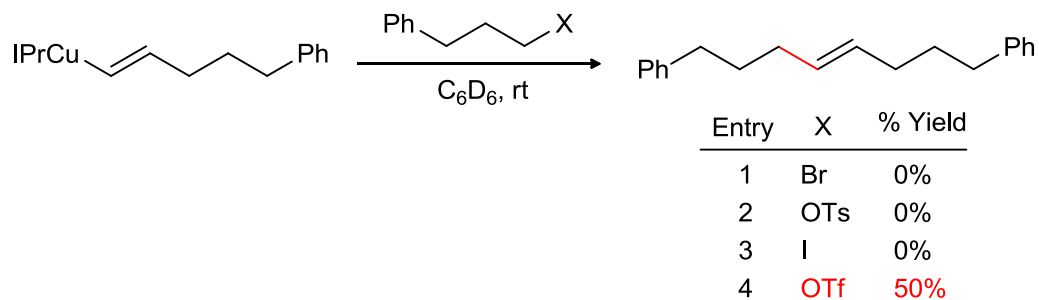
Scheme 34. Known Alkyne Hydroalkylation Strategies

Copper-catalyzed hydrofunctionalization reactions have been developed that achieve alkyne semireduction,¹³ hydrocarboxylation,¹⁴ hydroamination,¹⁵ and hydrobromination.¹⁶ All of these catalytic reactions depend upon alkyne hydrocupration with NHCCuH , first unambiguously described by Sadighi and coworkers.¹⁷ These catalytic reactions are proposed to proceed by a similar mechanism, catalytic hydrocupration of an alkyne, followed by electrophilic functionalization. In theory, as long as an electrophile is able to react with alkenyl copper, building a copper-catalyzed alkyne hydrofunctionalization reaction around this stoichiometric reaction is possible. We were drawn to simple alkyl electrophiles as those types of substrates have been underutilized in reductive couplings in general.

In addition, we hoped that a hydroalkylation reaction developed using copper-catalyzed hydrofunctionalization of alkynes would provide synthetic access to (*E*)-alkenes because hydrocupration is known to be highly regio- and stereoselective for the *cis*, anti-Markovnikov hydrometallation product.

4.2 Hydroalkylation of Alkynes Reaction Development

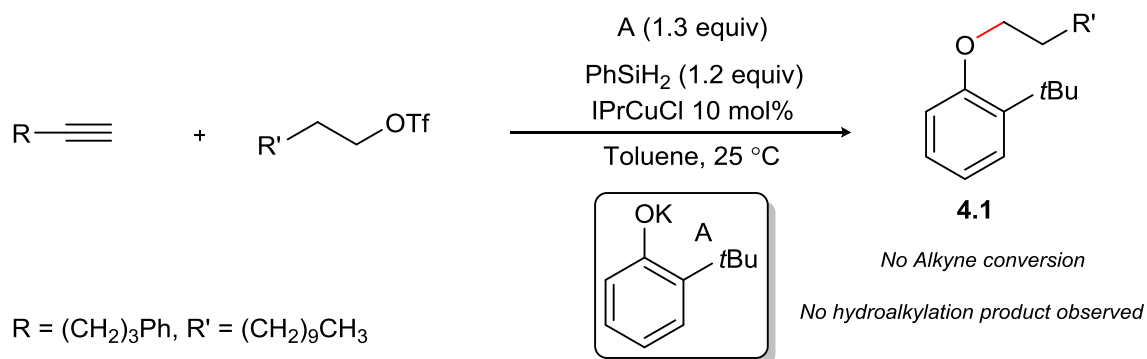
To identify an appropriate electrophile for hydroalkylation of alkynes, we explored the reactivity of the alkenyl copper with a range of alkyl electrophiles (Scheme 35). We observed that alkenyl copper did not react with common electrophiles including, alkyl tosylate, bromide, and iodide. However, in the presence of an alkyl triflate, the alkene product was formed in 50% yield. While the stoichiometric reaction between alkenyl copper complex and the alkyl triflate did not proceed to high yield, this experiment proved that it is possible to form an alkene from an NHCCuAlkenyl and an alkyl electrophile. In addition, this result showed us that we most likely will need to use an alkyl triflate electrophile in order to develop the hydroalkylation reaction.



Scheme 35. Stoichiometric Alkylation of Alkenyl Copper

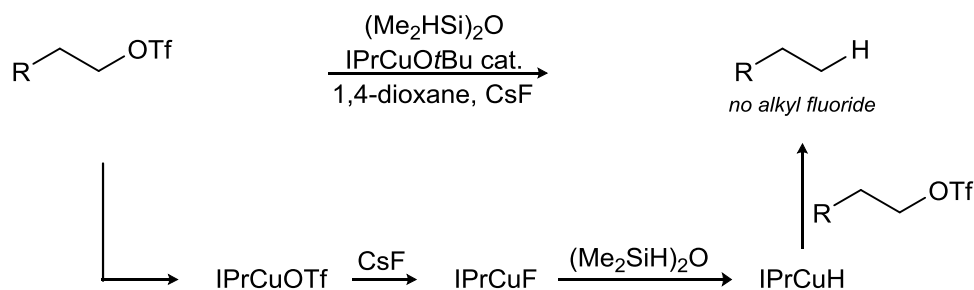
With the key insight that alkylation of alkenyl copper is most effective using an alkyl triflate, we attempted copper-catalyzed hydroalkylation of alkynes using conditions similar to those developed for catalytic hydrobromination of alkynes (Scheme 36). We observed no formation of product and minimal conversion of the alkyne. The major product that formed was the Williamson ether product **4.1**, formed through alkylation of the phenoxide with the alkyl triflate. Thus, we identified a key challenge of

hydroalkylation reaction optimization which is identification of an additive that can promote the formation of copper hydride but not react with alkyl triflate.



Scheme 36. First Attempt at Hydroalkylation of Alkynes

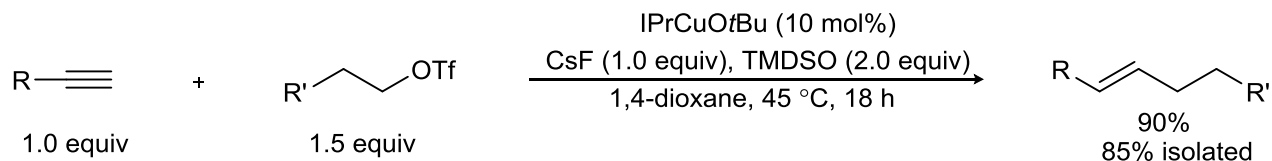
At around the same time, our lab was working on other copper-catalyzed reactions using alkyl triflates as electrophiles. For example, our lab published the copper-catalyzed reduction of alkyl triflates using silane as a hydride donor in 2014.¹⁸ A key discovery in this study was that CsF does not react with alkyl triflates unless copper is present, and if a copper fluoride species is formed, it can be trapped using silane selectively to form copper hydride as opposed to fluorination of the alkyl triflate (Scheme 37).



Scheme 37. Copper-Catalyzed Reduction of Alkyl Triflates

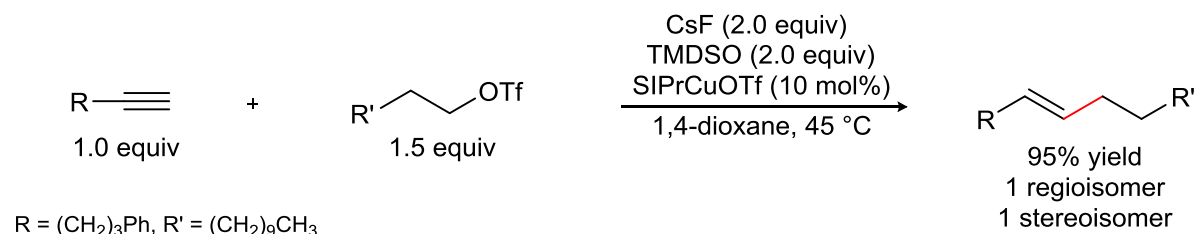
Based on the observations made during the development of alkyl triflate reduction, we proposed that if an alkyne is present, hydrocupration might be competitive with alkyl triflate reduction, and maybe hydroalkylation would proceed. We used reaction conditions optimized for alkyl triflate reduction but

simply added a terminal alkyne. Gratifyingly we observed the hydroalkylation product in 90% yield with a minimal amount of alkane formed via triflate reduction (<5%) (Scheme 38).¹⁹ With slight modification to the reaction conditions shown in scheme 38, we arrived at the fully optimized reaction shown in Table 13. The alkyl-alkyl substituted (*E*)-alkene was isolated in high yield and the (*Z*) isomer was not observable in the crude mixture by GC analysis.²⁰



Scheme 38. Optimization of Hydroalkylation of Alkynes.

Table 13. Reaction Parameters for Hydroalkylation of Alkynes



Entry	Change From Optimal Conditions	% Yield
1	ICyOTf instead of SIPrCuOTf	3%
2	PCy ₃ CuOTf instead of SIPrCuOTf	0%
3	PPh ₃ CuOTf instead of SIPrCuOTf	22%
4 ^a	toluene instead of 1,4-dioxane	70%
5 ^a	ether instead of 1,4-dioxane	82%
6 ^a	DCM instead of 1,4-dioxane	70%
7	triethoxysilane instead of TMDSO	27%
8	triethylsilane instead of TMDSO	20%

^a36 h reaction

During the development of the hydroalkylation reaction we made several observations. The choice of catalyst is crucial for the success of the reaction. SIPr- and IPrCuOTf catalyze the desired reaction efficiently (Table 13, Entries 1-3), while other catalysts bearing various NHC ligands are not

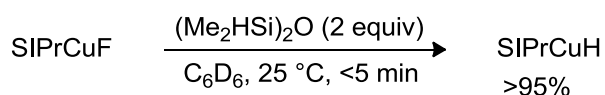
effective. The reaction proceeds in other common organic solvents (Entries 4-6), but at a substantially lower rate. Finally, Other common silanes did not perform nearly as well as $(\text{Me}_2\text{HSi})_2\text{O}$ under the optimized conditions (Entries 7-8).

4.3 Hydroalkylation of Alkynes Scope

The scope of the hydroalkylation reaction is shown in Table 14. We found that the both alkyl and aryl substituted alkynes are suitable substrates for the hydroalkylation reaction (Table 14). In addition, alkynes with α -branching are compatible substrates (Table 14, Entry 4). The hydroalkylation reaction is compatible with an array of functional groups such as ester, silyl ether, aryl bromide, alkyl bromide, alkyl tosylate, nitro, and tosyl protected amine. All compounds were isolated as one regio- and diastereoisomer. Lastly, we also found that hydrobenzylation using a benzylic triflate is possible (Table 14, Entry 9).

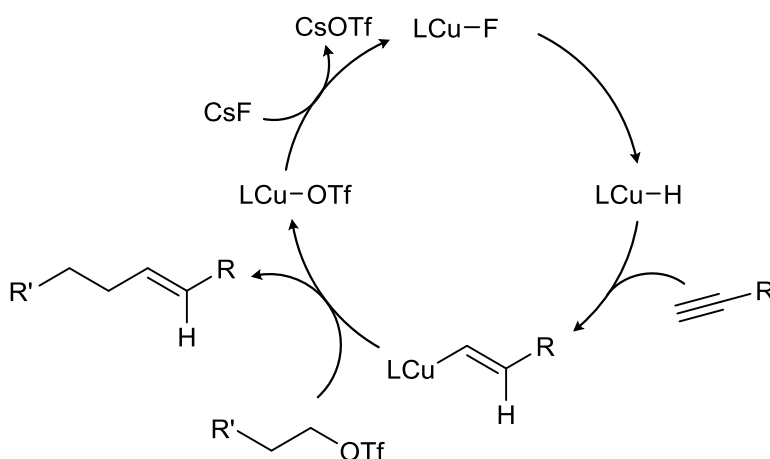
Table 14. Hydroalkylation of Alkynes Scope

Experimental evidence exists for each step of the proposed catalytic cycle. The formation of NHCCuH from NHCCuF has been studied in the context of alkyne hydrocarboxylation.²¹ In addition, we have shown that the formation of SIPrCuH from SIPrCuF through reaction with silane is efficient (Scheme 39).



Scheme 39. Formation of SIPrCuH

Hydrocupration of terminal alkynes is well established in the literature in the context of both stoichiometric experiments²² and catalytic reactions.²³ The experiment shown in Scheme 35 provides support that alkylation of alkenyl copper is possible, although the yield of this reaction is surprisingly low compared to the catalytic reaction.²⁴ After alkylation of alkenyl copper, SIPrCuOTf is converted to SIPrCuF through substitution with cesium fluoride. Our lab has recently studied the reaction between NHCCuOTf complexes and alkali metal fluorides and have shown that this type of reaction is catalytically relevant.²⁵



Scheme 40. Proposed Catalytic Cycle of Hydroalkylation of Alkynes

In an effort to provide further insight into the reaction mechanism and explore the relative rates of elementary steps involved in the catalytic cycle, we examined the kinetics of the hydroalkylation reaction. Initial experiments revealed a surprising induction period (see Figure 3). Furthermore, we found that both the induction period and the rate of the reaction strongly depend on the rate at which the reaction mixture is stirred (Figure 3, conditions A and B). We speculated that phase transfer of fluoride may limit the rate at which copper fluoride is initially formed and, in that way, cause the induction period. Indeed, when SIPrCuF was used as a catalyst there was no induction period (Figure 3, condition C). The induction period could also be reduced by vigorously stirring CsF in the heated reaction solvent for 25 min before addition of the other reagents. We also have established that the rate of the reaction does not depend upon the concentration of alkyne, silane, or alkyl triflate (See experimental). Taken together, we propose that the turnover limiting step of the catalytic cycle is phase transfer of CsF.

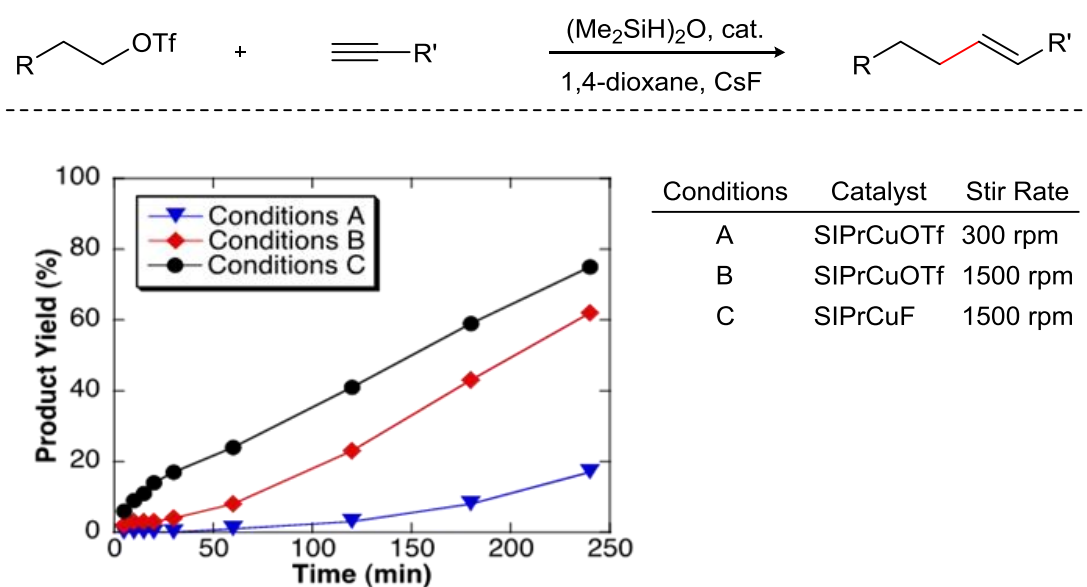


Figure 3. Hydroalkylation Reaction Time Courses Comparing Stir Rate and Catalyst

4.5 Conclusion

We have developed copper-catalyzed hydroalkylation of terminal alkynes using alkyl triflates as electrophiles. The hydroalkylation proceeds with complete control of regio- and diastereoselectivity and allows an efficient synthesis of (*E*)-alkenes from readily available starting materials. We have demonstrated that both alkyl- and aryl-substituted alkynes can be used as substrates, together with a range of primary alkyl triflates. In terms of the mechanism, we propose that the hydroalkylation reaction involves hydrocupration of the alkyne followed by electrophilic functionalization of the alkenyl copper intermediate. A preliminary study of the reaction mechanism suggests that the formation of the SIPrCuF intermediate is the turnover-limiting step of the catalytic cycle.

4.6 Experimental

General Information

All reactions were performed under an atmosphere of nitrogen with flame-dried or oven-dried (120 °C) glassware, using standard Schlenk techniques, or in a nitrogen-filled glovebox (Nexus II from Vacuum Atmospheres). Column chromatography was performed using a Biotage Iso-1SV flash purification system with silica gel from Agela Technologies Inc. (60Å, 40-60 µm, 230-400 mesh) or activated alumina purchased from Sigma Aldrich (CAS# 344-28-1). ¹H- and ¹³C-NMR spectra were recorded on a Bruker AV-300 or AV-500 spectrometer. ¹H NMR chemical shifts (δ) are reported in parts per million (ppm) downfield of TMS and are referenced relative to the residual solvent peak (CDCl₃ (7.26 ppm), C₆D₆ (7.16 ppm), or CD₂Cl₂ (5.32 ppm)). ¹³C chemical shifts are reported in parts per million downfield of TMS and are referenced to the carbon resonance of the solvent (CDCl₃: δ 77.2 ppm, C₆D₆: δ 128.1 ppm, CD₂Cl₂: δ 54.0 ppm). Data are represented as follows: chemical shift, multiplicity (s = singlet, bs = broad singlet, d = doublet, t = triplet, q = quartet, p = pentet, h = heptet m = multiplet), integration, and coupling

constants in Hertz (Hz). Mass spectra were collected on a JEOL HX-110 Mass Spectrometer, a Bruker Esquire 1100 Liquid Chromatograph – Ion Trap Mass Spectrometer, or a Hewlett Packard 5971A gas chromatograph Mass Spectrometer. GC analysis was performed on a Shimadzu GC-2010 instrument with a flame ionization detector and a SHRXI-5MS column (15 m, 0.25 mm inner diameter, 0.25 μm film thickness). The following temperature program was used: 2 min @ 60 $^{\circ}\text{C}$, 13 $^{\circ}\text{C}/\text{min}$ to 160 $^{\circ}\text{C}$, 30 $^{\circ}\text{C}/\text{min}$ to 250 $^{\circ}\text{C}$, 5.5 min @ 250 $^{\circ}\text{C}$. Infrared (IR) spectra were recorded on a Perkin Elmer Spectrum RX I spectrometer. IR peak absorbencies are represented as follows: s = strong, m = medium, w = weak, br = broad.

Materials: Toluene, benzene, ether, DCM, and THF were dried by passing through columns of neutral alumina. 1,4-dioxane was distilled over calcium hydride, degassed, and stored over activated molecular sieves. All other solvents were used as received. Deuterated solvents were purchased from Cambridge Isotope Laboratories, Inc. Common commercial reagents were purchased from Sigma-Aldrich Co., VWR International, LLC., TCI America, or STREM Chemicals, Inc. $(\text{Me}_2\text{SiH})_2\text{O}$ (TMDSO) was purchased from Oakwood Chemical and vacuum transferred over calcium hydride before use. Cesium fluoride was purchased from Matrix Scientific or Sigma Aldrich. The material was dried rigorously by flame-drying under vacuum followed by grinding with a mortar and pestle in a glove box. This process was repeated three times. 4-(trifluoromethyl)benzyl bromide and 4-nitrobenzyl bromide were purchased from Sigma-Aldrich. 2,6-Lutidine was purchased from TCI America and distilled over calcium hydride, then vacuum transferred over aluminum trichloride. Triflic anhydride was purchased from Oakwood Chemical and vacuum transferred over P_2O_5 .

4.6.1 Reaction Development

In a glovebox, a dram vial was charged with a stir bar, catalyst (either a preligated copper complex, or ligand and copper (I) triflate benzene complex [CAS #4215-46-5]), octyl ether (internal standard), cesium fluoride, and solvent. After allowing the mixture to stir vigorously at 45 °C for 20 minutes, silane was added followed by alkyne and alkyl triflate. The reaction temperature was maintained at 45 °C and stirred vigorously. After 4 hours, a GC aliquot was taken to measure the yield.

Table 15. Hydoalkylation Catalyst Screen

$$\begin{array}{c}
 \text{R}-\text{C}\equiv\text{C} \\
 \text{1.0 equiv}
 \end{array}
 +
 \begin{array}{c}
 \text{TfO}-\text{CH}_2\text{CH}_2-\text{R}' \\
 \text{1.5 equiv}
 \end{array}
 \xrightarrow[\text{1,4-dioxane, 45 }^\circ\text{C, 4h}]{\begin{array}{c} \text{CsF (2.0 equiv)} \\ (\text{Me}_2\text{SiH})_2\text{O (2.0 equiv)} \\ \text{catalyst (10 mol\%)} \end{array}}
 \begin{array}{c}
 \text{R}-\text{CH}=\text{CH}-\text{CH}_2-\text{CH}_2-\text{R}'
 \end{array}$$

entry	catalyst	% yield
1	SIPrCuOTf	95%
2	IPrCuOTf	85%
3	ICyCuOTf	3%
4	ItBuCuOTf	1%
5	IAdCuOTf	1%
6	PCy ₃ CuOTf	3%
7	PPh ₃ CuOTf	22%
8	XantphosCuOTf	0%
9	DPPPCuOTf	0%
10	DPPBCuOTf	1%
11	DPPFCuOTf	0%
12	BipyCuOTf	0%

R = (CH₂)₃Ph, R' = (CH₂)₉CH₃

Table 16. Solvent Screen

$\text{R}-\text{C}\equiv\text{C} + \text{TfO}-\text{CH}_2\text{CH}_2-\text{R}' \xrightarrow[\text{solvent, 45 }^\circ\text{C, 4h}]{\text{CsF (1.0 equiv), (Me}_2\text{SiH)}_2\text{O (2.0 equiv), SIPrCuOTf (10 mol\%)}$
 $\text{R}-\text{CH}=\text{CH}-\text{CH}_2\text{CH}_2-\text{R}'$

entry	catalyst	% yield ^a	% yield ^b
1	Dioxane	91% ^c	-
2	Toluene	12%	70%
3	Ether	37%	82%
4	DCM	16%	70%
5	Glyme	35% ^{c,d}	-
6	ClC ₆ H ₅	0%	21%
7	CH ₃ CN	20% ^{c,d}	-
8	DCE	1%	50%

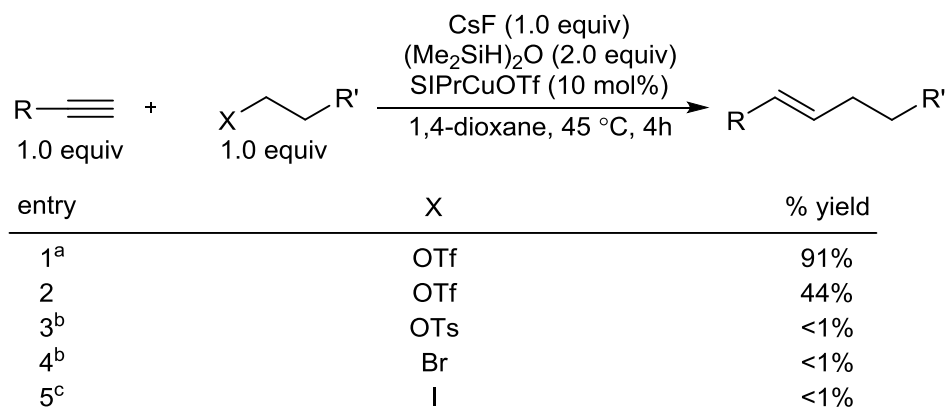
R = (CH₂)₃Ph, R' = (CH₂)₉CH₃, ^ayield after 5h, ^byield after 36 h, ^cyield was not measured at 36 h, ^dalkyl triflate was fully converted after 5 hours.

Table 17. Silane Screen

$\text{R}-\text{C}\equiv\text{C} + \text{TfO}-\text{CH}_2\text{CH}_2-\text{R}' \xrightarrow[\text{solvent, 45 }^\circ\text{C, 4h}]{\text{CsF (1.0 equiv), Silane (2.0 equiv), SIPrCuOTf (10 mol\%)}$
 $\text{R}-\text{CH}=\text{CH}-\text{CH}_2\text{CH}_2-\text{R}'$

entry	silane	% yield
1	TMDSO	91%
2	PMHS	32%
3	triethoxy silane	27%
4	diethoxy methyl silane	67%
5	diethoxy methyl silane	66% ^a
6	triethyl silane	20%

R = (CH₂)₃Ph, R' = (CH₂)₉CH₃, ^a4 equivalents of diethoxy methyl silane

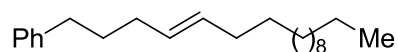
Table 18. Electrophile Screen in Catalytic Reaction

R = (CH₂)₃Ph, R' = (CH₂)₉CH₃. ^a1.5 equiv alkyl triflate. ^bIPrCuOtBu used as catalyst. 1.0 equiv TMDSO. ^cR' = CH₂Ph, 1.5 equiv alkyl iodide

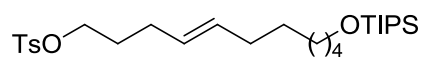
4.6.2 General Procedure for Hydroalkylation of Alkynes

In a glovebox, a scintillation vial was charged with a stir bar, SIPrCuOTf (30 mg, 0.05 mmol, 0.10 equiv), cesium fluoride (152 mg, 1 mmol, 2.0 equiv), and 1,4-dioxane (5 mL, 0.1 M). After allowing the mixture to stir at 45 °C for 20 minutes, (Me₂SiH)₂O (190 μL, 1 mmol, 2.0 equiv) was added, followed by alkyne (0.5 mmol, 1.0 equiv) and alkyl triflate (0.75 mmol, 1.5 equiv). The reaction was stirred vigorously at 45 °C. After the alkyne was no longer observable by TLC, the reaction was filtered through a pad of silica gel with EtOAc. The crude mixture was concentrated under reduced pressure and purified by column chromatography using silica gel or activated alumina.

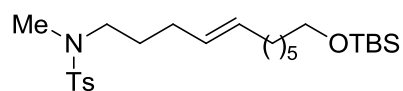
4.6.3 Characterization Data for Alkene Products



(4E)-heptadec-4-en-1-ylbenzene (4.2), compound was purified on a silica gel column with EtOAc/Hex (0→15%) and isolated as a clear oil, 141 mg, 90% yield, 95% yield measured by GC. ^1H NMR (300 MHz, Chloroform-*d*) δ 7.40 – 7.22 (m, 2H, CHCl_3 overlap), 7.24 – 7.05 (m, 3H), 5.51 – 5.30 (m, 2H), 2.73 – 2.50 (m, 2H), 2.13 – 1.89 (m, 4H), 1.69 (q, $J = 7.7$ Hz, 2H), 1.26 (bs, 20H, slight impurity), 0.88 (t, $J = 6.6$ Hz, 3H). ^{13}C NMR (126 MHz, Chloroform-*d*) δ 131.2, 129.9, 128.6, 128.5, 128.4, 125.7, 35.5, 32.8, 32.3, 32.1, 31.5, 29.8, 29.8 (multiple resonances overlapping), 29.7, 29.5, 29.3, 22.8, 14.3. GC/MS calculated for $[\text{M}]^+$ 314.3, found 314.4. FTIR (neat, cm^{-1}): 3063 (w), 3027 (w), 2924 (s), 2853 (m), 1605 (w), 1496 (m), 1454 (m), 966 (m), 697 (m).

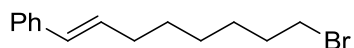


(4E)-11-[[tris(propan-2-yl)silyl]oxy]undec-4-en-1-yl 4-methylbenzene-1-sulfonate (4.7), compound was purified on an alumina column with EtOAc/Hex (0→20%) and isolated as a yellow oil, 220 mg, 89% yield. ^1H NMR (300 MHz, Chloroform-*d*) δ 7.79 (d, $J = 8.3$ Hz, 2H), 7.34 (d, $J = 8.0$ Hz, 2H), 5.41 – 5.14 (m, 2H), 4.02 (t, $J = 6.4$ Hz, 2H), 3.66 (t, $J = 6.6$ Hz, 2H), 2.45 (s, 3H), 2.00 (q, $J = 7.1$ Hz, 2H), 1.91 (q, $J = 6.4$ Hz, 2H), 1.69 (p, $J = 6.7$ Hz, 2H), 1.59 – 1.46 (m, 2H, water overlap), 1.41 – 1.21 (m, 6H), 1.17 – 0.94 (m, 21H). ^{13}C NMR (75 MHz, Chloroform-*d*) δ 144.7, 133.4, 132.3, 129.9, 128.1, 127.9, 70.0, 63.6, 33.2, 32.6, 29.6, 29.1, 28.8, 28.3, 25.8, 21.8, 18.2, 12.2. ESI MS calculated for $[\text{M} + \text{Na}]^+$ 519.3, found 519.4. FTIR (neat, cm^{-1}): 2939 (s), 2865 (s), 1599 (w), 1463 (m), 1366 (m), 1178 (s), 1099 (s), 882 (m), 664 (m).

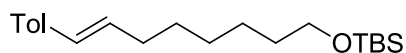


N-[(4E)-11-[(tert-butyldimethylsilyl)oxy]undec-4-en-1-yl]-N,4-dimethylbenzene-1-

sulfonamide (4.11), compound was purified on a silica gel column with EtOAc/Hex (0→30%) and isolated as a yellow oil, 225 mg, 96% yield. ¹H NMR (300 MHz, Chloroform-*d*) δ 7.66 (d, *J* = 8.2 Hz, 2H), 7.31 (d, *J* = 8.1 Hz, 2H), 5.47 – 5.31 (m, 2H), 3.59 (t, *J* = 6.6 Hz, 2H), 3.01 – 2.93 (m, 2H), 2.70 (s, 3H), 2.43 (s, 3H), 1.99 (dq, *J* = 14.2, 7.1 Hz, 4H), 1.64 – 1.44 (m, 4H, H₂O overlap), 1.37 – 1.23 (m, 6H), 0.89 (s, 9H), 0.04 (s, 6H). ¹³C NMR (75 MHz, Chloroform-*d*) δ 143.3, 134.8, 131.7, 129.7, 128.9, 127.6, 63.5, 50.1, 49.9, 34.8, 33.0, 32.6, 29.6, 29.1, 27.7, 26.1, 25.8, 21.6, 18.5, -5.1. ESI MS calculated for [M + Na]⁺ 490.3, found 490.4. FTIR (neat, cm⁻¹): 2926 (s), 2853 (s), 1596 (w), 1567 (m), 1342 (s), 1160 (s), 1088 (s), 834 (m), 714 (m).

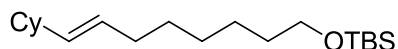


[(1E)-8-bromooct-1-en-1-yl]benzene (4.8), compound was purified on a silica gel column with EtOAc/Hex (0→25%) and isolated as a clear oil, 105 mg, 78% yield. ¹H NMR (300 MHz, Methylene Chloride-*d*₂) δ 7.38 – 7.24 (m, 4H), 7.23 – 7.12 (m, 1H), 6.39 (d, *J* = 16.0 Hz, 1H), 6.32 – 6.17 (m, 1H), 3.43 (t, *J* = 6.9 Hz, 2H), 2.22 (q, *J* = 6.8 Hz, 2H), 1.87 (p, *J* = 6.8 Hz, 2H), 1.67 – 1.01 (m, 6H, water overlap). ¹³C NMR (126 MHz, Chloroform-*d*) δ 138.0, 131.0, 130.1, 128.6, 127.0, 126.1, 34.1, 33.0, 32.9, 29.3, 28.4, 28.2. GC/MS calculated for [M]⁺ 266.1, found 266.1. FTIR (neat, cm⁻¹): 3019 (w), 2926 (s), 2843 (m), 1944 (w), 1876 (w), 1793 (w), 1596 (m), 1492 (m), 1254 (m), 963 (s), 745 (m), 692 (s).

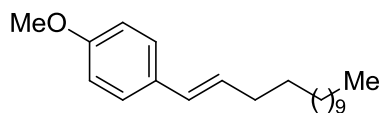


tert-butyldimethyl{[(7E)-8-(4-methylphenyl)oct-7-en-1-yl]oxy}silane (4.3), compound purified on a silica gel column with EtOAc/Hex (0→15%) and isolated as a yellow oil, 145 mg, 87% yield. ¹H NMR (300 MHz, Chloroform-*d*) δ 7.24 (d, *J* = 8.1 Hz, 2H), 7.10 (d, *J* = 8.0 Hz,

2H), 6.35 (d, $J = 15.8$ Hz, 1H), 6.16 (dt, $J = 15.8, 6.8$ Hz, 1H), 3.61 (t, $J = 6.5$ Hz, 2H), 2.32 (s, 3H), 2.19 (q, $J = 7.1$ Hz, 2H), 1.65 – 1.41 (m, 4H, H₂O overlap), 1.41 – 1.29 (m, 4H), 0.90 (s, 9H), 0.05 (s, 6H). ¹³C NMR (75 MHz, Chloroform-*d*) δ 136.6, 135.3, 130.2, 129.7, 129.3, 125.9, 63.4, 33.1, 33.0, 29.6, 29.2, 26.1, 25.9, 21.3, 18.5, -5.1. GC/MS calculated for [M]⁺ 332.3, found 332.3. FTIR (neat, cm⁻¹): 3022 (w), 2928 (s), 2856 (s), 1513 (m), 1471 (m), 1255 (s), 1100 (s), 836 (s), 744 (s).

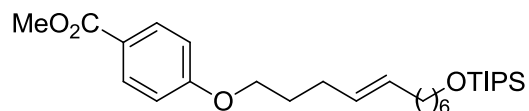


tert-butyl(7E)-8-cyclohexyloct-7-en-1-yl]oxy}dimethylsilane (4.5), compound purified on a silica gel column with EtOAc/Hex (0→15%) and isolated as a clear oil, 120 mg, 72% yield. ¹H NMR (300 MHz, Chloroform-*d*) δ 5.50 – 5.21 (m, 2H), 3.59 (t, $J = 6.6$ Hz, 2H), 2.01 – 1.85 (m, 3H), 1.77 – 1.62 (m, 5H), 1.57 – 1.45 (m, 2H), 1.39 – 0.98 (m, 12H, minor impurity), 0.89 (s, 9H), 0.05 (s, 6H). ¹³C NMR (75 MHz, Chloroform-*d*) δ 136.6, 127.8, 63.5, 40.8, 33.4, 33.0, 32.7, 29.8, 29.1, 26.4, 26.3, 26.1, 25.8, 18.5, -5.1. ESI MS calculated for [M + H]⁺ 325.3, found 325.4. FTIR (neat, cm⁻¹): 2926 (s), 2854 (s), 1471 (m), 1255 (m), 1102 (m), 835 (s).

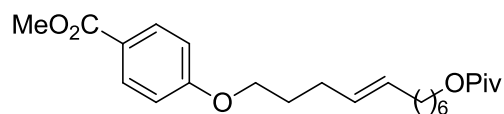


1-methoxy-4-[(1E)-tetradec-1-en-1-yl]benzene (4.9), compound was purified on a silica gel column with EtOAc/Hex (0→15%) and isolated as a yellow oil, 135 mg, 90% yield. ¹H NMR (300 MHz, Chloroform-*d*) δ 7.27 (d, $J = 8.6$ Hz, 2H), 6.84 (d, $J = 8.7$ Hz, 2H), 6.32 (d, $J = 15.8$ Hz, 1H), 6.08 (dt, $J = 15.7, 6.8$ Hz, 1H), 3.80 (s, 3H), 2.18 (q, $J = 6.9$ Hz, 2H), 1.51 – 1.37 (m, 2H), 1.27 (bs, 18H), 0.88 (t, $J = 6.6$ Hz, 3H). ¹³C NMR (126 MHz, Chloroform-*d*) δ 158.7, 131.0, 129.3, 129.1, 114.0, 55.4, 33.2, 32.1, 29.8 (multiple resonances) 29.7 (multiple resonances) ,

29.5, 29.4 , 22.8, 14.3. GC/MS calculated for $[M]^+$ 302.3, found 302.4. FTIR (neat, cm^{-1}): 3021 (w), 2920 (s), 2851 (s), 1701 (w), 1654 (w), 1608 (m), 1511 (s), 1466 (s), 1247 (s), 1175 (m), 1035 (m), 962 (m), 802 (m).

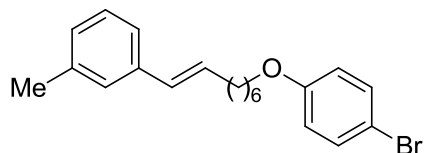


methyl 4-[[[(4E)-11-[[tris(propan-2-yl)silyl]oxy]undec-4-en-1-yl]oxy]benzoate, compound purified on an alumina column with EtOAc/Hex (0→25%) and isolated as a clear oil, 211 mg, 89% yield. ^1H NMR (300 MHz, Benzene- d_6) δ 8.16 (d, $J = 8.8$ Hz, 2H), 6.72 (d, $J = 8.9$ Hz, 2H), 5.52 – 5.28 (m, 2H), 3.66 (t, $J = 6.3$ Hz, 2H), 3.60 – 3.44 (m, 5H), 2.03 (dq, $J = 13.0, 6.4$ Hz, 4H), 1.80 – 1.52 (m, 4H), 1.47 – 1.28 (m, 6H), 1.26 – 1.03 (m, 21H, slight impurity). ^{13}C NMR (75 MHz, Chloroform- d) δ 167.0, 163.1, 131.8, 131.7, 128.9, 122.5, 114.2, 67.6, 63.6, 51.9, 33.1, 32.6, 29.7, 29.1, 29.1, 29.0, 25.8, 18.2, 12.2. ESI MS calculated for $[M + \text{Na}]^+$ 499.3, found 499.4. FTIR (neat, cm^{-1}): 2930 (s), 2865 (s), 1722 (s), 1607 (s), 1435 (m), 1279 (s), 1104 (s), 882 (m), 770 (m).

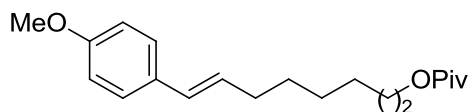


methyl 4-[[[(4E)-11-[(2,2-dimethylpropanoyl)oxy]undec-4-en-1-yl]oxy]benzoate, compound was purified on a silica gel column with EtOAc/Hex (0→25%) and isolated as a clear oil, 159 mg, 79% yield. ^1H NMR (300 MHz, Chloroform- d) δ 7.97 (d, $J = 8.9$ Hz, 2H), 6.89 (d, $J = 9.0$ Hz, 2H), 5.47 – 5.39 (m, 2H), 4.08 – 3.96 (m, 4H), 3.88 (s, 3H), 2.17 (q, $J = 6.9$ Hz, 2H), 2.04 – 1.93 (m, 2H), 1.85 (p, $J = 6.6$ Hz, 2H), 1.67 – 1.52 (m, 2H, H_2O overlap), 1.44 – 1.26 (m, 6H), 1.19 (s, 9H). ^{13}C NMR (75 MHz, Chloroform- d) δ 178.8, 167.0, 163.0, 131.7, 131.6, 129.0, 122.5, 114.2,

67.5, 64.5, 52.0, 38.9, 32.6, 29.5, 29.0, 29.0, 28.8, 28.7, 27.3, 25.9. ESI MS calculated for $[M + Na]^+$ 427.2, found 427.4. FTIR (neat, cm^{-1}): 2933 (s), 2856 (m), 2099 (w), 1918 (w), 1722 (s), 1715 (s), 1606 (s), 1511 (m), 1254 (m), 1104 (m), 847 (w).

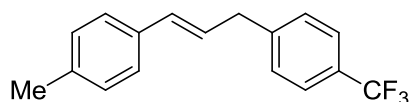


1-[(1E)-8-(4-bromophenoxy)oct-1-en-1-yl]-3-methylbenzene (4.6), compound purified on a silica gel column with EtOAc/Hex (0→15%) and isolated as a yellow oil, 153 mg, 82% yield. 1H NMR (300 MHz, Chloroform-*d*) δ 7.41 – 7.29 (m, 2H), 7.24 – 7.09 (m, 3H), 7.01 (d, $J = 6.9$ Hz, 1H), 6.83 – 6.71 (m, 2H), 6.35 (d, $J = 15.9$ Hz, 1H), 6.20 (dt, $J = 15.7, 6.7$ Hz, 1H), 3.92 (t, $J = 6.5$ Hz, 2H), 2.33 (s, 3H), 2.22 (q, $J = 6.6$ Hz, 2H), 1.78 (p, $J = 6.5$ Hz, 2H), 1.63 – 1.24 (m, 6H). ^{13}C NMR (75 MHz, Chloroform-*d*) δ 158.4, 138.1, 137.9, 132.3, 130.9, 130.1, 128.5, 127.7, 126.8, 123.2, 116.4, 112.7, 68.3, 33.1, 29.4, 29.2, 29.0, 26.0, 21.6. GC/MS calculated for $[M]^+$ 372.1, found 372.2. FTIR (neat, cm^{-1}): 3020 (w), 2929 (s), 2855 (m), 1870 (w), 1738 (w), 1650 (w), 1591 (m), 1489 (s), 1286 (m), 1244 (s), 1071 (m), 821 (s), 692 (m).

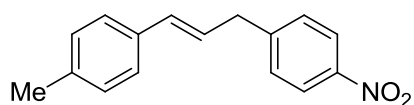


(7E)-8-(4-methoxyphenyl)oct-7-en-1-yl 2,2-dimethylpropanoate (4.4), compound purified on a silica gel column EtOAc/Hex (0→20%) and isolated as a yellow oil, 149 mg, 94% yield. 1H NMR (300 MHz, Chloroform-*d*) δ 7.27 (d, $J = 7.5$ Hz, 2H, $CHCl_3$ overlap), 6.84 (d, $J = 8.6$ Hz, 2H), 6.32 (d, $J = 15.7$ Hz, 2H), 6.07 (dt, $J = 15.7, 6.8$ Hz, 1H), 4.05 (t, $J = 6.5$ Hz, 2H), 3.80 (s, 3H), 2.19 (q, $J = 6.6$ Hz, 2H), 1.68 – 1.55 (m, 2H), 1.51 – 1.33 (m, 6H), 1.20 (s, 9H). ^{13}C NMR

(126 MHz, Chloroform-*d*) δ 178.8, 158.8, 130.9, 129.4, 128.9, 127.1, 114.1, 64.6, 55.4, 38.9, 33.0, 29.5, 28.9, 28.7, 27.4, 26.0. GC/MS calculated for $[M]^+$ 318.2, found 318.3. FTIR (neat, cm^{-1}): 3030 (w), 2957 (s), 2932 (s), 2857 (w), 2254 (m), 1720 (s), 1608 (m), 1511 (s), 1248 (s), 1174 (s), 909 (s), 734 (s).



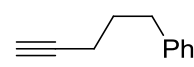
1-methyl-4-[(1E)-3-[4-(trifluoromethyl)phenyl]prop-1-en-1-yl]benzene, compound purified on a silica gel column with EtOAc/Hex (0 \rightarrow 15%) and isolated as a clear oil, 110 mg, 80% yield. ^1H NMR (300 MHz, Chloroform-*d*) δ 7.56 (d, $J = 8.1$ Hz, 2H), 7.35 (d, $J = 8.0$ Hz, 2H), 7.26 (d, $J = 8.1$ Hz, 2H, CHCl_3 overlap), 7.11 (d, $J = 8.0$ Hz, 2H), 6.44 (d, $J = 15.8$ Hz, 1H), 6.26 (dt, $J = 15.7, 6.8$ Hz, 1H), 3.59 (d, $J = 6.8$ Hz, 2H), 2.33 (s, 3H). ^{13}C NMR (126 MHz, Methylene Chloride-*d*₂) δ 145.3, 137.7, 134.8, 132.1, 129.6, 129.5, 128.6 (q, $J = 32.2$ Hz), 127.4, 126.4, 125.7 (q, $J = 3.8$ Hz), 124.9 (q, $J = 271.5$ Hz), 39.4, 21.3. ^{19}F NMR (471 MHz, Chloroform-*d*) δ -62.32. GC/MS calculated for $[M]^+$ 276.1, found 276.1. FTIR (neat, cm^{-1}): 3024 (w), 2924 (w), 1618 (m), 1512 (m), 1416 (m), 1325 (s), 1163 (m), 1124 (s), 1018 (m), 969 (m).

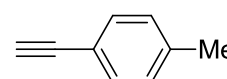


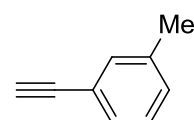
1-methyl-4-[(1E)-3-(4-nitrophenyl)prop-1-en-1-yl]benzene (4.10), compound purified on a silica gel column with EtOAc/Hex (0 \rightarrow 20%) and isolated as a yellow oil, 102 mg, 81% yield. ^1H NMR (300 MHz, Chloroform-*d*) δ 8.17 (d, $J = 8.7$ Hz, 2H), 7.40 (d, $J = 8.6$ Hz, 2H), 7.29 – 7.22 (m, 2H, CHCl_3 overlap), 7.12 (d, $J = 8.0$ Hz, 2H), 6.46 (d, $J = 15.9$ Hz, 1H), 6.25 (dt, $J = 15.8, 6.8$ Hz, 1H), 3.64 (d, $J = 6.4$ Hz, 2H), 2.33 (s, 3H). ^{13}C NMR (126 MHz, Chloroform-*d*) δ 148.3,

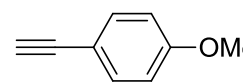
146.8, 137.6, 134.2, 132.6, 129.6, 129.5, 126.2, 126.0, 123.9, 39.2, 21.3. GC/MS calculated for $[M]^+$ 253.1, found 253.2. FTIR (neat, cm^{-1}): 3025 (w), 2923 (w), 1599 (m), 1518 (s), 1344 (s), 1109 (m), 969 (m), 857 (m), 737 (m).

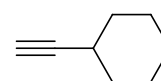
4.6.4 Alkyne Starting Materials

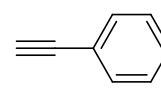
 **pent-4-yn-1-ylbenzene (4.12)**, was purchased from GSF Chemicals and distilled over calcium hydride under high vacuum before use.

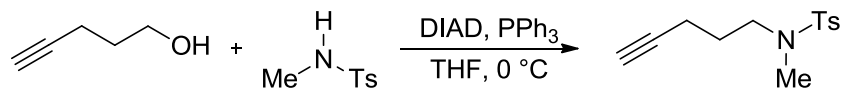
 **4-ethynyltoluene (4.13)** was purchased from Sigma-Aldrich and used as received.

 **3-ethynyltoluene (4.14)** was purchased from Sigma-Aldrich and used as received.

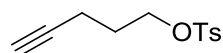
 **4-ethynylanisole (4.15)** was purchased from Sigma-Aldrich and used as received.

 **cyclohexylacetylene (4.16)** was purchased from Sigma-Aldrich and used as received.

 **phenylacetylene (4.17)** was purchased from Sigma-Aldrich and distilled over calcium hydride under high vacuum before use.

N-methyl-N-(pent-4-yn-1-yl) tosylsulfonamide (4.18):

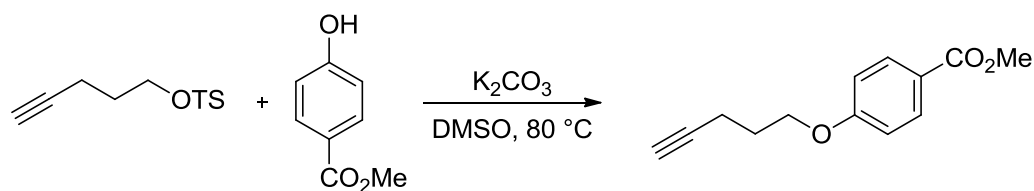
A round bottom flask was charged with a stir bar, 4-pentyne-1-ol (4.2 g, 1.0 equiv, 50 mmol), triphenylphosphine (14.4 g, 1.1 equiv, 55 mmol), N-methyl-*p*-toluenesulfonamide (9.3 g, 1.0 equiv, 50 mmol), and THF (1 M). The mixture was cooled to 0 °C with an ice bath. To the cooled mixture was added DIAD (10.8 mL, 1.1 equiv, 55 mmol) dropwise. The mixture was allowed to warm to room temperature and stir for 16 hours. At this time, the THF was removed under reduced pressure and the mixture was suspended in hexane and stirred vigorously for one hour. Solid triphenylphosphine oxide was removed by filtration through a silica plug with 20% EtOAc/Hex. The solvent was removed under reduced pressure and the product was purified on an activated alumina column with EtOAc/Hex (0 → 25%). The product was isolated as a white solid in 60 %, 7.5g. ¹H NMR (300 MHz, Chloroform-*d*) δ 7.66 (d, *J* = 8.3 Hz, 2H), 7.31 (d, *J* = 8.0 Hz, 2H), 3.08 (t, *J* = 7.0 Hz, 2H), 2.73 (s, 3H), 2.42 (s, 3H), 2.26 (td, *J* = 7.1, 2.6 Hz, 2H), 1.96 (t, *J* = 2.6 Hz, 1H), 1.77 (p, *J* = 7.1 Hz, 2H). ¹³C NMR (75 MHz, Chloroform-*d*) δ 143.5, 134.6, 129.8, 127.5, 83.3, 69.1, 49.3, 35.2, 27.0, 21.6, 15.8. ESI MS calculated for [M + Na]⁺ 274.1, found 274.2. FTIR (neat, cm⁻¹): 3280 (m), 2926 (m), 2871 (m), 1717 (w), 1598 (m), 1465 (m), 1339 (s), 1160 (s), 968 (w), 816 (w).



pent-4-yn-1-yl 4-methylbenzene-1-sulfonate (4.19) was prepared according to

a known procedure and has been previously characterized.²⁶

methyl 4-(pent-4-yn-1-yloxy)benzoate (4.20)



A flame dried reaction flask was charged with a stir bar, potassium carbonate (3.8 g, 1.4 equiv, 27.3 mmol), methyl 4-hydroxybenzoate (3.4 g, 1.2 equiv, 22.4 mmol), and DMSO (0.8 M, 10 mL). To this mixture was added pent-4-yn-1-yl 4-methylbenzene-1-sulfonate (4.6 g, 1.0 equiv, 19.5 mmol). The mixture was stirred at 80 °C until the tosylate was not observable by TLC. The mixture was diluted with 10 mL water and 40 mL ether and extracted 3 times. The organic phase was washed 3 times with 5 mL of water. The material was dried with magnesium sulfate and concentrated under reduced pressure. The crude product was purified on a silica gel column with EtOAc/Hex (0 →25%). The product was isolated as a white solid in 85% yield, 3.6 g. ¹H NMR (300 MHz, Chloroform-*d*) δ 7.96 (d, *J* = 8.5 Hz, 2H), 6.89 (d, *J* = 8.5 Hz, 2H), 4.09 (t, *J* = 6.0 Hz, 2H), 3.86 (s, 3H), 2.44 – 2.33 (m, 2H), 2.16 – 1.72 (m, 3H). ¹³C NMR (75 MHz, Chloroform-*d*) δ 166.8, 162.7, 131.6, 122.7, 114.1, 83.2, 69.2, 66.3, 51.9, 28.0, 15.1. ESI MS calculated for [M + Na]⁺ 241.2, found 241.2. FTIR (neat, cm⁻¹): 3288 (s), 2936 (m), 2118 (w), 1918 (w), 1715 (s), 1606 (s), 1511 (m), 1254 (s), 1106 (m), 847 (s).

4.6.5 Primary Alcohol Starting Materials


dodecan-1-ol (4.21) was purchased from Sigma-Aldrich and used as received.

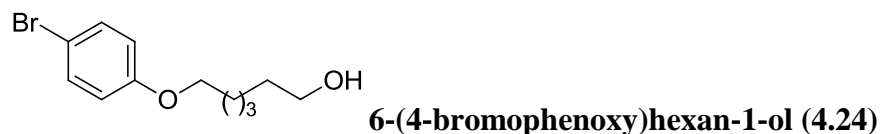

6-[(tert-butyldimethylsilyloxy)hexan-1-ol (4.22)

A 200 mL round bottom flask was charged with a stir bar, 1,6-hexanediol (8.9 g, 1.5 equiv, 75 mmol), imidazole (6.8 g, 2.0 equiv, 100 mmol), and DCM (50 mL, 1.0 M). The mixture was

stirred vigorously and a solution of TBSCl in DCM (7.5 g, 1.0 equiv, 50.0 mmol, in 25 mL DCM) was added with a syringe pump over 2 h. The mixture was allowed to stir overnight after which time the material was filtered through a silica gel plug with 40% EtOAc/Hex. The mixture was concentrated under reduced pressure and purified by silica gel column chromatography using EtOAc/Hex (10→60%) yielding 7.0 g of clear oil, 61% yield. This compound has been previously characterized.²⁷



A 200 mL round bottom flask was charged with a stir bar, 1,6-hexanediol (9.4 g, 80 mmol, 2 equiv), DCM (80 mL, 1 M), and pivaloyl chloride (4.9 mL, 40 mmol, 1 equiv). The mixture was cooled to 0 °C and pyridine (8 mL, 1.3 equiv, 52 mmol) was added dropwise. After 8 hours, the mixture was diluted in ether and washed with 1 M HCl, sodium bicarbonate, and brine. The mixture was then dried with magnesium sulfate and concentrated under reduced pressure. The product was purified on a silica gel column with EtOAc/Hex (5 → 60%) to yield 4.3 g of a clear oil, 68% yield. This compound has been previously characterized.²⁸



The preparation of this compound has been previously reported and this compound has been previously characterized.²⁹



A 200 mL round bottom flask was charged with a stir bar, 1,6-hexanediol (5.9 g, 1.0 equiv, 50.0 mmol), DCM (50 mL, 0.2 M), TIPSCl (11.7 mL, 1.1 equiv, 55.0 mmol), and 4-dimethyl amino pyridine (600 mg, 0.1 equiv, 5 mmol). The mixture was cooled to 0 °C and triethylamine (8.3 mL, 1.2 equiv, 60.0 mmol) was added dropwise. The mixture was allowed to warm to room temperature and stirred for 16 hours, at which time the mixture was filtered through a plug of silica gel with 50% EtOAc/Hex. The crude material was concentrated under reduced pressure and purified on a silica gel column with EtOAc/Hex (10 → 60%) to yield 5.5 g of a clear oil, 55% yield. This compound has been previously characterized.³⁰

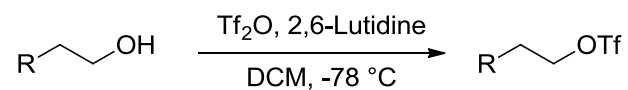


Step 1: A round bottom flask was charged with a stir bar, 6-[(tert-butyl dimethylsilyl)oxy]hexan-1-ol (3.7 g, 16 mmol, 1.0 equiv), carbon tetrabromide (5.3 g, 16 mmol, 1 equiv), and DCM (45 mL, 0.3 M). The mixture was cooled to 0 °C using an ice water bath. Triphenylphosphine was added portion-wise and the flask was removed from the ice bath and allowed to stir at room temperature for 24 hours. The mixture was then concentrated under reduced pressure and 200 mL hexane was added. The mixture was stirred vigorously for 30 minutes. The material was then filtered through a silica gel plug with hexane. The crude material was purified on a silica gel column. 4 g of pure [(6-bromohexyl)oxy](tert-butyl)dimethylsilane was isolated, 84% yield. This compound has been previously characterized.³¹

Step 2: A round bottom flask was charged with a stir bar, [(6-bromohexyl)oxy](tert-butyl)dimethylsilane (3 g, 1 mmol, 1.0 equiv), methanol (25 mL, 1 M), 2-chloroethyl chloroformate (50 µL, 0.05 mmol, 0.05 equiv). The mixture was allowed to stir at

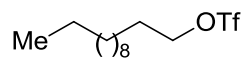
room temperature until all of the silyl ether starting material was consumed. The starting material was unobservable by TLC after 20 minutes. At this time the mixture was diluted with DCM and quenched with saturated sodium bicarbonate. The aqueous phase was extracted three times and the combined organic phase was dried with magnesium sulfate and concentrated under reduced pressure. The crude material was purified on a silica gel column using EtOAc/Hex (0 → 100%). 1.2 g of the target compound was isolated as a clear oil, 65%. This compound has been previously characterized.³²

4.6.7 General Procedure for the Triflation of Primary Alcohols



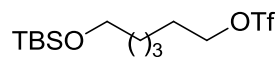
A reaction flask was flame-dried under vacuum and allowed to cool under nitrogen. The flask was then charged with a stir bar, alcohol (1.0 equiv), DCM (1.0 M), and 2,6-lutidine (1.6 equiv). The mixture was cooled to -78 °C with a dry ice acetone bath. Triflic anhydride (1.2 equiv) was added dropwise to the cooled mixture with stirring. The reaction progress was monitored by TLC and when full conversion of the alcohol had occurred, the cold mixture was poured into hexanes (3x the reaction volume) in an Erlenmeyer flask. The mixture was immediately poured onto a silica plug and the plug was washed with a mixture of hexane and ethyl acetate that moves the product to R_f 0.5. The clean fractions from the silica gel plug were concentrated under reduced pressure and used without further purification. We found that storing the alkyl triflates over activated molecular sieves in the glovebox freezer helps to improve their stability and slow down decomposition.

Alkyl Triflate Characterization Data



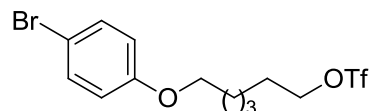
1-trifluoromethanesulfonyldodecane (4.27): compound was isolated as a

clear oil, 2.1 g, 95% yield. ^1H NMR (300 MHz, Benzene- d_6) δ 3.84 (t, J = 6.4 Hz, 2H), 1.53 – 1.04 (m, 16H), 0.75 – 1.15 (m, 7H).



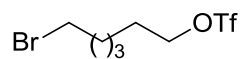
6-[(tert-butyl dimethylsilyl)oxy]hexyl trifluoromethanesulfonate (4.28):

compound was isolated as a clear oil, 2.5 g, 78% yield. ^1H NMR (300 MHz, Chloroform- d) δ 4.54 (t, J = 6.5 Hz, 2H), 3.61 (t, J = 6.2 Hz, 2H), 1.84 (p, J = 6.5 Hz, 2H), 1.66 – 1.26 (m, 6H), 0.89 (s, 9H), 0.05 (s, 6H).



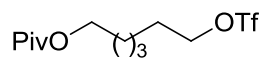
6-(4-bromophenoxy)hexyl trifluoromethanesulfonate (4.29):

compound isolated as a clear oil, 1.6 g, 80% yield. ^1H NMR (300 MHz, Chloroform- d) δ 7.47 – 7.29 (m, 2H), 6.94 – 6.52 (m, 2H), 4.55 (t, J = 6.4 Hz, 2H), 3.93 (t, J = 6.3 Hz, 2H), 2.00 – 1.69 (m, 4H), 1.62 – 1.30 (m, 4H).



6-bromohexyl trifluoromethanesulfonate (4.30): Compound isolated as a

clear oil, 1 g, 71% yield. ^1H NMR (300 MHz, Chloroform- d) δ 4.55 (t, J = 6.4 Hz, 2H), 3.42 (t, J = 6.6 Hz, 2H), 1.97 – 1.78 (m, 4H), 1.61 – 1.24 (m, 4H).



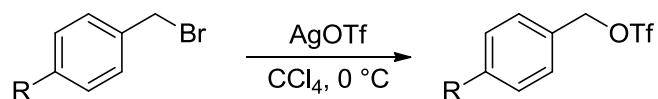
6-(trifluoromethanesulfonyloxy)hexyl 2,2-dimethylpropanoate (4.31):

Compound isolated as a clear oil, 2.2 g, 90% yield. ^1H NMR (300 MHz, Benzene- d_6) δ 3.90 (t, J = 6.6 Hz, 2H), 3.78 (t, J = 6.4 Hz, 2H), 1.31 – 1.15 (m, 11H), 1.01 (dt, J = 13.8, 6.6 Hz, 2H), 0.93 – 0.66 (m, 4H).



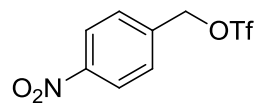
Compound isolated as a clear oil, 2.5 g, 83% yield. $^1\text{H NMR}$ (300 MHz, Benzene- d_6) δ 3.83 (t, $J = 6.4$ Hz, 2H), 3.56 (t, $J = 6.2$ Hz, 2H), 1.49 – 1.25 (m, 2H), 1.22 – 1.01 (m, 25H), 0.99 – 0.86 (m, 2H).

4.6.8 General Procedure for the Synthesis of Benzylic Triflates³³



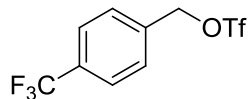
A reaction flask was flame-dried under vacuum and allowed to cool under a nitrogen atmosphere. The flask was then charged with a stir bar, benzylic bromide (1.0 equiv), and carbon tetrachloride (0.5 M). The mixture was cooled to 0 °C with an ice bath. Silver triflate (1.0 equiv) was added and the mixture was allowed to warm to room temperature. The reaction progress was monitored by $^1\text{H NMR}$. After the benzylic bromide was consumed, the solid was filtered off and the material was concentrated under reduced pressure. The material was used as quickly as possible after concentration. The benzylic bromides synthesized are stable for multiple days if stored under inert atmosphere in the dark in carbon tetrachloride.

Benzylic Triflate Characterization Data



(4-nitrophenyl)methyl trifluoromethanesulfonate (4.33): Compound

isolated as an amber oil, 1.2 g, 84% yield. $^1\text{H NMR}$ (300 MHz, Chloroform- d) δ 8.32 (d, $J = 8.7$ Hz, 2H), 7.62 (d, $J = 8.6$ Hz, 2H), 5.56 (s, 2H).

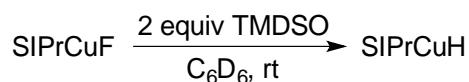


[4-(trifluoromethyl)phenyl]methyl trifluoromethanesulfonate (4.34):

Compound isolated as a brown oil, 1.2 g, 78% yield. ^1H NMR (300 MHz, Chloroform-*d*) δ 7.72 (d, $J = 8.1$ Hz, 2H), 7.56 (d, $J = 8.0$ Hz, 2H), 5.53 (s, 2H).

4.6.9 Mechanism and Kinetics Experiments

Synthesis of SIPrCuH from SIPrCuF and TMDSO



Scheme 41. Formation of SIPrCH from SIPrCuF

In a nitrogen-filled glovebox, SIPrCuF (11.9 mg, 0.025 mmol) and internal standard methyl 4-methoxybenzoate (1.6 mg, 0.010 mmol) were suspended in C_6D_6 (1.0 mL). TMDSO (8.8 μL , 0.050 mmol) was added to the suspension. The reaction solution turned bright yellow and the precipitate dissolved immediately upon mixing. Quantitative yield of SIPrCuH was observed by NMR spectroscopy in a J. Young tube with Teflon plug valve, referenced to methyl 4-methoxybenzoate internal standard.

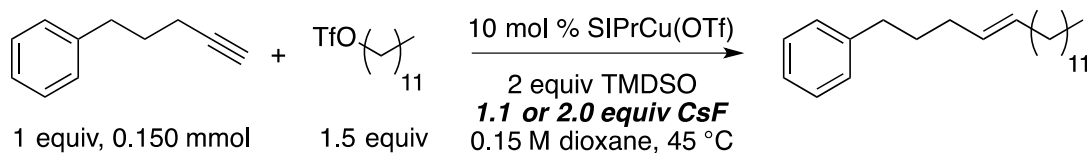
General Procedure for GC Analysis of Reaction Rate

Reactions were performed in a nitrogen-filled glovebox. CsF (2 equiv, 45.6 mg, 0.300 mmol) was weighed into a 1-dram vial and pre-stirred in 1,4-dioxane (0.60 mL) at 45 $^\circ\text{C}$ for 25 min. The following reagents were weighed and then added to the reaction vial within 3 minutes of each other: SIPrCuF (0.1 equiv, 7.1 mg, 0.015 mmol, added as a solid), TMDSO (2 equiv, 40.3 mmol, 0.300 mmol, washed in with 3 aliquots of 0.10 mL 1,4-dioxane), phenylpentyne (1 equiv, 21.6 mg, 0.150 mmol, washed in with 3 aliquots of 0.10 mL 1,4-dioxane), dioctyl ether internal

standard (0.2 equiv, 7.3 mmol, 0.030 mmol, weighed into alkyne), and dodecyl triflate (1.5 equiv, 71.6 mg, 0.225 mmol, washed in with 3 aliquots of 0.10 mL 1,4-dioxane). A total of 1.5 mL of 1,4-dioxane were used to give a reaction that is 100 mM in phenylpentynes concentration. The reactions were vigorously stirred (1500 rpm) at 45 °C.

At each desired timepoint, a 50- μ L aliquot of the well-shaken reaction mixture was removed and diluted in 400 μ L pentane to precipitate copper and CsF. The solution was removed from the glovebox, filtered through celite and cotton, then analyzed by GC.

Reaction Rate Dependence on use of 1.1 equiv or 2.0 equiv CsF



The reaction profiles were analyzed by GC according to the general procedure. Product formation occurs considerably faster with 2.0 equiv rather than 1.1 equiv CsF.

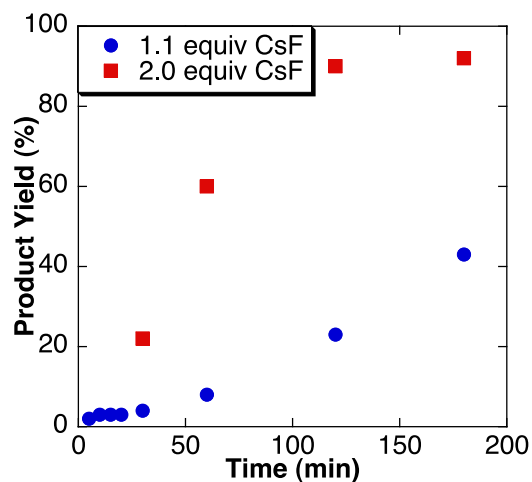
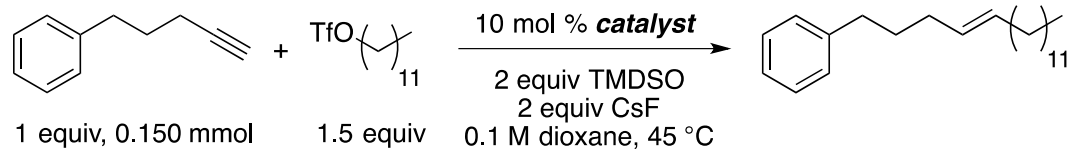


Figure 4. Product Yield Over Time Using 1.1 equiv or 2.0 equiv CsF

11.4. Reaction Profiles for SIPrCuOTf and SIPrCuF Catalyst with 2.0 equiv CsF



The reaction profiles were analyzed by GC according to the general procedure. SIPrCuOTf and SIPrCuF catalysts give similar yields over time when using 2.0 equiv CsF, however, use of SIPrCuF removes the induction period. SIPrCuF was therefore selected for the following kinetic studies.

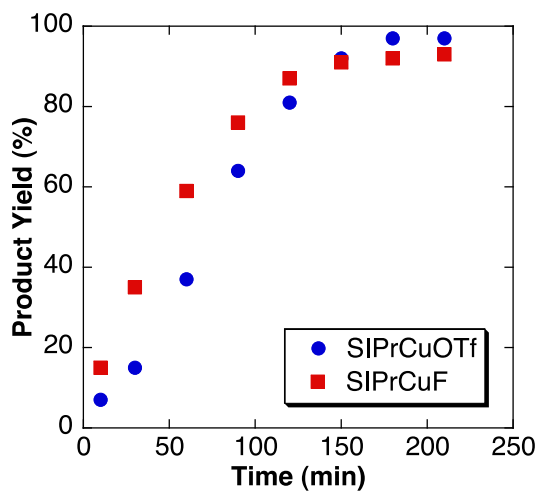
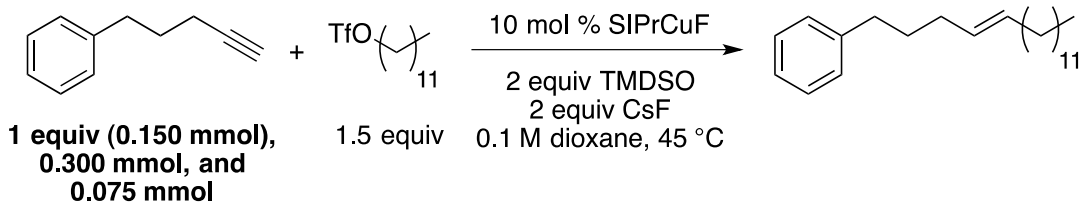


Figure 5. Product Yield Over Time Using SIPrCuOTf or SIPrCuF

Reaction Rate Dependence on Concentration of Phenylpentyne



The reaction profiles were analyzed by GC according to the general procedure. There was no significant change in reaction rate when using different concentrations of phenylpentyne.

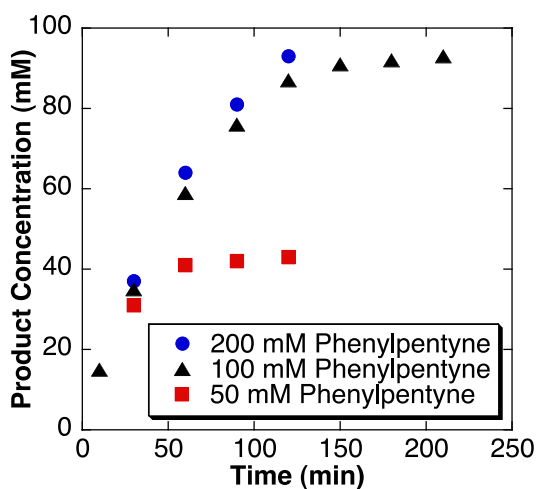
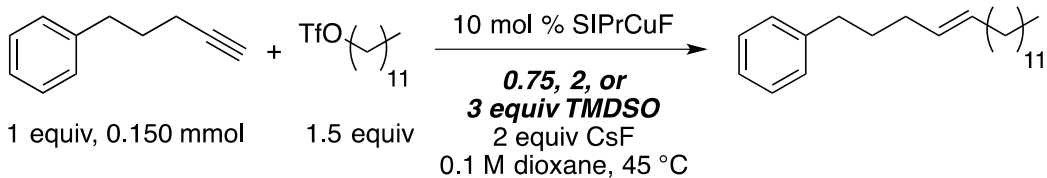


Figure 6. Product Yield over Time with Varying Concentrations of Alkyne

Reaction Rate Dependence on Concentration of TMDSO



The reaction profiles were analyzed by GC according to the general procedure. There was no significant change in reaction rate when using different concentrations of $(\text{Me}_2\text{SiH})_2\text{O}$ (TMDSO).

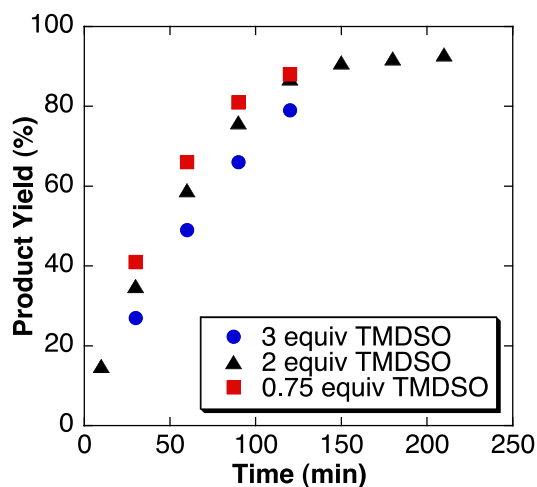
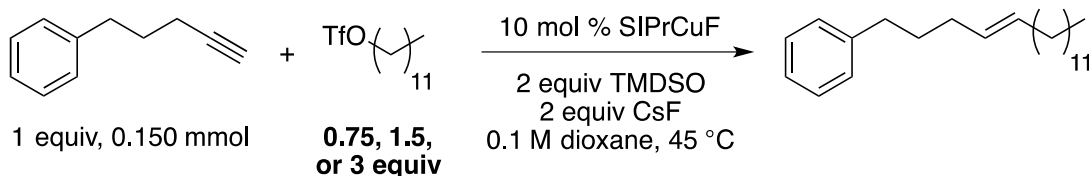


Figure 7. Product Yield over Time with Varying Concentrations of TMDSO

11.7. Reaction Rate Dependence on Dodecyl Triflate Concentration using 1.1 equiv CsF



The reaction profiles were analyzed by GC according to the general procedure. There was no significant change in reaction rate when using different concentrations of dodecyl triflate with 1.1 equiv CsF. Reactions were stopped before full conversion. The reaction profile is also linear when using standard conditions with 2.0 equiv CsF and that reaction goes to full conversion.

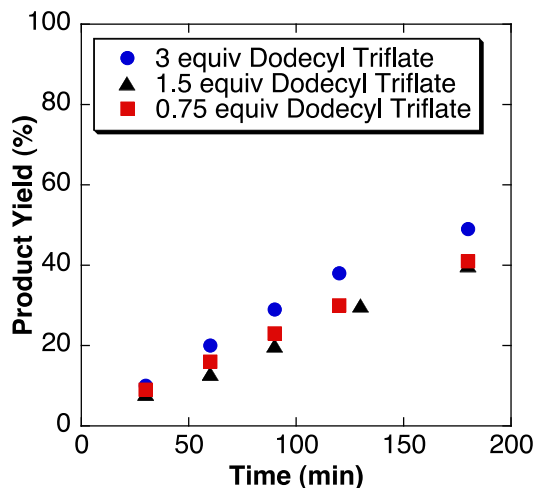
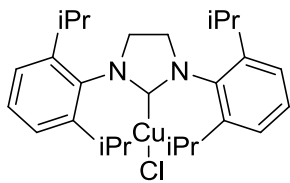


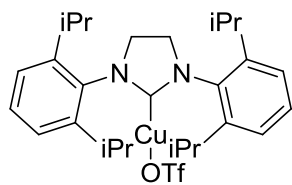
Figure 8. Product Yield over Time With Varying Concentration of Alkyl Triflate.

4.6.10. Synthesis of Organometallic Starting Materials and Intermediates

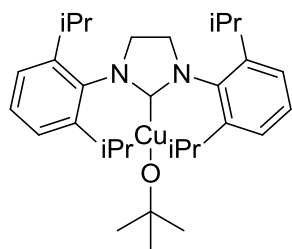


SIPrCuCl: In a nitrogen-filled glovebox, a 100-mL round bottom flask

was charged with 1,3-bis(2,6-di-iso-propylphenyl)imidazolinium chloride³⁴ (3.0g, 1.00 equiv, 7.0 mmol), sodium *t*-butoxide (682 mg, 1.01 equiv, 7.1 mmol), and 30 mL THF. The mixture was allowed to stir at 23 °C for 15 minutes then CuCl (696 mg, 1.00 equiv, 7.0 mmol) was added. After 16 hours, the reaction mixture was removed from the glovebox and concentrated under reduced pressure. The white-green solid was purified by silica plug filtration using dry DCM. Upon removal of the solvent under reduced pressure, 2.8 g of SIPrCuCl was obtained as a white solid, 80% yield. This compound has been previously characterized.³⁵

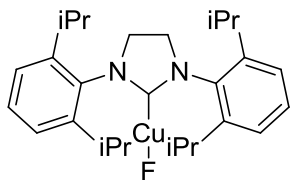


SIPrCuOTf: In a nitrogen-filled glovebox, a 20-mL scintillation vial was charged with a stir bar, SIPrCuCl (1.7g, 1.0 equiv, 3.48 mmols), and AgOTf (894 mg, 1.0 equiv, 3.48 mmols). The mixture was diluted in 9 mL THF and stirred for 3 hours. At this time, the solids were filtered off using a celite pad and the THF solution was removed under reduced pressure to yield an off-white solid. After crystallization in THF and pentane, 1.6 g of SIPrCuOTf was obtained as a white solid, 76% yield. ^1H NMR (300 MHz, Chloroform-*d*) δ 7.44 (t, $J = 7.8$ Hz, 2H), 7.27 (d, $J = 7.7$ Hz, 4H), 4.08 (s, 4H), 3.03 (hept, $J = 6.6$ Hz, 4H), 1.34 (t, $J = 6.8$ Hz, 24H). ^{13}C NMR (126 MHz, Methylene Chloride-*d*₂) δ 201.2, 147.1, 134.4, 130.4, 125.0, 119.7 (q, $J = 318.1$ Hz), 54.3, 29.3, 25.5, 24.1. ^{19}F NMR (471 MHz, Chloroform-*d*) δ -81.1.

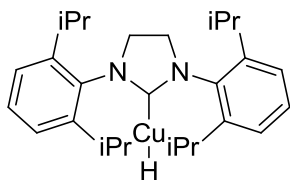


SIPrCuOtBu: In a nitrogen-filled glovebox, a reaction flask was charged with SIPrCuCl (2 g, 1 equiv, 4 mmols), sodium *t*-butoxide (784 mg, 2 equiv, 8 mmols), a stir bar, and THF (40 mL, 0.1 M). The reaction was stirred overnight. The THF was then removed under reduced pressure and the crude product was suspended in toluene. After 30 minutes of vigorous stirring a fine white solid was suspended. The mixture was then filtered through celite and concentrated under reduced pressure to afford a white powder. The white powder was recrystallized in THF/pentane yielding 1.5 g, 70%. ^1H NMR (300 MHz, Benzene-*d*₆) δ 7.23 – 7.13 (m, 2H, C₆H₆ overlap), 7.08 – 7.02 (m, 4H), 3.17 (s, 1H), 2.98 (hept, $J = 6.6$ Hz, 4H), 1.49

(d, $J = 6.8$ Hz, 12H), 1.27 (s, 9H), 1.17 (d, $J = 6.9$ Hz, 12H). ^{13}C NMR (75 MHz, Benzene- d_6) δ 206.2, 146.9, 135.6, 129.8, 124.6, 69.1, 53.3, 37.2, 29.1, 25.6, 24.1.



SIPrCuF: In a nitrogen-filled glovebox, a reaction flask was charged with SIPrCuOtBu (262 mg, 1 equiv, 0.5 mmol), a stir bar, and benzene (24 mL, 0.02 M). The reaction flask was sealed, removed from the glove box, and attached to a Schlenk line under positive pressure of nitrogen gas. With stirring, triethylamine trihydrofluoride (26 μL , 0.32 equiv, 0.16 mmol) was added via needle and syringe. The reaction was allowed to stir overnight. The volatiles were removed on the Schlenk line under reduced pressure and the leftover material was sealed under vacuum in the reaction flask and pumped back into the glove box. The white solid material was washed with pentane on a frit to yield 176 mg of a white powder, 75%. ^1H NMR (300 MHz, Chloroform- d) δ 7.75 – 7.34 (m, 2H), 7.33 – 7.11 (m, 4H, CHCl_3 overlap), 4.03 (s, 4H), 3.06 (hept, $J = 6.8$ Hz, 4H), 1.36 (dd, $J = 8.8, 6.9$ Hz, 24H). ^{13}C NMR (75 MHz, Chloroform- d) δ 203.5, 146.7, 134.6, 129.9, 124.7, 53.8, 29.0, 25.5, 24.1.



SIPrCuH: SIPrCuH was prepared in situ as previously described in Section 11: Mechanism Experiments. ^1H NMR (500 MHz, Benzene- d_6) δ 7.11 (t, $J = 7.7$ Hz, 2H), 6.99 (d, $J = 7.7$ Hz, 4H), 3.32 (s, 4H), 3.21 (h, $J = 6.9$ Hz, 4H), 1.93 (s, 1H), 1.37 (d, $J = 6.7$ Hz, 12H), 1.23 (d, $J = 7.0$ Hz, 12H).

Chapter 4 References

- ¹ a) Campbell, K. N.; Eby, L. T. *J. Am. Chem. Soc.* **1941**, 63, 216 b) Pasto, D. J. In *Comprehensive Organic Synthesis*; Trost, B. M., Fleming, I., Eds.; Pergamon: Oxford, **1991**; Vol. 8, p 471
- ² a) Schlosser, M.; Christmann, K. F. *Angew. Chem., Int. Ed.* **1966**, 5, 126 b) Wang, Q.; Deredas, D.; Huynh, C.; Schlosser, M. *Chem. Eur. J.* **2003**, 9, 570
- ³ a) Horner, L.; Hoffman, H.; Wippel, H. G. *Chem. Ber.* **1958**, 91, 61. b) Horner, L.; Hoffman, H.; Wippel, H. G.; Klahre, G. *Chem. Ber.* **1959**, 92, 2499. c) Wardworth, W. S. Jr.; Emmons, W. D. *J. Am. Chem. Soc.* **1961**, 83, 1733. d) Wadsworth, D. H.; Schupp, I. O.E.; Sous, E.J.; Ford, J.J. A. *Org. Chem.* **1965**, 30, 680
- ⁴ a) Julia, M.; Paris, J.-M. *Tetrahedron Lett.* **1973**, 14, 4833. (b) Baudin, J. B.; Hareau, G.; Julia, S. A.; Ruel, O. *Tetrahedron Lett.* **1991**, 32, 1175. (c) Blakemore, P. R.; Cole, W. J.; Kocienski, P. J.; Morley, A. *Synlett* **1998**, 26.
- ⁵ a) Heck, R. F. *J. Am. Chem. Soc.* **1968**, 90, 5518. b) Mizoroki, T.; Mori, K.; Ozaki, A. *Bull. Chem. Soc. Jpn.* **1971**, 44, 581. c) Heck, R. F.; Nolley, J. P. *J. Org. Chem.* **1972**, 37, 2320. d) Beletskaya, I. P.; Cheprakov, A. V. *Chem. Rev.* **2000**, 100, 3009
- ⁶ de Meijere, A.; Brase, S.; Oestreich, M., Eds. *Metal Catalyzed CrossCoupling Reactions and More*; Wiley-VCH Verlag GmbH & Co. KGaA.; Berlin, Germany, **2014**.
- ⁷ See chapter 3
- ⁸ a) Trost, B. M.; Ball, Z. T.; Jö ge, T. *J. Am. Chem. Soc.* **2002**, 124, 7922 b) Radkowski, K.; Sundararaju, B.; Füstner, A. *Angew. Chem. Int. Ed.* **2013**, 52, 355.
- ⁹ These Nakamura reaction achieves hydroalkylation with β -carbonyl compounds, See: Endo, K.; Hatakeyama, T.; Nakamura, M.; Nakamura, E. *J. Am. Chem. Soc.* **2007**, 129, 5264
- ¹⁰ Reactions with aldehydes: a) Oblinger, E.; Montgomery, J. *J. Am. Chem. Soc.* **1997**, 119, 9065. b) Miller, K. M.; Huang, W.-S.; Jamison, T. F. *J. Am. Chem. Soc.* **2003**, 125, 3442. c) Mahandru, G. M.; Liu, G.; Montgomery, J. *J. Am. Chem. Soc.* **2004**, 126, 3698. d) Herath, A.; Thompson, B. B.; Montgomery, J. *J. Am. Chem. Soc.* **2007**, 129, 8712. e) Patman, R. L.; Chaulagain, M. R.; Williams, V. M.; Krische, M. J. *J. Am. Chem. Soc.* **2009**, 131, 2066. f) Malik, H. A.; Sormunen, G. J.; Montgomery, J. *J. Am. Chem. Soc.* **2010**, 132, 6304. g) Leung, J. C.; Patman, R. L.; Sam, B.; Krische, M. J. *Chem. Eur. J.* **2011**, 17, 12437. For reactions in which aldehydes are formed in situ, see: a) McInturff, E. L.; Nguyen, K. D.; Krische, M. J. *Angew. Chem., Int. Ed.* **2014**, 53, 3232. b) Nakai, K.; Yoshida, Y.; Kurahashi, T.; Matsubara, S. *J. Am. Chem. Soc.* **2014**, 136, 7797. Reactions with ketones: Ngai, M.-Y.; Barchuk, A.; Krische, M. J. *J. Am. Chem. Soc.* **2006**, 129, 280. Reactions with enones: a) Wang, C.-C.; Lin, P.-S.; Cheng, C.-H. *J. Am. Chem. Soc.* **2002**, 124, 9696. b) Li, W.; Herath, A.; Montgomery, J. *J. Am. Chem. Soc.* **2009**, 131, 17024. c) Wei, C.-H.; Mannathan, S.; Cheng, C.-H. *J. Am. Chem. Soc.* **2011**, 133, 6942. Reaction with imines: Zhou, C.-Y.; Zhu, S.-F.; Wang, L.-X.; Zhou, Q.-L. *J. Am. Chem. Soc.* **2010**, 132, 10955. Reaction with foramide: Nakao, Y.; Idei, H.; Kanyiva, K. S.; Hiyama, T. *J. Am. Chem. Soc.* **2009**, 131, 5070.
- ¹¹ a) Molinaro, C.; Jamison, T. F. *J. Am. Chem. Soc.* **2003**, 125, 8076. b) Beaver, M. G.; Jamison, T. F. *Org. Lett.* **2011**, 13, 4140.
- ¹² Saito, S.; Yamamoto, Y. *Chem. Rev.* **200**, 100, 2901
- ¹³ a) Semba, K.; Fujihara, T.; Xu, T.; Terao, J.; Tsuji, Y. *Adv. Synth. Catal.* **2012**, 354, 1542. b) Whittaker, A. M.; Lalic, G. *Org. Lett.* **2013**, 15, 1112. c) Wang, G.-H.; Bin, H.-Y.; Sun, M.; Chen, S.-W.; Liu, J.-H.; Zhong, C.-M. *Tetrahedron* **2014**, 70, 2175
- ¹⁴ Fujihara, T.; Xu, T.; Semba, K.; Terao, J.; Tsuji, Y. *Angew. Chem. Int. Ed.* **2011**, 50, 523

-
- ¹⁵ Shi, S. L.; Buchwald, S. L. *Nature Chemistry*, **2015**, 7, 38-44
- ¹⁶ Uehling, M. R.; Rucker, R. P.; Lalic, G. *J. Am. Chem. Soc.* **2014**, 136, 8799
- ¹⁷ Mankad, N. P.; Laitar, D. S.; Sadighi, J. P. *Organometallics* **2004**, 23, 3369
- ¹⁸ Dang, H.; Cox, N.; Lalic, G. *Angew. Chem. Int. Ed.* **2014**, 53, 752
- ¹⁹ This chemoselectivity is remarkable as alkyl triflates are very reactive
- ²⁰ We prepared the Z diastereoisomer independently
- ²¹ See Reference 14
- ²² See Reference 17
- ²³ See References 13-16
- ²⁴ At this time, it is unclear why this is the case
- ²⁵ Dang, H.; Mailig, M.; Lalic, G. *Angew. Chem. Int. Ed.* **2014**, 53, 6473
- ²⁶ Pereira de Freitas, R.; Lehl, J.; Delavaux-Nicot, B.; Nierengarten, J. *Tetrahedron*, **2008**, 64, 11409
- ²⁷ Kaiser, F.; Schwink, L.; Velder, J.; Schmalz, H. *J. Org. Chem.* **2002**, 67, 9248
- ²⁸ Tucker, J. W.; Narayanam, J. M. R.; Shah, P. S.; Stephenson, C. R. J. *Chem. Commun.* **2011**, 47, 5040
- ²⁹ Dang, H.; Cox, N.; Lalic, G. *Angew. Chem. Int. Ed.* **2014**, 53, 752
- ³⁰ Martín-Matute, B.; Pereira, S. I.; Peña-Cabrera, E.; Adrio, J.; Silva, A. M. S.; Carretero, J. C. *Adv. Synth. Catal.* **2007**, 349, 1714
- ³¹ Kalivrestenos, A.; Stille, J. K.; Hegedus, L. S. *J. Org. Chem.* **1990**, 56, 2883
- ³² Mattes, H.; Benezra, C. *J. Org. Chem.* **1988**, 53, 2732
- ³³ Dietze, P.; Jencks, W. P. *J. Am. Chem. Soc.* **1989**, 111, 5880
- ³⁴ Thomson, J. E.; Cambell, C. D.; Concellón, C.; Duguet, N.; Rix, K.; Slawin, A. M. Z.; Smith, A. D. *J. Org. Chem.* **2007**, 2784-2791
- ³⁵ Landers, B.; Navarro, O. *Eur. J. Inorg. Chem.* **2012**, 2980-2982